1. Near-Infrared Blinking Carbon Dots Designed for Quantitative Nanoscopy

Accession number: 20230113345609

Authors: Mao, Jian (1); Xue, Minmin (1); Guan, Xin (1); Wang, Qian (2); Wang, Zhirui (1); Qin, Guangyong (1); He, Hua (1)

Author affiliation: (1) State Key Laboratory of Heavy Oil Processing, College of Chemistry and Chemical Engineering, China University of Petroleum (East China), Qingdao; 266580, China; (2) College of Chemistry and Chemical Engineering, Xi'an Shiyou University, Xi'an; 710065, China

Corresponding author: He, Hua(huahe@upc.edu.cn)

Source title: Nano Letters
Abbreviated source title: Nano Lett.
Volume: 23
Issue: 1
Issue date: January 11, 2023
Publication year: 2023
Pages: 124-131
Language: English
ISSN: 15306984
E-ISSN: 15306992
CODEN: NALEFD
Document type: Journal article (JA)
Publisher: American Chemical Society

Abstract: Blinking carbon dots (CDs) have attracted attention as a probe for single molecule localization microscopy (SMLM), yet quantitative analysis is limited because of inept blinking and low signal-to-noise ratio (SNR). Here we report the design and synthesis of near-infrared (NIR) blinking CDs with a maximum emission of around 750 nm by weaving a nitrogen-doped aromatic backbone with surplus carboxyl groups on the surface. The NIR-CDs allow conjugation to monovalent antibody fragments for labeling and imaging of cellular receptors as well as afford increases of 52% in SNR and 33% in localization precision over visible CDs. Analysis of fluorescent bursts allows for accurate counting of cellular receptors at the nanoscale resolution. Using NIR-CDs-based SMLM, we demonstrate oligomerization and internalization of programmed cell death-ligand 1 by a small molecule inhibitor for checkpoint blockade. Our NIR-CDs can become a generally applicable probe for quantitative nanoscopy in chemistry and biology. © 2023 American Chemical Society. All rights reserved.

Number of references: 44
Main heading: Probes
Controlled terms: Carbon - Cell death - Doping (additives) - Infrared devices - Molecules - Signal to noise ratio
Uncontrolled terms: Blinking - Carbon dots - Cellular receptors - Low signal-to-noise ratio - Maximum emissions - Molecular counting - Near Infrared - Near-infrared - Single molecule localization microscopy - Single-molecule localizations
Classification code: 461.9 Biology - 716.1 Information Theory and Signal Processing - 804 Chemical Products Generally - 931.3 Atomic and Molecular Physics
Numerical data indexing: Percentage 3.30E+01%, Percentage 5.20E+01%, Size 7.50E-07m
DOI: 10.1021/acs.nanolett.2c03711

Compendex references: YES
Database: Compendex
Data Provider: Engineering Village

2. Plasma resonance enhanced electric field and adsorption properties of Ag nanowire based triangular @ circle dimer structures

Accession number: 20225213306147

Authors: Xu, Chao (1); Chen, Haixia (1); Ding, Jijun (1); Fu, Haiwei (1)

Author affiliation: (1) Shaanxi Engineering Research Center of Oil and Gas Resource Optical Fiber Detection, Shaanxi Key Laboratory of Measurement and Control Technology for Oil and Gas Wells, College of Science, Xi'an Shiyou University, Xi'an; 710065, China

Corresponding author: Chen, Haixia(chenhx@xsyu.edu.cn)

Source title: Physica E: Low-Dimensional Systems and Nanostructures

Abstract: The triangle @ circle dimer structures based on Ag nanowires are designed. Firstly, the resonance frequency $_\omega$ of dimer with strong electric field is determined by theoretical simulation. Then, the triangular nanowires are rotated 60° and 90°, respectively. The effect of the triangular nanowire with different rotation angles on the electric field in the gap is investigated. Results indicate that the triangle-0°@circle dimer structure shows a very sharp dipole resonance peak. In addition, the tip located along the polarization direction of the electric field can significantly modulate the resonance peak to shift towards the visible region. The neff of the dimer shows that triangle-0° @circle dimer structure can obtain a drastic resonance in the gap without a large energy loss. Finally, the enhancement mechanism of shape parameter e and dispersion relationship on plasma resonance frequency is discussed. It is of great significance to provide a theoretical basis for optical devices to modulate plasma resonance frequency under a low loss. © 2022 Elsevier B.V.

Number of references: 26
Main heading: Electric fields
Controlled terms: Dimers - Dispersions - Electron resonance - Energy dissipation - Nanowires - Natural frequencies
Uncontrolled terms: Ag nanowires - Dimer structure - Dispersion relationship - Plasma resonance - Plasmon resonances - Resonance enhanced - Resonance frequencies - Resonance peak - Simulation - The triangle @ circle dimer structure
Classification code: 525.4 Energy Losses (industrial and residential) - 701.1 Electricity: Basic Concepts and Phenomena - 761 Nanotechnology - 815.1.1 Organic Polymers - 933 Solid State Physics - 951 Materials Science
DOI: 10.1016/j.physe.2022.115629

Compendex references: YES
Database: Compendex
Data Provider: Engineering Village

3. Quantitative analysis of phenanthrene in soil by fluorescence spectroscopy coupled with the CARS-PLS model   (*Open Access*)

Accession number: 20231513874797

Authors: Li, Haonan (1); Li, Maogang (1); Tang, Hongsheng (1); Li, Hua (1, 2); Zhang, Tianlong (1); Yang, Xiao-Feng (1)
Author affiliation: (1) Key Laboratory of Synthetic and Natural Functional Molecule of the Ministry of Education, College of Chemistry & Materials Science, Northwest University, Xi'an; 710127, China; (2) College of Chemistry and Chemical Engineering, Xi'an Shiyou University, Xi'an; 710065, China
Corresponding authors: Zhang, Tianlong(tlzhang@nwu.edu.cn); Yang, Xiao-Feng(xfyang@nwu.edu.cn)
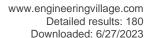
Document type: Journal article (JA)
Publisher: Royal Society of Chemistry
Abstract: Polycyclic aromatic hydrocarbons (PAHs) are typical organic pollutants in soil and are teratogenic and carcinogenic. Therefore, rapid and accurate analysis of PAHs in soil can provide a theoretical basis and data support for soil contamination risk assessment. In this work, a fluorescence spectroscopy technique combined with partial least squares (PLS) was proposed for rapid quantitative analysis of phenanthrene (PHE) in soil. At first, the fluorescence spectra of 29 soil samples with different concentrations (0.3-10 mg g-1) of PHE were collected by RF-5301 PC fluorescence spectrophotometer. Secondly, the effects of different spectral preprocessing methods were investigated on the prediction performance of the PLS calibration model. And then, the influence of competitive adaptive reweighted sampling (CARS) wavelength points on the prediction performance of PLS calibration model was discussed. Finally, according to the selected wavelength points, a quantitative analytical model for PHE content in soil was constructed using the PLS calibration method. To further explore the predictive performance of the CARS-PLS calibration model, the predictive results were compared with those of the RAW spectrum-partial least squares calibration model (RAW-PLS) and the wavelet transform-standard normal variation (WT-SNV) calibration model. The CARS-PLS calibration model showed the optimal predictive performance and its coefficient of determination of cross-validation (Rcv2) and root mean square error of 10-fold cross-validation (RMSEcv) were 0.9957 and 18.98%, respectively. The coefficient of determination of prediction set (Rp2) and root mean square error of prediction set (RMSEp) were 0.9963 and 16.13%, respectively. Hence, the CARS algorithm based on fluorescence spectrum coupled with PLS can give a rapid and accurate quantitative analysis of the PHE content in soil. © 2023 The Royal Society of Chemistry.
Number of references: 45
Main heading: Soils
Controlled terms: Anthracene - Coherent scattering - Fluorescence - Fluorescence spectroscopy - Forecasting - Mean square error - Organic pollutants - Risk assessment - Spectrum analysis - Wavelet transforms
Uncontrolled terms: Calibration model - Carcinogenics - Coefficient of determination - Fluorescence spectra - Partial least squares calibrations - Partial least squares models - Partial least-squares - Prediction performance - Predictive performance - Rapid analysis
Classification code: 483.1 Soils and Soil Mechanics - 711 Electromagnetic Waves - 741.1 Light/Optics - 741.3 Optical Devices and Systems - 804.1 Organic Compounds - 914.1 Accidents and Accident Prevention - 921.3 Mathematical Transformations - 922.2 Mathematical Statistics - 941.3 Optical Instruments - 941.4 Optical Variables Measurements
Numerical data indexing: Percentage 1.613E+01%, Percentage 1.898E+01%, Percentage 9.957E-01%, Percentage 9.963E-01%, null 3.00E-01null to 1.00E+01null
DOI: 10.1039/d2ra08279a
Compendex references: YES
Open Access type(s): All Open Access, Gold, Green
Database: Compendex
Data Provider: Engineering Village

4. Seismic performance of interlocking compressed-earth block composite walls

Accession number: 20230413441714
Authors: Lan, Guanqi (1, 2); Wang, Tianya (3); Wang, Yihong (3); Zhang, Kun (1)
Author affiliation: (1) School of Civil Engineering, Xi'an Shiyou University, China; (2) State Key Laboratory of Green Building in Western China, Xian University of Architecture & Technology, China; (3) Key Laboratory of Low-carbon Urban Construction of Xi'an, Chang' an University, China
Corresponding author: Lan, Guanqi(langq@xsyu.edu.cn)
Source title: Composite Structures
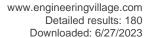**Abbreviated source title:** Compos. Struct.
Volume: 308
Issue date: March 15, 2023
Publication year: 2023
Article number: 116704
Language: English
ISSN: 02638223
CODEN: COMSE2
Document type: Journal article (JA)
Publisher: Elsevier Ltd

Abstract: This study proposes a novel interlocking compressed-earth block (ICEB) composite wall. The composite walls consist of stabilized interlocking compressed-earth blocks, reinforced concrete core columns, structural columns, and lateral strengthening strips. Nine interlocking compressed-earth block composite walls are designed and prepared at a scale of 1:2 based on the shear wall of traditional residences in Chinese villages. The effects of different structural measures on the seismic performance of composite walls are investigated through low-frequency cyclic loading tests. The failure mode, hysteretic behavior, stiffness degradation, ductility, and energy dissipation ability of the walls under lateral loads are obtained and analyzed. Based on analysis of test curves, the characteristic envelope curves model, calculation method of loading and unloading stiffness, and hysteretic trends are established and a trilinear restoring force model suitable for the wall obtained. © 2023 Elsevier Ltd

Number of references: 46
Main heading: Stiffness
Controlled terms: Cyclic loads - Energy dissipation - Hysteresis - Reinforced concrete - Seismic waves - Seismology - Unloading
Uncontrolled terms: Composite wall - Compressed earth blocks - Concrete core columns - Earthen structures - Hysteretic model - Interlocking block - Interlockings - Reinforced concrete core - Seismic Performance - Structural measures
Classification code: 408.1 Structural Design, General - 412 Concrete - 484 Seismology - 484.1 Earthquake Measurements and Analysis - 525.4 Energy Losses (industrial and residential) - 691.2 Materials Handling Methods - 951 Materials Science - 961 Systems Science
DOI: 10.1016/j.compstruct.2023.116704

Compendex references: YES
Database: Compendex
Data Provider: Engineering Village

5. The regulation of the withstand voltage performance of ZnO/GaN vertical heterostructures using external electric field and vacancy defects

Accession number: 20230513472603

Authors: Yang, Mingya (1); Ding, Jijun (1); Wang, Xiangyu (1); Chen, Haixia (1); Fu, Haiwei (1)
Author affiliation: (1) Shaanxi Engineering Research Center of Oil and Gas Resource Optical Fiber Detection, Shaanxi Key Laboratory of Measurement and Control Technology for Oil and Gas Wells, College of Science, Xi'an Shiyou University, Xi'an; 710065, China
Corresponding author: Ding, Jijun(jjding@xsyu.edu.cn)

Abstract: The band gap of the heterostructure determines the withstand voltage. It is very important to regulate the band gap of heterojunctions and to investigate their electrical properties by applying external electric field. Based on density functional theory (DFT), ZnO/GaN vertical heterostructures with two stacking configurations (AB/BA and AB/AB, named H1 and H2, respectively) are constructed. The external electric field and vacancy defects of Zn, Ga, O

and N atoms (VZn, VGa, VO and VN) are applied to analyze the electrical properties. The band gap can be tuned from 2.07 eV to 0 eV in H1 and 1.53 eV–0 eV in H2. As the electric field increases, H1 has stronger withstand voltage (-0.84–0.56 V/Å) than H2 (-0.26–0.26 V/Å). In addition, the structures deform obviously with the effect of vacancy defects, but remain stable. The presence of VGa and VN enables H1 and H2 to exhibits metal conductivity and VO change the band types of H1 and H2 from direct to indirect. The results of charge density difference (CDD) prove that a zero potential region and a weak electric field occur at the position of VZn and VO, respectively. Likewise, the external electric field is applied to the defective heterostructures. The bandgap also exhibits strong tunability, and the heterostructure with VO has the largest electric field modulation width. The above results indicate that ZnO/GaN exhibits excellent electrical properties with the influence of VO, which represents potential applications in electronic devices. © 2023 Elsevier Inc.

Number of references: 35
Main heading: Zinc oxide
Controlled terms: Binary alloys - Defects - Density functional theory - Electric fields - Energy gap - Heterojunctions - II-VI semiconductors
Uncontrolled terms: Charge density difference - Density-functional-theory - External electric field - Metal conductivity - Performance - Stacking configurations - Vacancy Defects - Vertical heterostructure - Withstand voltage - ZnO/GaN heterostructure
Classification code: 701.1 Electricity: Basic Concepts and Phenomena - 712.1 Semiconducting Materials - 714.2 Semiconductor Devices and Integrated Circuits - 804.2 Inorganic Compounds - 922.1 Probability Theory - 931.3 Atomic and Molecular Physics - 931.4 Quantum Theory; Quantum Mechanics - 951 Materials Science
Numerical data indexing: Electron volt 0.00E00eV, Electron volt 1.00E00eV, Electron volt 1.53E+00eV, Electron volt 2.07E+00eV to 0.00E00eV, Voltage 2.60E-01V, Voltage 8.40E-01V to 5.60E-01V
DOI: 10.1016/j.jmgm.2023.108424
Funding Details: Number: YCS22213170, Acronym: -, Sponsor: -; Number: 11804273, Acronym: NSFC, Sponsor: National Natural Science Foundation of China; Number: 2019GY-170, Acronym: -, Sponsor: Key Research and Development Projects of Shaanxi Province;
Funding text: This work is supported by the National Natural Science Foundations of China (Grant No. 11804273), Key Research and Development Projects of Shaanxi Province (Grant No. 2019GY-170), Graduate Student Innovative and Practical Ability Training Program of Xi'an Shiyou University (Grant No. YCS22213170).
Compendex references: YES
Database: Compendex
Data Provider: Engineering Village

Compilation and indexing terms, Copyright 2023 Elsevier Inc.

6. Wave propagation of bending jet in electrospinning process (*Open Access*)

Authors: Xu, Lei (1); Lv, Jiao (1); Wang, Xiang (2); Qu, Wentao (3)
Author affiliation: (1) School of Mechanical and Electric Engineering, Jingdezhen Ceramic University, Jingdezhen; 333403, China; (2) School of Mechanical and Automotive Engineering, Xiamen University of Technology, Xiamen; 361024, China; (3) College of Mechanical Engineering, Xi'An Shiyou University, Xi'an; 710065, China
Corresponding authors: Xu, Lei(charlie1975@163.com); Qu, Wentao(wtqu@xsyu.edu.cn)
Abstract: The electrospinning process features bending jets in space and solidified nanofibers on a collector. Although electrospun nanofibers have been widely applied, the wave characteristics, especially the first jet bend and tapered envelope cone profile, of bending jets are not fully comprehended. In this work, a spatial normal mode k- is true to characterize the convective instability of a bending jet. Some real wave variables are measured and calculated. It is observed that the first jet bend occurs at the jet end. The instability grows quickly at the early stage of a wave. Underdeveloped dispersive waves are temporally and spatially unstable. When dispersive waves develop to a mature stage, the instability grows slowly, and developed dispersive waves are only spatially unstable. Furthermore, the energy ratio of electric energy to kinematic energy accounts for the wave characteristics of a bending jet. A high

energy ratio may stabilize the jet, and a very low energy ratio destabilizes the jet. The stabilizing effect of the high energy ratio suppresses the growth of dispersive waves at the jet source. Once residual charges within the jet trigger small perturbations to the electric field near the plate owing to the Coulomb repulsive effect of like charges, the destabilizing effect of the low energy ratio causes the rapid development of small perturbation first at the jet end. The inhomogeneous distribution of electric energy contributes to the tapered envelope cone profile of a bending jet. Numerically and experimentally, the wave speed is in the order of 1 m/s, and the growth rate is in the order of 102 m-1. The numerical results are in accordance with the experimental results. © 2023 Author(s).

Number of references: 37
Main heading: Nanofibers
Controlled terms: Dispersion (waves) - Electric fields - Electrospinning - Wave propagation
Uncontrolled terms: Convective instabilities - Dispersive waves - Electric energies - Electrospinning process - Electrospun nanofibers - Energy ratio - Lower energies - Normal modes - Small perturbations - Wave characteristics
Classification code: 701.1 Electricity: Basic Concepts and Phenomena - 761 Nanotechnology - 819.3 Fiber Chemistry and Processing - 933 Solid State Physics
Numerical data indexing: Size 1.02E+02m, Velocity 1.00E00m/s
DOI: 10.1063/5.0126064
Funding Details: Number: 11762007,51805460,52071261, Acronym: NSFC, Sponsor: National Natural Science Foundation of China; Number: 2021J011196,2022H6036, Acronym: -, Sponsor: Science and Technology Planning Project of Guangdong Province; Number: 2022GY-401, Acronym: -, Sponsor: Key Research and Development Projects of Shaanxi Province;
Funding text: This work was funded by the National Natural Science Foundation of China (Grant Nos. 11762007, 51805460, and 52071261), the Science and Technology Planning Project of Fujian Province (Grant Nos. 2021J011196 and 2022H6036), and the Key Research and Development Projects of Shaanxi Province (Grant No. 2022GY-401).
Compendex references: YES
Open Access type(s): All Open Access, Gold
Database: Compendex
Data Provider: Engineering Village
Compilation and indexing terms, Copyright 2023 Elsevier Inc.

7. Rapid quantitative analysis of rare earth elements Lu and Y in rare earth ores by laser induced breakdown spectroscopy combined with iPLS-VIP and partial least squares (*Open Access*)

Accession number: 20232314204069
Authors: Liu, Xiangqian (1); Yan, Chunhua (1); An, Duanyang (1); Yue, Chengen (1); Zhang, Tianlong (2); Tang, Hongsheng (2); Li, Hua (1, 2)
Author affiliation: (1) College of Chemistry and Chemical Engineering, Xi'an Shiyou University, Xi'an; 710065, China; (2) Key Laboratory of Synthetic and Natural Functional Molecule of the Ministry of Education, College of Chemistry & Materials Science, Northwest University, Xi'an; 710127, China
Corresponding authors: Yan, Chunhua(huahua18254@163.com); Li, Hua(huali@nwu.edu.cn)
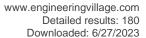**Source title:** RSC Advances
Abbreviated source title: RSC Adv.
Volume: 13
Issue: 22
Issue date: May 22, 2023
Publication year: 2023
Pages: 15347-15355
Language: English
E-ISSN: 20462069
CODEN: RSCACL
Document type: Journal article (JA)
Publisher: Royal Society of Chemistry
Abstract: Rare earth ores are complex in composition and diverse in mineral composition, requiring high technical requirements for the selection of rare earth ores. It is of great significance to explore the on-site rapid detection and analysis methods of rare earth elements in rare earth ores. Laser induced breakdown spectroscopy (LIBS) is an important tool to detect rare earth ores, which can be used for in situ analyses without complicated sample preparation. In this study, a rapid quantitative analysis method for rare earth elements Lu and Y in rare earth ores was established by LIBS combined with an iPLS-VIP hybrid variable selection strategy and partial least squares (PLS) method. First, the LIBS spectra of 25 samples were studied using laser induced breakdown spectrometry. Second, taking the

spectrum processed by wavelet transform (WT) as the input variables, PLS calibration models based on interval partial least squares (iPLS), variable importance projection (VIP) and iPLS-VIP hybrid variable selection were constructed to quantitatively analyze rare earth elements Lu and Y, respectively. The results show that the WT-iPLS-VIP-PLS calibration model has better prediction performance for rare earth elements Lu and Y, and the optimal coefficient of determination (R^2) of Lu and Y were 0.9897 and 0.9833, the root mean square error (RMSE) were 0.8150 µg g-1 and 97.1047 µg g-1, and the mean relative error (MRE) were 0.0754 and 0.0766, respectively. It shows that LIBS technology combined with the iPLS-VIP and PLS calibration model provides a new method for in situ quantitative analysis of rare earth elements in rare earth ores. © 2023 The Royal Society of Chemistry.

Number of references: 38
Main heading: Wavelet transforms
Controlled terms: Atomic emission spectroscopy - Laser induced breakdown spectroscopy - Least squares approximations - Mean square error - Ores - Rare earths - Spectrum analysis
Uncontrolled terms: Analysis method - Calibration model - Hybrid variables - Laserinduced breakdown spectroscopy (LIBS) - Partial least squares calibrations - Partial least-squares - Rare earth ores - Spectra's - Variable importances - Variables selections
Classification code: 804.2 Inorganic Compounds - 921.3 Mathematical Transformations - 921.6 Numerical Methods - 922.2 Mathematical Statistics - 931.1 Mechanics
Numerical data indexing: Mass 1.00E-09kg, Mass 8.15E-10kg, Mass 9.71047E-08kg
DOI: 10.1039/d3ra02102e
Funding Details: Number: 22173071, Acronym: NSFC, Sponsor: National Natural Science Foundation of China; Number: 22JP064, Acronym: -, Sponsor: Education Department of Shaanxi Province; Number: 2023-JC-QN-0169, Acronym: -, Sponsor: Natural Science Basic Research Program of Shaanxi Province;
Funding text: This work was supported by the National Natural Science Foundation of China (No. 22173071); Scientific Research Program Funded by Shaanxi Provincial Education Department (No. 22JP064); Natural Science Basic Research Program of Shaanxi (No. 2023-JC-QN-0169).
Compendex references: YES
Open Access type(s): All Open Access, Gold
Database: Compendex
Data Provider: Engineering Village

8. Cloud service provisioning strategy using data center consortium clustering

Accession number: 20231013682209
Authors: Liang, Bin (1); Wu, Di (2); Wu, Pengfei (3)
Author affiliation: (1) School of Computer Science, Xi'an Shiyou University, Xi'an; 710065, China; (2) College of Physics and Electronic Engineering, Northwest Normal University, Lanzhou; 730070, China; (3) School of Automation and Information Engineering, Xi'an University of Technology, Xi'an; 710049, China
Corresponding author: Wu, Pengfei(howlaser@163.com)

Abstract: The rapid growth of data centers provides cloud users with better choices and services. An increasing number of companies are involved in the construction of data centers; at the same time, the original cloud service providers are constantly expanding new data centers to meet the needs of users. Therefore, the joint scheduling of multiple data centers has become a difficult problem that cloud service providers must face. Joint scheduling refers to the resource allocation among multiple data centers of a cloud service provider. That is, how can the virtual machine application of cloud users be deployed on the physical machine in multiple data centers. A single data center provisioning strategy can solve the scheduling problem within the data center. However, multiple data centers can make the previous provisioning strategy invalid due to geographical location and other differences. In this paper, the characteristics of different data centers are analyzed and clustered to form a data center consortium. Then, the virtual machine (VM) is classified according to the deadline. As cloud users purchase virtual machine resources from cloud service providers, they are billed by time in most cases. The deadline of the virtual machine refers to the time when

the virtual machine ends its service. Then, we analyze the power consumption of the data center and deploy VMs based on the rule of avoiding hotspot deployment of VMs with priority energy consumption. Finally, a cloud service provisioning strategy using data center consortium clustering (PSDC3) is proposed and verified. It can be seen from the results that the algorithm can significantly reduce the number of hotspots and energy consumption of cloud data centers. © 2023 Elsevier Ltd

Number of references: 28
Main heading: Machine learning
Controlled terms: Distributed database systems - Energy utilization - Network security - Virtual machine
Uncontrolled terms: Cloud service providers - Cloud services - Clusterings - Data center consortium - Datacenter - Joint scheduling - Machine-learning - Multiple data - Provisioning strategy - Service provisioning
Classification code: 525.3 Energy Utilization - 723 Computer Software, Data Handling and Applications - 723.3 Database Systems - 723.4 Artificial Intelligence - 723.5 Computer Applications
DOI: 10.1016/j.eswa.2023.119744
Compendex references: YES
Database: Compendex
Data Provider: Engineering Village

9. On-line Raman spectroscopy combined with multivariate curve resolution-alternating least squares (MCR-ALS) to investigate the synthesis mechanism of 3,5-diamino-1,2,4-triazole (DAT)

Accession number: 20225113273327
Authors: Fu, Han (1); Li, Maogang (1); Guo, Mengjun (1); Tang, Hongsheng (1); Zhang, Tianlong (1); Li, Hua (1, 2)
Author affiliation: (1) Key Laboratory of Synthetic and Natural Functional Molecule of the Ministry of Education, College of Chemistry & Materials Science, Northwest University, Xi'an; 710127, China; (2) College of Chemistry and Chemical Engineering, Xi'an Shiyou University, Xi'an; 710065, China
Corresponding author: Zhang, Tianlong(tlzhang@nwu.edu.cn)
Source title: Spectrochimica Acta - Part A: Molecular and Biomolecular Spectroscopy
Abbreviated source title: Spectrochim. Acta Part A Mol. Biomol. Spectrosc.
Volume: 289
Issue date: March 15, 2023
Publication year: 2023
Article number: 122231
Language: English
ISSN: 13861425
CODEN: SAMCAS
Document type: Journal article (JA)
Publisher: Elsevier B.V.
Abstract: The precise and accurate synthesis mechanism of typical energetic materials (EMs) intermediate is extremely important for the optimization of synthesis technology of EMs. In this research, on-line Raman spectroscopy technique combined with multivariate curve resolution-alternating least squares(MCR-ALS) method was proposed and used to investigate the synthesis mechanism of EMs intermediate (3,5-diamino-1,2,4-triazole, DAT). Initially, on-line Raman spectroscopy was applied to collect the Raman spectral data of DAT synthesis process. Secondly, principal component analysis (PCA), coupled with singular value decomposition (SVD) were used to determine the number of component of the reaction system and the components was 5. Thirdly, MCR-ALS was used to extract the pure Raman spectra and concentration curves of each substance of DAT synthesis process. During the MCR-ALS operation, evolving factor analysis (EFA) was choose to acquire the initial concentration estimation for MCR-ALS. Several constraints were selected to apply to ALS optimization including non-negative, closure, equality and correlation constraint. And the correlation coefficient between the Raman spectra and the actual Raman spectra of the hydrazine hydrochloride, dicyandiamide and DAT was calculated, their correlation coefficient R^2 were 0.9522, 0.9446, 0.9908 respectively which showed a good data fit of MCR-ALS method. Finally, according to the results of MCR-ALS analysis, the structure of the synthetic intermediates was successfully deduced and the mechanism of DAT synthesis was proposed. Hence, a precise and comprehensive method for analyzing the DAT synthesis reaction mechanism

is proposed, which is helpful to provide a new idea for the analysis of the synthesis reaction mechanism of energetic materials. © 2022 Elsevier B.V.

Number of references: 47
Main heading: Raman scattering
Controlled terms: Least squares approximations - Nitrogen compounds - Principal component analysis - Raman spectroscopy - Singular value decomposition - Spectrum analysis
Uncontrolled terms: Alternating least square methods - Chemometrices - Correlation coefficient - Multivariate curve resolution alternating least-squares - Multivariate curve resolution-alternating least squares - On-line raman - Optimisations - Synthesis mechanism - Synthesis process - Triazole
Classification code: 741.1 Light/Optics - 921 Mathematics - 921.6 Numerical Methods - 922.2 Mathematical Statistics
DOI: 10.1016/j.saa.2022.122231
Funding Details: Number: 21873076,22073074,22173071, Acronym: NSFC, Sponsor: National Natural Science Foundation of China;
Funding text: This work was supported by the National Natural Science Foundation of China (No. 22173071 , 22073074 , and 21873076).
Compendex references: YES
Database: Compendex
Data Provider: Engineering Village

10. Study on the uneven flow distribution and non-uniform heat transfer in microchannels

Accession number: 20232114140755
Authors: Gao, Zhigang (1); Shang, Xiaolong (1); Bai, Junhua (2); Yang, Yuxin (3); Li, Peng (1)
Author affiliation: (1) Institute of Precision Guidance and Control, Northwestern Polytechnical University, Xi'an; 710072, China; (2) College of Petroleum Engineering, Xi'an Shiyou University, Xi'an; 710065, China; (3) Science and Technology on Combustion, Internal flow and Thermo-Structure Laboratory, Xi'an; 710025, China
Corresponding author: Gao, Zhigang(gaozhigang@nwpu.edu.cn)
Source title: Applied Thermal Engineering
Abbreviated source title: Appl Therm Eng
Volume: 230
Issue date: July 25, 2023
Publication year: 2023
Article number: 120824
Language: English
ISSN: 13594311
CODEN: ATENFT
Document type: Journal article (JA)
Publisher: Elsevier Ltd
Abstract: The power module is one of the main heating sources with non-uniform heat flux in high-power electrical servo systems used for flight vehicles. Faults in the power module are usually caused by a high or a non-uniform temperature. Given the environment of heat dissipation during flight, a regenerative cooling method is typically used, and the cooling system is designed as a microchannel heat sink with supercritical fuel. This is an effective means of solving thermal problems in the flight vehicles. However, because of the high heating power and non-uniform heat distribution of the power module, it is necessary to optimize its heat sink to restrict the high temperature rise and suppress the non-uniform distribution of temperature. In light of these considerations, a 3D numerical model of the microchannel heat sink of a power module with non-uniform heat flux was established in this study to examine the heat transfer and the thermal performance of the cooling channels. Based on the validation of the mesh and numerical method, the simulations of the flow distributions of the channels were performed to assess the thermal performance of the heat sink. It included investigating the effects of the inlet location of the manifold and its injection angle on the flow distribution in the channels, and the influences of the flow distribution and the operational parameters on the thermal performance of the heat sink. The results revealed that the Z30 configuration provided the best location and injection angle of the inlet to match the non-uniform heat flux of the power module. In this case, the values of Stanton number and buoyancy parameter of channel 4 yielded the minimum values of all channels owing to its higher flow rate and gradual rise in temperature. The deviation in the rate of mass flow Φ changed slightly corresponding to the various operational parameters, only the total heat flux would bring a bigger fluctuation. The tiny difference in temperatures among the observation areas on the substrate verified the positive influence of the flow distribution in matching the non-uniform heat flux. © 2023 Elsevier Ltd
Number of references: 35
Main heading: Heat sinks
Controlled terms: 3D modeling - Cooling - Heat flux - Microchannels - Numerical methods

Uncontrolled terms: Flight vehicles - Flow distribution - Micro channel heat sinks - Non-uniform - Non-uniform heat fluxes - Power module - Supercritical - Supercritical methane - Temperature uniformity - Thermal Performance

Classification code: 616.1 Heat Exchange Equipment and Components - 641.2 Heat Transfer - 723.2 Data Processing and Image Processing - 921.6 Numerical Methods

DOI: 10.1016/j.applthermaleng.2023.120824

Compendex references: YES

Database: Compendex

Data Provider: Engineering Village

11. Prediction and Analysis of Daily Oil Production in Block T of A Oil Production Plant Based on ARIMA Model

Accession number: 20232014104144

Authors: Hu, Mingyuan (1); Zhang, Yi (1); Guo, Jun (1); Chen, Yazhou (2); Wei, Feng (3); Gou, Mengjiao (1)

Author affiliation: (1) School of Petroleum Engineering, Xi'an ShiYou University, Shaanxi, Xi'an; 710065, China; (2) No.3 Oil Production Plant of Changqing Oilfield Branch Company, CNPC, Ningxia, Yinchuan; 750005, China; (3) Development Department of Zhanjiang Branch, CNOOC (China), Guangdong, Zhanjiang; 524057, China

Corresponding author: Zhang, Yi(zhyfly@163.com)

Source title: Proceedings of SPIE - The International Society for Optical Engineering

Abbreviated source title: Proc SPIE Int Soc Opt Eng

Volume: 12462

Part number: 1 of 1

Issue title: Third International Symposium on Computer Engineering and Intelligent Communications, ISCEIC 2022

Issue date: 2023

Publication year: 2023

Article number: 124621I

Language: English

ISSN: 0277786X

E-ISSN: 1996756X

CODEN: PSISDG

ISBN-13: 9781510660298

Document type: Conference article (CA)

Conference name: 3rd International Symposium on Computer Engineering and Intelligent Communications, ISCEIC 2022

Conference date: September 16, 2022 - September 18, 2022

Conference location: Xi'an, China

Conference code: 187947

Sponsor: Academic Exchange Information Center; Dalian Maritime University

Publisher: SPIE

Abstract: Oil production plant A has entered the stage of high water cut in the middle and late stages of development, and its benefits are getting worse and worse, In order to formulate a reasonable production plan for the enterprise, avoid blind investment and improve production efficiency, Based on the current situation, this paper introduces the modeling process of the ARIMA model in detail. Based on the oil production data of block T of the A oil production plant from January 2007 to September 2021, the ARIMA model is used to analyze the oil production. Four different ARIMA models were obtained through judgment, and after comparison, the study found that the prediction error metrics of the ARIMA(3, 1, 1)(2, 0, 0)[12] model were all small, and the model The effect of the short-term prediction of the daily oil production sequence in block T of the A oil production plant is relatively accurate, and it is of great significance for the short-term prediction of oil production. © The Authors. Published under a Creative Commons Attribution CC-BY 3.0 License.

Number of references: 15

Main heading: Production efficiency

Controlled terms: Forecasting - Investments - Production control - Time series analysis

Uncontrolled terms: ARIMA models - High water-cut - Late stage - Oil-production - Prediction and analysis - Production forecasts - Production plant - Short term prediction - Short-term forecasts - Time series forecasts
Classification code: 913 Production Planning and Control; Manufacturing - 913.2 Production Control - 913.4 Manufacturing - 922.2 Mathematical Statistics
DOI: 10.1117/12.2660959
Compendex references: YES
Database: Compendex
Data Provider: Engineering Village
Compilation and indexing terms, Copyright 2023 Elsevier Inc.

12. Special issue "New advancements and challenges in unconventional reservoirs" (*Open Access*)

Accession number: 20230913631917
Authors: Davarpanah, Afshin (1); Xu, Jinze (2, 3); Zhang, Tao (4)
Author affiliation: (1) Aberystwyth University, Aberystwyth; SY23 3BZ, United Kingdom; (2) Department of Chemical and Petroleum Engineering, University of Calgary, Calgary; AB, Canada; (3) College of Petroleum Engineering, Xi'an Shiyou University, Shaanxi, Xi'an, China; (4) Southwest Petroleum University, Sichuan, Chengdu; 610500, China
Corresponding author: Davarpanah, Afshin(afshindpe@gmail.com)
Compilation and indexing terms, Copyright 2023 Elsevier Inc.

13. SOC estimation and fault diagnosis framework of battery based on multi-model fusion modeling

Accession number: 20231613892096
Authors: Li, Jiabo (1, 2); Ye, Min (2); Ma, Xiaokang (3); Wang, Qiao (2); Wang, Yan (1)
Author affiliation: (1) Mechanical Engineering College, Xi'an Shiyou University, Xi'an; 710065, China; (2) Engineering Research Center of Expressway Construction & Maintenance Equipment and Technology of MOE, Chang'an University, Xi'an; 710064, China; (3) School of Physics and Electronic Information, Yan'an University, Yan'an; 716000, China
Corresponding authors: Li, Jiabo(ljb92_7@163.com); Ye, Min(mingye@chd.edu.cn)
Abstract: Accurate estimation of the battery state characteristics can ensure the safe driving of electric vehicles(EVs). This paper aims to propose a new method for state of charge (SOC) estimation and fault diagnosis based on multiple equivalent circuit models(ECMs) fusion approach. This paper improves the accuracy of SOC estimation and fault

diagnosis from the following four aspects. Firstly, the Thevenin model and second-order ECM are selected to describe the dynamic characteristics of the battery and the least square method is then used to determine the model parameters. Besides, the unscented Kalman filter(UKF) is employed to estimate the SOC from the two models and the Bayesian theorem is employed to determine the optimal weights for synthesizing the SOCs estimated from the two models. Moreover, the voltage residual innovation sequence(RIS) is introduced to adaptively adjust the size of the window width in real-time, which can promote the iterative performance of traditional UKF and the prediction ability of the models. Finally, an adaptive fault diagnosis framework based on multiple ECMs fusion is constructed to determine the current battery operation status based on the probability weight of each model, and also to achieve accurate early warning of the current sensor fault. The experimental results show that the SOC estimation errors are controlled within 1 %, and the battery status and current sensor fault can also be accurately diagnosed. © 2023 Elsevier Ltd

Number of references: 40
Main heading: Failure analysis
Controlled terms: Battery management systems - Charging (batteries) - Electric vehicles - Equivalent circuits - Fault detection - Iterative methods - Kalman filters - Least squares approximations - Secondary batteries
Uncontrolled terms: Current sensors - Equivalent circuit model - Faults diagnosis - Model fusion - Multi-model fusion - Multi-modelling - Sensors faults - State-of-charge estimation - States of charges - Unscented Kalman Filter
Classification code: 702.1.2 Secondary Batteries - 921.6 Numerical Methods
Numerical data indexing: Percentage 1.00E00%
DOI: 10.1016/j.est.2023.107296

Compendex references: YES
Database: Compendex
Data Provider: Engineering Village

14. An Amphiphilic Nano Calcium Carbonate: Preparation, Emulsification, Interface Properties, and Displacement Mechanism in Low Permeability Reservoir

Accession number: 20230167497

Authors: Tian, Kaiping (1, 2); Pu, Wanfen (1); Wang, Qianlong (3); Liu, Shun (3); Li, Siying (2)
Author affiliation: (1) State Key Laboratory of Oil and Gas Reservoir Geology and Exploitation, Southwest Petroleum University, Chengdu; 610500, China; (2) School of Petroleum and Natural Gas Engineering, Southwest Petroleum University, Chengdu; 610500, China; (3) School of Petroleum Engineering, Xi'an Shiyou University, Xi'an; 710065, China
Corresponding authors: Tian, Kaiping(1250259737@qq.com); Pu, Wanfen(pwf58@163.com); Wang, Qianlong(153326100@qq.com)

Source title: SSRN
Issue date: May 24, 2023
Publication year: 2023
Language: English
ISSN: 15565068
Document type: Preprint (PP)
Publisher: SSRN

Abstract: More extensive attention has been directed toward amphiphilic nanomaterials in the field of chemical enhanced oil recovery owing to they have the same excellent properties as surfactants. In this work, an amphiphilic nano calcium carbonate(ANCC) was prepared by chemical one-pot synthesis. ANCC had a lipophilic property, which can make the oil and water were completely emulsified at the concentration of 500ppm to form W/O emulsion with a particle size of 0.2~2.6μm. ANCC had best dispersion effect at the solution of 0.1% Tween80. In the oil-water phase, ANCC can be adsorbed on the oil-water interface to reduce interface tension, and increase interface strength, and improve emulsion stability. The lipophilic slide can be changed from lipophilic to hydrophilic when immersed in the nanofluid. Using TW-ANCC (0.1% of Tween80+500ppm of ANCC) as the oil displacement fluid, water flooding, TW-

ANCC improved oil recovery by 23.3% in the single core displacement experiment and by 36.9% in the flat panel visualization experiment with comparing primary water flooding. The oil displacement mechanism of TW-ANCC was obtained by the etched glass micromodel experiment and the nuclear magnetic resonance experiment, the result shown that TW-ANCC can enhance oil recovery by reducing interface tension, changing rock wettability, reducing flow in high permeability zone, and expanding sweep volume in low permeability zone. © 2023, The Authors. All rights reserved.

Number of references: 52
Main heading: Wetting
Controlled terms: Calcium carbonate - Emulsification - Enhanced recovery - Floods - Low permeability reservoirs - Oil well flooding - Particle size - Petroleum reservoir engineering - Phase interfaces - Reservoirs (water)
Uncontrolled terms: Amphiphilic nano calcium carbonate - Amphiphilics - Displacement mechanisms - Enhance oil recoveries - Floodings - Interface displacements - Interface property - Interface strength - Nano calcium carbonate - Tween 80
Classification code: 441.2 Reservoirs - 511.1 Oil Field Production Operations - 512.1 Petroleum Deposits - 512.1.2 Petroleum Deposits : Development Operations - 801.4 Physical Chemistry - 802.3 Chemical Operations - 804 Chemical Products Generally
Numerical data indexing: Percentage 1.00E-01%, Percentage 2.33E+01%, Percentage 3.69E+01%, Size 2.00E-07m to 2.60E-06m
DOI: 10.2139/ssrn.4458317
Compendex references: YES
Preprint ID: 4458317
Preprint source website: https://papers.ssrn.com/sol3/papers.cfm
Preprint ID type: SSRN
Database: Compendex
Data Provider: Engineering Village
Compilation and indexing terms, Copyright 2023 Elsevier Inc.

15. Hydraulic fracture network propagation in a naturally fractured shale reservoir based on the "well factory" model

Accession number: 20224413052031
Authors: Zhang, Haoyu (1); Chen, Junbin (1); Zhao, Zhengyan (2); Qiang, Jianli (3)
Author affiliation: (1) College of Petroleum Engineering, Xi'an Shiyou University, Shaanxi, Xi'an; 710065, China; (2) Changqing Oilfield Oil & Gas Technology Research Institute, PetroChina, Shaanxi, Xi'an; 710018, China; (3) Exploration and Development Research Institute of Tarim Oilfield Company, PetroChina, Xinjiang, Korla; 841000, China
Corresponding author: Zhang, Haoyu(20111010006@stumail.xsyu.edu.cn)
Source title: Computers and Geotechnics
Abbreviated source title: Comput. Geotech.
Volume: 153
Issue date: January 2023
Publication year: 2023
Article number: 105103
Language: English
ISSN: 0266352X
E-ISSN: 18737633
CODEN: CGEOEU
Document type: Journal article (JA)
Publisher: Elsevier Ltd
Abstract: In different geological and engineering conditions, it is important to study the stress interference of multiple fractures and interaction of natural fractures in "well factory" fracturing to improve the complexity of fracture networks. For this purpose, a 2D, coupled stress-seepage-damage field cohesive model with random propagation of hydraulic fracture was developed, and a random function was used to simulate the natural fractures distribution in a real reservoir. Orthogonal test was designed to investigate the geological and engineering parameters impacting the evolution of zipper fracturing and modified zipper fracture networks. The results show that in naturally fractured reservoirs, hydraulic fracture can open natural fractures and promote the formation of complex fracture networks by combined, induced manner. Higher stress differences lead to simpler fracture networks and straighter hydraulic fracture propagation paths; When pre-existing natural fracture is longer, the propagation direction of hydraulic fracture is more likely to be paralleled with natural fracture; However, the stress shadow effect of multiple fractures may potentially lead to failure of some hydraulic fracture initiation. In addition, the fracture initiation sequence of multiple

fractures has a significant effect on the evolution of the fracture networks. The results of the study have important significance for parameter optimization of well factory fracturing in naturally fractured reservoirs. © 2022 Elsevier Ltd

Number of references: 43
Main heading: Fracture
Controlled terms: Complex networks - Geology - Hydraulic fracturing
Uncontrolled terms: Condition - Fracture initiation - Fracture network - Hydraulic fracture network - Multiple fracture - Multiple interactions - Natural fracture - Naturally fractured reservoirs - Naturally fractured shales - Well factory
Classification code: 481.1 Geology - 512.1.2 Petroleum Deposits : Development Operations - 722 Computer Systems and Equipment - 951 Materials Science
DOI: 10.1016/j.compgeo.2022.105103

Compendex references: YES
Database: Compendex
Data Provider: Engineering Village

16. Method of Wear Evaluation on Sliding Supports in Expansion Joints Based on Theories of Mechanism Motion and Wear

Accession number: 20232314193921
Title of translation:

Authors: Li, Guang-Ling (1); Su, Quan-Ke (2, 3); Han, Wan-Shui (2); Xu, Xin (2)
Author affiliation: (1) College of Civil Engineering, Xi'An Shiyou University, Shaanxi, Xi'an; 710065, China; (2) School of Highway, Chang'An University, Shaanxi, Xi'an; 710064, China; (3) Center for Technology Leadership, The Hong Kong University of Science and Technology (Guangzhou), Guangdong, Guangzhou; 511453, China
Corresponding author: Li, Guang-Ling(ligl0127@163.com)

Abstract: To evaluate the service state of the large-displacement swivel joist expansion joints under the action of traffic flow and wind loads during the operation period, the wear life evaluation method of the expansion joints component was established based on the combination of mechanism motion and wear theory of the mechanism. Based on the motion theory of variable length double rocker and slider four-bar linkage, the kinematics model of multi rocker and slider expansion joints mechanism was established. The wear depth calculation model of sliding supports in expansion joints was proposed based on Archard wear theory, and the evaluation method of wear life of sliding supports in expansion joints was established with index of failure probability. Taking a single span suspension bridge as an example, the service life and annual replacement times of sliding supports in expansion joints were quantitatively evaluated. The results indicated that movement simulation model of expansion joints has been established. By comparing with the motion test data of the 8-joints expansion mechanism, the accuracy of the simulation model was verified. The cumulative distributed probability characteristics of the wear depth of sliding supports in expansion joints could be simulated by using the gamma distribution. Under the action of random traffic flow and wind loads, the service life of the expansion joints sliding support of suspension bridge decreased with the closer to the sliding side, and the failure probability was on the contrary. The service life of more than 82% sliding supports was less than 15 years under the general flow and wind speed conditions of 10 m · s-1. The combined action of different traffic densities and wind speeds had a great influence on the service life of sliding supports in expansion joints, and it is suggested that a reasonable replacement period for sliding supports in expansion joints should be formulated according to the traffic

load level and wind field condition. The established wear life evaluation method of rotary shaft expansion joints could provide reference for the wear life evaluation of the same type expansion joints mechanism. © 2023 Xi'an Highway University. All rights reserved.

Number of references: 31
Main heading: Wind stress
Controlled terms: Aerodynamic loads - Failure (mechanical) - Probability distributions - Service life - Suspension bridges - Suspensions (components)
Uncontrolled terms: Bridge engineering - Evaluation methods - Failure Probability - Life evaluation - Mechanism motion simulation - Mechanism motions - Motion simulations - Sliding support - Wear evaluation - Wear-life
Classification code: 401.1 Bridges - 443.1 Atmospheric Properties - 601.2 Machine Components - 651.1 Aerodynamics, General - 922.1 Probability Theory
Numerical data indexing: Age 1.50E+01yr, Percentage 8.20E+01%, Velocity 1.00E+01m/s
DOI: 10.19721/j.cnki.1001-7372.2023.02.014
Funding Details: Number: 300102212521, Acronym: CHD, Sponsor: Chang'an University; Number: 2019YFB1600702, Acronym: NKRDPC, Sponsor: National Key Research and Development Program of China; Number: -, Acronym: -, Sponsor: Fundamental Research Funds for the Central Universities; Number: 2022JQ-467, Acronym: -, Sponsor: Natural Science Basic Research Program of Shaanxi Province;
Funding text: National Key R & D Program of China (2019YFB1600702) ; Natural Science Basic Research Program of Shaanxi (2022JQ-467) ; Fundamental Research Funds for the Central Universities, CHD (300102212521)
Compendex references: YES
Database: Compendex
Data Provider: Engineering Village
Compilation and indexing terms, Copyright 2023 Elsevier Inc.

17. Ultrasensitive temperature sensor based on optic fiber Fabry–Pérot interferometer with Vernier effect

Accession number: 20232014101325
Authors: Liu, Qinpeng (1, 3); Wang, Danyang (1); Wang, Chunfang (2); Gao, Hong (4); Cheng, Feng (3)
Author affiliation: (1) Xi'an Shiyou University, Key Laboratory of Measurement and Control Technology for Oil and Gas Wells, Xi'an; 710065, China; (2) AVIC Jonhon Optronic Technology Co., Ltd., China; (3) CNPC Logging Co., LTD, Xi'an; 710076, China; (4) School of Physics, Northwest University, Xi'an; 710065, China
Corresponding author: Wang, Danyang(danyangwang006@163.com)
Source title: Optics Communications
Abbreviated source title: Opt Commun
Volume: 541
Issue date: August 15, 2023
Publication year: 2023
Article number: 129567
Language: English
ISSN: 00304018
CODEN: OPCOB8
Document type: Journal article (JA)
Publisher: Elsevier B.V.

Abstract: An ultrahigh sensitivity optic fiber temperature sensor with cascaded two Fabry–Pérot interferometers (FPIs) based on the Vernier effect has been fabricated and experimentally demonstrated. One polymer-cavity FPI is used as a sensing FPI and another fiber-cavity is used as a reference FPI to generate the Vernier effect. The experimental results show that the fabricated FPIs sensor has the high temperature sensitivity of -83.130 nm/°C and a high linear response (R-square: 0.9976), which is almost ~ 39 times higher than that of an individual polymer-cavity FPI sensor (~ 2.080 nm/°C). The stability experiment is also carried out, and the maximal variation of the wavelength shift of the interference fringes is 2.005 nm for a long-term testing. With its advantages of easy fabrication, low cost and small volume, the proposed sensor has significant benefits in terms of various practical applications that need high precision temperature measurement. © 2023 Elsevier B.V.

Number of references: 31
Main heading: Temperature sensors
Controlled terms: Fibers - Interferometers - Temperature measurement
Uncontrolled terms: Fabry-Perot interferometer sensors - Fiber fabry-perot interferometers - Fiber temperature sensors - Optic-fiber - Optic-fiber sensors - Polymer cavity - Ultra-high-sensitivity - Ultrasensitive - Ultrasensitive temperature sensor - Vernier effect

Classification code: 941.3 Optical Instruments - 944.5 Temperature Measuring Instruments - 944.6 Temperature Measurements
Numerical data indexing: Size 2.005E-09m, Size 2.08E-09m, Size 8.313E-08m
DOI: 10.1016/j.optcom.2023.129567

Compendex references: YES
Database: Compendex
Data Provider: Engineering Village

18. Preparation of Ce/ferroferric oxide/food waste-derived biochar for aqueous Cr(VI) adsorption (*Open Access*)

Accession number: 20224012842809

Authors: Tie, Jingxi (1); Zhang, Meng (1); Shen, Chenliang (2); Liu, Haiyuan (2); Du, Chunbao (3)
Author affiliation: (1) School of Environmental and Municipal Engineering, North China University of Water Resources and Electric Power, Zhengzhou, China; (2) Technology Research and Development Center, Zhongzhou Water Holding Co., Ltd., Zhengzhou, China; (3) College of Chemistry and Chemical Engineering, Xi'an Shiyou University, Xi'an, China
Corresponding author: Du, Chunbao(duchunbao218@126.com)

Source title: Journal of Chemical Technology and Biotechnology
Abbreviated source title: J. Chem. Technol. Biotechnol.
Volume: 98
Issue: 1
Issue date: January 2023
Publication year: 2023
Pages: 168-178
Language: English
ISSN: 02682575
E-ISSN: 10974660
CODEN: JCTBDC
Document type: Journal article (JA)
Publisher: John Wiley and Sons Ltd

Abstract: BACKGROUND: Cr(VI) in aqueous solution is a serious concern that can harm human health by accumulating in the food chain. Meanwhile, the most common form of food waste (FW) disposal by landfill takes up a lot of area and pollutes the environment. As a consequence, FW was employed as a raw material in the production of food waste-derived biochar (FWB), which was then modified to produce a $Ce/Fe_3O_4/FWB$ composite for high-efficiency Cr(VI) removal. RESULTS: The structure, morphology, and properties of the $Ce/Fe_3O_4/FWB$ composite were thoroughly investigated, as well as its Cr(VI) adsorption ability. The composite exhibited the highest Cr(VI) adsorption of 20.4 mg/g at pH 2. Furthermore, the adsorption fitted the pseudo-second-order kinetic model and the Langmuir model, with intra-particle diffusion acting as the rate-controlling step. The thermodynamic investigation demonstrated that Cr (VI) adsorption by $Ce/Fe_3O_4/FWB$ was a spontaneous endothermic process. With increasing concentrations of Cl^-, SO_4^{2-} and PO_4^{3-}, the Cr(VI) adsorption was weakened in the sequence of Cl^-, SO_4^{2-} and PO_4^{3-}. CONCLUSION: Adsorbent preparation utilizing FW as raw material is a sustainable and environmentally beneficial method for FW reclaimation and Cr(VI)-bearing wastewater treatment. © 2022 Society of Chemical Industry (SCI). © 2022 Society of Chemical Industry (SCI).

Number of references: 71
Main heading: Adsorption
Controlled terms: Cerium oxide - Chemical industry - Chromium compounds - Wastewater disposal - Wastewater treatment
Uncontrolled terms: Adsorption ability - Biochar - Ferroferric oxides - Food chain - Food waste - Hexavalent chromium - Higher efficiency - Human health - Property - Pseudo-second-order kinetic models
Classification code: 452.4 Industrial Wastes Treatment and Disposal - 802.3 Chemical Operations - 804.2 Inorganic Compounds - 805 Chemical Engineering, General

19. Tribological properties of NiMo matrix composite containing in-situ formed Sr2NiMoO6and SrO at elevated temperatures   (*Open Access*)

Authors: Liu, Feng (1); Ren, Jingshu (1); Zhao, Wenwen (1); Li, Guang (1); Jia, Junhong (2)
Author affiliation: (1) Xi'An Key Laboratory of High Performance Oil and Gas Field Materials, School of Materials Science and Engineering, Xi'An Shiyou University, Xi'an; 710065, China; (2) College of Mechanical and Electrical Engineering, Shaanxi University of Science and Technology, Xi'an; 710021, China
Corresponding author: Liu, Feng(fliu@xsyu.edu.cn)

Abstract: NiMo alloy and NiMo-5SrSO4 composite were fabricated to reveal the effect mechanism of Sr2NiMoO6 and SrO derived from the decomposition characteristics of SrSO4 in vacuum on the microstructure, density, microhardness, and tribological properties against Al2O3 ball at different temperatures. The formation of Sr2NiMoO6 and SrO led to a negligible increase in the density and microhardness of the sintered composite. Below 400 °C, compared to NiMo alloy, the poor tribological properties were observed in NiMo-5SrSO4 composite, which was responsible for the appearance of Sr2NiMoO6 and SrO on the worn surface. However, with the further increase in the temperature, the friction coefficient and wear rate of NiMo-5SrSO4 composite reached as low around 0.26 and 1.32 × 10-5 mm3/Nm at 800 °C respectively, which was attributed to the synergistic lubricating effect of SrMoO4 generated from the tribochemical reaction between SrO and MoO3, Sr2NiMoO6, and oxides (MoO3, NiO, and NiMoO4) on the rubbing surface. © 2022 The Author(s).

Number of references: 48
Main heading: Aluminum oxide
Controlled terms: Alumina - Binary alloys - Friction - Microhardness - Molybdenum alloys - Molybdenum oxide - Nickel oxide - Strontium compounds - Tribology - Wear of materials
Uncontrolled terms: Decomposition characteristics - Effect mechanism - Elevated temperature - In-vacuum - Matrix composite - Microstructures properties - Ni-Mo alloys - Tribochemical reaction - Tribological properties - Wear mechanisms
Classification code: 543.3 Molybdenum and Alloys - 804 Chemical Products Generally - 804.2 Inorganic Compounds - 931 Classical Physics; Quantum Theory; Relativity - 931.2 Physical Properties of Gases, Liquids and Solids - 951 Materials Science
Numerical data indexing: Temperature 1.073E+03K, Temperature 6.73E+02K, Volume 1.32E-14m3, Volume 2.60E-10m3
DOI: 10.1016/j.jmrt.2022.12.111

20. Research of a novel fracturing-production integral fluid based on cationic surfactant

Authors: Yan, Jiao (1, 2); Li, Yongfei (1, 3); Xie, Xuan (4); Slaný, Michal (5, 6); Dong, Sanbao (1); Wu, Yuanpeng (2); Chen, Gang (1, 3)
Author affiliation: (1) State Key Laboratory of Petroleum Pollution Control, Xi'an Shiyou University, Xi'an; 710065, China; (2) State Key Laboratory of Oil and Gas Reservoir Geology and Exploitation, Southwest Petroleum University, Chengdu; 610500, China; (3) Shaanxi Province Key Laboratory of Environmental Pollution Control and Reservoir Protection Technology of Oilfields, Xi'an Shiyou University, Xi'an; 710065, China; (4) Xi'an Changqing Chemical Group Co. Ltd, Xi'an Shaanxi, China; (5) Institute of Inorganic Chemistry, Slovak Academy of Sciences, Dúbravská cesta 9, Bratislava; 845 36, Slovakia; (6) Institute of Construction and Architecture, Slovak Academy of Sciences, Dúbravská cesta 9, Bratislava; 845 03, Slovakia
Corresponding author: Wu, Yuanpeng

Abstract: Fracturing plays an extremely important role in increasing oil and gas production, however, the fracturing flowback fluid has problems such as large volume, difficult treatment, high processing cost, and environmental pollution. In order to expand the application range and reuse of clean fracturing fluid, a fracturing-production integral fluid based on small molecule surfactants, cetyl trimethyl ammonium chloride (CTAC), salicylic acid (SA) and oleic acid amide methyl hydroxypropyl ammonium chloride (OAMDC) is proposed. At 90 °C the resistance of the fracturing-production integral fluid reached values up to 63.5 mPa·s. The surface and interface tension of the fracturing-production integral fluid broken by crude oil were 28.5 and 8.19 × 10-3 mN/m, respectively. It shows good oil flooding ability (up to 16.35 %), static oil washing rate (up to 21.5 %) and outstanding emulsification effect. Meanwhile, the application scope clean fracturing flowback fluid will be expanded to achieve its efficient and comprehensive application in the field of oilfield chemistry, thereby improving the benefits of oilfield development. © 2022 Elsevier B.V.

Number of references: 45
Main heading: Cationic surfactants
Controlled terms: Amides - Chlorine compounds - Dyes - Emulsification - Floods - Oil well flooding - Washing
Uncontrolled terms: Comprehensive utilizations - Environmental pollutions - Fracturing flowback - Fracturing-production integral fluid - Large volumes - Oil and gas production - Oil flooding - Oil flooding ability - Processing costs - Static oil washing
Classification code: 511.1 Oil Field Production Operations - 802.3 Chemical Operations - 803 Chemical Agents and Basic Industrial Chemicals - 804.1 Organic Compounds
Numerical data indexing: Percentage 1.635E+01%, Percentage 2.15E+01%, Pressure 6.35E-05Pa, Surface tension 2.85E-02N/m, Surface tension 8.19E-06N/m, Temperature 3.63E+02K
DOI: 10.1016/j.molliq.2022.120858

Compendex references: YES

21. Experimental and computational investigations on foaming properties of anionic-nonionic-zwitterionic surfactants and amino acid compounds to address the liquid loading of natural gas wells

Authors: Dong, Sanbao (1); Fan, Jiabao (1); Liu, Chenwei (2); Yan, Yongli (1); Han, Weiwei (1)
Author affiliation: (1) College of Chemistry and Chemical Engineering, Xi'an Shiyou University, No. 18, East Dianzi 2nd Road, Shaanxi, Xi'an; 710065, China; (2) College of Petroleum Engineering, China University of Petroleum (East China), No. 66 Changjiang Road, Huangdao District, Shandong, Qingdao; 266580, China
Corresponding author: Han, Weiwei(hanweiwei@xsyu.edu.cn)

Abstract: Liquid buildup in gas wells would undoubtedly obstruct the gas production. The use of foaming surfactants to generate foams and remove the loaded liquid is very common. Due to the undesirable conditions (e.g., high condensate cut (ratio of condensate oil volume to total liquid volume) and high salinity, etc.) that often encountered in the wells, different foaming surfactants were often compounded together to unload liquid in gas wells. In this paper, lauramide propyl dimethylamine (C12 Amine), palmitamide propyl dimethylamine (C16 Amine) and cocamidopropyl betaine (CAPB) were synthesized and compounded with L-aspartic acid (Asp) and N-lauroylsarcosine sodium (LSS) to form foaming supramolecular complexes through optimization (with Waring blender method and liquid unloading tests) to quantify their application potentials in foam-based deliquification treatment for gas wells. The C12 Amine-Asp-LSS-CAPB complex (in an optimized mole ratio of 10:4:14:7) exhibited superior condensate tolerance than the C16 Amine-Asp-LSS-CAPB complex (in an optimized mole ratio of 10:4:14:42). The salinity posed a significant influence on the liquid unloading performance (k) and foaming efficiency (, defined as the ratio of the foam mass to the initial liquid mass) of the C12 Amine-Asp-LSS-CAPB complex, however, the nitrilotriacetic acid trisodium (NTA) can greatly enhance the properties of the C12 Amine-Asp-LSS-CAPB complex against the salinity (up to 6×10^4 mg/L). The temperature (25 °C -90 °C) favored the performances (as indicated by k and) of the C12 Amine-Asp-LSS-CAPB complex, which achieved k and values of 85.0% and 100% at 90 °C, respectively. Meanwhile, the synergy observed in the foaming ability, foam stability and liquid unloading performance tests using the C12 Amine-Asp-LSS-CAPB mixture was also proved by the surface tension analysis and the calculations of the supramolecular interactions (interaction energies and electrostatic interactions). © 2023 Elsevier B.V.

Main heading: Efficiency
Controlled terms: Amines - Amino acids - Anionic surfactants - Blending - Gases - Natural gas well production - Natural gas wells - Nonionic surfactants - Phase equilibria - Supramolecular chemistry - Synthesis (chemical) - Unloading
Uncontrolled terms: Cocamidopropyl betaine - Dimethylamines - Foaming efficiency - Foaming surfactant - Gas well - Gas well deliquifying - Liquid unloading - Liquid unloading efficiency - Supramolecular interactions - Synergistic effect
Classification code: 512.2.1 Natural Gas Fields - 691.2 Materials Handling Methods - 801.4 Physical Chemistry - 802.2 Chemical Reactions - 802.3 Chemical Operations - 803 Chemical Agents and Basic Industrial Chemicals - 804.1 Organic Compounds - 913.1 Production Engineering
Numerical data indexing: Mass density 4.00E-03kg/m3, Percentage 1.00E+02%, Percentage 8.50E+01%, Temperature 2.98E+02K, Temperature 3.63E+02K

Compendex references: YES
Database: Compendex
Data Provider: Engineering Village

22. Pilot test of polymer microsphere alternate surfactant flood (PMAS) with mixtures of anionic-cationic surfactants under harsh conditions in a sandstone reservoir

Accession number: 20230913644804
Authors: Li, Yingcheng (1); Jin, Jun (1); Su, Zhiqing (1); Zhang, Weidong (1); Bao, Xinning (1); Niu, Baolun (2); Yang, Changhua (3); Wu, Xinyue (1); Zhai, Xiaodong (1); Zhang, Li (1); Guo, Rong (1); Meng, Yong (1); He, Xiujuan (1); Shen, Zhiqin (1); Zhang, Hui (1); Sha, Ou (1)
Author affiliation: (1) Sinopec Shanghai Research Institute of Petrochemical Technology, Shanghai, China; (2) Sinopec Zhongyuan Oil Field Company, Puyang, China; (3) Xi'an Petroleum University, Xi'an, China
Corresponding author: Li, Yingcheng(liyc.sshy@sinopec.com)
Source title: Petroleum Research
Abbreviated source title: Pet. Res.
Issue date: 2023
Publication year: 2023
Language: English
ISSN: 20962495
E-ISSN: 25241729
Document type: Article in Press
Publisher: KeAi Publishing Communications Ltd.
Abstract: The first pilot test of polyacrylamide microsphere alternate surfactant flood (PMAS) with mixtures of anionic-cationic surfactants (Sa/c) was carried out for a high-temperature, high-salinity, and high-hardness sandstone reservoir to demonstrate the potential of this novel technique to improve oil recovery. A critical micelle concentration (CMC) of 4.82 mg/L, an ultralow interfacial tension (IFT) of 8 × 10-4 mN/m, and a high oil solubilization of 22 were obtained. Static and dynamic adsorptions of Sa/c on natural core containing 15 wt% clay were reduced to about 2.20 and 0.30 mg/g-core, respectively, with the addition of adsorption inhibitor (AI). Since June 2014, the pilot test of PMAS was carried out in a Sinopec reservoir with a temperature of 87 °C, a salinity of 260,393 mg/L, and a hardness of 6,401 mg/ L. Twelve cycles of alternative injection of 0.0125 PV Sa/c with a concentration of 0.1% and 0.0125 PV polyacrylamide microsphere with a concentration of 0.2% were conducted at an injection rate of 0.1 PV/yr, for a total of 0.3 PV chemical injection. As a result, the net daily oil production increased from 0 t to 6.5 t, and the water cut decreased from 96.3% to 93.8%, leading to an ultimate improved oil recovery of 6.3% original oil-in-place. © 2023 Chinese Petroleum Society
Number of references: 26
Main heading: Anionic surfactants
Controlled terms: Cationic surfactants - Critical micelle concentration - Dyes - Floods - Hardness - Micelles - Microspheres - Oil well flooding - Reservoirs (water) - Sandstone
Uncontrolled terms: Condition - High hardness - High salinity - Highest temperature - Mixture of anionic and cationic surfactant - Pilot tests - Polyacrylamide microsphere - Polymer microspheres - Sandstones reservoirs - Surfactant floods
Classification code: 441.2 Reservoirs - 482.2 Minerals - 511.1 Oil Field Production Operations - 801.3 Colloid Chemistry - 803 Chemical Agents and Basic Industrial Chemicals - 804.1 Organic Compounds - 951 Materials Science
Numerical data indexing: Mass density 2.60393E+02kg/m3, Mass density 4.82E-03kg/m3, Mass density 6.401E +00kg/m3, Percentage 1.00E-01%, Percentage 2.00E-01%, Percentage 6.30E+00%, Percentage 9.63E+01% to 9.38E +01%, Surface tension 8.00E-07N/m, Temperature 3.60E+02K, Voltage 1.00E-13V, Voltage 1.25E-14V, Voltage 3.00E-13V, null 2.20E+00null, null 3.00E-01null
DOI: 10.1016/j.ptlrs.2023.01.001
Compendex references: YES
Database: Compendex
Data Provider: Engineering Village

23. A Generalized Modularity for Computing Community Structure in Fully Signed Networks (*Open Access*)

Authors: He, Xiaochen (1); Zhang, Ruochen (2); Zhu, Bin (3)
Author affiliation: (1) School of Public Policy and Administration, Xi'An Jiaotong University, Shaanxi, Xi'an; 710049, China; (2) School of Economics and Management, Xi'An Shiyou University, Shaanxi, Xi'an; 710065, China; (3) School of Public Health and Emergency Management, Southern University of Science and Technology, Guangdong, Shenzhen; 518055, China
Corresponding author: Zhu, Bin(zhub6@sustech.edu.cn)
Abstract: The community structure in fully signed networks that considers both node attributes and edge signs is important in computational social science; however, its physical description still requires further exploration, and the corresponding measurement remains lacking. In this paper, we present a generalized framework of community structure in fully signed networks, based on which a variant of modularity is designed. An optimization algorithm that maximizes modularity to detect potential communities is also proposed. Experiments show that the proposed method can efficiently optimize the objective function and perform effective community detection. © 2023 Xiaochen He et al.
Number of references: 70
Uncontrolled terms: Community IS - Community structures - Computational social science - Computing community - Generalized modularity - Network-based - Node attribute - Objective functions - Optimization algorithms - Signed networks
DOI: 10.1155/2023/8767131
Compendex references: YES
Open Access type(s): All Open Access, Gold
Database: Compendex
Data Provider: Engineering Village

24. Evaluation of viscosity reduction effect of oil-soluble viscosity reducer on crude oil (*Open Access*)

Authors: Lei, Haoran (1); Huang, Chen (2); Liu, Jiangbo (3); Dou, Miao (2); Gu, Xuefan (4)
Author affiliation: (1) Oil Production No.11, Changqing Oilfield Company, Xi'an; 710068, China; (2) Oil and Gas Technology Research Institute Changqing Oilfield Company, Xi'an; 710068, China; (3) Xi'An Changqing Chemical Group Co., Ltd, Xi'an; 710068, China; (4) Shaanxi University Engineering Research Center of Oil and Gas Field Chemistry, Xi'An Shiyou University, Xi'an; 710065, China
Corresponding author: Lei, Haoran(1078125919@qq.com)

E-ISSN: 17426596
Document type: Conference article (CA)
Conference name: 5th International Symposium on Hydrogen Energy and Energy Technologies, HEET 2022
Conference date: November 18, 2022 - November 19, 2022
Conference location: Osaka, Virtual, Japan
Conference code: 187331
Publisher: Institute of Physics
Abstract: In this paper, several crude oil viscosity reducers were selected to evaluate their performance on the heavy oil Henan Oilfield, China. Through investigation, the viscosity reducing ability of these viscosity reducers were relatively general. Among them, EVA had the highest performance, reaching a viscosity reduction rate of 45.6%. The results were characterized by DSC analysis, wax crystal micromorphology analysis of saturated hydrocarbons and IR spectroscopy. Finally, possible viscosity reduction mechanism was discussed. © Published under licence by IOP Publishing Ltd.
Number of references: 10
Main heading: Crude oil
Controlled terms: Heavy oil production - Viscosity
Uncontrolled terms: Crude oil viscosity - Micromorphologies - Oil soluble - Performance - Reduction effects - Reduction rate - Saturated hydrocarbons - Viscosity reducer - Viscosity reduction - Wax crystals
Classification code: 511.1 Oil Field Production Operations - 512.1 Petroleum Deposits - 631.1 Fluid Flow, General - 931.2 Physical Properties of Gases, Liquids and Solids
Numerical data indexing: Percentage 4.56E+01%
DOI: 10.1088/1742-6596/2454/1/012018
Compendex references: YES
Open Access type(s): All Open Access, Gold
Database: Compendex
Data Provider: Engineering Village

25. Generation of the switchable dual-state solitons and the octave-spanning supercontinuum in a single-mode Er-doped fibre laser system

Accession number: 20225113271022
Authors: Lin, Qimeng (1); Gang, Tingting (1); Zhang, Chun (1); Lu, Baole (2, 3); Hou, Lei (2, 3); Bai, Jintao (2, 3)
Author affiliation: (1) School of Science, Xi'an Shiyou University, Xi'an; 710065, China; (2) State Key Laboratory of Energy Photon-Technology in Western China, Shaanxi Engineering Technology Research Center for Solid State Lasers and Application, Northwest University, Xi'an; 710069, China; (3) Institute of Photonics & Photon-technology, Northwest University, Xi'an; 710069, China
Corresponding author: Hou, Lei(lhou@ustc.edu.cn)
Source title: Infrared Physics and Technology
Abbreviated source title: Infrared Phys Technol
Volume: 128
Issue date: January 2023
Publication year: 2023
Article number: 104512
Language: English
ISSN: 13504495
CODEN: IPTEEY
Document type: Journal article (JA)
Publisher: Elsevier B.V.
Abstract: We experimentally demonstrate the generation of the switchable dual-state solitons in a compact ultrashort pulse Er-doped fibre laser. The octave-spanning supercontinuum is obtained in an Er-doped fibre amplifier seeded by the self-similar soliton. The mode-locked oscillator produces 205.5 fs dispersion-managed soliton at 1556.6 nm and 115.6 fs self-similar soliton at 1558 nm. The switchable generation of dual-state solitons is only needed to adjust the pump power and the polarization state. The amplifier generates a 147.2 fs ultrashort pulse with a spectral bandwidth of more than 650 nm after compressing the pulse duration. The maximum output power of the laser system is 195 mW. Our experimental results provide a possibility of achieving supercontinuum generation based on the switchable dual-state solitons ultrashort pulse in a standard single-mode fibre-format energetic ultrashort laser system. © 2022 Elsevier B.V.
Number of references: 42
Main heading: Solitons

Controlled terms: Fiber lasers - Single mode fibers - Supercontinuum generation - Ultrashort pulses
Uncontrolled terms: Dual state soliton - Er-doped fiber amplifier - Er-doped fiber laser - Laser systems - Octave-spanning supercontinuum - Self-similar - Single mode - Super continuum - Switchable - Ultrashort-pulse
Classification code: 741.1.1 Nonlinear Optics - 741.1.2 Fiber Optics - 744.4 Solid State Lasers
Numerical data indexing: Power 1.95E-01W, Size 1.5566E-06m, Size 1.558E-06m, Size 6.50E-07m, Time 1.156E-13s, Time 1.472E-13s, Time 2.055E-13s
DOI: 10.1016/j.infrared.2022.104512

Compendex references: YES
Database: Compendex
Data Provider: Engineering Village

26. Leakage and diffusion behavior of a buried pipeline of hydrogen-blended natural gas

Accession number: 20224613129856
Authors: Zhu, Jianlu (1); Pan, Jun (1); Zhang, Yixiang (1, 4); Li, Yuxing (1); Li, He (2); Feng, Hui (2); Chen, Dongsheng (3); Kou, Yimin (3); Yang, Rui (3)
Author affiliation: (1) College of Pipeline and Civil Engineering, China University of Petroleum (East China), Qingdao; 266580, China; (2) Petroleum Pipeline Engineering Technology Research Institute, CNPC, Xi 'an; 710000, China; (3) Shaanxi Provincial Natural Gas Co. Ltd, Xi 'an; 710000, China; (4) College of Petroleum Engineering, Xi'an Shiyou University, Xi'an; 710065, China
Corresponding author: Zhu, Jianlu(upczjl@upc.edu.cn)
Source title: International Journal of Hydrogen Energy
Abbreviated source title: Int J Hydrogen Energy
Volume: 48
Issue: 30
Issue title: ProfSpecial issue on the 4th International Symposium on Hydrogen Energy and Energy Technologies (HEET 2021)
Issue date: April 8, 2023
Publication year: 2023
Pages: 11592-11610
Language: English
ISSN: 03603199
CODEN: IJHEDX
Document type: Journal article (JA)
Publisher: Elsevier Ltd

Abstract: Buried pipelines are one method of conservation transfer for widely used gases such as natural gas and hydrogen. The safety of these pipelines is of great importance because of the potential leakage risks posed by the flammable gas and the special properties of the hydrogen mixture. Estimating the leakage behavior and quantifying the diffusion range outside the pipeline are important but challenging goals due to the hydrogen mixture and presence of soil. This study provides essential information about the diffusion behavior and concentration distribution of underground hydrogen and natural gas mixture leakages. Therefore, a large-scale experimental system was developed to simulate high-pressure leaks of hydrogen mixture natural gas from small holes in three different directions from a pipeline buried in soil. The diffusion of hydrogen-doped natural gas in soil was experimentally measured under different conditions, such as different hydrogen mixture ratios, release pressures, and leakage directions. The experimental results verified the applicability of the gas leakage mass flow model, with an error of 6.85%. When a larger proportion of a single component was present in the hydrogen-doped natural gas, the leakage pressure showed a greater diffusion range. In addition, the diffusion range of hydrogen-doped natural gas in the leakage direction was larger at 3 o'clock than that at 12 o'clock. The hydrogen blend carried methane and diffused, which shortened the methane saturation time. Moreover, a quantitative relationship between the concentration of hydrogen-doped natural gas and the diffusion distance over which the hydrogen-doped natural gas reached the lower limit of the explosion was obtained by quantitative analysis of the experimental data. © 2022 Hydrogen Energy Publications LLC
Number of references: 28
Main heading: Hydrogen
Controlled terms: Clocks - Diffusion - Gases - Methane - Natural gas - Natural gas pipelines - Soils

Uncontrolled terms: Buried pipelines - Concentration distributions - Diffusion behavior - Diffusion concentrations - Diffusion range - Flammable gas - Leakage and diffusion - Leakage behaviors - Natural gas mixture - Special properties

Classification code: 483.1 Soils and Soil Mechanics - 522 Gas Fuels - 619.1 Pipe, Piping and Pipelines - 804 Chemical Products Generally - 804.1 Organic Compounds - 943.3 Special Purpose Instruments

Numerical data indexing: Percentage 6.85E+00%

DOI: 10.1016/j.ijhydene.2022.10.185

Funding Details: Number: 2021YFB4001603, Acronym: NKRDPC, Sponsor: National Key Research and Development Program of China;

Funding text: This paper is funded by the National Key R&D Program of China (2021YFB4001603).

Compendex references: YES

Database: Compendex

Data Provider: Engineering Village

Compilation and indexing terms, Copyright 2023 Elsevier Inc.

27. Quantitative analysis of polycyclic aromatic hydrocarbons (PAHs) in water by surface-enhanced Raman spectroscopy (SERS) combined with Random Forest

Accession number: 20225013246864

Authors: Guo, Mengjun (1); Li, Maogang (1); Fu, Han (1); Zhang, Yi (3); Chen, Tingting (1); Tang, Hongsheng (1); Zhang, Tianlong (1); Li, Hua (1, 2)

Author affiliation: (1) Key Laboratory of Synthetic and Natural Functional Molecule of the Ministry of Education, College of Chemistry & Materials Science, Northwest University, Xi'an; 710127, China; (2) College of Chemistry and Chemical Engineering, Xi'an Shiyou University, Xi'an; 710065, China; (3) Xi'an Wanlong Pharmaceutical Co., Ltd., Xi'an; 710119, China

Corresponding author: Zhang, Tianlong(tlzhang@nwu.edu.cn)

Source title: Spectrochimica Acta - Part A: Molecular and Biomolecular Spectroscopy

Abbreviated source title: Spectrochim. Acta Part A Mol. Biomol. Spectrosc.

Volume: 287

Issue date: February 15, 2023

Publication year: 2023

Article number: 122057

Language: English

ISSN: 13861425

CODEN: SAMCAS

Document type: Journal article (JA)

Publisher: Elsevier B.V.

Abstract: Polycyclic aromatic hydrocarbons (PAHs) have strong carcinogenicity, teratogenicity, mutagenicity and other adverse effects on human beings. They are one of the most dangerous pollutants, which have attracted great attention in the past decades. In this work, aiming at the actual problems that water environment is polluted and human health is threatened by PAHs, surface enhanced Raman spectroscopy (SERS) combined with Random Forest (RF) calibration models were used to quantitative analysis of phenanthrene and fluoranthene in water. Firstly, the SERS data was collected after samples mixed with Ag NPs, after 31 PAHs samples were prepared. Secondly, it was discussed how spectral preprocessing integration strategies affect on the prediction performance of the RF calibration models. And then, the effect of mutual information (MI) variable selection method on the performance of RF calibration models was explored. Finally, the RF calibration models were established for phenanthrene and fluoranthene. For the prediction set, a lowest mean relative error (MRE) and a largest determination coefficient (R2) were obtained. For quantitative analysis of phenanthrene, the final prediction performance results show that R2p is 0.9780, and MREp is 0.0369 based on the D1st-WT-RF calibration model. For fluoranthene, WT-D1st-MI-RF is a better calibration model, and corresponding to R2p and MREp are 0.9770 and 0.0694, respectively. Hence, a rapid and accurate quantitative method of PAHs is established for the real-time detection of water environmental pollution, which is intended to provide new ideas and methods for the quantitative analysis of PAHs in water. © 2022

Number of references: 46

Main heading: Forecasting

Controlled terms: Anthracene - Aromatization - Forestry - Light transmission - Mineral oils - Raman spectroscopy - Spectrum analysis - Water pollution

Uncontrolled terms: Calibration model - Fluoranthene - Mean relative error - Method integration - Mutual informations - Pre-processing method - Prediction performance - Preprocessing method integration - Random forests - Surface enhanced Raman spectroscopy

28. Plasma etched Ag nanospheres for large increases of ZnO fluorescence emission: A combined theoretical-experimental study

Authors: Xu, Chao (1); Ding, Jijun (1); Chen, Haixia (1); Wang, Xiaojun (2)
Author affiliation: (1) Shaanxi Engineering Research Center of Oil and Gas Resource Optical Fiber Detection, Shaanxi Key Laboratory of Measurement and Control Technology for Oil and Gas Wells, College of Science, Xi'an Shiyou University, Xi'an; 710065, China; (2) Department of Physics, Georgia Southern University, Statesboro; GA; 30460, United States
Corresponding authors: Ding, Jijun(jjding@xsyu.edu.cn); Wang, Xiaojun(xwang@georgiasouthern.edu)

Abstract: Ag nanoparticles are prepared on p-type silicon substrates by magnetron sputtering, and then Ag nanospheres are constructed using appropriate plasma etching conditions. By comparing and analyzing the AFM and SEM morphologies, the experimental parameters are optimized continuously to achieve Ag nanospheres with uniform size distribution. Finally, ZnO films are deposited on the upper layer to form Ag/ZnO composite films. Compared with Ag/ZnO with unetched Ag nanoparticles, its fluorescence emission is enhanced 140 times by adjusting the optimum coupling distance of Ag nanospheres. In this work, based on the experimental results, the coupling effect of Ag nanospheres and ZnO films is theoretically simulated using COMSOL Multiphysics. According to the plasmon electromagnetic coupling theory, the dielectric function relationship is deduced. At the same time, the relationship between the electric field distribution, scattering cross section, skin depth and fluorescence emission is analyzed, which also confirm theoretically that the plasma resonance of Ag nanospheres enhance the fluorescence emission of ZnO. It provides reliable theoretical and experimental parameters for improving the light response and fluorescence emission efficiency of optical devices. © 2022 Elsevier Ltd and Techna Group S.r.l.

29. An Image Construction Based on the VTLF Fusion Technique for Oil-Water Two-Phase Flow of Noncontact Electrical Impedance Tomography

Accession number: 20230313394418
Authors: Wang, Xiaoxin (1); Xi, Wei (1); Wang, Bo (2); Dang, Bo (1); Hu, Hongli (3)

Author affiliation: (1) Xi'an Shiyou University, Shaanxi Key Laboratory of Measurement and Control Technology for Oil and Gas Wells, Xi'an; 710065, China; (2) Xi'an Research Institute, China Coal Research Institute, Xi'an; 710077, China; (3) Xi'an Jiaotong University, State Key Laboratory of Electrical Insulation and Power Equipment, Xi'an; 710049, China
Corresponding author: Wang, Xiaoxin(wxiaoxin@xsyu.edu.cn)

Source title: IEEE Transactions on Instrumentation and Measurement
Abbreviated source title: IEEE Trans. Instrum. Meas.
Volume: 72
Issue date: 2023
Publication year: 2023
Article number: 9501214
Language: English
ISSN: 00189456
E-ISSN: 15579662
CODEN: IEIMAO
Document type: Journal article (JA)
Publisher: Institute of Electrical and Electronics Engineers Inc.

Abstract: Electrical tomography (ET) has attracted extensive attention in the petroleum multiphase flow field due to its advantages of nonintrusion, nonradiation, and simple equipment structure. Some contactless impedance imaging methods, such as capacitively coupled electrical resistance tomography (CCERT) and phase-based dielectric spectroscopy tomography, or displacement current phase tomography (DCPT), have been studied for the parameter measurement of two-phase flow. The mentioned research mainly focuses on the separate imaging by real part, imaginary part, or phase information of the voltage/current. However, the distribution change of media in the region of interest (RoI), especially the presence of high permittivity and conductivity materials, involves the distribution change of conductivity, permittivity, and loss factor. Developing a proper image fusion technique based on the three components can provide more comprehensive image information for tomographic imaging. This article proposed an improved logic filter image fusion algorithm based on a variable threshold (VTLF), and a noncontact electrical impedance tomography (NEIT) system for imaging water-oil two-phase flow is carried out. Image reconstruction is implemented by the VTLF image fusion algorithm under different media distributions, conductivities, and excitation frequencies, and the image fusion algorithms of a weighted average (WA) and logic filter (LF) are also used for comparison. The simulation results show that the reconstructed images by the proposed fusion method of VTLF had the lowest artifacts and the highest correlation coefficient (above 0.7) compared with other methods. Also, in the experiment, the VTLF also got the best performance, so it is effective to improve the reconstruction accuracy. © 1963-2012 IEEE.

Number of references: 39
Main heading: Image reconstruction
Controlled terms: Computer circuits - Construction equipment - Electric impedance - Electric impedance measurement - Electric impedance tomography - Image enhancement - Image fusion - Image segmentation - Permittivity - Two phase flow
Uncontrolled terms: Conductivity - Electrical impe dance tomography (EIT) - Excitation frequency - Images reconstruction - Impedance - Impedance measurement - Non-contact - Non-contact electrical impedance tomography - Variable threshold improved logic filter - Variable thresholds
Classification code: 405.1 Construction Equipment - 631.1 Fluid Flow, General - 701.1 Electricity: Basic Concepts and Phenomena - 721.3 Computer Circuits - 723.2 Data Processing and Image Processing - 942.2 Electric Variables Measurements
DOI: 10.1109/TIM.2022.3232618

30. An uncertainty quantitative model of wellbore failure risk for underground gas storage in depleted gas reservoir during the construction process

Authors: Zhang, Shengyue (1, 2); Shi, Lan (3); Jia, Delong (4)
Author affiliation: (1) School of Electronic Engineering, Xi'an Shiyou University, Xi'an, Shanxi; 710077, China; (2) Key Laboratory of Oil and Gas Well Measurement and Control Technology, Xi'an, Shanxi; 710077, China; (3) Xi 'an Rare Metal Materials Institute Co. Ltd, Xi'an; 710077, China; (4) College of Mechanical and Electrical Engineering, Qingdao University, Shandong, Qingdao; 266580, China
Corresponding author: Zhang, Shengyue(syz_safe@xsyu.edu.cn)
Abstract: The sensitivity of wellbore-wall failure risk under depleted formation-pressure coefficients and underground gas storage in depleted gas reservoirs during the construction process is quantitatively assessed, especially the failure risk of wellbore collapse and fracture in depleted reservoirs with ultralow formation-pressure coefficients, and to effectively guide safe construction. Based on the Mohr–Coulomb failure theory and multilevel confidence model, three typical in situ stress states (normal fault, slip fault, and reverse fault) are considered to establish an analytical model for wellbore-wall failure risk under different depleted reservoir pressure coefficients. Taking a depleted sandstone reservoir as the main reservoir for wellbore-wall stability analysis as an example, a wellbore-wall stability state visualization analysis model with three typical in situ stress states under arbitrary orientations and well deviation angles is obtained, and the uncertain probability distribution law of wellbore-wall collapse and fracture failure in a reservoir with an ultralow formation-pressure coefficient is constructed using a stochastic uncertainty simulation method with interval confidence. The distribution patterns of wellbore-wall stress fields and borehole safety density windows during the construction of depleted reservoirs are quantitatively analyzed. The results show that a safety density window with interval uncertainty estimates would be more intuitive for assessing the stability of the reservoir wellbore wall in a quantitative form, and it is observed that inclined well sections in depleted reservoirs typically have narrower safety density windows. In conclusion, the lower and upper limits of the safety density window in numerical examples are 1.4 to 1.6 g/cm3 (normal fault state), 1.2 to 1.5 g/cm3 (slip fault state), and 1.2 to 1.65 g/cm3 (reverse fault state), respectively. The research results can provide effective guidance for wellbore instability control, design, and construction of directional wells in depleted gas reservoirs. © 2022 Elsevier Ltd

31. Feasibility evaluation of CO2 EOR and storage in tight oil reservoirs: A demonstration project in the Ordos Basin

Accession number: 20223712727400

Authors: Ren, Dazhong (1); Wang, Xiangzeng (2); Kou, Zuhao (3); Wang, Shouchuan (4); Wang, Heng (4); Wang, Xiaoguang (4); Tang, Yong (5); Jiao, Zunsheng (6); Zhou, Desheng (1); Zhang, Rongjun (1, 7)
Author affiliation: (1) Shaanxi Key Laboratory of Advanced Stimulation Technology for Oil&Gas Reservoirs, College of Petroleum Engineering, Xi'an Shiyou University, Xi'an; 710065, China; (2) Shaanxi Yanchang Petroleum (Group) Corp. Ltd., Xi'an; 710075, China; (3) Department of Chemical Engineering, University of Wyoming, 1000 E. University Avenue, Laramie; WY; 82071, United States; (4) State Key Laboratory of Oil and Gas Reservoir Geology and Exploitation, Chengdu University of Technology, Chengdu; 610059, China; (5) State Key Laboratory of Oil and Gas Reservoir Geology and Exploitation, Southwest Petroleum University, Chengdu; 610500, China; (6) Center for Economic Geology Research, University of Wyoming, 1000 E. University Avenue, Laramie; WY; 82071, United States; (7) Xi'an Key Laboratory of Tight Oil (Shale Oil) Development, Xi'an Shiyou University, Xi'an; 710065, China
Corresponding author: Kou, Zuhao(zkou@uwyo.edu)

Source title: Fuel
Abbreviated source title: Fuel
Volume: 331
Issue date: January 1, 2023
Publication year: 2023
Article number: 125652
Language: English
ISSN: 00162361
CODEN: FUELAC
Document type: Journal article (JA)
Publisher: Elsevier Ltd

Abstract: Among the techniques to mitigate CO2 emissions into atmosphere, CO2 geological storage is the only option for gigaton removal of CO2. This study performs a pilot test of CO2-EOR and storage in a tight reservoir of Baibao oilfield, located at the Ordos Basin of China. Two scenarios: CO2 injection through two newly drilled wells and total nine wells, with two CO2 injection schemes: continuous injection (CI) and water alternative gas (WAG) injection, are considered. Simulation results show that both CO2 injection schemes can substantially increase oil production, compared to the current waterflooding. To be more specific, WAG, in contrast to CI, increases oil production by 7.9% and 16.2% for the two- and nine-injection well scenarios, respectively. Yet, as for CO2 storage, WAG, compared with CI, finally leads to a decrease of stored CO2 by 9.6% and 15%, for the two- and nine-CO2 injection well scenarios, respectively. From the aspect of CO2 utilization efficiency, net CO2 utilization ratio of WAG is smaller than the one from CI regardless of the number of CO2 injection well. Besides, for the two- and nine-injection well scenarios, maximum net utilization ratios are achieved after 7–8 years' and 4–5 years' injections, respectively. The sensitive analyses reveal that the impact of CO2 injection rate of WAG on total oil production is more significant than the water injection in WAG. Water injection rate in WAG negatively affects the total CO2 storage and CO2 net utilization ratio whereas the higher CO2 injection rate dramatically increases the total CO2 storage. Overall, this study not only sheds light on achieving double-win goal via CO2 injection, but also can be a valuable reference for other CO2-EOR and storage pilot tests in tight reservoirs. © 2022 Elsevier Ltd

Number of references: 51
Main heading: Carbon dioxide
Controlled terms: Aspect ratio - Enhanced recovery - Infill drilling - Injection (oil wells) - Metamorphic rocks - Petroleum reservoir engineering - Petroleum reservoirs
Uncontrolled terms: Co 2 injections - CO2 storage - Continuous gas injections - Continuous injections - Enhanced-oil recoveries - Injection wells - Oil reservoirs - Oil-production - Tight oil reservoir - Water alternative gas injection
Classification code: 511.1 Oil Field Production Operations - 512.1.1 Oil Fields - 512.1.2 Petroleum Deposits : Development Operations - 804.2 Inorganic Compounds
Numerical data indexing: Age 4.00E+00yr to 5.00E+00yr, Age 7.00E+00yr to 8.00E+00yr, Percentage 1.50E+01%, Percentage 1.62E+01%, Percentage 7.90E+00%, Percentage 9.60E+00%
DOI: 10.1016/j.fuel.2022.125652

Compendex references: YES
Database: Compendex
Data Provider: Engineering Village

32. Identification of watered-out zones in carbonate reservoirs using resistivity curve reconstruction based on reservoir classification   (*Open Access*)

Accession number: 20224313013792
Authors: Wang, Fei (1); Zhao, Lun (2); Bian, Huiyuan (3); Tan, Chengqian (4); Li, Jianxin (2)
Author affiliation: (1) School of Earth Science and Resources, Chang'an University, Shaanxi, Xi'an; 710054, China; (2) PetroChina Research Institute of Petroleum Exploration & Development, Beijing; 100083, China; (3) College of Geology & Environment, Xi'an University of Science and Technology, Shaanxi, Xi'an; 710054, China; (4) School of Earth Science and Engineering Xi'an Shiyou University, Shaanxi, Xi'an; 710065, China
Corresponding author: Wang, Fei(wangfeijlu-147@163.com)
Source title: Energy Geoscience
Abbreviated source title: Energy Geosci.
Volume: 4
Issue: 2
Issue date: April 2023
Publication year: 2023
Article number: 100092
Language: English
E-ISSN: 26667592
Document type: Journal article (JA)
Publisher: KeAi Communications Co.
Abstract: The KT–II layer in the Zananor Oilfield, Caspian Basin, Kazakhstan, contains carbonate reservoirs of various types. The complex pore structure of the reservoirs have made it difficult to identify watered-out zones with traditional logging interpretation methods. This study classifies the reservoirs on the basis of core analysis and establishes an identification model for watered-out layers in the field to effectively improve the interpretation accuracy. Thin section analysis shows that there are three types of pores in the reservoirs, i.e., the matrix pore, fracture and dissolution vug. A triple porosity model is used to calculate the porosities of the reservoirs and the results are combined with core analysis to classify the reservoirs into the fractured, matrix pore, fracture-pore as well as composite types. A classification standard is also proposed. There are differences in resistivity logging responses from the reservoirs of different types before and after watering-out. The pre–watering-out resistivities are reconstructed using generalized neural network for different types of reservoirs. The watered-out layers can be effectively identified according to the difference in resistivity curves before and after watering-out. The results show that the watered-out layers identified with the method are consistent with measured data, thus serving as a reference for the evaluation of watered-out layers in the study area. © 2022 Sinopec Petroleum Exploration and Production Research Institute
Number of references: 20
Main heading: Porosity
Controlled terms: Fracture - Oil well logging - Petroleum prospecting - Pore structure
Uncontrolled terms: Carbonate reservoir - Curve reconstruction - Log evaluation - Matrix pore - Neural-networks - Reconstructed resistivity - Reservoir classification - Resistivity curves - Watered-out zone - Watering-out
Classification code: 512.1.2 Petroleum Deposits : Development Operations - 931.2 Physical Properties of Gases, Liquids and Solids - 951 Materials Science
DOI: 10.1016/j.engeos.2022.01.004
Compendex references: YES
Open Access type(s): All Open Access, Gold
Database: Compendex
Data Provider: Engineering Village

33. Effect of the interfacial microstructure on hardness of multi-layer diamond coatings

Authors: Liu, Yanming (1); Wang, Mengrui (1, 2); Liu, Lusheng (2); Song, Haozhe (2); Hu, Tianwen (2); Xiong, Jiaji (2, 3); Zhai, Zhaofeng (2); Zhao, Xiao (1, 2); Zhang, Chuyan (2); Yang, Bing (2); Jiang, Xin (2); Huang, Nan (2, 3)
Author affiliation: (1) College of Materials Science and Engineering, Xi'an Shiyou University, Xi'an; 710065, China; (2) Shenyang National Laboratory for Materials Science, Institute of Metal Research, Chinese Academy of Sciences, Wenhua Road 72, Shenyang; 110016, China; (3) School of Materials Science and Engineering, University of Science and Technology of China, Wenhua Road 72, Shenyang; 110016, China
Corresponding authors: Jiang, Xin(xjiang@imr.ac.cn); Huang, Nan(nhuang@imr.ac.cn)

Abstract: Multi-layer diamond coatings have been widely employed in cutting tools due to their superior mechanical performance, which mainly stems from their complex multi-layer structures and versatile interfaces. However, it is still lack of investigation on how these interfaces may be tuned to enhance the mechanical properties. Herein, the multi-layer diamond coatings with different modulation periods (= 1.70, 0.87, 0.29 μm), containing microcrystalline diamond (MCD), sub-microcrystalline diamond (SMCD) and nanocrystalline diamond (NCD) as sub-layers, were synthetized by hot filament chemical vapor deposition (HFCVD). The interfacial microstructures were characterized by scanning transmission electron microscopy (STEM). The hardness (H) and Young's modulus (E) of the coatings were evaluated by nanoindentation tests with two different modes. The planar defects including stacking faults (SFs) and twinning boundaries (TBs) are observed at both MCD/SMCD and NCD/MCD interfaces but absent at SMCD/NCD interfaces. Owing to more interfaces, SFs and TBs as barriers inhibiting the dislocation motion effectively, the H and E of the coatings are enhanced with the decrease of . Hence, the coating with of 0.29 μm, possessing more SFs, TBs and more sharp interfaces, obtains the highest hardness (78.39 ± 1.10 GPa). In summary, the mechanical properties of the multi-layer diamond coatings can be greatly improved by the elaborately designed interfacial microstructure, which is of great significance to promote the far-ranging application of diamond coatings. © 2023

Number of references: 58
Main heading: Nanoindentation
Controlled terms: Chemical vapor deposition - Coatings - Diamonds - Elastic moduli - Hardness - High resolution transmission electron microscopy - Microstructure - Nanocrystals - Physical vapor deposition - Scanning electron microscopy
Uncontrolled terms: Diamond coating - Interfacial microstructure - Mechanical performance - Microcrystalline diamond - Modulation period - Multi-layer diamond coating - Multi-layers - Multilayer structures - Nano indentation - Nanocrystalline diamonds
Classification code: 482.2.1 Gems - 741.3 Optical Devices and Systems - 761 Nanotechnology - 802.2 Chemical Reactions - 813.2 Coating Materials - 933.1 Crystalline Solids - 943.2 Mechanical Variables Measurements - 951 Materials Science
Numerical data indexing: Pressure 7.839E+10Pa, Size 2.90E-07m
DOI: 10.1016/j.surfcoat.2023.129541

Compendex references: YES
Database: Compendex
Data Provider: Engineering Village

34. Rapid quantitative analysis of slag acidity by laser induced breakdown spectroscopy combined with random forest

Authors: LONG, Shi-Jia (1); LI, Mao-Gang (2); ZHOU, Jia-Jun (2); ZHANG, Tian-Long (2); TANG, Hong-Sheng (2); LI, Hua (2, 3)
Author affiliation: (1) College of Chemical Engineering and Technology, Tianshui Normal University, Tianshui; 741000, China; (2) Key Laboratory of Synthetic and Natural Functional Molecule of the Ministry of Education, College of Chemistry & Materials Science, Northwest University, Xi'an; 710127, China; (3) College of Chemistry and Chemical Engineering, Xi'an Shiyou University, Xi'an; 710065, China
Corresponding author: ZHANG, Tian-Long(tlzhang@nwu.edu.cn)

Abstract: Slag is one of the industrial wastes of iron and steel smelting, the recycling of which is a research hotspot in recent years. The acidity of slag is one of the important indexes affecting the reuse of slag. Therefore, the rapid analysis of slag acidity is particularly important for industrial production and resource recovery. The feasibility of laser induced breakdown spectroscopy (LIBS) technology combined with machine learning method for the acidity analysis of slag was explored in the present work. Firstly, the LIBS spectral data of 30 slag samples were collected, and an optimal spectral pretreatment method was explored. On this basis, the variable importance measurement (VIM) based on random forest (RF) algorithm is used to screen the feature variables of LIBS spectral data of slag samples. Then, the grid search method is used to optimize the parameters of the RF calibration model. Based on the optimized spectral data and model parameters, a quantitative analysis model of slag acidity was established. In order to further verify the prediction performance of this model, it is compared with other models. The results show that the best prediction performance of slag acidity is obtained based on the combination of LIBS and VIM-RF model, of which the determination coefficient of prediction set (R^2) is 0.9412, the relative analysis error (RPD) is 4.123, the root mean square error (RMSE) is 0.5358, and the average relative error (MRE) is 0.4166. This study shows that LIBS combined with VIM-RF is an effective method for rapid quantitative analysis of metallurgical slag, which can provide a reference for other index analysis in the metallurgical industry. © 2022

Number of references: 27
Main heading: Slags
Controlled terms: Atomic emission spectroscopy - Errors - Forecasting - Forestry - Industrial research - Laser induced breakdown spectroscopy - Learning systems - Mean square error - Spectrum analysis
Uncontrolled terms: Hotspots - Iron and steel - Iron-smelting - Laserinduced breakdown spectroscopy (LIBS) - Prediction performance - Random forests - Reuse - Spectral data - Steel smelting - Variable importances
Classification code: 821 Agricultural Equipment and Methods; Vegetation and Pest Control - 901.3 Engineering Research - 912.1 Industrial Engineering - 922.2 Mathematical Statistics - 931.1 Mechanics
DOI: 10.1016/j.cjac.2022.100210

Compendex references: YES
Database: Compendex
Data Provider: Engineering Village

35. The impact of isolation kernel on agglomerative hierarchical clustering algorithms   (*Open Access*)

Authors: Han, Xin (1, 2); Zhu, Ye (3); Ting, Kai Ming (4); Li, Gang (3)
Author affiliation: (1) School of Computer Science, Xi'an Shiyou University, Shaanxi; 710065, China; (2) Asia-Pacific Academy of Economics and Management, University of Macau, Macau; 999078, China; (3) Centre for Cyber Resilience and Trust, Deakin University, Geelong; 3125, Australia; (4) National Key Laboratory for Novel Software Technology, Nanjing University, Nanjing; 210023, China
Corresponding author: Zhu, Ye(ye.zhu@ieee.org)
Abstract: Agglomerative hierarchical clustering (AHC) is one of the popular clustering approaches. AHC generates a dendrogram that provides richer information and insights from a dataset than partitioning clustering. However, a major problem with existing distance-based AHC methods is: it fails to effectively identify adjacent clusters with varied densities, regardless of the cluster extraction methods applied to the resultant dendrogram. This paper aims to reveal the root cause of this issue and provides a solution by using a data-dependent kernel. We analyse the condition under which existing AHC methods fail to effectively extract clusters, and give the reason why the data-dependent kernel is an effective remedy. This leads to a new approach to kernerlise existing hierarchical clustering algorithms including the traditional AHC algorithms, HDBSCAN, GDL, PHA and HC-OT. Our extensive empirical evaluation shows that the recently introduced Isolation Kernel produces a higher quality or purer dendrogram than distance, Gaussian Kernel and adaptive Gaussian Kernel in all the above mentioned AHC algorithms. © 2023 The Author(s)
Number of references: 44
Main heading: Gaussian distribution
Controlled terms: Clustering algorithms
Uncontrolled terms: Agglomerative hierarchical clustering - Clustering approach - Data dependent - Dendrogram purity - Dendrograms - Gaussian kernels - Hierarchical clustering algorithms - Hierarchical clustering methods - Isolation kernel - Varied density
Classification code: 903.1 Information Sources and Analysis - 922.1 Probability Theory - 922.2 Mathematical Statistics
DOI: 10.1016/j.patcog.2023.109517
Compendex references: YES
Open Access type(s): All Open Access, Hybrid Gold, Green
Database: Compendex
Data Provider: Engineering Village

36. Cantilever vibration sensor based on Fiber Bragg Grating temperature compensation

Authors: Jia, Zhen'an (1, 2, 3, 4); Dang, Shuo (1, 2, 3, 4); Yu, Dakuan (1, 2, 3, 4); Fan, Wei (1, 2, 3, 4)
Author affiliation: (1) School of Science, Xi'an Shiyou University, Xi'an; 710065, China; (2) Shaanxi Engineering Research Center of Oil and Gas Resource Optical Fiber Detection, Xi'an; 710065, China; (3) Shaanxi Key Laboratory of Measurement and Control Technology for Oil and Gas Wells, Xi'an; 710065, China; (4) Key Laboratory of CNPC, Research Laboratory for Optical Fiber Dynamic Detection of Oil Reservoirs, Xi'an; 710065, China
Corresponding author: Dang, Shuo(ds_15289461196@163.com)

Abstract: To improve the sensitivity of fiber Bragg grating (FBG) vibration sensor and reduce the influence of temperature on vibration detection, an FBG vibration sensor with equal strength beam as elastic structure and temperature self-compensated is proposed. The working principle of the sensor is analyzed, the resonant frequency and the sensitivity are derived through the formula, the structural parameters are optimized, and its good response characteristics are proved by experiments. The theory of the proposed sensor is verified by experiments, and the experimental results show that the temperature impact on the sensor structure is reduced to 0.17 pm/°C in the range of 30–75°C. The sensor has a good response flat region at 20–220 Hz, the sensitivity is 149.8 pm/g. and the transverse sensitivity is only 3.95 % of the sensitivity in the working direction. Experiments show that the sensor has good comprehensive characteristics. Therefore, the sensor has great application prospect in vibration signal detection in the environment with obvious temperature changes, such as oil exploration, aerospace and so on. © 2022 Elsevier Inc.

Number of references: 34
Main heading: Fiber Bragg gratings
Controlled terms: Cantilever beams - Nanocantilevers - Natural frequencies - Petroleum prospecting - Ventilation exhausts
Uncontrolled terms: Cantilever vibrations - Elastic structures - Equal strengths - Response characteristic - Structural parameter - Temperature compensation - Temperature impact - Temperature self-compensated - Vibration detection - Vibration sensors
Classification code: 408.2 Structural Members and Shapes - 512.1.2 Petroleum Deposits : Development Operations - 619.1 Pipe, Piping and Pipelines - 643.5 Ventilation - 761 Nanotechnology - 933 Solid State Physics
Numerical data indexing: Frequency 2.00E+01Hz to 2.20E+02Hz, Percentage 3.95E+00%, Size 1.498E-10m, Size 1.70E-13m, Temperature 3.03E+02K to 3.48E+02K
DOI: 10.1016/j.yofte.2022.103183

Compendex references: YES
Database: Compendex
Data Provider: Engineering Village

37. Process characteristics of V-shaped coupling dual GTA-based additive manufacturing (*Open Access*)

Accession number: 20231113703492

Authors: Qiang, Wei (1, 2); Wang, Kehong (2); Gao, Cheng (1); Peng, Yong (2); Lu, Yongxin (1); Wen, Guodong (3)
Author affiliation: (1) School of Materials Science and Engineering, Xi'an Shiyou University, Xi'an; 710065, China; (2) Key Laboratory of Controlled Arc Intelligent Additive Technology, Ministry of Industry and Information Technology, Nanjing University of Science and Technology, Nanjing; 210094, China; (3) Xi'an Research Institute of China Coal Technology&Engineering Group Corp, Xi'an; 710077, China
Corresponding authors: Qiang, Wei(qiangw@xsyu.edu.cn); Wen, Guodong(wenguodong@cctegxian.com)

Abstract: The deposition efficiency of gas tungsten arc (GTA) additive manufacturing is quite low despite its superior quality in comparison with other arc-based manufacturing processes. Therefore, V-shaped coupling dual GTA-based additive manufacturing (VCG-AM) process was proposed in this study to solve the problem. Thin-wall part with sound formation was acquired by VCG-AM, with the deposition efficiency reaching more than twice of conventional single

GTA-based additive manufacturing (SG-AM) process. The microstructure of mainly polygonal ferrite and pearlite was obtained via both processes, and the grain size of VCG-AM was slightly larger than that of SG-AM, related with the higher heat input. The pearlite assembled near the grain boundary of the polygonal ferrite, and a larger volume fraction of pearlite formed in the VCG-AM sample due to the lower cooling rate. The average microhardness of the VCG-AM sample was a little lower than that of the SG-AM sample, while the impact absorbing energy and ultimate tensile strength was close. Both VCG-AM and SG-AM part demonstrates ductile fracture based on the tensile fracture analysis. © 2023 The Authors

Number of references: 27
Main heading: Microstructure
Controlled terms: 3D printing - Additives - Deposition - Ductile fracture - Ferrite - Grain boundaries - Pearlite - Tensile strength
Uncontrolled terms: Additive manufacturing process - Deposition efficiencies - Gas tungsten arc - Grainsize - Manufacturing IS - Manufacturing process - Polygonal ferrites - Process characteristics - Thin wall part - V-shaped coupling dual gas tungsten arc-based additive manufacturing
Classification code: 531.2 Metallography - 745.1.1 Printing Equipment - 802.3 Chemical Operations - 803 Chemical Agents and Basic Industrial Chemicals - 951 Materials Science
DOI: 10.1016/j.jmrt.2023.01.139

Compendex references: YES
Open Access type(s): All Open Access, Gold
Database: Compendex
Data Provider: Engineering Village

38. Enhanced corrosion resistance of high speed laser-cladded Ni/316L alloy coating by heat treatment   (*Open Access*)

Accession number: 20231213781439

Authors: Dong, Hui (1); Guo, Peng-Fei (1); Han, Yan (2); Bai, Ru-Xue (1); Yang, Zi-Chen (1); Zhang, San-Qi (1)
Author affiliation: (1) Xi'an Key Laboratory of High Performance Oil and Gas Field Materials, School of Materials Science and Engineering, Xi'an Shiyou University, Shaanxi, Xi'an; 710065, China; (2) CNPC Tubular Goods Research Institute, State Key Laboratory for Performance and Structure Safety of Petroleum Tubular Goods and Equipment Materials, Shaanxi, Xi'an; 710077, China
Corresponding author: Dong, Hui(donghui@xsyu.edu.cn)

Abstract: The heat treatment was performed on the high speed laser-cladded Ni/316L coating to improve the corrosion resistance. The coatings were heat treated at temperatures of 650 °C, 700 °C, 750 °C and 800 °C, respectively. The results show that the porosity of the coating was independent of the annealing temperature and the chemical composition of the coating could be perfectly retained after heat treatment. The grain size first decreased and then increased with heat treatment temperature. The content of equiaxed grains and the Fe19Ni precipitation phase increased with increasing temperature. Due to the precipitation, the corrosion resistance of the heat-treated coating was higher than that of the as-cladded coating. Based on the coupled effect of precipitation and grain morphology, the corrosion resistance of the heat-treated coating first increased and then decreased. Therefore, the corrosion resistance could be improved by annealing, but need applicable parameters. © 2023 The Author(s)

Number of references: 59

Main heading: Corrosion resistance
Controlled terms: Binary alloys - Corrosion resistant alloys - Corrosion resistant coatings - Heat resistance - Heat treatment - Iron alloys - Laser cladding - Metal cladding - Nickel alloys - Textures
Uncontrolled terms: 316L - After-heat treatment - Alloy coatings - Annealing temperatures - Chemical compositions - Grainsize - Heat-treated coatings - High speed laser - High speed laser cladding - Ni/316l coating
Classification code: 531 Metallurgy and Metallography - 537.1 Heat Treatment Processes - 539.1 Metals Corrosion - 539.2 Corrosion Protection - 545.2 Iron Alloys - 548.2 Nickel Alloys - 744.9 Laser Applications - 813.1 Coating Techniques
Numerical data indexing: Temperature 1.023E+03K, Temperature 1.073E+03K, Temperature 9.23E+02K, Temperature 9.73E+02K, Volume 3.16E-01m3
DOI: 10.1016/j.jmrt.2023.03.070
Funding Details: Number: YS37020203, Acronym: -, Sponsor: -; Number: YCS22111018, Acronym: -, Sponsor: -; Number: 51904331, Acronym: NSFC, Sponsor: National Natural Science Foundation of China;
Funding text: The research was funded by the National Natural Science Foundation of China (51904331), the Materials Science and Engineering of Provincial Advantage Disciplines in Xi'an Shiyou University (No. YS37020203), and the Xi'an Shiyou University Graduate Innovation and Practice Ability Training Pro-ject (YCS22111018).
Compendex references: YES
Open Access type(s): All Open Access, Gold
Database: Compendex
Data Provider: Engineering Village

Compilation and indexing terms, Copyright 2023 Elsevier Inc.

39. The microscopic pore crude oil production characteristics and influencing factors by DME-assisted CO2 injection in shale oil reservoirs

Accession number: 20223712704937
Authors: Huang, Xing (1, 2, 3); Tian, Zhen (1); Zuo, Xiongdi (1); Li, Xiang (4); Yang, Weipeng (4); Lu, Jun (4)
Author affiliation: (1) School of Petroleum Engineering, Xi'an Shiyou University, Shaanxi, Xi'an; 710065, China; (2) Shaanxi Key Laboratory of Carbon Dioxide Sequestration and Enhanced Oil Recovery (under Planning), Shaanxi, Xi'an; 710065, China; (3) Shaanxi Cooperative Innovation Center of Unconventional Oil and Gas Exploration and Development, Shaanxi, Xi'an; 710065, China; (4) McDougall School of Petroleum Engineering, The University of Tulsa, Tulsa; OK; 74104, United States
Corresponding author: Zuo, Xiongdi(zuoxiongdizxd@163.com)
Source title: Fuel
Abbreviated source title: Fuel
Volume: 331
Issue date: January 1, 2023
Publication year: 2023
Article number: 125843
Language: English
ISSN: 00162361
CODEN: FUELAC
Document type: Journal article (JA)
Publisher: Elsevier Ltd
Abstract: CO2 injection into shale oil reservoirs can effectively enhance recovery while simultaneously realizing geological storage. However, shale oil recovery by CO2 injection remains low. In this paper, classification and evaluation standards for shale oil reservoirs were established. Based on this, comparative experiments between pure CO2 flooding and dimethyl ether (DME)-assisted CO2 flooding were conducted, supplemented by nuclear magnetic resonance testing. The microscopic production characteristics of shale oil under different injection methods were analyzed. The effects of injection pressure, gas injection volume, and DME concentration on oil recovery were studied, and the potential of DME-assisted CO2 flooding was explored. The results show three types of shale samples: I, II, and III, with their corresponding physical properties, pore-throat structures, and percolation capacities decreasing in the same order. With the addition of DME, the CO2 solubility increased, while the produced oil viscosity significantly decreased. DME-assisted CO2 flooding has higher recovery compare with CO2 flooding. The increase is more significant as pressure increases. The increase in ultimate recovery was the largest for type III samples. In addition, regardless of whether pure CO2 flooding or DME-assisted CO2 flooding was applied, a higher injection pressure and injection volume mean higher recovery. The increase by DME-assisted CO2 flooding is much greater than that by pure CO2 flooding. During the miscible stage, the recovery is greater than that during the immiscible stage. The recovery increased with increasing DME molar concentration and then slowed down; therefore, the recommended

molar concentration of DME in the mixed gas is 20 mol%. The research results provide new methods and ideas for enhancing shale oil recovery and realizing geological storage by CO2 injection. © 2022 Elsevier Ltd

Number of references: 69
Main heading: Carbon dioxide
Controlled terms: Crude oil - Enhanced recovery - Floods - Geology - Oil well flooding - Petroleum reservoir engineering - Petroleum reservoirs - Pore structure - Recovery - Reservoirs (water) - Solvents
Uncontrolled terms: Co 2 injections - Crude oil production - Crude oil production characteristic - Dimethyl ether-assisted CO2 injection - Influencing factor - Microscopic pore structures - Oil reservoirs - Production characteristics - Shale oil reservoir
Classification code: 441.2 Reservoirs - 481.1 Geology - 511.1 Oil Field Production Operations - 512.1 Petroleum Deposits - 512.1.1 Oil Fields - 512.1.2 Petroleum Deposits : Development Operations - 803 Chemical Agents and Basic Industrial Chemicals - 804.2 Inorganic Compounds - 931.2 Physical Properties of Gases, Liquids and Solids
Numerical data indexing: Amount of substance $2.00E+01mol$
DOI: 10.1016/j.fuel.2022.125843

Compendex references: YES
Database: Compendex
Data Provider: Engineering Village

40. Highly crinkled and interconnected N, O and S co-doped carbon nanosheet modified separators for efficient Li-S batteries

Accession number: 20230713579996
Authors: Zhu, Yanan (1, 2); Deng, Yuanfu (3); Chen, Guohua (1)
Author affiliation: (1) Department of Mechanical Engineering, Research Institute for Smart Energy, The Hong Kong Polytechnic University, Hung Hom, Kowloon, Hong Kong; (2) College of Chemistry and Chemical Engineering, Xi'an Shiyou University, Xi'an; 710065, China; (3) The Key Laboratory of Fuel Cell for Guangdong Province, School of Chemistry and Chemical Engineering, South China University of Technology, Guangzhou, China
Corresponding authors: Zhu, Yanan(zhuyanan@xsyu.edu.cn); Chen, Guohua(ghchen1963@gmail.com)
Source title: Materials Chemistry Frontiers
Abbreviated source title: Mater. Chem. Front.
Volume: 7
Issue: 6
Issue date: January 17, 2023
Publication year: 2023
Pages: 1072-1081
Language: English
E-ISSN: 20521537
Document type: Journal article (JA)
Publisher: Royal Society of Chemistry
Abstract: Carbon materials with large exposed surfaces and heteroatom doping have great potential in suppressing the shuttle effect in Li-S batteries. In this study, crosslinked triazine frameworks were successfully utilized to synthesize heteroatom-doped carbon nanosheets utilizing g-C3N4 nanosheets as the hard template and porogen. Characterization studies show that the nanosheets were highly crinkled and interconnected with a large surface area (1060 m2 g-1) and pore volume (2.14 cm3 g-1), and with highly dispersed N, O and S. After coating them on commercial Celgard separators, batteries with the modified separators showed a low self-discharge and an improved rate performance even at 4 C. At 0.5 C, the initial discharge capacity was 1240 mA h g-1 with a capacity decay of 0.059% per cycle for over 1000 cycles. Moreover, excellent cycling performances at 2 C for 500 cycles were also achieved. The excellent performance can be attributed to the large surface area and porous structure of NOS-C, the superior wettability toward the electrolyte, enhanced Li+ diffusion, strong interactions between polysulfides and doped atoms, and the accelerated redox kinetics of polysulfides. © 2023 The Royal Society of Chemistry.
Number of references: 67

Main heading: Separators
Controlled terms: Carbon - Electrolytes - Lithium batteries - Lithium compounds - Lithium sulfur batteries - Nanosheets - Polysulfides
Uncontrolled terms: Carbon material - Carbon nanosheets - Co-doped - Crosslinked - Doped carbons - Exposed surfaces - Hard templates - Heteroatoms - Large surface area - Polysulphides
Classification code: 702 Electric Batteries and Fuel Cells - 702.1.1 Primary Batteries - 702.1.2 Secondary Batteries - 761 Nanotechnology - 803 Chemical Agents and Basic Industrial Chemicals - 804 Chemical Products Generally - 815.1.1 Organic Polymers - 818.2.1 Synthetic Rubber - 933 Solid State Physics
Numerical data indexing: Electric current 1.24E+00A, Force 3.00E+00N, Percentage 5.90E-02%, Size 1.06E+03m, Size 2.14E-02m
DOI: 10.1039/d2qm00968d

Compendex references: YES
Database: Compendex
Data Provider: Engineering Village

41. Temperature-sensitive polymer based nano-SiO2 composite multi-component synergistic improvement of shale stability in water-based drilling fluids

Accession number: 20232214153678
Authors: Lai, Nanjun (1, 2, 3); Fan, Wei (1); Zhang, Xiaochen (1); Liu, Liang (1); Zhou, Xuefeng (1); Chen, Siqi (1)
Author affiliation: (1) College of Chemistry and Chemical Engineering, Southwest Petroleum University, Sichuan Province, Chengdu City; 610500, China; (2) The Key Laboratory of Well Stability and Fluid & Rock Mechanics in Oil and Gas Reservoir of Shaanxi Province, Xi'an Shiyou University, Xi'an; 710065, China; (3) Oil and Gas Fields Applied Chemistry Key Laboratory of Sichuan Province, Southwest Petroleum University, Sichuan Province, Chengdu City; 610500, China
Corresponding author: Lai, Nanjun(lainanjun@126.com)
Source title: Geoenergy Science and Engineering
Abbreviated source title: Geoenergy. Sci. Eng.
Volume: 224
Issue date: May 2023
Publication year: 2023
Article number: 211498
Language: English
E-ISSN: 29498910
Document type: Journal article (JA)
Publisher: Elsevier B.V.
Abstract: Shale instability caused by the development of nano-micron-scale fractures, pores, and bedding is always a challenge for drilling complex formations. In this work, two additives (Temperature-sensitive polymer based nano-SiO2 composite (SNAS) and poly (NVP-TAAC-AMPS) (NTA)) were synthesized. The lower critical solution temperature (LCST) value of SNAS could be controlled by adjusting the monomer ratio. As temperature-sensitive nanocomposites, SNAS has the rheological control of drilling fluid. The effects of SNAS and NTA on shale stability were tested based on analytical approaches, including shale wettability, microporous membrane fluid loss, pressure transmission rate, shale specific surface area, shale pore volume, shale strength, linear swelling percentage and shale cuttings recovery. When the temperature is higher than the LCST value, due to the transition from hydrophilicity to hydrophobicity of SNAS, it not only changes the wetting angle of shale, but also enhances the plugging effect of SNAS. The composite system could form tight plugging layer and hydrophobic region compared with single SNAS, which was more conducive to improve plugging performance of shale. Finally, the synergistic improvement mechanism of shale stability combined with SNAS and NTA were further proposed. © 2023
Number of references: 53
Main heading: Nanocomposites

42. Experimental study on the effects of an electric field on the pore characterization in anode, middle and cathode regions of tight sandstone samples

Authors: Zhang, Wentong (1, 2, 3); Ning, Zhengfu (1, 2); Wang, Qing (1, 2); Cheng, Zhilin (1, 2, 4); Lyu, Chaohui (1, 2); Wang, Yanwei (5); Liu, Zongke (1, 2); Wang, Hengli (1, 2)
Author affiliation: (1) State Key Laboratory of Petroleum Resources and Prospecting, China University of Petroleum, Beijing, China; (2) School of Petroleum Engineering, China University of Petroleum, Beijing, China; (3) Department of Chemistry, Faculty of Science, University of Alberta, Edmonton; AB; T6G2G2, Canada; (4) School of Petroleum Engineering, Xi'an Shiyou University, Xi'an, China; (5) College of Construction Engineering, Jilin University, Changchun; 130026, China
Corresponding authors: Zhang, Wentong(wentong0202@126.com); Ning, Zhengfu(nzf@cup.edu.cn)
Abstract: Electric field stimulation is more favour for the enhancement of oil recovery from tight sandstones compared to conventional resources, since electroosmotic flow of fluids in smaller pores is stronger. However, the question concerning the character of electric field on the pore structure of tight sandstones (PSTS) remains open, especially the effects in three treated regions: the anode (A), middle (M), and cathode (C) regions. Therefore, in this study, for the first time, several techniques including nuclear magnetic resonance (NMR), high-pressure mercury intrusion (HPMI), and low-temperature nitrogen adsorption (LNA), were combined to explore this topic. First, the T2 relaxation time distribution was converted to the pore size distribution (PSD) through a power-law relation. After that, the changes in the PSTS before and after applying an electric field in the three treated regions were analyzed. The differences in the anode and cathode regions occur in the changes in pore types and pore volume. The reason for this difference is attributed to the effect of electrophoresis and the motion of polar water molecules. Apart from the effect of the dissolution of clay minerals due to the presence of hydrogen ions, the negatively charged particles move to the anode region to fill the pore space, consequently decreasing the number of micropores there. However, the escape of polar water molecules from the anode region increases the number of nanopores in the anode region. This study offers useful information concerning the application of electric fields, which could help electric field-related technologies greatly improve the oil recovery of unconventional resources. © 2023 Elsevier B.V.
Number of references: 71

Main heading: Pore structure
Controlled terms: Anodes - Cathodes - Charged particles - Electric fields - Electroosmosis - Electrophoresis - Gas adsorption - Molecules - Nanopores - Nuclear magnetic resonance - Pore size - Sandstone - Temperature
Uncontrolled terms: Cathode region - High pressure mercury - High-pressure mercury intrusion - Low-temperature nitrogen - Low-temperature nitrogen adsorption - Mercury intrusion - Nitrogen adsorption - Oil recoveries - Pores structure - Tight sandstones
Classification code: 482.2 Minerals - 641.1 Thermodynamics - 701.1 Electricity: Basic Concepts and Phenomena - 714.1 Electron Tubes - 761 Nanotechnology - 801.3 Colloid Chemistry - 801.4.1 Electrochemistry - 802.3 Chemical Operations - 931.2 Physical Properties of Gases, Liquids and Solids - 931.3 Atomic and Molecular Physics - 933 Solid State Physics - 951 Materials Science
DOI: 10.1016/j.geoen.2023.211500
Funding Details: Number: 51774298,51974330, Acronym: -, Sponsor: -; Number: 202006440064, Acronym: UofA, Sponsor: University of Alberta; Number: -, Acronym: CSC, Sponsor: China Scholarship Council;
Funding text: The foundation of National Science in China (Nos. 51974330 , and 51774298) supported this work. Meanwhile, the first author, Wentong Zhang deeply thanks the China Scholarship Council (CSC) for supporting a visit to the University of Alberta (No. 202006440064).The foundation of National Science in China (Nos. 51974330, and 51774298) supported this work. Meanwhile, the first author, Wentong Zhang deeply thanks the China Scholarship Council (CSC) for supporting a visit to the University of Alberta (No.202006440064).
Compendex references: YES
Database: Compendex
Data Provider: Engineering Village
Compilation and indexing terms, Copyright 2023 Elsevier Inc.

43. Investigation on gas/water two-phase flow in quartz nanopores from molecular perspectives

Accession number: 20230113333793
Authors: Lyu, Fangtao (1, 2); Ning, Zhengfu (1, 2); Jia, Zejiang (1, 2); Mu, Zhongqi (1, 2); Zhang, Wentong (3); Liu, Bei (4)
Author affiliation: (1) State Key Laboratory of Petroleum Resources and Prospecting, China University of Petroleum (Beijing), Beijing; 102249, China; (2) Key Laboratory of Petroleum Engineering of the Ministry of Education, China University of Petroleum (Beijing), Beijing; 102249, China; (3) School of New Energy, Xi'an Shiyou University, Xi'an; 710065, China; (4) State Key Laboratory of Heavy Oil Processing, China University of Petroleum (Beijing), Beijing; 102249, China
Corresponding author: Ning, Zhengfu(ningzhengfu313@163.com)
Source title: Journal of Molecular Liquids
Abbreviated source title: J Mol Liq
Volume: 371
Issue date: February 1, 2023
Publication year: 2023
Article number: 121145
Language: English
ISSN: 01677322
CODEN: JMLIDT
Document type: Journal article (JA)
Publisher: Elsevier B.V.
Abstract: Understanding the gas/water two-phase occurrence, flow patterns, and underlying mechanisms in quartz nanopores is crucial for gas transport and production in shale reservoirs. In this study, we investigated the flow characteristics of methane and water in hydroxylated quartz nanopores employing the grand canonical Monte Carlo (GCMC) and molecular dynamics (MD) simulations and focused on elucidating the effects of water saturation, pressure gradient and ion concentration in various aperture nanopores. Results show that water molecules preferentially adsorb on the hydrophilic quartz surface to form water film, increasing methane flow friction and reducing its slippage velocity significantly. Water bridges are formed to wrap gas bubbles and hinder the gas flow with increased water saturation. The water phase occupies a larger pore space with increasing water saturation resulting in an increase in methane effective viscosity and a decrease in apparent permeability. The water bridge is broken under the joint action of external force and gas driving when the pressure gradient is much larger, leading to a dramatic growth of gas flow, and the high-speed gas will produce a shear driving effect on the thick water layers. Ions will weaken the formation of hydrogen bonds between water molecules, but the flux of the water phase decreases with the increasing ion concentration due to the combined impact of ion spatial structure and electroviscous effects and counteracts the

gas phase, thus impeding its flow. This study shed light on the flow phenomena of gas/water phases in hydrophilic nanopores. The results are expected to provide some insight into energy and environmental issues, such as fracturing fluid optimization, enhanced gas recovery (EGR) by water flooding, and the fabrication of microfluidic chips. © 2022 Elsevier B.V.

Number of references: 76
Main heading: Molecular dynamics
Controlled terms: Flow of gases - Flow patterns - Fracturing fluids - Gases - Hydrogen bonds - Hydrophilicity - Ions - Methane - Molecules - Monte Carlo methods - Nanopores - Pressure gradient - Quartz - Shale - Shear flow
Uncontrolled terms: Gas-water - Gas/water flow - Hydrophilics - Ion concentrations - Quartz nanopore - Water bridges - Water flows - Water molecule - Water phasis - Water saturations
Classification code: 482.2 Minerals - 631.1 Fluid Flow, General - 631.1.2 Gas Dynamics - 761 Nanotechnology - 801.4 Physical Chemistry - 804.1 Organic Compounds - 922.2 Mathematical Statistics - 931.3 Atomic and Molecular Physics - 933 Solid State Physics - 944.4 Pressure Measurements
DOI: 10.1016/j.molliq.2022.121145

Compendex references: YES
Database: Compendex
Data Provider: Engineering Village

44. Characteristics and prediction model of hydrogen production of oily sludge by supercritical water gasification

Accession number: 20223312578315
Authors: Wang, Yulong (1, 2, 3); Wang, Shuzhong (1); Qi, Hongyuan (2, 3); Jiang, Huayi (2, 3); Duan, Yuanwang (1)
Author affiliation: (1) Key Laboratory of Thermo-Fluid Science and Engineering of MOE, School of Energy and Power Engineering, Xi'an Jiaotong University, Shaanxi, Xi'an; 710049, China; (2) College of Petroleum Engineering, Xi'an Shiyou University, Shaanxi, Xi'an; 710065, China; (3) Engineering Research Center of Oil and Gas Storage and Transportation Safety and Energy Saving, Universities of Shaanxi Province, Shaanxi, Xi'an; 710065, China
Corresponding author: Wang, Shuzhong(szwang@aliyun.com)
Source title: International Journal of Hydrogen Energy
Abbreviated source title: Int J Hydrogen Energy
Volume: 48
Issue: 30
Issue title: ProfSpecial issue on the 4th International Symposium on Hydrogen Energy and Energy Technologies (HEET 2021)
Issue date: April 8, 2023
Publication year: 2023
Pages: 11191-11204
Language: English
ISSN: 03603199
CODEN: IJHEDX
Document type: Journal article (JA)
Publisher: Elsevier Ltd

Abstract: Harmless treatment and resource utilization of oily sludge are urgent and related to the sustainable green, and low-carbon development of the petroleum industry. Aiming to the supercritical water gasification (SCWG) of oily sludge for hydrogen production, this paper investigated the effects of critical factors, including reaction temperature, initial pressure, retention time, and feed concentration, on the mole fraction, the gas yield, the gasification efficiency, and the hydrogen yield potential. The interaction mechanisms among these four factors were discussed and revealed with a reasonable prediction model of hydrogen production. Results showed that the longer retention time, higher temperature, and lower feed concentration could accelerate hydrogen production from oily sludge by SCWG. The synthetic promotion of the hydrogen yield exists between the temperature and the retention time, while the temperature predominates. A 2.63-fold increase in the H2 yield was obtained when the condition changed from 135 min to 380 °C to

10 min and 555 °C. The hydrogen production of oily sludge by SCWG, at lower temperature and higher pressure was worse than that at higher temperature and lower pressure. © 2022 Hydrogen Energy Publications LLC

Number of references: 45
Main heading: Hydrogen production
Controlled terms: Forecasting - Gasification - Petroleum industry
Uncontrolled terms: Characteristic model - Coupling mechanism - Feed concentration - High-low - Highest temperature - Hydrogen yields - Oily sludges - Prediction modelling - Retention time - Supercritical water gasification
Classification code: 522 Gas Fuels - 802.3 Chemical Operations
Numerical data indexing: Temperature 6.53E+02K, Temperature 8.28E+02K, Time 6.00E+02s, Time 8.10E+03s
DOI: 10.1016/j.ijhydene.2022.06.312

Compendex references: YES
Database: Compendex
Data Provider: Engineering Village

45. Effect of dispersants on the stability of calcite in non-polar solutions

Accession number: 20232214172885

Authors: Liu, Shuai (1, 2); Zhang, Cheng (1); Du, Jiaxin (1); Huang, Hai (2); Fang, Shenwen (1); Li, Xinliang (1); Duan, Ming (1)
Author affiliation: (1) Oil & Gas Field Applied Chemistry Key Laboratory of Sichuan Province, College of Chemistry and Chemical Engineering, Southwest Petroleum University, Sichuan Province, Chengdu, China; (2) Engineering Research Center of Development and Management for Low to Ultra-Low Permeability Oil & Gas Reservoirs in West China, Ministry of Education, Xi'an Shiyou University, Shanxi Province, Xi'an, China
Corresponding authors: Liu, Shuai(ShuaiLiu@pku.org.cn); Duan, Ming(swpua124@126.com)

Source title: Colloids and Surfaces A: Physicochemical and Engineering Aspects
Abbreviated source title: Colloids Surf. A Physicochem. Eng. Asp.
Volume: 672
Issue date: September 5, 2023
Publication year: 2023
Article number: 131730
Language: English
ISSN: 09277757
E-ISSN: 18734359
CODEN: CPEAEH
Document type: Journal article (JA)
Publisher: Elsevier B.V.

Abstract: The surface modification of calcite has been widely used to improve the compatibility of calcite with non-polar solutions, but this method is complex, time-consuming and uneconomical. Thus, we propose to use dispersants for improving the compatibility of calcite with non-polar solutions and systematically study the dispersion effect and mechanism of various dispersants. Anionic bis (2-ethylhexyl) sulfosuccinate sodium (AOT), non-ionic sorbitol monooleate sodium (Span 80) and sorbitol trioleate (Span 85), cationic cetyltrimethylammonium bromide (CTAB), oleic acid (OA) and stearic acid (SA), are used to change the surface properties of calcite in nonpolar solutions. The results of sedimentation and rheology showed that the anionic dispersant AOT had the best dispersion performance and efficiency. All dispersants, except CTAB, can significantly improve the wettability of particle surface, and the calcite adsorbed AOT has the best hydrophobicity. XRD results showed that all dispersants were adsorbed on the surface of calcite. FT-IR and XPS confirmed that AOT adsorbed on the particle surface through the coordination between AOT and Ca^{2+}. Zeta potential shows that the calcite system with anionic AOT has the highest surface charges, indicating that the strong electrostatic interaction is one reason of the stabilization of calcite particles. This work has guiding implications for the selection of dispersants to improve the compatibility of calcite with non-polar solvents. © 2023

Number of references: 43
Main heading: Surface properties
Controlled terms: Alcohols - Calcite - Dispersions - Sodium
Uncontrolled terms: Cetyltrimethylammonium bromide - Dispersants - Dispersion effect - Dispersion mechanisms - Non-polar - Non-polar solution - Particle surface - Polar solutions - Sulfosuccinate - Surface-modification

46. The relationships between heavy metals and bacterial communities in a coal gangue site

Accession number: 20230613555336

Authors: Kou, Bing (1, 2); He, Yue (3); Wang, Yang (1); Qu, Chengtun (2); Tang, Jun (1); Wu, Yuman (1, 2); Tan, Wenbing (1); Yuan, Ying (1); Yu, Tingqiao (4)
Author affiliation: (1) State Environmental Protection Key Laboratory of Simulation and Control of Groundwater Pollution, Chinese Research Academy of Environmental Sciences, Beijing; 100012, China; (2) College of Chemistry and Chemical Engineering, Xi'an Shiyou University, Xi'an; 710065, China; (3) Beijing Guozhong Biotechnology Co., LTD, Beijing; 102211, China; (4) International Education College, Beijing Vocational College of Agriculture, Beijing; 102442, China
Corresponding author: Yuan, Ying(yuanying19880214@126.com)

Source title: Environmental Pollution
Abbreviated source title: Environ. Pollut.
Volume: 322
Issue date: April 1, 2023
Publication year: 2023
Article number: 121136
Language: English
ISSN: 02697491
E-ISSN: 18736424
CODEN: ENPOEK
Document type: Journal article (JA)
Publisher: Elsevier Ltd

Abstract: Coal is the main source of energy for China's economic development, but coal gangue dumps are a major source of heavy metal pollution. Bacterial communities have a major effect on the bioremediation of heavy metals in coal gangue dumps. The effects of different concentrations of heavy metals on the composition of bacterial communities in coal gangue sites remain unclear. Soil bacterial communities from four gangue sites that vary in natural heavy metal concentrations were investigated using high-throughput sequencing in this study. Correlations among bacterial communities, heavy metal concentrations, physicochemical properties of the soil, and the composition of dissolved organic matter of soil in coal gangue dumps were also analyzed. Our results indicated that Actinobacteriota, Proteobacteria, Chloroflexi, Acidobacteriota, and Gemmatimonadota were the bacterial taxa most resistant to heavy metal stress at gangue sites. Heavy metal contamination may be the main cause of changes in bacterial communities. Heavy metal pollution can foster mutually beneficial symbioses between microbial species. Microbial-derived organic matter was the main source of soil organic matter in unvegetated mining areas, and this could affect the toxicity and transport of heavy metals in soil. Polar functional groups such as hydroxyl and ester groups (A226-400) play an important role in the reaction of cadmium (Cd) and lead (Pb), and organic matter with low molecular weight (SR) tends to bind more to mercury (Hg). In addition to heavy metals, the content of nitrogen (N), phosphorus (P), and total organic carbon (TOC) also affected the composition of the bacterial communities; TOC had the strongest effect, followed by N, SOM, and P. Our findings have implications for the microbial remediation of heavy metal-contaminated soils in coal gangue sites and sustainable development. © 2023 Elsevier Ltd

Number of references: 113
Main heading: Heavy metals
Controlled terms: Bacteria - Biogeochemistry - Bioremediation - Coal - Mining - Organic carbon - Physicochemical properties - Soil pollution - Soil pollution control - Soils

Uncontrolled terms: Bacterial community - Coal gangues - Economic development - Gangue site - Heavy metal concentration - Heavy metals pollution - Soil bacterial community - Soil organic matters - Sources of energy - Total Organic Carbon

Classification code: 454.2 Environmental Impact and Protection - 481.2 Geochemistry - 483.1 Soils and Soil Mechanics - 502.1 Mine and Quarry Operations - 524 Solid Fuels - 531 Metallurgy and Metallography - 801.2 Biochemistry - 801.4 Physical Chemistry - 804.1 Organic Compounds

DOI: 10.1016/j.envpol.2023.121136

Compendex references: YES
Database: Compendex
Data Provider: Engineering Village

47. Factors influencing fault-propagation folding in the Kuqa Depression: Insights from geomechanical models

Accession number: 20230913633702

Authors: Ju, Wei (1, 2); Zhong, Yu (1); Liang, Yan (1); Gong, Lei (3); Yin, Shuai (4); Huang, Peiming (1)

Author affiliation: (1) School of Resources and Geosciences, China University of Mining and Technology, Xuzhou; 221116, China; (2) Key Laboratory of Coalbed Methane Resources and Reservoir Formation Process, Ministry of Education, Xuzhou; 221008, China; (3) Bohai-Rim Energy Research Institute, Northeast Petroleum University, Qinhuangdao; 066004, China; (4) School of Earth Science and Engineering, Xi'an Shiyou University, Xi'an; 710065, China

Corresponding author: Ju, Wei(wju@cumt.edu.cn)

Source title: Journal of Structural Geology
Abbreviated source title: J. Struct. Geol.
Volume: 168
Issue date: March 2023
Publication year: 2023
Article number: 104826
Language: English
ISSN: 01918141
Document type: Journal article (JA)
Publisher: Elsevier Ltd

Abstract: Understanding the rock mass deformation and strain state is critical to a range of endeavors. Geomechanical modeling is an excellent approach simulating the formation processes of faulting and folding, which can reproduce the geometry of fold structures and track strain and stress through the whole deformation process. In this study, five series of two-dimensional (2D) elastic-plastic finite element models were built to investigate the influences of shortening distance, ramp cutoff angle, interlayer slip, fault friction, fault number and fault slice width on structural styles and strain distribution patterns during fault-propagation folding in the Kuqa Depression of Tarim Basin. The results indicate that, i) All above mentioned factors can influence the structural style and strain distribution of fault-propagation fold (FPF) to varying degrees. Fault friction, interlayer slip and fault slice width are the most important parameters influencing the deformation geometry and strain patterns of FPF; ii) There are critical values for fault friction coefficient and shortening distance to create a secondary fold besides the FPF; iii) A "step pattern" occurs both in the forelimb and backlimb of the FPF when fault slice width reaches a certain high value; iv) Structural position in the FPF controls volumetric changes. The evolution of FPF can be divided into two stages: layer parallel shortening and volume loss, and folding; v) The steep forelimb region of FPF develops more natural fractures, which may serve as a favorable location for potential reservoirs in the Kuqa Depression. The results are also expected to provide clues for the exploration and development of oil and gas in regions with similar geological conditions. © 2023 Elsevier Ltd

Number of references: 52
Main heading: Elastoplasticity
Controlled terms: Ductile fracture - Faulting - Friction - Geomechanics - Petroleum prospecting
Uncontrolled terms: Fault friction - Fault slice width - Fault-propagation folding - Fault-propagation folds - Foldings - Geomechanical model - Interlayer slip - Kuqa depression - Structural strain - Structural styles

Compendex references: YES
Database: Compendex
Data Provider: Engineering Village

48. Preparation of a recyclable and high-performance photocatalyst AgInS2/CN/PAN for RhB and phenol degradation

Authors: Liang, Xuhua (1); Liu, Jifang (2); Guo, Hongxia (3); Li, Haohao (1, 4); Liu, Enzhou (5); Zhao, Yanyan (1); Ji, Yuliang (1); Fan, Jun (6)
Author affiliation: (1) College of Biology Pharmacy and Food Engineering, Shangluo University, Shangluo; 726000, China; (2) College of Life Sciences, Northwest University, Xi'an; 710069, China; (3) Nursing College of Anhui Sanlian University, 230000, China; (4) College of Chemistry and Chemical Engineering, Xi'an Shiyou University, Xi'an; 710000, China; (5) School of Chemical Engineering, Northwest University, Xi'an; 710069, China; (6) College of Food Science and Technology, Northwest University, Xi'an; 710069, China
Corresponding author: Liang, Xuhua(liangxuhua2012@126.com)
Abstract: Photocatalysis technology is considered as an important strategy to solve the environmental and energy crisis, but the powdered photocatalyst is difficult to recover from water environment and may lead secondary pollution, restricts its practical applications. In this work, a novel AgInS2/CN/PAN photocatalytic film with recyclable and high-performance was successfully prepared for RhB and phenol degradation. The microstructure of this photocatalytic film was evaluated by XRD, FTIR, XPS, SEM, TEM, UV–vis, Photoluminescence spectra, Transient photocurrent, etc. The as-prepared AgInS2/CN/PAN photocatalytic film exhibited the excellent photocatalytic activity, about 94.48% of RhB and about 77.71% of phenol can be degraded after 60 min visible light irradiation, respectively. The enhanced photocatalytic activity of the photocatalytic film was believed to be related to the improved light-harvest ability and the facilitated carrier transport ability between AgInS2 and CN. The AgInS2/CN/PAN photocatalytic film could be easily separate from water after photocatalytic process only through a sample filtering method, which can be reused via a simple washing and drying process. Meanwhile, biology and environment toxicities of the as-prepared samples towards Mung bean seeds were performed. This study may develop a novel strategy to rationally design the novel recyclable and high-performance photocatalysts for water pollution remediation. © 2023 Elsevier Ltd
Number of references: 45
Main heading: Biodegradation
Controlled terms: Film preparation - Fourier transform infrared spectroscopy - Indium compounds - Phenols - Photocatalytic activity - Photodegradation - Photoluminescence - Rhodium compounds - Silver compounds - Water pollution - Water treatment

Compendex references: YES
Database: Compendex
Data Provider: Engineering Village

49. Adaptive Spatiotemporal Transformer Graph Network for Traffic Flow Forecasting by IoT Loop Detectors

Authors: Huang, Boyu (1, 2); Dou, Haowen (1, 2); Luo, Yu (3); Li, Junchao (4); Wang, Jiaqi (5); Zhou, Teng (1, 2)
Author affiliation: (1) Intelligent Manufacturing Key Laboratory, Ministry of Education, Shantou; 515000, China; (2) Guangdong Provincial Key Laboratory of Infectious Diseases and Molecular Immunopathology, Shantou; 515000, China; (3) Guangdong University of Technology, School of Computer Science and Technology, Guangzhou; 510006, China; (4) Xi'an Shiyou University, Mechanical Engineering College, Xi'an; 710312, China; (5) Sun Yat-sen University, School of Pharmaceutical Sciences (Shenzhen), Guangzhou; 510275, China
Corresponding author: Zhou, Teng(zhouteng@stu.edu.cn)
Abstract: Extensive traffic flow data are received from the loop detector networks every second, which requires us to develop an effective and efficient algorithm to predict future traffic flow. However, dynamic traffic conditions on a road are not just influenced by sequential patterns in the temporal dimension, but also by other roadways in the spatial dimension. Although many successful models have been developed in previous studies to forecast future traffic flows, most of them have shortcomings in modeling spatial and temporal dependencies. In this article, we focus on spatial-temporal factors and propose a new adaptive spatial-temporal transformer graph network (ASTTGN) to improve the accuracy of traffic forecasting by jointly modeling the spatial-temporal information of road networks. Specifically, we propose an adaptive spatial-temporal transformer module, which contains two developed adaptive transformer modules for capturing dynamic spatial dependence and temporal dependence across multiple time steps, respectively. Finally, feature fusion is performed through a gated feature aggregation layer to simulate the effect of complex spatial-temporal factors on traffic conditions. In particular, the multihead attention mechanism employed by the transformer can effectively explore the potential spatial-temporal dependence patterns in different subspaces. Experimental results on two real-world traffic data sets demonstrate the superiority of the proposed model compared to existing techniques. © 2014 IEEE.
Number of references: 44
Main heading: Forecasting

Controlled terms: Deep learning - Flow graphs - Intelligent systems - Motor transportation - Roads and streets - Time series analysis - Traffic control
Uncontrolled terms: Adaptation models - Correlation - Deep learning - Intelligent transportation systems - Predictive models - Road - Spatial temporal model - Time-series analysis - Traffic flow forecasting - Transformer
Classification code: 406.2 Roads and Streets - 461.4 Ergonomics and Human Factors Engineering - 723.4 Artificial Intelligence - 921.4 Combinatorial Mathematics, Includes Graph Theory, Set Theory - 922.2 Mathematical Statistics
DOI: 10.1109/JIOT.2022.3209523
Compendex references: YES
Database: Compendex
Data Provider: Engineering Village

50. Identification of coal structures by semi-supervised learning based on limited labeled logging data

Accession number: 20225213301184

Authors: Shi, Jinxiong (1, 2, 3); Zhao, Xiangyuan (4); Zeng, Lianbo (3); Zhang, Yunzhao (5); Dong, Shaoqun (3)
Author affiliation: (1) Key Laboratory of Exploration Technologies for Oil and Gas Resources of the Ministry of Education, Yangtze University, Wuhan; 430100, China; (2) School of Geosciences, Yangtze University, Wuhan; 430100, China; (3) College of Geosciences, China University of Petroleum (Beijing), Beijing; 102249, China; (4) Petroleum Exploration and Production Research Institute of SINOPEC, Beijing; 100083, China; (5) School of Earth Sciences and Engineering, Xi'an Shiyou University, Xi'an; 710065, China
Corresponding author: Zeng, Lianbo(lbzeng@sina.com)

Source title: Fuel
Abbreviated source title: Fuel
Volume: 337
Issue date: April 1, 2023
Publication year: 2023
Article number: 127191
Language: English
ISSN: 00162361
CODEN: FUELAC
Document type: Journal article (JA)
Publisher: Elsevier Ltd

Abstract: Coal structure is a critical parameter in coalbed methane (CBM) development due to its significant impacts on methane enrichment, fluid flow and hydraulic fracturing. Traditional statistical analysis and data-driven machine learning methods for coal structure identification are highly dependent on the labeled logging data and have potential limitations when labeled logging data is limited. To address this issue, this paper proposed a semi-supervised learning method based on Laplacian support vector machine (LapSVM) to identify coal structure by using few labeled logging data. By mining the structure information from abundant unlabeled data, LapSVM can improve the model performance and alleviate the over-reliance on labeled data. To evaluate and verify the effectiveness and reliability of the proposed LapSVM method in coal structure identification, datasets collected from 32 CBM wells in the southern Qinshui Basin, China, are utilized in this study. The particle swarm optimization (PSO) is adopted for parameter optimization of LapSVM models. For the LapSVM model, the addition of unlabeled data is conducive to enhance model accuracy, and unavoidably increases the computational cost at the same time. The comparison of training, testing and blind-well test results between the LapSVM and standard support vector machine (SVM) models indicates that the LapSVM outperforms traditional SVM and possesses higher accuracy and generalization in coal structure identification. It has been demonstrated that the LapSVM can be a reliable tool for coal structure identification when limited labeled logging data is available. © 2022 Elsevier Ltd

Number of references: 60
Main heading: Methane
Controlled terms: Coal - Coal bed methane - Coal deposits - Firedamp - Flow of fluids - Laplace transforms - Learning algorithms - Learning systems - Natural gas wells - Particle swarm optimization (PSO)   - Support vector machines - Well testing
Uncontrolled terms: Coal structure - Laplacian support vector machine - Laplacians - Limited labeled-sample - Logging data - Semi-supervised learning - Structure identification - Support vector machine models - Support vectors machine - Well logging data
Classification code: 503 Mines and Mining, Coal - 512.2 Natural Gas Deposits - 512.2.1 Natural Gas Fields - 522 Gas Fuels - 524 Solid Fuels - 631.1 Fluid Flow, General - 723 Computer Software, Data Handling and Applications -

51. Numerical study of gas-liquid two-phase flow distribution of refrigerant mixtures in a vertically-upward T-junction

Authors: Feng, Zongrui (1); Li, Huixiong (1); Loh, Wai Lam (2); Lei, Xianliang (1); Liu, Jialun (3); Guo, Kaikai (4)
Author affiliation: (1) State Key Laboratory of Multiphase Flow in Power Engineering, School of Energy & Power Engineering, Xi'an Jiaotong University, Shaanxi, Xi'an; 710049, China; (2) Department of Mechanical Engineering, National University of Singapore, Singapore, 9 Engineering Drive 1, 117575, Singapore; (3) School of Mechanical Engineering, Xi'an Shiyou University, Xi'an; 710065, China; (4) Facility Design & Instrumentation institute, China Aerodynamics Research and Development Center, Sichuan, MianYang; 621000, China
Corresponding author: Li, Huixiong(huixiong@mail.xjtu.edu.cn)

Abstract: The maldistribution of gas-liquid two-phase flow will decline the efficiency of the refrigeration system as the heat transfer performance of the heat exchangers decreases. The distribution characteristics of gas-liquid two-phase flow of refrigerant mixtures R134a in the vertically-upward T-junction were investigated in this work by 3D numerical simulation using the Eulerian model. The simulations were conducted for inlet quality from 0.005 to 0.8 and inlet mass flux from 100 to 1000 kg·m-2s-1 at a saturated temperature of 272.0 K, respectively. The effect of inlet quality on the two-phase flow distribution was studied when the inlet flow patterns were intermittent flow, annular flow, stratified-wave flow, and mist flow, respectively. The fractions of the gas phase and liquid phase flowing to the branch were used to represent the gas and liquid phase distribution characteristics in the T-junction. Numerical results showed that the fraction of the gas phase flowing through the branch decreased with an increase in inlet quality within the scope of this study. The distribution uniformity of the liquid phase in the vertically-upward T-junction was the best for mist flow and the worst for stratified-wave flow at the inlet. Calculation results indicated that a decrease in the difference in the inertia forces acting on the two phases would promote the uniformity of the gas phase distribution in the vertically-upward T-junction and an increase in pressure difference at the intersection zone would lead to a larger amount of liquid phase diverting to the branch. © 2022

Number of references: 40
Main heading: Two phase flow
Controlled terms: Gases - Heat exchangers - Numerical models - Refrigerants - Refrigeration
Uncontrolled terms: 3-D numerical simulation - Distribution characteristics - Gas/liquid two phase flow - Inlet quality - Liquid phasis - Phase distribution - Phase distribution characteristic - Refrigerant r134a - T junctions - Two phases flow
Classification code: 616.1 Heat Exchange Equipment and Components - 631.1 Fluid Flow, General - 644.1 Refrigeration Methods - 644.2 Refrigerants - 803 Chemical Agents and Basic Industrial Chemicals - 921 Mathematics
Numerical data indexing: Mass 1.00E+02kg to 1.00E+03kg, Temperature 2.72E+02K, Time 2.00E+00s

Compendex references: YES
Database: Compendex
Data Provider: Engineering Village

52. Porous media flooding mechanism of nanoparticle-enhanced emulsification system

Accession number: 20231113701682
Authors: Liu, Jianbin (1, 2, 3); Liu, Shun (1, 2, 3); Zhong, Liguo (4); Li, Zelin (5); Zhang, Yalong (1, 2, 3); Du, Hengyi (1, 2, 3)
Author affiliation: (1) Xi'an Shiyou University, Xi'an; 710065, China; (2) Shaanxi Key Laboratory of Advanced Stimulation Technology for Oil & Gas Reservoirs, Xi'an; 710065, China; (3) Eng. Res. Ctr. of Devmt. and Mgmt. for Low to Ultra-low Permeability Oil Gas Reservoirs in W. China, Ministry of Education, Xi'an; 710065, China; (4) China University of Petroleum-Beijing, Beijing; 102249, China; (5) No. 8 Oil Extraction Plant of PetroChina Changqing Oilfield Company, Xi'an; 710018, China
Corresponding author: Liu, Jianbin(deleap@163.com)
Source title: Physics of Fluids
Abbreviated source title: Phys. Fluids
Volume: 35
Issue: 3
Issue date: March 2023
Publication year: 2023
Article number: 033304
Language: English
ISSN: 10706631
E-ISSN: 10897666
CODEN: PHFLE6
Document type: Journal article (JA)
Publisher: American Institute of Physics Inc.
Abstract: This study carried out interfacial tension (IFT) testing, sand surface element analysis and scanning electron microscope imaging, rock-oil-emulsification system interaction testing, and microstructure, droplet size distribution, and stability of oil in water (O/W) emulsion to clarify the porous media flooding mechanism of a hydrophilic nano-SiO2 enhanced emulsification system. The results show that by adding a small amount of nano-SiO2 (0.01 wt. %) into an anionic surfactant fatty alcohol polyoxyethylene ether sodium hydroxypropyl sulfonate (AEOSHS) solution (0.5 wt. %), the IFT of oil-water was effectively reduced, the adsorption loss of AEOSHS on the formation sand surface was reduced by more than 70%, and the droplet size of the formed O/W emulsion was reduced by 50%. This greatly improves the effective concentration of AEOSHS and emulsifies the heavy oil ability in the formation away from the injection well. Moreover, the spreading ability of oil on the core surface is greatly reduced, and the width of the diffusion zone is narrowed. Meanwhile, a very clear dividing line of oil can be seen, which shows that the wettability of the core has changed to water wet. The stability of the formed O/W emulsion was further enhanced, and the coalescence and migration process of the droplet is extremely slow. The oil recovery of the AEOSHS + nano-SiO2 system can effectively increase 21.95% of the original oil in place. Both the sand-packed tube experiment and the microscopic visual oil flooding experiment show that the system can not only expand the swept volume but also improve the oil displacement efficiency, which means that the combined system can significantly improve the oil displacement effect. © 2023 Author(s).
Number of references: 46
Main heading: Porous materials
Controlled terms: Alcohols - Anionic surfactants - Crude oil - Drops - Emulsification - Floods - Heavy oil production - Injection (oil wells) - Microemulsions - Nonionic surfactants - Oil well flooding - Scanning electron microscopy - Silica - Silicon
Uncontrolled terms: Emulsification systems - Flooding mechanism - Microscope imaging - Nano-SiO2 - Oil-in-water - Porous medium - Scanning electrons - Surface-element analysis - System interactions - Water emulsion
Classification code: 511.1 Oil Field Production Operations - 512.1 Petroleum Deposits - 549.3 Nonferrous Metals and Alloys excluding Alkali and Alkaline Earth Metals - 802.3 Chemical Operations - 803 Chemical Agents and Basic Industrial Chemicals - 804 Chemical Products Generally - 804.1 Organic Compounds - 951 Materials Science

Compendex references: YES
Database: Compendex
Data Provider: Engineering Village

53. Microstructure and Tribological Properties Evolution of Ni-Mo-Srso4 Composites as a Function of Mo Contents at Different Temperatures

Accession number: 20230062284
Authors: Liu, Feng (1); Wang, Xianfang (1); Ren, Jingshu (1); Cao, Weifeng (1); Guo, Ruisheng (2); Zhao, Wenwen (1); Jia, Junhong (3)
Author affiliation: (1) Xi'an Key Laboratory of High Performance Oil and Gas Field Materials, School of Materials Science and Engineering, Xi'an Shiyou University, Xi'An; 710065, China; (2) State Key Laboratory of Solidification Processing, Center of Advanced Lubrication and Seal Materials, School of Materials Science and Engineering, Northwestern Polytechnical University, Xi'An; 710072, China; (3) College of Mechanical and Electrical Engineering, Shaanxi University of Science and Technology, Xi'An; 710021, China
Corresponding authors: Liu, Feng(fliu@xsyu.edu.cn); Guo, Ruisheng(guoruisheng@nwpu.edu.cn)
Source title: SSRN
Issue date: February 21, 2023
Publication year: 2023
Language: English
ISSN: 15565068
Document type: Preprint (PP)
Publisher: SSRN
Abstract: Ni-Mo-SrSO4 composites with different Mo amount were prepared by hot pressing in a vacuum. The oxygen-deficient environment derived from the degradation of SrSO4 during fabrication process led to the formation of SrMoO4, Sr2NiMoO6, and SrO in the sintered composites. With the increment in the contents of Mo, excessive dissolved molybdenum atoms accelerated the oxidation of nickel in the oxygen-deficient environment, which eradicated SrMoO4 phase. As compared to sintered material containing Sr2NiMoO6 and SrO, the appearance of SrMoO4 led to a distinct decrease in the density and microhardness. To reveal the effect of SrMoO4 on the wear mechanism, the tribological properties of the sintered composites against Al2O3 ball were investigated at room temperature and 800 . The result indicated that the in-situ composite consisting of 80.75 wt.% Ni, 14.25 wt.% Mo, and 5 wt.% SrSO4 exhibited good friction and wear properties at room temperature and 800 , which was attributed to the development of the intact tribofilm with grooves consisting of SrMoO4, Sr2NiMoO6, NiO, and h-MoO3 at room temperature and the synergistic lubricating effect of SrMoO4, Sr2NiMoO6, and oxides (NiO, α–MoO3, SrMoO4, α–NiMoO4, and β–NiMoO4) at 800 . © 2023, The Authors. All rights reserved.
Number of references: 45
Main heading: Tribology
Controlled terms: Alumina - Aluminum oxide - Dissolved oxygen - Hot pressing - Layered semiconductors - Molybdenum - Molybdenum oxide - Nickel oxide - Sintering - Strontium compounds - Wear of materials
Uncontrolled terms: Lubricating effect - Microstructures properties - Mo content - Ni-mo-SrSO4 composite - Oxygen deficient - Property - Synergistic lubricating effect - Tribologcial property - Tribological properties - Wear mechanisms
Classification code: 543.3 Molybdenum and Alloys - 712.1 Semiconducting Materials - 804 Chemical Products Generally - 804.2 Inorganic Compounds - 931 Classical Physics; Quantum Theory; Relativity - 931.2 Physical Properties of Gases, Liquids and Solids - 951 Materials Science
DOI: 10.2139/ssrn.4365825
Compendex references: YES
Preprint ID: 4365825
Preprint source website: https://papers.ssrn.com/sol3/papers.cfm
Preprint ID type: SSRN
Database: Compendex

54. Microstructure and tribological properties evolution of Ni–Mo–SrSO4 composites as a function of Mo contents at different temperatures

Authors: Liu, Feng (1); Wang, Xianfang (1); Ren, Jingshu (1); Cao, Weifeng (1); Guo, Ruisheng (2); Zhao, Wenwen (1); Jia, Junhong (3)
Author affiliation: (1) Xi'an Key Laboratory of High Performance Oil and Gas Field Materials, School of Materials Science and Engineering, Xi'an Shiyou University, Xi'an; 710065, China; (2) State Key Laboratory of Solidification Processing, Center of Advanced Lubrication and Seal Materials, School of Materials Science and Engineering, Northwestern Polytechnical University, Xi'an; 710072, China; (3) College of Mechanical and Electrical Engineering, Shaanxi University of Science and Technology, Xi'an; 710021, China
Corresponding authors: Liu, Feng(fliu@xsyu.edu.cn); Guo, Ruisheng(guoruisheng@nwpu.edu.cn)

Abstract: Ni–Mo–SrSO4 composites with different Mo amount were prepared by hot pressing in a vacuum. The oxygen-deficient environment derived from the degradation of SrSO4 during fabrication process led to the formation of SrMoO4, Sr2NiMoO6, and SrO in the sintered composites. With the increment in the contents of Mo, excessive dissolved Mo atoms accelerated the oxidation of Ni in the oxygen-deficient environment, which eradicated SrMoO4 phase. As compared to sintered material containing Sr2NiMoO6 and SrO, the appearance of SrMoO4 led to a distinct decrease in the density and microhardness. To reveal the effect of SrMoO4 on the wear mechanism, the tribological properties of the sintered composites against Al2O3 ball were investigated at different temperatures. The result indicated that the in-situ composite consisting of 80.75 wt.% Ni, 14.25 wt.% Mo, and 5 wt.% SrSO4 exhibited good friction and wear properties at room temperature (RT) and 800 °C, which was attributed to the development of the intact tribofilm with grooves consisting of SrMoO4, Sr2NiMoO6, NiO, and h-MoO3 at RT and the synergistic lubricating effect of SrMoO4, Sr2NiMoO6, and oxides (NiO, α_MoO3, SrMoO4, α_NiMoO4, and β_NiMoO4) at 800 °C. © 2023 The Author(s)

55. Achieving comprehensive temperature-stable energy storage properties in core-shell Na0.4K0.1Bi0.5TiO3@(SrZrO3-BiMg0.5Sn0.5O3)@SiO2 ceramics via a multi-scale synergistic optimization

Authors: Zhang, Xiaoting (1, 2); Zhao, Lili (3); Qiu, Yu (2); Wang, Yan (1); Fan, Yueyao (4); Liu, Xueru (1); Cui, Bin (1)
Author affiliation: (1) Key Laboratory of Synthetic and Natural Functional Molecule of the Ministry of Education, Shaanxi Key Laboratory of Physico-Inorganic Chemistry, College of Chemistry and Materials Science, Northwest University, Shaanxi Province, Xi'an; 710127, China; (2) College of Chemistry & Chemical Engineering, Yan'an University, Shaanxi Province, Yan'an; 716000, China; (3) School of Information Science and Technology, Northwest University, Shaanxi Province, Xi'an; 710127, China; (4) School of Electronic Engineering, Xi'an Shiyou University, Shaanxi Province, Xi'an; 710065, China
Corresponding author: Cui, Bin(cuibin@nwu.edu.cn)

Abstract: At present, to improve the energy storage properties and wide-range temperature stability synergistically is the bottleneck of Na0.5Bi0.5TiO3 (NBT)-based energy storage ceramics. In this paper, it is expected to breakthrough this bottleneck through a multi-scale synergistic optimization (including composition, structure and preparation) integrated by the design of core–shell structure. This unique structure is constructed by coating SrZrO3-BiMg0.5Sn0.5O3 (SZ-BMS) on the surface of Na0.4K0.1Bi0.5TiO3 (NKBT), and then coating SiO2 glass to prepare NKBT@(SZ-BMS)@SiO2 ceramics. The SZ-BMS phase plays multi roles in alleviating interfacial polarization, domain reconstruction and defect regulation. The outer SiO2 layer benefits to grain size refinement and defect control. The energy storage performance of NKBT@(SZ-BMS)@SiO2 ceramics are affected by the BMS amount. When the BMS amount is 15 mol%, high breakdown strength of 301 kV/cm and polarization of 29.1 μC/cm2 are achieved in the ceramics. Ultimately, large recoverable energy density of 3.94 J/cm3 with high efficiency of 87.1% are simultaneously obtained. It also has an ultra-wide temperature stability (30–467) of dielectric properties and excellent thermal endurance of energy storage within 20–150 . The prepared NKBT@(SZ-BMS)@SiO2 ceramic is a favorable alternative for temperature-stable energy storage capacitors. © 2023 Elsevier B.V.

56. Study on the emulsification characteristics of heavy oil during chemical flooding (*Open Access*)

Accession number: 20232314195399

Authors: Liu, Jianbin (1, 2, 3); Liu, Shun (1, 2, 3); Zhong, Liguo (4); Yuan, Shibao (1, 2, 3); Wang, Qianlong (1, 2, 3); Wei, Chaoping (4, 5)
Author affiliation: (1) College of Petroleum Engineering, Xi'an Shiyou University, Xi'an; 710065, China; (2) Shaanxi Key Laboratory of Advanced Stimulation Technology for Oil & Gas Reservoirs, Xi'an; 710065, China; (3) Engineering Research Center of Development and Management for Low to Ultra-low Permeability Oil & Gas Reservoirs in West China (Ministry of Education), Xi'an; 710065, China; (4) Unconventional Petroleum Research Institute, China University of Petroleum, Beijing; 102249, China; (5) Exploration and Development Research Institute, Shengli Oilfield Company, SINOPEC, Dongying; 257015, China
Corresponding author: Liu, Jianbin(deleap@163.com)

Source title: Physics of Fluids
Abbreviated source title: Phys. Fluids
Volume: 35
Issue: 5
Issue date: May 1, 2023
Publication year: 2023
Article number: 053330
Language: English
ISSN: 10706631
E-ISSN: 10897666
CODEN: PHFLE6
Document type: Journal article (JA)
Publisher: American Institute of Physics Inc.

Abstract: Chemical flooding is a very important method to the efficient development of a heavy oil reservoir. A clear understanding of the relationship between emulsification characteristics of heavy oil during chemical flooding and test methods that current used to evaluate the properties of chemical flooding agent can be useful for oilfields development of the heavy oil. In this study, the oil-water interfacial tension (IFT) and oil in water (O/W) emulsion properties (emulsification state, droplet size, viscoelasticity, and stability) formed by six chemical flooding agents at different concentration are tested. Then, combined with the heavy oil flooding dynamics, the emulsification characteristics of heavy oil during the chemical flooding process of are studied and the influence mechanisms of O/W emulsion on oil recovery are clarified. Finally, the emulsification effect of heavy oil on the injection profile turnover is studied by parallel sand-packed tube experiments. Studies show that all six chemical flooding agents can greatly reduce the IFT of heavy oil-water (more than 90%). However, the stronger the emulsification ability, the smaller the droplet size, the better the viscoelasticity, the stronger the stability of O/W emulsion, and the better the heavy oil recovery of the chemical flooding agent. This is mainly because the most effective action stage is the time that before the O/W emulsion front flow reaches the production outlet, chemical flooding agent is injected into the formation. During this period, the amount of emulsified heavy oil, the width of emulsification zone, and the properties of formed O/W emulsion affect the heavy oil flooding efficiency. Therefore, when screening chemical flooding agents, the emulsification speed, the droplet size, and the viscoelasticity of formed O/W emulsion are the primary evaluation factors. In addition, through the parallel sand-packed tube experiment, it is found that the stronger the emulsification ability of chemical flooding agent, the better the performance of formed O/W emulsion, the stronger the profile turnover ability. For reservoirs that the water flow channel has formed, using profile control agents to effectively block dominant flow channels can improve the emulsification ability of chemical flooding agents, thus achieving the purpose of improving the swept area. The research results can provide guidance for the screening of chemical flooding agent with emulsification characteristic and construction process optimizing in the heavy oil reservoirs' development. © 2023 Author(s).

Number of references: 51
Main heading: Emulsification
Controlled terms: Chemical stability - Crude oil - Drops - Floods - Flow of water - Heavy oil production - Oil well flooding - Petroleum reservoir engineering - Petroleum reservoirs - Reservoirs (water) - Viscoelasticity
Uncontrolled terms: Chemical flooding - Droplets sizes - Emulsification characteristics - Flooding agent - Heavy oil reservoirs - Oil flooding - Oil-in-water - Oil/water - Property - Water emulsion
Classification code: 441.2 Reservoirs - 511.1 Oil Field Production Operations - 512.1 Petroleum Deposits - 512.1.1 Oil Fields - 512.1.2 Petroleum Deposits : Development Operations - 631.1.1 Liquid Dynamics - 801 Chemistry - 802.3 Chemical Operations - 931.2 Physical Properties of Gases, Liquids and Solids
Numerical data indexing: Percentage 9.00E+01%

57. A Minireview of the Influence of CO2Injection on the Pore Structure of Reservoir Rocks: Advances and Outlook

Authors: Gao, Hui (1, 2, 3); Xie, Yonggang (4, 5); Cheng, Zhilin (1, 2, 3); Wang, Chen (1, 2, 3); Li, Teng (1, 2, 3); Zhu, Xiulan (1, 2, 3); Luo, Kaiqing (1, 2, 3); Cao, Jiangfeng (1, 2, 3); Li, Ning (1, 2, 3)
Author affiliation: (1) School of Petroleum Engineering, Xi'An Shiyou University, Xi'an; 710065, China; (2) Ministry of Education, Eng. Res. Ctr. of Devmt. and Mgmt. for Low to Ultra-Low Permeability Oil Gas Reservoirs in W. China, Xi'an; 710065, China; (3) Xi'An Key Laboratory of Tight Oil (Shale Oil) Development, Xi'an; 710065, China; (4) Oil and Gas Technology Institute of Changqing Oilfield Company, PetroChina, Xi'an; 710018, China; (5) National Engineering Laboratory for Exploration and Development of Low-permeability Oil Gas Fields, Xi'an; 710018, China
Corresponding author: Gao, Hui(ghtopsun1@163.com)
Abstract: The recoverable hydrocarbon reserves of conventional oil and gas resources are very limited in China. As important alternative resources, unconventional oil and gas have become a research hotspot. Though tight reservoirs have great potential to alleviate the increasing demand, issues during the development process, such as the rapid pressure depletion, fast decline in production, low productivity, and difficulties in water injection, are usually encountered due to poor physical properties like small pore throats and strong heterogeneity of the pore structure. The CO2flooding technique could effectively replace crude oil from micro-nanopores, which is considered as a promising way to enhance the development performance of tight oil. However, precipitation and dissolution phenomena usually occur along with the CO2injection process into reservoirs, affecting the pore structure evolution and oil displacement efficiency. In addition, artificial and natural fractures will even make this process more complicated. This paper presents the commonly used experimental approaches for CO2injection into tight reservoirs and summarizes the main methods for investigating the influence of CO2injection on the pore structure of reservoir rocks. Based on this, we highlighted that more attention should be paid to the influence of fractures and their dynamic changes on the evolution of pore structure during CO2injection and the study of the solid-liquid interactions. To establish a method that could quantitatively evaluate the full-scale evolution of pore throats after CO2injection is necessary. Meanwhile, the interaction strength of precipitation and dissolution and their effects on pore structure also remain open. Finally, a rigorous framework that could reveal the evolution mechanism and characterize the multiscale pore structure involving multiple influencing factors is urgently warranted. © 2023 American Chemical Society. All rights reserved.
Number of references: 103
Main heading: Pore structure
Controlled terms: Carbon dioxide - Dissolution - Energy resources - Fracture - Nanopores - Petroleum reservoir engineering - Petroleum reservoirs - Proven reserves - Rocks

58. Surface wettability of sandstone and shale: Implication for CO2 storage

Accession number: 20232214165464
Authors: Zhang, Juan (1, 2); Zhao, Zhongjun (3); Xu, Zhenping (4); Zhang, Xiaohui (4); Zhang, Liang (5)
Author affiliation: (1) Earth Science and Engineering, Xi'an Shiyou University, Shaanxi, Xi'an; 710000, China; (2) State Key Laboratory of Oil and Gas Reservoir Geology and Exploitation (Southwest Petroleum University), Sichuan, Chengdu; 610000, China; (3) Changbei Operation Company, Fengcheng 8 Road, Weiyang District, Shaanxi, Xi'an; 710000, China; (4) Exploration and Development Research Institute, Changqing Oilfield Branch Company, PetroChina, Shaanxi, Xi'an; 710000, China; (5) Exploration and Development Research Institute, Tarim Oilfield Branch Company, PetroChina, Xinjiang, Korla; 841000, China
Corresponding author: Zhang, Juan(zhangjuan@xsyu.edu.cn)
Abstract: Reservoir wettability is an important factor controlling the CO2 geosequestration. In this study, temperature pressure and salinity effects were implemented to analyze the CO2 wettability alteration of the sandstone and shale reservoir. Previous studies on CO2 sequestration were mostly from the point of view of caprock wettability. This research is from the point of view of caprock and reservoir wettability, considers the sandstone and shale interbeded situation, which is less studied. Research results show that the contact angle of CO2/sandstone and CO2/shale decreases with pressure, which indicates that the reservoir is more CO2-wet in high pressure. In addition, the contact angle was not related to the temperature. Thirdly, the sandstones show strong hydrophilicity that has little relation with liquid salinity under standard temperature and pressure. Compared with sandstones, the hydrophilicity of the shales is weak. The CO2 wettability of shales increase with the salinity, due to the reason that shales have higher clay content and better oil saturation than the sandstones. Tests predict that low-pressure sandstone is suitable for the caprocks, high-pressure-low-temperature sandstone with better oil saturation, high-pressure-high-temperature sandstone with poor oil saturation, and low-temperature-high-pressure shale are ideal for CO2 storage. © 2023 Elsevier Ltd
Number of references: 38
Main heading: Wetting
Controlled terms: Carbon dioxide - Contact angle - Hydrophilicity - Sandstone - Shale - Temperature
Uncontrolled terms: Cap rock - CO2 storage - Geo sequestrations - High pressure - Lows-temperatures - Oil saturation - Reservoir wettability - Salinity effects - Surface wettability - Wettability alteration
Classification code: 482.2 Minerals - 641.1 Thermodynamics - 804.2 Inorganic Compounds - 931.2 Physical Properties of Gases, Liquids and Solids
DOI: 10.1016/j.ijggc.2023.103917

Compendex references: YES
Database: Compendex
Data Provider: Engineering Village

59. Halide Perovskite: A Promising Candidate for Next-Generation X-Ray Detectors (*Open Access*)

Accession number: 20225013223017
Authors: Wu, Ya (1, 2); Feng, Jiangshan (2); Yang, Zhou (2); Liu, Yucheng (2); Liu, Shengzhong (2, 3)
Author affiliation: (1) College of Chemistry and Chemical Engineering, Xi'an Shiyou University, Xi'an; 710065, China; (2) Key Laboratory of Applied Surface and Colloid Chemistry, National Ministry of Education, Shaanxi Engineering Lab for Advanced Energy Technology, School of Materials Science and Engineering, Shaanxi Normal University, Xi'an; 710119, China; (3) State Key Laboratory of Catalysis, Dalian National Laboratory for Clean Energy, Dalian Institute of Chemical Physics, Chinese Academy of Sciences, Dalian; 116023, China
Corresponding author: Liu, Yucheng(liuyc@snnu.edu.cn)
Source title: Advanced Science
Abbreviated source title: Adv. Sci.
Volume: 10
Issue: 1
Issue date: January 4, 2023
Publication year: 2023
Article number: 2205536
Language: English
E-ISSN: 21983844
Document type: Journal article (JA)
Publisher: John Wiley and Sons Inc
Abstract: In the past decade, metal halide perovskite (HP) has become a superstar semiconductor material due to its great application potential in the photovoltaic and photoelectric fields. In fact, HP initially attracted worldwide attention because of its excellent photovoltaic efficiency. However, HP and its derivatives also show great promise in X-ray detection due to their strong X-ray absorption, high bulk resistivity, suitable optical bandgap, and compatibility with integrated circuits. In this review, the basic working principles and modes of both the direct-type and the indirect-type X-ray detectors are first summarized before discussing the applicability of HP for these two types of detection based on the pros and cons of different perovskites. Furthermore, the authors expand their view to different preparation methods developed for HP including single crystals and polycrystalline materials. Upon systematically analyzing their potential for X-ray detection and photoelectronic characteristics on the basis of different structures and dimensions (0D, 2D, and 3D), recent progress of HPs (mainly polycrystalline) applied to flexible X-ray detection are reviewed, and their practicability and feasibility are discussed. Finally, by reviewing the current research on HP-based X-ray detection, the challenges in this field are identified, and the main directions and prospects of future research are suggested. © 2022 The Authors. Advanced Science published by Wiley-VCH GmbH.
Number of references: 222
Main heading: Perovskite
Controlled terms: Metal halides - Polycrystalline materials - Single crystals - X ray absorption - X ray detectors
Uncontrolled terms: Bulk resistivity - Halide - Halide perovskites - Optical-bandgap - Photo-voltaic efficiency - Photoelectrics - Photovoltaics - X-ray absorptions - X-ray detections - X-ray detector
Classification code: 482.2 Minerals - 711 Electromagnetic Waves - 804 Chemical Products Generally - 933.1 Crystalline Solids
DOI: 10.1002/advs.202205536

Compendex references: YES
Open Access type(s): All Open Access, Gold, Green
Database: Compendex
Data Provider: Engineering Village

60. Preparation of SiO2-Fluorinated Acrylate Polymer Nanoemulsions (SCFs) and Their Application as Depressurization and Injection Treatment Agents

Accession number: 20225213289180
Authors: Wu, Chunping (1, 2, 3); Ye, Zhongbin (3); Qiao, Dongyu (4); Wang, Junqi (2); Tang, Lei (5); Lai, Nanjun (1, 2, 3)
Author affiliation: (1) College of Chemistry and Chemical Engineering, Southwest Petroleum University, Sichuan, Chengdu; 610500, China; (2) The Key Lab. of Well Stability and Fluid Rock Mechanics in Oil and Gas Reservoir of Shaanxi Prov., Xi'An Shiyou University, Shaanxi, Xi'an; 710065, China; (3) Oil and Gas Field Applied Chemistry Key Laboratory of Sichuan Province, Southwest Petroleum University, Sichuan, Chengdu; 610500, China; (4) Engineer Technology Research Institute, CNPC Xibu Drilling Engineering Company Limited, Xinjiang, Urumqi; 830000, China; (5) Sichuan Ruidong Technology Co., Ltd, Sichuan, Chengdu; 610500, China
Corresponding authors: Lai, Nanjun(lainanjun@126.com); Ye, Zhongbin(yezb@swpu.edu.cn)
Source title: Energy and Fuels
Abbreviated source title: Energy Fuels
Volume: 37
Issue: 1
Issue date: January 5, 2023
Publication year: 2023
Pages: 350-359
Language: English
ISSN: 08870624
E-ISSN: 15205029
CODEN: ENFUEM
Document type: Journal article (JA)
Publisher: American Chemical Society
Abstract: For water injection development in low-permeability reservoirs, nanoscale SiO2-fluorinated acrylate polymer nanoemulsions (SCFs) with good properties were prepared through core-shell emulsion polymerization. The results show that nano-SiO2 particles are well dispersed, the average particle size of the SCFs is 113 nm, and the synergy among fluoride chain segments is good and effectively improves the utilization of fluorine atoms. SCFs form a low-surface-energy nanoscale hydrophobic film on the rock surface, which changes the original rock surface micro- or nanostructure, resulting in a water contact angle of up to 120° at the core. At 60 °C, the interfacial tension (IFT) between a 1500 mg/L SCF dispersion and white mineral oil is 1.86 mN/m, decreasing by 95.67% relative to the oil-water IFT at room temperature. The core flooding experiment shows that the depressurization rate reaches 29.62% in the 1500 mg/L SCF dispersion. Therefore, SCFs have broad application prospects in processes that eliminate water lock, reduce injection pressure, and increase injection volume. © 2022 American Chemical Society.
Number of references: 57
Main heading: Silica
Controlled terms: Contact angle - Dispersions - Emulsification - Emulsion polymerization - Fluorine compounds - Nanotechnology - Particle size - Reservoirs (water) - Silicon
Uncontrolled terms: Acrylate polymers - Core shell emulsion - Depressurizations - Fluorinated acrylate - Low-permeability reservoirs - Nano scale - Nano-SiO2 - Nanoemulsion - Property - Rock surfaces
Classification code: 441.2 Reservoirs - 549.3 Nonferrous Metals and Alloys excluding Alkali and Alkaline Earth Metals - 761 Nanotechnology - 802.3 Chemical Operations - 815.2 Polymerization - 931.2 Physical Properties of Gases, Liquids and Solids - 951 Materials Science

61. Process Intensification in Gas–Liquid Mass Transfer by Modification of Reactor Design: A Review

Authors: Zhang, Huan (1, 2); Song, Naijian (1); Yu, Tao (3); Qu, Chengtun (3, 4)
Author affiliation: (1) College of Chemistry and Material, Weinan Normal University, Weinan; 714099, China; (2) Oil & Gas Field Applied Chemistry Key Laboratory of Sichuan Province, Chengdu; 610500, China; (3) College of Chemistry and Chemical Engineering, Shaanxi Province Key Laboratory of Environmental Pollution Control and Reservoir Protection Technology of Oilfields, Xi'an Shiyou University, Xi'an; 710065, China; (4) State Key Laboratory of Petroleum Pollution Control, CNPC Research Institute of Safety and Environmental Technology, Beijing; 102206, China
Corresponding author: Zhang, Huan(zhuan@wnu.edu.cn)

Abstract: Process intensification is one way of developing new efficient production pathways for the chemical industry to overcome the increasing global energy demand and solve global energy and environmental problems. Process intensification plays an important role in the gas–liquid mass transfer processes. Herein, an overview of the development in gas–liquid mass transfer enhancement is provided. Classical mass transfer models such as two-film theory, penetration theory, and surface renewal theory are analyzed. Major enhancement methods, namely, mechanical modification of reactor, are summarized and discussed here. The most recent accomplishments in gas–liquid mass transfer engineering are also provided. This review is expected to inspire new research on gas–liquid mass transfer engineering to enhance the future development and potential applications of gas–liquid mass transfer in scientific and industrial fields. Suggestions for the enhancement of gas–liquid mass transfer are also provided. © 2023 Wiley-VCH GmbH.

62. Study on sustained-release kinetics of intelligent tracer for water search in horizontal wells

Authors: Jing, Cheng (1, 2); Wang, Qiang (3); Ma, Rui (3); Deng, Qingyong (4); Qi, Aojiang (1, 2); Wang, Jian (5); Lin, Jia'en (1, 2); Xu, Jianping (1, 2)
Author affiliation: (1) School of Petroleum Engineering, Xi'an Shiyou University, Shaanxi, Xi'an; 710065, China; (2) Engineering Research Center of Development and Management for Low to Extra-Low Permeability Oil & Gas Reservoirs in West China, Ministry of Education, Shaanxi, Xi'an; 710065, China; (3) Northwest Oilfield Company, Sinopec, Xinjiang, Urumqi; 830011, China; (4) Petrochina ChangQing Oilfield Company Oil Production Plant, NO.11, Ningxia, Guyuan; 756500, China; (5) Research Institute of Exploration and Development, Shengli Oilfield Co., Sinopec, Shandong, Dongying; 257015, China
Corresponding author: Jing, Cheng(jich.0704@163.com)

Abstract: At present, finding and plugging water in horizontal wells has become both the main difficulty and also the key for the sustainable and effective development of horizontal wells. Intelligent tracer technology for finding water can directly indicate the position and intensity of water outlets in a horizontal interval and it has broad application prospects. Currently, however, the interpretation of this technology in the field assumes that the intelligent tracer in each section of the horizontal well is released at an equal speed, which reduces the reliability of interpretation results. In order to improve the interpretation model for finding water in horizontal wells with intelligent tracers, it is necessary to further clarify the controlling factors of intelligent tracer release and its variation law. Therefore, using an independently developed water-soluble intelligent tracer, macroscopic static and dynamic release experiments were carried out, as well as CT scanning microscopic experiments, and a one-dimensional sustained-release dynamical model of the intelligent tracer was established based on the microexperimental results. A static non-scour experiment showed that the polymer skeleton is the fundamental reason for the tracer's sustained release. A dynamic scour experiment showed that temperature and external scour flow rate are the main factors affecting the release of intelligent tracer and that the greater the temperature and scour flow rate, the greater the cumulative release amount. Microcosmic release experiments showed that the release of intelligent tracer is a process of gradual dissolution from outside to inside, as well as diffusion from outside, with an obvious dynamic interface. Furthermore, the results of the dynamic model analysis were in agreement with those of the macroscopic scour experiments. The results of this study confirm that the influence of temperature and scour speed on intelligent tracer release should be considered in the interpretation model of intelligent tracer water search in horizontal wells, and they provide guidance and have practical significance for expanding the application of these tracers in oil and gas field development. © 2023 Elsevier B.V.

Main heading: Gas industry
Controlled terms: Computerized tomography - Horizontal wells - Scour
Uncontrolled terms: Dynamical modeling - Fluid flushing velocity - Intelligent tracer - Interpretation model - Release experiments - Sustained release - Sustained release kinetics - Sustained-release dynamical model - Tracer concentration - Tracer technology
Classification code: 512.1.1 Oil Fields - 522 Gas Fuels - 723.5 Computer Applications - 951 Materials Science
Compendex references: YES

63. An X-ray activatable gold nanorod encapsulated liposome delivery system for mitochondria-targeted photodynamic therapy (PDT)

Authors: Gu, Xuefan (1, 4, 5); Shu, Tiantian (1); Deng, Wei (3); Shen, Chao (5); Wu, Youshen (2)
Author affiliation: (1) College of Chemistry and Chemical Engineering, Xi'an Shiyou University, Shaanxi, Xi'an; 710065, China; (2) Department of Chemistry, School of Science, Xi'an Jiaotong University, Shaanxi, Xi'an; 710049, China; (3) School of Biomedical Engineering, University of Technology Sydney, Sydney, Australia; (4) ARC Centre of Excellence for Nanoscale Biophotonics, Graduate School of Biomedical Engineering, University of New South, Wales Kensington, NSW; 2052, Australia; (5) Faculty of Science and Engineering, Macquarie University, Sydney; NSW; 2109, Australia
Corresponding author: Wu, Youshen(wuyoushen@mail.xjtu.edu.cn)
Abstract: In this work, we developed a mitochondria-targeted nanomaterial for neoadjuvant X-ray-triggered photodynamic therapy of rectal cancer. Herein, we designed a biodegradable liposome incorporating a photosensitizer, verteporfin, to generate X-ray-induced reactive oxygen species, gold nanorods as radiation enhancers, and triphenylphosphonium as the mitochondrial targeting moiety. The average size of the nanocarrier was about 150 nm. Due to the synergetic effect between X-ray and a combination of verteporfin and gold nanorods, as well as precise site-targeted TPP-modified liposomal nanocarriers, our nanoconjugates generated sufficient cytotoxic singlet oxygen within the mitochondria under X-ray irradiation, triggering the loss of membrane potential and mitochondria-related apoptosis of cancer cells. © 2023 The Royal Society of Chemistry
Number of references: 46
Main heading: Mitochondria
Controlled terms: Cancer cells - Cell death - Diseases - Gold - Nanorods - Oxygen - Photodynamic therapy - Photosensitizers - Plasmons
Uncontrolled terms: Average size - Delivery systems - Gold nanorod - Mitochondrias - Nanocarriers - Photosensitiser - Radiation enhancers - Reactive oxygen species - Rectal cancer - Synergetic effect
Classification code: 461.2 Biological Materials and Tissue Engineering - 461.6 Medicine and Pharmacology - 461.9 Biology - 547.1 Precious Metals - 741.1 Light/Optics - 761 Nanotechnology - 804 Chemical Products Generally - 931.3 Atomic and Molecular Physics - 932.3 Plasma Physics - 933 Solid State Physics
Numerical data indexing: Size 1.50E-07m
Compendex references: YES

64. Direct Observation and Real-Time Tracking of an Extraordinarily Stable Folding Intermediate in Mitotic Arrest Deficient Protein 2 Folding by Single-Molecule Fluorescence Resonance Energy Transfer

Accession number: 20230413428194

Authors: Hu, Xiang (1, 2); Zhao, Jincheng (1, 2); Zhao, Yuanyuan (1, 3); Zhang, Huiting (1, 2); Wang, Qian (1, 4); Ge, Baosheng (1, 2); Wang, Xiaoqiang (1, 2); He, Hua (1, 2); Nau, Werner M. (5); Wang, Xiaojuan (1, 2); Huang, Fang (1, 2)

Author affiliation: (1) State Key Laboratory of Heavy Oil Processing, China University of Petroleum (East China), Qingdao; 266580, China; (2) Department of Biological and Energy Chemical Engineering, China University of Petroleum (East China), Qingdao; 266580, China; (3) Department of Chronic and Non-communicable Disease Control and Prevention, Qingdao Center for Disease Control and Prevention, Qingdao; 266033, China; (4) College of Chemistry and Chemical Engineering, Xi'An Shiyou University, Xi'an; 710065, China; (5) School of Science, Constructor University, Bremen; 28759, Germany

Corresponding authors: Wang, Xiaojuan(xwang@upc.edu.cn); Huang, Fang(fhuang@upc.edu.cn)

Abstract: Although ensemble experiments have suggested that mitotic arrest deficient protein 2 (Mad2), a metamorphic protein, has folding intermediates, direct evidence and characterization are not available. It remains an outstanding challenge to capture the folding intermediates in real time, which is crucial to elucidate the folding mechanism, but the folding intermediates are normally unstable and only exist transiently. By combining confocal-microscopy-based and total internal reflection fluorescence (TIRF)-microscopy-based single-molecule Förster resonance energy transfer (sm-FRET) techniques, we have investigated the folding/unfolding process of Mad2 and captured its folding intermediate at the single-molecule level. This provides direct evidence for the existence of an intermediate along the folding pathway of Mad2. The folding intermediate proved to be extraordinarily stable, with an extremely long average dwell time of 2.3 s under the conditions of 3 M GdmCl at ambient temperature. The folding trajectories obtained from TIRF experiments further suggest that the intermediate is on-pathway to native Mad2. © 2023 American Chemical Society.

Number of references: 40
Main heading: Proteins
Controlled terms: Energy transfer - Forster resonance energy transfer - Molecules - Refractive index
Uncontrolled terms: Direct observations - Fluorescence resonance energy transfer - Folding intermediates - Folding mechanism - Foldings - Mitotic arrest - Real time tracking - Real- time - Single molecule fluorescence - Total internal reflection fluorescence microscopy
Classification code: 741.1 Light/Optics - 804.1 Organic Compounds - 804.2 Inorganic Compounds - 931 Classical Physics; Quantum Theory; Relativity - 931.3 Atomic and Molecular Physics
Numerical data indexing: Time 2.30E+00s
DOI: 10.1021/acs.jpclett.2c03181

Compendex references: YES
Database: Compendex
Data Provider: Engineering Village

65. Microstructure and properties of X100 large-deformability pipeline steel based on heating on-line partitioning

Accession number: 20231113708011

Authors: Cheng, Shixia (1, 2); Lv, Rensa (3); Cheng, Fei (4); Han, Bin (5); Fu, Anqing (2); Zhang, Xiaoyong (6); Zhang, Jianxun (1); Feng, Yaorong (2); Gao, Huilin (6)

Author affiliation: (1) State Key Laboratory for Mechanical behavior of Materials, Xi'an Jiaotong University, Xi'an; 710049, China; (2) CNPC Tubular Goods Research Institute, Xi'an; 710077, China; (3) NO. 3 Oil Production Plant

of Changqing Oilfield Company, Yinchuan; 750000, China; (4) NO. 8 Oil Production Plant of PetroChina Changqing Oilfield Company, Xi'an; 710016, China; (5) NO. 4 Oil Production Plant of PetroChina Changqing Oilfield Company, Jingbian; 718500, China; (6) School of Materials Science and Engineering, Xi'an Shiyou University, Xi'an; 710065, China

Corresponding authors: Cheng, Shixia; Feng, Yaorong
Abstract: It is often assumed that high strength and good plasticity cannot be obtained at the same time. However, a kind of X100 pipeline steel with a multiphase structure of bainite and fine M/A constituent has not only high strength and toughness but also excellent plasticity. In this paper, Heating on-line partitioning (HOP) was performed on a type of X100 pipeline steel to achieve the multiphase structure. Carbon atoms diffuse from bainite to austenite during the HOP process, improving the stability of austenite and increasing the volume fraction of retained austenite. Meanwhile, bainite laths widen and dislocation density drops, increasing the plasticity. On the other hand, carbides precipitation and the formation of martensite provide the steel with high strength. © 2023 Elsevier Ltd

Number of references: 49
Main heading: Bainite
Controlled terms: Austenite - Bainitic transformations - Carbides - High strength steel - Microstructure - Pipelines - Plasticity - Steel pipe
Uncontrolled terms: (B+M/A) x100 pipeline steel - Excellent deformability - Heating on-line partitioning - High strength and toughness - High-strength - M/A constituents - Microstructure and properties - Multi-phase structures - Pipeline steel - X100 pipeline steels
Classification code: 531.2 Metallography - 545.3 Steel - 619.1 Pipe, Piping and Pipelines - 804.2 Inorganic Compounds - 812.1 Ceramics - 951 Materials Science
DOI: 10.1016/j.mtcomm.2023.105771
Compendex references: YES
Database: Compendex
Data Provider: Engineering Village

66. A Bithiazole-Substituted Donor for High-Efficiency Thick Ternary Organic Solar Cells via Regulation of Crystallinity and Miscibility

Accession number: 20231914063053
Authors: Zou, Wentao (1); Han, Chenyang (1, 2); Zhang, Xu (1); Qiao, Jiawei (3); Yu, Jifa (4); Xu, Huajun (1); Gao, Huanhuan (2); Sun, Yanna (1); Kan, Yuanyuan (1); Hao, Xiaotao (3); Lu, Guanghao (4); Yang, Yingguo (5); Gao, Ke (1)
Author affiliation: (1) Shandong Provincial Key Laboratory for Science of Material Creation and Energy Conversion, Science Center for Material Creation and Energy Conversion, Institute of Frontier and Interdisciplinary Science, Shandong University, Qingdao; 266237, China; (2) College of New Energy, Xi'an Shiyou University, Xi'an; 710065, China; (3) School of Physics, State Key Laboratory of Crystal Materials, Shandong University, Jinan; 250100, China; (4) Frontier Institute of Science and Technology, Xi'an Jiaotong University, Xi'an; 710054, China; (5) School of Microelectronics, Fudan University, Shanghai; 200433, China
Corresponding authors: Sun, Yanna(ynsun@sdu.edu.cn); Kan, Yuanyuan(yykan@sdu.edu.cn); Gao, Ke(kegao@sdu.edu.cn)
Source title: Advanced Energy Materials
Abbreviated source title: Adv. Energy Mater.

Abstract: Organic solar cells (OSCs) with thick active layers exhibit great potential for future roll-to-roll mass production. However, increasing the thickness of the active layer generally leads to unfavorable morphology, which decreases the device's performance. Therefore, it is a critical challenge to achieve OSCs with high efficiency and thick film simultaneously. Herein, a small molecular donor, ZW1, incorporating a bithiazole unit along with a thiophene group as a π_bridge is reported. ZW1 with high crystallinity is employed to fabricate D18:ZW1:Y6 ternary devices, which enhances the crystallization, optimizes the morphology, and suppresses bimolecular recombination. Additionally, ZW1 shows better miscibility with D18, resulting in the preferred vertical phase distribution. As a result, an outstanding power conversion efficiency (PCE) of 18.50% is realized in ternary OSCs with 120 nm active layer thickness. Importantly, the thick ternary OSCs attain a high PCE of 16.67% (thickness ≈ 300 nm), significantly higher than the corresponding binary devices (13.50%). The PCE of 16.67% is one of the highest values for thick-film OSCs reported to date. This work demonstrates that the incorporation of highly crystalline small-molecule donors into ternary OSCs, possessing good miscibility with host materials, presents an effective strategy for fabricating highly efficient thick OSCs. © 2023 Wiley-VCH GmbH.

Number of references: 46
Main heading: Thick films
Controlled terms: Conversion efficiency - Crystallinity - Molecules - Morphology - Organic solar cells - Solubility
Uncontrolled terms: Active Layer - Bithiazole - Cristallinity - Higher efficiency - Power conversion efficiencies - Roll to Roll - Small molecule donor - Small molecules - Ternary organic solar cell - Thick active layers
Classification code: 525.5 Energy Conversion Issues - 702.3 Solar Cells - 801.4 Physical Chemistry - 931.2 Physical Properties of Gases, Liquids and Solids - 931.3 Atomic and Molecular Physics - 933.1 Crystalline Solids - 951 Materials Science
Numerical data indexing: Percentage 1.35E+01%, Percentage 1.667E+01%, Percentage 1.85E+01%, Size 1.20E-07m, Size 3.00E-07m
DOI: 10.1002/aenm.202300784

Compendex references: YES
Database: Compendex
Data Provider: Engineering Village

67. Petrogenesis and tectonic implications of the early Mesozoic granitoids in the northern Alxa region, Central Asian Orogenic Belt

Accession number: 20231914067293

Authors: Zhao, Xiaochen (1); Liu, Chiyang (2); Wang, Jianqiang (2); Niu, Yazhuo (3); Huang, Lei (2); Zhang, Shaohua (4); Du, Fangpeng (1); Peng, Heng (2); Chen, Yingtao (1); Peng, Tao (1); Mao, Zhengzheng (1)
Author affiliation: (1) College of Geology and Environment, Xi'an University of Science and Technology, Xi'an; 710054, China; (2) State Key Laboratory of Continental Dynamics, Department of Geology, Northwest University, Xi'an; 710069, China; (3) Key Laboratory for the Study of Focused Magmatism and Giant Ore Deposits, Xi'an Centre of Geological Survey (Northwest China Centre of Geoscience Innovation), China Geological Survey, Xi'an; 710054, China; (4) Shaanxi Key Laboratory of Petroleum Accumulation Geology, School of Earth Sciences and Engineering, Xi'an Shiyou University, Xi'an; 710065, China
Corresponding authors: Zhao, Xiaochen(zxcnwu@126.com); Wang, Jianqiang(wjq@nwu.edu.cn)

Abstract: The northern Alxa region is located in the central segment of the southern Central Asian Orogenic Belt. Many controversies and deficiencies still exist regarding the magma source characteristics, petrogenesis and tectonic regimes during the late Palaeozoic - early Mesozoic period within this region. This study presents whole-rock compositions and zircon U-Pb and Lu-Hf isotopic data for three early Mesozoic I- and A-type granitic plutons occurring in the northern Alxa region. The Haerchaoenji and Chahanhada I-type granitoids yielded zircon ^{206}Pb-^{238}U ages of 245 ± 5 Ma and 245 ± 2 Ma, respectively. The variable positive zircon $I\mu Hf(t)$ values between +1.8 and +11.8, with young TDM ages of 425-837 Ma, indicate that these I-type granitoids were mainly derived from juvenile crustal materials. The Wulantaolegai pluton has a zircon ^{206}Pb-^{238}U age of 237 ± 2 Ma and is classified as having high-K calc-alkaline A-type affinity. Furthermore, the positive zircon $I\mu Hf(t)$ values of the Wulantaolegai granite range from +3.3 to +8.7 with young TDM ages of 545-778 Ma, suggesting the involvement of a juvenile crustal source as well. Furthermore, the major-element compositions of the Chahanhada and Wulantaolegai granites suggest the input of metasedimentary components. Geochemically, the Haerchaoenji and Chahanhada I-type granitoids show an arc affinity, while the Wulantaolegai granite exhibits a post-collisional affinity. However, with regional data, we suggest that the Haerchaoenji and Chahanhada I-type granitoids were also emplaced in a post-collisional setting, and the arc affinity was probably inherited from recycled subduction-related materials. These lines of evidence obtained in this study enable us to argue that the Palaeo-Asian Ocean in the central segment of the Central Asian Orogenic Belt closed before Middle Triassic time. © The Author(s), 2022. Published by Cambridge University Press.

Number of references: 171
Main heading: Zircon
Controlled terms: Binary alloys - Geochemistry - Geochronology - Granite - Hafnium - Hafnium alloys - Isotopes - Lead alloys - Lutetium alloys - Petrology - Tectonics - Uranium alloys
Uncontrolled terms: Central Asian orogenic belt - Collisional - Granitoids - Hf isotopic composition - Isotopic composition - Mesozoic - Northern alxa region - Petrogenesis - Tectonic implications - U-Pb geochronology
Classification code: 481.1 Geology - 481.1.2 Petrology (Before 1993, use code 482) - 481.2 Geochemistry - 481.3 Geophysics - 482.2.1 Gems - 546.1 Lead and Alloys - 547 Minor, Precious and Rare Earth Metals and Alloys - 547.2 Rare Earth Metals - 549.3 Nonferrous Metals and Alloys excluding Alkali and Alkaline Earth Metals - 622.1 Radioactive Materials, General
Numerical data indexing: Age 2.37E+08yr, Age 2.45E+08yr, Age 4.25E+08yr to 8.37E+08yr, Age 5.45E+08yr to 7.78E+08yr

68. Ultra-low interfacial tension Anionic/Cationic surfactants system with excellent emulsification ability for enhanced oil recovery

Authors: Liu, Jianbin (1, 3, 4); Liu, Shun (1, 3, 4); Zhong, Liguo (2); Wang, Pan (5); Gao, Pengchao (6); Guo, Qihua (7)
Author affiliation: (1) Xi'an Shiyou University, Xi'an; 710065, China; (2) China University of Petroleum-Beijing, Beijing; 102249, China; (3) Shaanxi Key Laboratory of Advanced Stimulation Technology for Oil & Gas Reservoirs, Xi'an; 710065, China; (4) Engineering Research Center of Development and Management for Low to Ultra-low Permeability Oil & Gas Reservoirs in West China (Ministry of Education), Xi'an; 710065, China; (5) Shaanxi Yanchang Petroleum (Group) Co., Ltd, Yanan; 716000, China; (6) Changqing Oilfield Branch of CNPC, Xi'an; 710018, China; (7) Changqing Drilling Company of CNPC Chuanqing Drilling Engineering Co., Ltd., Xi'an; 710021, China
Corresponding author: Liu, Jianbin(deleap@163.com)

Abstract: Droplet size and stability of the O/W emulsion formed by heavy oil determine its fluidity in formation porous media. Hence, an anionic/cationic surfactants system of with excellent emulsification ability, ultra-small droplet size, and reduced oil–water interfacial tension (IFT) to ultra-low level was developed in this study. The AEOSHS/DTAC system can reduce oil–water IFT to ultra-low level within the molar ratio of 4:6 to 6:4. Due to the hydrophilicity of sulfonic acid group and ether group, the precipitation-dissolution balance of AEOSHS/DTAC system is well improved, and its solubility in is enhanced, and transparent solutions can be formed in a molar ratio of 10:0 to 0:10. The droplet size of O/W emulsion formed can as low as 0.6 μm when the molar ratio is 5:5. Moreover, the stability of O/W emulsion is greatly improved. The coalescence and migration process of O/W emulsion is very slow, and the stability is excellent. The dehydration rate after 24 h is only 6%, with the dehydration speed of only 0.25 %·h-1. AEOSHS/DTAC can enhance the heavy oil recovery by 22.05%. Because the droplet size of W/O emulsion is much smaller than porous diameter, the pressure does not increase during the system injection and subsequent water flooding. The AEOSHS/DTAC system is composed by anionic and cationic surfactant, which can attract each other at the interface to form a compound molecular layer. So, the repulsion between molecules on the oil–water interface is greatly reduced, making the arrangement of molecular is tighter, and the adsorption layer is more stable (The occupied area of a single molecule is only 0.06 nm2). The surface activity and interfacial activity are higher, and the droplet size is smaller, and the stability is stronger. © 2023 Elsevier B.V.

Number of references: 62
Main heading: Porous materials
Controlled terms: Anionic surfactants - Cationic surfactants - Crude oil - Dehydration - Drops - Dyes - Emulsification - Emulsions - Enhanced recovery - Heavy oil production - Hydrophilicity - Molar ratio - Molecules - Stability
Uncontrolled terms: Droplet stability - Droplets sizes - Enhanced-oil recoveries - Molar ratio - O/W emulsions - Oil/water - Porous medium - Surfactant system - Ultra-low interfacial tension - Ultra-small
Classification code: 511.1 Oil Field Production Operations - 512.1 Petroleum Deposits - 801.4 Physical Chemistry - 802.2 Chemical Reactions - 802.3 Chemical Operations - 803 Chemical Agents and Basic Industrial Chemicals - 804 Chemical Products Generally - 804.1 Organic Compounds - 931.3 Atomic and Molecular Physics - 951 Materials Science
Numerical data indexing: Percentage 2.205E+01%, Percentage 2.50E-01%, Percentage 6.00E+00%, Size 6.00E-07m, Size 6.00E-11m, Time 8.64E+04s
DOI: 10.1016/j.molliq.2023.121989

Compendex references: YES
Database: Compendex
Data Provider: Engineering Village

69. Size effect of failure mode of thermally damaged torus granite

Accession number: 20230413442716
Authors: Li, Pengfei (1); Sun, Qiang (1, 2); Gao, Qian (3); Jia, Hailiang (4); Zhang, YuLiang (5); Hu, Jianjun (6)
Author affiliation: (1) College of Geology and Environment, Xi'an University of Science and Technology, Shaanxi, Xi'an; 710054, China; (2) Shaanxi Provincial Key Laboratory of Geological Support for Coal Green Exploitation, 710054, China; (3) College of Petroleum Engineering, Xi'an Shiyou University, Shanxi, Xi'an; 710065, China; (4) College of Architecture and Civil Engineering, Xi'an University of Science and Technology, Shaanxi, Xi'an; 710054, China; (5) School of Civil and Transportation Engineering, Hebei University of Technology, Tianjin; 300401, China; (6) College of Water Resource and Hydropower, Sichuan University, Sichuan, Chengdu; 610065, China
Corresponding authors: Li, Pengfei(lipengfei@stu.xust.edu.cn); Sun, Qiang(sunqiang04@cumt.edu.cn)
Source title: International Journal of Rock Mechanics and Mining Sciences
Abbreviated source title: Int. J. Rock Mech. Min. Sci.
Volume: 163
Issue date: March 2023
Publication year: 2023
Article number: 105331
Language: English
ISSN: 13651609
CODEN: IRMGBG
Document type: Journal article (JA)
Publisher: Elsevier Ltd
Abstract: The rocks around wellbores in energy-storage areas are affected by high temperatures and thermal stresses during the extraction of geothermal resources. In this study, the mechanical properties of torus granite samples with different aperture ratios and sizes are experimentally investigated at high temperatures. Further, Acoustic Emission (AE) and Digital Image Correlation (DIC) technology are used to monitor the deformation and failure process of torus granites. The research results show that the radial peak load decreases exponentially with increases in the aperture ratio, temperature, and thermal damage. 400 °C is the critical threshold for the strength instability of the torus granite. According to the failure characteristics. When the aperture ratio λ © 2023 Elsevier Ltd
Number of references: 86
Main heading: Granite
Controlled terms: Acoustic emission testing - Cracks - Failure (mechanical) - Failure modes - Geothermal fields - Image correlation
Uncontrolled terms: Acoustic-emissions - Aperture ratio - Digital image correlations - Disruption trace - Highest temperature - Supercritical - Supercritical geothermal - Tensile crack - Von mise strain - Von Mises
Classification code: 481.3.1 Geothermal Phenomena - 615.1 Geothermal Energy - 723.2 Data Processing and Image Processing - 751.2 Acoustic Properties of Materials
Numerical data indexing: Temperature 6.73E+02K, Temperature 8.73E+02K
DOI: 10.1016/j.ijrmms.2023.105331
Compendex references: YES
Database: Compendex
Data Provider: Engineering Village

70. Recent development of sludge biochar-based catalysts in advanced oxidation processes for removing wastewater contaminants: A review

Accession number: 20231814044053
Authors: Zhang, Huan (1, 2); Zhang, Ming (3); Zhang, Hongli (1); Yu, Tao (4); Qu, Chengtun (4, 5)
Author affiliation: (1) College of Chemistry and Material, Weinan Normal University, Weinan; 714099, China; (2) Oil &Gas Field Applied Chemistry Key Laboratory of Sichuan Province, Chengdu; 610500, China; (3) China Railway Water Group Co. Ltd, Xi'an; 710100, China; (4) College of Chemistry and Chemical Engineering, Shaanxi Province Key Laboratory of Environmental Pollution Control and Reservoir Protection Technology of Oilfields, Xi'an Shiyou University, Xi'an; 710065, China; (5) State Key Laboratory of Petroleum Pollution Control, CNPC Research Institute of Safety and Environmental Technology, Beijing; 100000, China
Corresponding author: Zhang, Huan(zh_228611@163.com)
Source title: Fuel
Abbreviated source title: Fuel
Volume: 348
Issue date: September 15, 2023
Publication year: 2023
Article number: 128444
Language: English
ISSN: 00162361
CODEN: FUELAC
Document type: Journal article (JA)
Publisher: Elsevier Ltd

Abstract: Sewage sludge (SS) is a by-product of sewage treatment plant and a typical solid waste, which has dual properties of pollution and recycling. Using SS as raw material to prepare biochar-based catalytic materials for catalysis in water environment is a new way of sludge reduction and resource utilization. Sludge is a mixture of biomass organic matter, various inorganic oxides, metal ions and microorganisms; hence, carbon-based catalyst or carrier material prepared by sludge has readily available raw materials, excellent pore structure, dispersed active sites, easy regulation of surface chemical functional groups, and high specific surface area. It has been widely used in advanced oxidation processes (AOPs) and catalysis fields, such as catalytic H_2O_2 heterogeneous Fenton reaction, catalytic degradation based on persulfate (PS) and peroxymonosulfate (PMS), composite photocatalytic reaction, heterogeneous catalytic wet air oxidation and electrochemical catalytic oxidation. In this paper, the modification method for sludge biochar-based catalyst material is described. The key active sites and catalytic mechanism of sludge biochar-based catalysts in different oxidation systems are further revealed by examining the structure–activity relationship between the physical and chemical properties of the material and catalysis and their characteristics in the field of catalysis in water environment. Lastly, the main problems in this field and the future development direction were put forward to provide important reference for the further realization of the high-value-added resource utilization of sludge biochar. © 2023 Elsevier Ltd

Number of references: 207
Main heading: Catalytic oxidation
Controlled terms: Catalysis - Catalyst activity - Degradation - Metal ions - Pore structure - Sewage sludge - Sewage treatment plants - Wastewater treatment
Uncontrolled terms: Activation method - Active site - Advanced Oxidation Processes - Biochar - Catalysis in water - Catalyst material - Resources utilizations - Sludge biochar-based catalyst - Water environments -]+ catalyst
Classification code: 451.2 Air Pollution Control - 452.2 Sewage Treatment - 452.4 Industrial Wastes Treatment and Disposal - 531.1 Metallurgy - 802.2 Chemical Reactions - 803 Chemical Agents and Basic Industrial Chemicals - 804 Chemical Products Generally - 931.2 Physical Properties of Gases, Liquids and Solids
DOI: 10.1016/j.fuel.2023.128444
Funding Details: Number: 2022ZDYFJH-80, Acronym: -, Sponsor: -; Number: YQKF202213, Acronym: -, Sponsor: -; Number: 2022RC14, Acronym: WNU, Sponsor: Weinan Normal University;
Funding text: This work was carried out with the financial supports of the Key Research and Development Project of Weinan City (Grant No. 2022ZDYFJH-80), Opening Project of Oil & Gas Field Applied Chemistry Key Laboratory of Sichuan Province (Grant No. YQKF202213) and Talent project of Weinan Normal University (Grant No. 2022RC14).
Compendex references: YES
Database: Compendex
Data Provider: Engineering Village

71. Preface   (*Open Access*)

Authors: Hu, Sanbao (1); Gong, Bian (2); Hu, Dongtao (3); Deng, Xiaohe (1); Wang, Wei (4); Xu, Jianjun (5); Liu, Feng (6); Du, Qifei (7); Niu, Jianghao (8); Shi, Jianpeng (9); Shi, Y.D. (10); Li, X.L. (11); Li, D.M. (12); Chen, H. (13); Zhu, S. (14); Tian, X.W. (15); Dou, Y.H. (16); Zhou, Xintian (17); Jiang, Lei (18); Ma, H. (19); Ma, R.J. (20); Wang, Yong (21); Fang, Zhigang (1)
Author affiliation: (1) Wuhan University of Technology, China; (2) Shenzhen Technology University, China; (3) China University of Geosciences, China; (4) Chongqing Jiaotong University, China; (5) Northeast Petroleum University, China; (6) Huazhong University of Science and Technology, China; (7) Tiangong University, Tianjin, China; (8) Civil Aviation University of China, Tianjin, China; (9) Xi'an Jiaotong University, China; (10) Zhejiang University, China; (11) Peking University, China; (12) Shandong University of Science and Technology, China; (13) Shanghai University of Engineering Science, China; (14) Wuhan University, China; (15) Xi'an University of Science and Technology, China; (16) Xi'an Shiyou University, China; (17) Jiangsu Ocean University, China; (18) Nanjing University of Science and Technology, China; (19) Qingdao University of Science and Technology, China; (20) Tongji University, China; (21) Chongqing University, China

72. Effect of nanoparticles and nanosheets on improving the oil/water interface performance of surfactants in enhancing oil recovery: A comparative study by molecular simulation

Authors: Fu, Lipei (1, 2); Gu, Feng (1); Liao, Kaili (1, 3); Ma, Qianli (1); Shao, Minglu (1); Cheng, Yuan (1); Huang, Weiqiu (1); Li, Bing (2, 4); Si, Wenzhe (2); Wang, Yu (5)
Author affiliation: (1) School of Petroleum Engineering, Changzhou University, Changzhou; 213164, China; (2) State Key Joint Laboratory of Environment, Simulation and Pollution Control, National Engineering Laboratory for Multi Flue Gas Pollution Control Technology and Equipment, School of Environment, Tsinghua University, Beijing; 100084, China; (3) The Key Laboratory of Well Stability and Fluid & Rock Mechanics in Oil and Gas Reservoir of Shaanxi Province, Xi'an Shiyou University, Xi'an; 710065, China; (4) Jiangsu Zhongchuang Qingyuan Technology Co., Ltd., Yancheng; 224000, China; (5) School of Environmental Science and Engineering, Yancheng Institute of Technology, Yancheng; 224051, China
Corresponding authors: Liao, Kaili(liaokaili@cczu.edu.cn); Si, Wenzhe(siwenzhe115@tsinghua.edu.cn); Wang, Yu(wy252@126.com)

Abstract: In recent years, nanoparticles have become the most potential enhanced oil recovery technology because of their unique small size effect and specific surface area effect. With the research and application of graphene and its derivative materials, nanosheets are one of the research hotspots of nanomaterials for enhanced surfactant flooding. However, as far as we know, the molecular simulation comparison of nanoparticles and nanosheets to enhance the performance of surfactants has not been reported so far. Therefore, in this paper, we constructed nano-SiO2 particles grafted with hydroxyl and pentyl alkane activator, graphene nanosheets grafted with carboxylic acid chain and pentyl alkane activator for the first time. On this basis, the interfacial tension, interfacial density, interfacial generation energy and radial distribution function were analyzed by molecular dynamics simulation. The results show that nanoparticles and nanosheets have synergistic effect with amphoteric surfactant dodecyl dimethyl aminoethyl lactone (BS-12). The synergistic effect of nanosheets and BS-12 was stronger after carboxylic acid chain and pentyl alkane activator are grafted on the surface of nanosheets. The interfacial tension of n-dodecane/water could be reduced to 13.58 mN/m after the modified nanosheets are compounded with BS-12. The interfacial tension of n-dodecane/water could be reduced to 4.15 mN/m by the modified nanosheets are compounded with BS-12, and the ability of reducing the interfacial tension between oil and water is significantly improved. The calculation of n-dodecane/water interface thickness and interface formation energy showed that compared with the modified nanoparticles and BS-12 compound system, the interface thickness of the modified nanosheets and BS-12 compound system increased by 9.24%, and the interface formation energy increased by 17.85%. In addition, the results of radial distribution function analysis also demonstrated that the modified nanosheets had strong hydration with water molecules after being compounded with BS-12. The results of this work can provide new ideas for further research on the synergistic effect of surfactants and nanomaterials, as well as the development of oil displacement technology based on surfactants/nanomaterials. © 2023

Number of references: 56
Main heading: Molecular dynamics
Controlled terms: Carboxylic acids - Distribution functions - Enhanced recovery - Grafting (chemical) - Graphene - Molecular structure - Molecules - Nanosheets - Paraffins - Silica nanoparticles - SiO2 nanoparticles
Uncontrolled terms: Acid chains - Formation energies - Graphene nanosheets - Interface formation - Interface thickness - Molecular simulations - N -dodecane - Radial distribution functions - SiO2 nanoparticle - Synergistic effect
Classification code: 511.1 Oil Field Production Operations - 761 Nanotechnology - 801.4 Physical Chemistry - 802.2 Chemical Reactions - 804 Chemical Products Generally - 804.1 Organic Compounds - 922.1 Probability Theory - 931.3 Atomic and Molecular Physics - 933 Solid State Physics
Numerical data indexing: Percentage 1.785E+01%, Percentage 9.24E+00%, Surface tension 1.358E-02N/m, Surface tension 4.15E-03N/m
DOI: 10.1016/j.geoen.2023.211468

Compendex references: YES
Database: Compendex
Data Provider: Engineering Village

73. Comprehensive temperature-stable energy storage performance in core-shell structural Na0.5Bi0.5TiO3@SrSn0.1Ti0.9O3-(Bi2O3-B2O3-SiO2) composites via morphology engineering

Accession number: 20231914053772

Authors: Zhang, Xiaoting (1); Cui, Bin (2); Qiu, Yu (1); Ma, Rong (3); Fan, Yueyao (4)
Author affiliation: (1) College of Chemistry & Chemical Engineering, Yan'an University, Shaanxi Province, Yan'an; 716000, China; (2) Key Laboratory of Synthetic and Natural Functional Molecule of the Ministry of Education, Shaanxi Key Laboratory of Physico-Inorganic Chemistry, College of Chemistry and Materials Science, Northwest University, Xi'an; 710127, China; (3) Faculty of Chemistry and Chemical Engineering, Engineering Research Center of Advanced Ferroelectric Functional Materials, Key Laboratory of Phytochemistry of Shaanxi Province, Baoji University of Arts and Sciences, Shaanxi Province, Baoji; 721013, China; (4) School of Electronic Engineering, Xi'an Shiyou University, Shaanxi Province, Xi'an; 710065, China
Corresponding author: Zhang, Xiaoting(zxt@yau.edu.cn)

Source title: Materials Research Bulletin
Abbreviated source title: Mater Res Bull
Volume: 165
Issue date: September 2023
Publication year: 2023
Article number: 112324
Language: English
ISSN: 00255408
CODEN: MRBUAC
Document type: Journal article (JA)
Publisher: Elsevier Ltd

Abstract: In this paper, morphology engineering was developed to optimize the overall temperature-stable energy storage performance of ceramic capacitors. First, SrSn0.1Ti0.9O3 (SST) particles were coated on Na0.5Bi0.5TiO3 (NBT) rods to form "core-shell" NBT@SST rods by a co-precipitation method to improve the relaxor behavior. And the rods were compounded with the Bi2O3-B2O3-SiO2 (BBS) glass to dense into NBT@SST-BBS composites. The nanorods morphology of ceramic grains can increase the charge storage sites to induce higher polarization value. The moderate-#r SST shell with highly lattice matching could lower the interfacial polarization between ceramic and glass phase so as to boost the breakdown strength. Comparatively, composites with nanorod morphology can reach the highest recoverable energy density of 2.19 J/cm3 at 229 kV/cm with superior temperature stability $(\Delta E/E150\ ^{\circ}C \leq$ 15% at 30–395 °C). We hope this work will give guidance to fabricate the next-generation dielectric capacitors through morphology engineering. © 2023 Elsevier Ltd

Number of references: 43
Main heading: Energy storage
Controlled terms: Bismuth compounds - Dielectric properties - Glass - Morphology - Oceanography - Polarization - Precipitation (chemical) - Shells (structures) - Silica - Silicon - Sodium compounds
Uncontrolled terms: A composite - A interface - B: chemical synthesis - Core shell - D energy storage - D-dielectric properties - Nanorod morphologies - Storage performance - Temperature stable - TiO
Classification code: 408.2 Structural Members and Shapes - 471.1 Oceanography, General - 525.7 Energy Storage - 549.3 Nonferrous Metals and Alloys excluding Alkali and Alkaline Earth Metals - 802.3 Chemical Operations - 812.3 Glass - 931.2 Physical Properties of Gases, Liquids and Solids - 951 Materials Science
Numerical data indexing: Electric field strength 2.29E+04V/m, Energy 2.19E+00J, Percentage 1.50E+01%, Temperature 3.03E+02K to 6.68E+02K, Temperature 4.23E+02K
DOI: 10.1016/j.materresbull.2023.112324

Compendex references: YES
Database: Compendex
Data Provider: Engineering Village

74. Recent Progress in All-Small-Molecule Organic Solar Cells

Accession number: 20224913210816

Authors: Gao, Huanhuan (1); Sun, Yanna (2); Meng, Lingxian (3); Han, Chenyang (1); Wan, Xiangjian (4); Chen, Yongsheng (4)

Author affiliation: (1) College of New Energy, Xi'an Shiyou University, Xi'an; 710065, China; (2) Science Center for Material Creation and Energy Conversion, Institute of Frontier and Interdisciplinary Science, Shandong University, Qingdao; 266237, China; (3) School of Materials Science and Engineering, Henan Key Laboratory of Advanced Nylon Materials and Application, Henan Innovation Center for Functional Polymer Membrane Materials, Zhengzhou University, Zhengzhou; 450001, China; (4) Key Laboratory of Functional Polymer Materials, State Key Laboratory of Elemento-Organic Chemistry, Centre of Nanoscale Science and Technology, College of Chemistry, Nankai University, Tianjin; 300071, China

Corresponding authors: Gao, Huanhuan(gaohuanhuan@xsyu.edu.cn); Wan, Xiangjian(xjwan@nankai.edu.cn)

Abstract: Active layer material plays a critical role in promoting the performance of an organic solar cell (OSC). Small-molecule (SM) materials have the merits of well-defined chemical structures, few batch-to-batch variations, facile synthesis and purification procedures, and easily tuned properties. SM-donor and non-fullerene acceptor (NFA) innovations have recently produced all-small-molecule (ASM) devices with power conversion efficiencies that exceed 17% and approach those of their polymer-based counterparts, thereby demonstrating their great future commercialization potential. In this review, recent progress in both SM donors and NFAs to illustrate structure–property relationships and various morphology-regulation strategies are summarized. Finally, ASM-OSC challenges and outlook are discussed. © 2022 Wiley-VCH GmbH.

Number of references: 100
Main heading: Fullerenes
Controlled terms: Conversion efficiency - Molecules - Morphology - Organic solar cells - Synthesis (chemical)
Uncontrolled terms: Active Layer - All-small molecule organic solar cell - Layer materials - Morphology modulation - Non-fullerene acceptor - Power conversion efficiencies - Recent progress - Small molecule donor - Small molecules - Small-molecule organic solar cells
Classification code: 525.5 Energy Conversion Issues - 702.3 Solar Cells - 761 Nanotechnology - 802.2 Chemical Reactions - 804 Chemical Products Generally - 931.2 Physical Properties of Gases, Liquids and Solids - 931.3 Atomic and Molecular Physics - 951 Materials Science
Numerical data indexing: Percentage 1.70E+01%
DOI: 10.1002/smll.202205594

Compendex references: YES
Database: Compendex
Data Provider: Engineering Village

75. Frictional heat induced morphological responses at the interface in rotary friction welding of austenitic alloys: corona-bond and heat-pattern (*Open Access*)

Authors: Jin, Feng (1); Shi, Junmiao (2); Wen, Guodong (3); Fu, Banglong (4); Shen, Junjun (4); Wang, Shiqing (5); Wu, Yanbo (6); Xiong, Jiangtao (1); Li, Jinglong (1)
Author affiliation: (1) Shaanxi Key Laboratory of Friction Welding Technologies, Northwestern Polytechnical University, Xi'an; 710072, China; (2) Key Laboratory of Pressure Systems and Safety, Ministry of Education, East China University of Science and Technology, Shanghai; 200237, China; (3) Xi'an Research Institute of China Coal Technology & Engineering Group Corp, Xi'an; 710077, China; (4) Helmholtz-Zentrum Hereon, Institute of Materials Mechanics, Solid State Materials Processing, Max-Planck-Str. 1, Geesthacht; 21502, Germany; (5) School of Materials Science and Engineering, Xi'an Shiyou University, Xi'an; 710065, China; (6) Office of the People's Government of Inner Mongolia Autonomous Region in Dongfeng Aerospace City, Jiuquan; 735305, China
Corresponding authors: Shi, Junmiao(shijunmiao@ecust.edu.cn); Wen, Guodong(wenguodong@cctegxian.com)

Abstract: Frictional heat induced morphological responses of austenitic alloys SUS304, A286, and Inconel 718 at the interface in rotary friction welding was focused in this study, addressing initiation, evolution of corona-bond and the formation of heat-pattern. Summative models that describe the location and width of corona-bond at initiation, the corona-bond evolution mode and the formation of heat-patterns were given. The results show that when the corona-bond initiates at 0.33 R ∼ R, it fills the interface to form a lens-shaped heat-pattern. Inside this morphology, recrystallized ultrafine grains are formed to provide a superior performance. When the corona-bond initiates at 0–0.33 R with a width >0.4 R, it spreads to periphery to form a straight-line-shaped heat-pattern. Inside this heat-pattern, deformed grains and sub-boundaries are formed. The tensile strength of straight-line heat-pattern is lower than that of lens-shaped heat-pattern. When the corona-bond initiates at 0–0.33 R with a width ≤ 0.4 R, it does not spread but concentrates itself at center to form a spindle-shaped heat-pattern consisted of a 'spindle body' at center and a 'friction line' at periphery. Spindle body corresponds to a region made up of equiaxed recrystallized ultrafine grains, whereas the friction line corresponds to recrystallized grains and substructured grains. The formation of the friction line makes neglectable effect on local the strength but it does lower the elongation, where the local elongation of the friction line decreases to 6%–9% compared to 18% of a spindle body. © 2023 The Author(s)

Number of references: 34
Main heading: Friction
Controlled terms: Austenite - Austenitic stainless steel - Friction welding - Recrystallization (metallurgy) - Tensile strength - Textures
Uncontrolled terms: Austenitic alloys - Bond patterns - Corona-bond - Frictional heat - Heat patterns - Inconel-718 - Morphological response - Rotary friction welding - Spindle body - Ultra fine grain
Classification code: 531.1 Metallurgy - 531.2 Metallography - 538.2.1 Welding Processes - 545.3 Steel
Numerical data indexing: Percentage 1.80E+01%, Percentage 6.00E+00% to 9.00E+00%
DOI: 10.1016/j.jmrt.2023.02.221

Compendex references: YES
Open Access type(s): All Open Access, Gold
Database: Compendex
Data Provider: Engineering Village

76. Revisiting the contact splitting hypothesis: An effective route for enhancing adhesion on rough surface

Authors: Hu, Hong (1); Tian, Hongmiao (2); Gao, Yuan (3); Wan, Zhiguo (4); Wang, Lei (1); Xu, Hailong (1); Wang, Chunhui (2); Shao, Jinyou (2); Zheng, Zijian (1, 5, 6, 7)
Author affiliation: (1) Laboratory for Advanced Interfacial Materials and Devices, School of Fashion and Textiles, The Hong Kong Polytechnic University, Hong Kong; (2) State key Laboratory for Manufacturing Systems Engineering, Xi'an Jiaotong University, Xi'an, Shaanxi, 710049, China; (3) Information Science Academy of China Electronics Technology Group Corporation, Beijing; 100043, China; (4) School of Mechanical Engineering, Xi'an Shiyou University, Xi'an, Shaanxi, 710049, China; (5) Department of Applied Biology and Chemical Technology, Faculty of Science, The Hong Kong Polytechnic University, Hong Kong; (6) Research Institute for Smart Energy (RI-IWEAR), The Hong Kong Polytechnic University, Hong Kong; (7) Research Institute for Intelligent Wearable Systems (RISE), The Hong Kong Polytechnic University, Hong Kong
Corresponding author: Shao, Jinyou(jyshao@xjtu.edu.cn)
Abstract: The contact splitting hypothesis (CSH) has been proposed for around 20 years, which suggests that the patterned or fibrillar surfaces enable very efficient biological attachment systems (e.g., Geckos' seta). However, there is still a debate in academic community on the necessity of the CSH in man-made adhesives, since experiments have indicated that the non-fibrillar surface can also show strong adhesion. This study demonstrates that the surface roughness plays a key role in evaluating the influence of CSH on adhesion by a simple finite element (FE) model. The highly split structures are essentially required for strong adhesion on highly rough surface, but may in turn cause slight adhesion reduction on smooth surface due to the areal loss in the splitting process. With our results, the debate in CSH is explained as an incomplete understanding of an adhesive contact problem, in which the surface roughness is overlooked. Our results further sheds light on the natural selection that climbing animals with heavier body usually evolve finer adhesive structures on their pads, by considering both the surface roughness and its length scale dependence. © 2022 Elsevier Ltd
Number of references: 69
Main heading: Adhesion
Controlled terms: Adhesives - Biomimetics - Surface measurement - Surface roughness
Uncontrolled terms: Academic community - Bio-inspired adhesion - Contact modeling - Contact splitting hypothesis - Fibrillar structures - Finite element modelling (FEM) - Non-fibrillar - Rough surfaces - Simple++ - Splittings
Classification code: 461.8 Biotechnology - 461.9 Biology - 931.2 Physical Properties of Gases, Liquids and Solids - 943.2 Mechanical Variables Measurements - 951 Materials Science
Numerical data indexing: Age 2.00E+01yr
DOI: 10.1016/j.jmps.2022.105121
Compendex references: YES
Database: Compendex
Data Provider: Engineering Village

77. Experimental study on hydraulic fracture propagation in heterogeneous glutenite rock

Authors: Shi, Xian (1, 2); Qin, Yong (3, 4); Gao, Qi (5); Liu, Shun (6); Xu, Hongxing (7); Yu, Tianxi (8)
Author affiliation: (1) Key Laboratory of Unconventional Oil & Gas Development (China University of Petroleum (East China)), Ministry of Education, Qingdao; 266580, China; (2) College of Petroleum Engineering, China University of

Petroleum (East China), Qingdao; 266580, China; (3) School of Energy Resources, China University of Geosciences, Beijing; 100083, China; (4) Research Institute of Petroleum Exploration & Development, PetroChina, Beijing; 100083, China; (5) School of Engineering, The University of Western Australia, 35 Stirling Highway, Perth; WA; 6009, Australia; (6) Xi'an Shiyou University, Shaanxi, Xi'an; 710065, China; (7) CCDC Changqing Down Hole Technology Company, Xi'an; 710000, China; (8) Xinjiang Oilfield Company, PetroChina, Karamay; 843000, China
Corresponding author: Shi, Xian(xianshi@upc.edu.cn)

Abstract: To understand the fracture behavior and discuss the possibility of the reservoir-stimulated volume concept on glutenite rock, true triaxial hydraulic fracturing experiments were performed on glutenite rocks with acoustic emission monitoring. Experimental results indicate that a curved hydraulic fracture (HF) can be created. In addition, in situ stress plays the greatest role in HF propagation direction regardless of gravel characteristics; however, the gravel with high mechanical strength could affect hydraulic fracture path locally. Intense fluctuate extension pressure and discrete surged acoustic emission (AE) events not only occur during the breakdown stage but also during the shut-in stage, indicating embedded gravels tend to influence HF process. The breakdown pressure is the highest for sample with low horizontal stress difference, while breakdown pressure for large-size sample with small gravel numbers is the lowest. The highest AE amplitude can be observed for sample where fracture positions on gravels are at the initial stage, while continuous high AE amplitude is observed for samples with high pump rates during the entire process, indicating intense fracture and gravel interactions. Moreover, four possible interaction behaviors between HF and gravels, namely, fracture penetration, deflection, diversion and arrest, can be identified near wellbore and far-field failure zones. In general, fracture penetration behavior is exclusively observed within the near wellbore failure zone. Additionally, the fracture width for a penetration fracture is the largest due to high fracturing energy, while fracture diversion and arrest exhibit the smallest fracture width. Given the existence of gravels, branch fractures are difficult to merge with residual fracturing energy. An extremely coarse HF surface and tortuous HF path can be found for all samples; thus, the selection of a suitable pump rate and fracturing fluid is necessary to migrate near wellbore tortuosity. © 2023 Elsevier B.V.

Number of references: 43
Main heading: Hydraulic fracturing
Controlled terms: Acoustic emission testing - Boreholes - Fracture mechanics - Fracturing fluids - Gravel - Oil field equipment
Uncontrolled terms: Acoustic emission amplitudes - Acoustic-emissions - Breakdown pressure - Fracture path - Glutenite - Gravel - Hydraulic fracture propagation - Near wellbore - Pump rate - True triaxial
Classification code: 511.2 Oil Field Equipment - 512.1.2 Petroleum Deposits : Development Operations - 751.2 Acoustic Properties of Materials - 931.1 Mechanics
DOI: 10.1016/j.geoen.2023.211673

Compendex references: YES
Database: Compendex
Data Provider: Engineering Village

78. Atomic Cu-N-P-C Active Complex with Integrated Oxidation and Chlorination for Improved Ethylene Oxychlorination (*Open Access*)

Accession number: 20230513468428
Authors: Ma, Hongfei (1); Zheng, Xiuhui (2); Zhang, Hao (3, 4); Ma, Guoyan (5); Zhang, Wei (1); Jiang, Zheng (4); Chen, De (1)

Author affiliation: (1) Department of Chemical Engineering, Norwegian University of Science and Technology, Sem sælands vei 4, Trondheim; 7034, Norway; (2) State Key Laboratory of Heavy Oil Processing, China University of Petroleum, Shandong, Qingdao; 266580, China; (3) Institute of Functional Nano & Soft Materials Laboratory, (FUNSOM), Jiangsu Key Laboratory for Carbon-Based Functional Materials & Devices, Joint International Research Laboratory of Carbon-Based Functional Materials and Devices, Soochow University, Suzhou; 215123, China; (4) Shanghai Synchrotron Radiation Facility, Zhangjiang Lab, Shanghai Advanced Research Institute, Chinese Academy of Sciences, Shanghai; 201210, China; (5) College of Chemistry and Chemical Engineering, Xi'an Shiyou University, Shaanxi, Xi'an; 710065, China
Corresponding author: Chen, De(de.chen@ntnu.no)

Abstract: Fine constructing the chemical environment of the central metal is vital in developing efficient single-atom catalysts (SACs). Herein, the atomically dispersed Cu on the N-doped carbon is modulated by introducing Cu-P moiety to Cu-N-C SAC. Through fine-tuning with another heteroatom P, the Cu SAC shows the superior performance of ethylene oxychlorination. The Cu site activity of Cu-NPC is four times higher than the P-free Cu-NC catalyst and 25 times higher than the Ce-promoted $CuCl_2/Al_2O_3$ catalyst in the long-term test (>200 h). The selectivity of ethylene dichloride can be splendidly kept at $\approx 99\%$. Combined experimental and simulation studies provide a theoretical framework for the coordination of Cu, N, and P in the complex active center and its role in effectively catalyzing ethylene oxychlorination. It integrates the oxidation and chlorination reactions with superior catalytic performance and unrivaled ability of corrosive-HCl resistance. The concept of fine constructing with another heteroatom is anticipated to provide with inspiration for rational catalyst design and expand the applications of carbon-based SACs in heterogeneous catalysis. © 2023 The Authors. Advanced Science published by Wiley-VCH GmbH.

79. A novel triple responsive smart fluid for tight oil fracturing-oil expulsion integration   (*Open Access*)

Accession number: 20231213777870

Authors: Gao, Ming-Wei (1, 2, 3); Zhang, Ming-Shan (3); Du, Heng-Yi (4); Zhao, Ming-Wei (1, 2); Dai, Cai-Li (1, 2); You, Qing (5); Liu, Shun (4); Jin, Zhe-Hui (3)

Author affiliation: (1) Shandong Key Laboratory of Oilfield Chemistry (China University of Petroleum (East China)), Shandong, Qingdao; 266580, China; (2) Key Laboratory of Unconventional Oil & Gas Development (China University of Petroleum (East China)), Ministry of Education, Shandong, Qingdao; 266580, China; (3) Department of Civil and Environmental Engineering, University of Alberta, Edmonton; AB; T6G 1H9, Canada; (4) Shaanxi Key Laboratory of Advanced Stimulation Technology for Oil & Gas Reservoirs, Engineering Research Center of Development and Management for Low to Ultra-low Permeability Oil & Gas Reservoirs in West China (Ministry of Education), Xi'an Shiyou University, Shaanxi, Xi'an; 710065, China; (5) School of Energy Resources, China University of Geosciences, Beijing; 100083, China

Corresponding authors: Liu, Shun(liushun631@163.com); Dai, Cai-Li(daicl@upc.edu.cn); You, Qing(youqing@cugb.edu.cn)

Abstract: The traditional multi-process to enhance tight oil recovery based on fracturing and huff-n-puff has obvious deficiencies, such as low recovery efficiency, rapid production decline, high cost, and complexity, etc. Therefore, a new technology, the so-called fracturing-oil expulsion integration, which does not need flowback after fracturing while making full use of the fracturing energy and gel breaking fluids, are needed to enable efficient exploitation of tight oil. A novel triple-responsive smart fluid based on "pseudo-Gemini" zwitterionic viscoelastic surfactant (VES) consisting of N-erucylamidopropyl-N,N-dimethyl-3-ammonio-2-hydroxy-1-propane-sulfonate (EHSB), N,N,N#,N⁄_ tetramethyl-1,3-propanediamine (TMEDA) and sodium p-toluenesulfonate (NaPts), is developed. Then, the rheology of smart fluid is systematically studied at varying conditions (CO_2, temperature and pressure). Moreover, the mechanism of triple-response is discussed in detail. Finally, a series of fracturing and spontaneous imbibition performances are systematically investigated. The smart fluid shows excellent CO_2-, thermal-, and pressure-triple responsive behavior. It can meet the technical requirement of tight oil fracturing construction at 140 °C in the presence of 3.5 MPa CO_2. The gel breaking fluid shows excellent spontaneous imbibition oil expulsion $(\sim 40\%)$, salt resistance (1.2 × 104 mg/L Na+), temperature resistance (140 °C) and aging stability (30 days). © 2023 The Authors

Number of references: 73
Main heading: Carbon dioxide
Controlled terms: Fracturing fluids - Integration - Surface active agents
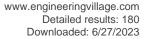**Uncontrolled terms:** Breakings - Fracturing-oil expulsion integration - Multi-Processes - Oil expulsion - Smart fluids - Spontaneous imbibition - Tight oil - Triple responsive smart fluid - Zwitterionic surfactants - "pseudo-geminus" zwitterionic surfactant
Classification code: 803 Chemical Agents and Basic Industrial Chemicals - 804.2 Inorganic Compounds - 921.2 Calculus
Numerical data indexing: Age 8.22E-02yr, Mass density 4.00E-03kg/m3, Percentage 4.00E+01%, Pressure 3.50E+06Pa, Temperature 4.13E+02K
DOI: 10.1016/j.petsci.2023.01.008

Compendex references: YES
Open Access type(s): All Open Access, Gold
Database: Compendex
Data Provider: Engineering Village

80. Dynamic variations of oil components and microbial communities during indigenous microbial stimulation pilot study in low-permeability reservoirs

Accession number: 20231714007927

Authors: He, Yanlong (1, 2); Hu, Yujie (3, 4, 5); Huang, Hai (1, 2); Zeng, Hao (3, 4, 5); Ni, Jun (6); Dong, Hao (7); Zhang, Fan (8, 9); She, Yuehui (3, 4, 5)
Author affiliation: (1) School of Petroleum Engineering, Xi'an Shiyou University, Shaanxi, Xi'an; 710065, China; (2) Engineering Research Center of Development and Management for Low to Ultra-Low Permeability Oil & Gas Reservoirs in West China, Ministry of Education, Shaanxi, Xi'an; 710065, China; (3) School of Petroleum Engineering, Yangtze University, Hubei, Wuhan; 430010, China; (4) Hubei Cooperative Innovation Center of Unconventional Oil and Gas, Hubei, Wuhan; 430010, China; (5) Hubei Key Laboratory of Drilling and Production Engineering for Oil and Gas, Hubei, Wuhan; 430010, China; (6) Shaanxi Yanchang Petroleum (Group) Co., Ltd, Shannxi, Xian; 716000, China; (7) College of Chemistry and Environmental Engineering, Yangtze University, Hubei, Jingzhou; 434023, China; (8) Key Laboratory of Marine Reservoir Evolution and Hydrocarbon Accumulation Mechanism, Ministry of Education, Beijing; 100083, China; (9) School of Energy Resources, China University of Geosciences (Beijing), Beijing; 100083, China
Corresponding author: She, Yuehui(sheyuehui@163.com)

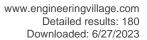**Abstract:** Indigenous microbial stimulation is considered as a highly promising technology for enhanced oil recovery (EOR) of low-permeability reservoirs. In this paper, oil components and microbial communities of indigenous microorganisms before and after bio-stimulation in the largest low-permeability oil field of China were discussed. The results showed that Pseudomonas aeruginosa was dominant in the original samples, followed by some sulfate-reducing bacteria (SRB) and iron-reducing bacteria (IRB), such as Desulfovibrio oxyclinae, and Methylopila capsulata, Deferribacter abyssi. After bio-stimulation, the species of microorganisms gradually decreased, the content of Pseudomonas aeruginosa reached $2{\sim}3$ times than that of the original samples. The harmful bacteria, such as SRB and IRB, gradually disappeared. The Pr/Ph of the oil decreased, whereas the Pr/nC 17, Ph/nC 18, and #nC 21-/#nC 22+ increased. The average molecular weight of oil decreased after the microorganisms were stimulated, in which the contents of N1-containing compounds increased, and that of O1-containing compounds decreased. The contents of biphenyls, naphthalene, and its derivatives decreased. Whereas those of aromatic compounds, such as phenanthrene, quaternary, fluorene, and their homologs increased. Pilot study was applied in LD field block, the average water cut of 27–47 well group decreased from 87.60% to 74.86%, the oil production increased from 12.18 t/d to 29.58 t/d. © 2023 The Author(s)

Number of references: 54
Main heading: Bacteria
Controlled terms: Enhanced recovery - Low permeability reservoirs - Mechanical permeability - Naphthalene - Petroleum reservoir engineering - Sulfur compounds

Compendex references: YES
Database: Compendex
Data Provider: Engineering Village

81. System design of ultrasonic oil production flowmeter based on time difference method

Accession number: 20232114124402

Authors: Wang, Wenzhen (1); Kai, Yan (1)
Author affiliation: (1) Xi'an Shiyou University, Xi'an, China
Corresponding author: Wang, Wenzhen(wzwang@xsyu.edu.cn)

Abstract: The flowmeter uses the TDC-GP22 chip as the acoustic wave processing core, uses the TDC-GP22 module to generate pulse waves, and sends them to the corresponding ultrasonic signal drive circuit to improve the amplitude of the ultrasonic signal. The echo is sent to TDC-GP22 to calculate the forward and reverse time difference; the main control module selects the STM32F407 chip, controls the TDC-GP22 module to transmit forward and reverse ultrasonic signals, enters the signal drive circuit to receive the echo signal and loads it into the TDC -GP22 chip calculates the time difference, and finally sends the corresponding time difference data to the main control module, which is connected to the PC through the serial port to display the measured data; the test is carried out in the fluid circulation device in the laboratory, and the speed of the screw pump is controlled to adjust the pipeline. The mass flowmeter

is used as the calibration instrument, and the final test results demonstrate that the measurement accuracy of the ultrasonic flowmeter meets the requirements of oilfield use. © 2023 SPIE.

Number of references: 5
Main heading: Digital storage
Controlled terms: Display devices - Flow measurement - Flowmeters
Uncontrolled terms: Acoustics waves - Control module - Difference method - Drive circuits - Liquid ultrasonic flowmeter - Oil-production - TDC-gp22 - Time difference method - Time-differences - Ultrasonic signals
Classification code: 631.1 Fluid Flow, General - 722.1 Data Storage, Equipment and Techniques - 722.2 Computer Peripheral Equipment - 943.1 Mechanical Instruments - 943.2 Mechanical Variables Measurements
DOI: 10.1117/12.2670205

Compendex references: YES
Database: Compendex
Data Provider: Engineering Village

82. Atomic-scale insight into interaction mechanism between screw dislocation and HCP phase in high-entropy alloy

Accession number: 20230413451354
Authors: Li, R.N. (1, 2); Song, H.Y. (1, 2); Xiao, M.X. (1, 2); An, M.R. (1, 2)
Author affiliation: (1) College of New Energy, Xi'An Shiyou University, Xi'an; 710065, China; (2) College of Material Science and Engineering, Xi'An Shiyou University, Xi'an; 710065, China
Corresponding author: Song, H.Y.(hysong@xsyu.edu.cn)
Source title: Journal of Applied Physics
Abbreviated source title: J Appl Phys
Volume: 133
Issue: 3
Issue date: January 21, 2023
Publication year: 2023
Article number: 034302
Language: English
ISSN: 00218979
E-ISSN: 10897550
CODEN: JAPIAU
Document type: Journal article (JA)
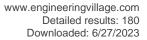**Publisher:** American Institute of Physics Inc.
Abstract: The face-centered cubic (FCC)/hexagonal close-packed (HCP) dual-phase structure is a new design strategy proposed in recent years to achieve high strength and excellent plasticity of high-entropy alloys (HEAs). Here, the effect of HCP phase thickness, strain rate, and temperature on the interaction mechanism between screw dislocation and the HCP phase in the FCC structured CoCrFeMnNi HEAs is investigated by molecular dynamics simulation. The results show that there are two types of interaction modes between dislocations and the HCP phase: one is the dislocation passing through the HCP phase, that is, the penetration mechanism, and the other is the dislocation being absorbed by the HCP phase, that is, the absorption mechanism. The generation of these two mechanisms mainly depends on the relative ability of the HCP phase to prevent dislocation slip, which is closely related to the HCP phase thickness, strain rate, and temperature. When the relative ability of the HCP phase to block dislocation is large, the interaction between dislocations and the HCP phase presents an absorption mechanism; otherwise, it presents a penetration mechanism. The research can provide theoretical guidance for the development and design of new high-performance HEAs to achieve high strength and high ductility of materials. © 2023 Author(s).
Number of references: 56
Main heading: High-entropy alloys
Controlled terms: Chromium alloys - Cobalt alloys - Entropy - High strength alloys - Iron alloys - Manganese alloys - Molecular dynamics - Screw dislocations - Screws - Strain rate
Uncontrolled terms: Face-centred cubic - Hexagonal close packed - Hexagonal close-packed - High entropy alloys - Interaction mechanisms - Penetration mechanisms - Phase thickness - Strain-rates - Strain-temperature - Thickness strain

83. Effect of rare earth element yttrium on migration behavior of twin boundary in magnesium alloys: a molecular dynamics study   (*Open Access*)

Authors: Li, S. (1, 2); Song, H.Y. (1); Han, L. (1); Su, W.L. (1)
Author affiliation: (1) College of New Energy, Xi'an Shiyou University, Xi'an; 710065, China; (2) College of Material Science and Engineering, Xi'an Shiyou University, Xi'an; 710065, China
Corresponding author: Song, H.Y.(hysong@xsyu.edu.cn)

Abstract: The addition of rare earth (RE) elements can effectively improve the mechanical properties of Mg alloys, which is attributed to its ability to regulate the plastic deformation behavior of Mg alloys. Here, the effects of the concentration of RE element Y and temperature on the migration behavior of twin boundary (TB) in the Mg alloys are investigated by molecular dynamics simulation. The results show that Y element has a softening effect on the migration of TB and promoted TB migration in the Mg alloys. The higher concentration of Y element, the stronger the softening effect on TB migration, and also the faster the migration speed of TB. The results indicate that higher temperature is beneficial to TB migration, and the softening effect of Y element on TB migration in the Mg alloys decreases with the increase of temperature. In addition, the migration mechanism of TB in the Mg alloys is analyzed in detail. This work provides a theoretical basis for the design and preparation of high-performance Mg alloys. © 2023 The Authors

84. An evolutional deep learning method based on multi-feature fusion for fault diagnosis in sucker rod pumping system   (*Open Access*)

Authors: Li, Juanni (1); Shao, Jun (2); Wang, Wei (1); Xie, Wenhao (3)
Author affiliation: (1) Shaanxi Key Laboratory of Measurement and Control Technology for Oil and Gas Wells, Xi'an Shiyou University, Shaanxi, Xi'an; 710065, China; (2) Mechanical Engineering College, Xi'an Shiyou University, Shaanxi, Xi'an; 710065, China; (3) School of Science, Xi'an Shiyou University, Shaanxi, Xi'an; 710065, China
Corresponding author: Li, Juanni(3072270@qq.com)
Abstract: As the smart oilfield has grown, various deep learning technologies are being utilized to recognize the graphic feature of the indicator diagram in order to detect the fault type of rod pump system, so as to maintain the oilfield's regular production. However, the original data for the indicator diagrams from various oil fields are influenced by different geographic conditions, sensor equipment, acquisition software, etc. and exhibit specific environmental characteristics. This poses difficulties for indicator diagram-based fault diagnosis methodologies and necessitates the use of a more generalizable diagnosis model. To address the issue, a multi-feature fusion fault diagnostic model is proposed. The model fuses the Fourier descriptor of the indicator diagram as a feature with the graphic feature to enhance the robustness of the feature. Firstly, the two backbone networks perform feature extraction on the single-modal input data of their own networks. Secondly, the information from the indicator diagram and the Fourier descriptor are learned together as features through the interactive fusion module. And finally the integrated features are used for feature classification to obtain the output of the network. The accuracy of the diagnostic model when using only a single feature is respectively: 0.8233(the graphic feature), 0.9422(the Fourier descriptor feature) according to the findings of the validation experiment, and when using the fusion of the two features is 0.9724. The results demonstrate that the suggested multi-input feature fusion model performs better than the single-input model. The technique makes use of the correlation between the features to realize their complementary benefits and enhance the effectiveness of the diagnostic model. © 2022 THE AUTHORS

85. Polydopamine microcapsules loaded Ag nanoparticles for catalytic reduction of organic pollutants

Accession number: 20230613559304

Authors: Chen, Xuelian (1); Zhou, Tong (1); Pan, Xiqiang (2); Li, Hong (2)
Author affiliation: (1) College of Materials Science and Engineering, Xi'an Shiyou University, Xi'an; 710065, China; (2) College of Chemistry and Chemical Engineering, Xi'an Shiyou University, Xi'an; 710065, China
Corresponding author: Chen, Xuelian(chenxl@xsyu.edu.cn)

Source title: Colloids and Surfaces A: Physicochemical and Engineering Aspects
Abbreviated source title: Colloids Surf. A Physicochem. Eng. Asp.
Volume: 663
Issue date: April 20, 2023
Publication year: 2023
Article number: 131085
Language: English
ISSN: 09277757
E-ISSN: 18734359
CODEN: CPEAEH
Document type: Journal article (JA)
Publisher: Elsevier B.V.

Abstract: We demonstrate a simple approach for fabricating polydopamine microcapsules decorated with silver nanoparticles (Ag@PDA MCs) as highly efficient catalysts for water purification. Polydopamine microcapsules (PDA MCs) were formed on the $MnCO_3$ template from self-polymerization and the removal of template under mild EDTA solution, followed by in situ reduction of Ag^+ by PDA and growth of monodispersed Ag nanoparticles. Under optimized conditions, the Ag@PDA MCs exhibits 41.56 wt% of Ag loading contents and superior catalytic performance for the degradation of organic pollutants with rate constant of 2.93 min-1 for methylene blue and 1.03 min-1 for 4-nitrophenol. The excellent catalytic activity can mainly be ascribed to high surface roughness of microcapsules, high Ag loading ratio, and uniform distribution of Ag nanoparticles. In addition, this catalyst can be recycled for five times with degradation efficiency higher than 98%. The Ag@PDA MCs possessed fast reduction rate, high catalytic activity, and good recyclability as well as facile preparation and easy separation, showing great potential for the application in wastewater treatment. © 2023 Elsevier B.V.

Number of references: 40
Main heading: Silver nanoparticles
Controlled terms: Aromatic compounds - Catalyst activity - Degradation - Manganese compounds - Metal nanoparticles - Microstructure - Organic pollutants - Rate constants - Surface roughness - Wastewater treatment
Uncontrolled terms: Ag + - Ag loadings - Catalytic reduction - Efficient catalysts - Microcapsules - Polydopamine - Self-polymerization - Simple approach - Situ reduction - Water purification
Classification code: 452.4 Industrial Wastes Treatment and Disposal - 761 Nanotechnology - 802.2 Chemical Reactions - 803 Chemical Agents and Basic Industrial Chemicals - 804 Chemical Products Generally - 804.1 Organic Compounds - 931.2 Physical Properties of Gases, Liquids and Solids - 951 Materials Science
Numerical data indexing: Percentage 9.80E+01%, Time 1.758E+02s, Time 6.18E+01s
DOI: 10.1016/j.colsurfa.2023.131085

Compendex references: YES
Database: Compendex
Data Provider: Engineering Village

86. Design and simulation of widely tunable picosecond synchronously pumped terahertz parametric oscillator based on silicon waveguide platform

Accession number: 20224613096028

Authors: Sun, Wei (1); Wen, Jin (1); Qin, Weijun (1); He, Chenyao (1); Xiong, Keyu (1); Liang, Bozhi (1)
Author affiliation: (1) School of Science, Xi'an Shiyou University, Xi'an, China

Corresponding author: Wen, Jin(wenjin@xsyu.edu.cn)

Abstract: A picosecond synchronously pumped terahertz optical parametric oscillator based on silicon membrane waveguide (Si-based WTPO) is proposed and numerically simulated. Through designing the structure parameters of the silicon membrane waveguide, a broadband terahertz frequency range is obtained by satisfying the phase matching condition. The parametric oscillation process and output characteristics of Si-based WTPO are numerically analyzed by solving the four-wave mixing coupled-wave equations, and the result has indicated that the parametric oscillation within the resonant cavity can apparently enhance the output terahertz wave power. Meanwhile, high bandwidth and efficiency output terahertz wave can be obtained, and too high pump power will lead to a reaction of reverse conversion. Finally, the threshold pump power is calculated. The Si-based WTPO system we proposed is expected to make some contributions to the study of compact and efficient terahertz wave sources. © 2022 Wiley Periodicals LLC.
Number of references: 28
Main heading: Terahertz waves
Controlled terms: Four wave mixing - Optical parametric oscillators - Optical pumping - Phase matching - Silicon - Simulation platform - Wave equations - Wave power - Waveguides
Uncontrolled terms: Design and simulation - Membrane waveguides - Parametric oscillations - Picoseconds - Si-based - Silicon membranes - Silicon waveguide - Terahertz parametric oscillators - Terahertz pulse - Widely tunable
Classification code: 549.3 Nonferrous Metals and Alloys excluding Alkali and Alkaline Earth Metals - 615.6 Wave Energy - 711 Electromagnetic Waves - 713 Electronic Circuits - 714.3 Waveguides - 723.5 Computer Applications - 921.2 Calculus
DOI: 10.1002/mop.33515

Compendex references: YES
Database: Compendex
Data Provider: Engineering Village

87. Energy, exergy and economic analysis of different integrated systems for power generation using LNG cold energy and geothermal energy

Accession number: 20225013239482
Authors: Pan, Jie (1, 2); Li, Mofan (1); Zhu, Min (1); Li, Ran (1); Tang, Linghong (3); Bai, Junhua (1)
Author affiliation: (1) College of Petroleum Engineering, Xi'an Shiyou University, Xi'an; 710065, China; (2) Engineering Research Cente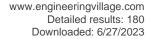r of Safety and Energy Saving in Oil & Gas Storage and Transportation, Universities of Shaanxi Province, Xi'an Shiyou University, Xi'an; 710065, China; (3) College of Mechanical Engineering, Xi'an Shiyou University, Xi'an; 710065, China
Corresponding authors: Pan, Jie(jackpan@xsyu.edu.cn); Li, Ran(rli@xsyu.edu.cn)
Source title: Renewable Energy
Abbreviated source title: Renew. Energy

Abstract: This paper constructs four integrated power generation systems using liquefied natural gas (LNG) cold energy and geothermal energy. These systems contain a geothermal single flash cycle, LNG expansion process and organic Rankine cycle (ORC). Different mathematical models are established to simulate the systems under steady-state conditions respectively. The influences of key working parameters on energy efficiency, exergy efficiency and levelized cost of energy (LCOE) are analyzed, and the comprehensive performances are estimated. The results show that increasing separator pressure, LNG turbine and Rankine turbine inlet pressures could increase the energy and exergy efficiencies. Also, a higher LNG turbine outlet pressure leads to a higher LCOE. To achieve the best system performance, single- and multi-objective genetic algorithm (GA) based optimizations are performed respectively. By single-objective optimization, GSF-TSORC and GSF-TPORC can reach the highest energy and exergy efficiencies of 34.80% and 52.61% respectively, and GSFC has the lowest total cost rate of 0.326 M$·year-1. After using multi-objective optimization, the energy and exergy efficiencies of GSF-TPORC are 29.56% and 51.29% respectively, which are superior to the other three systems, from the thermodynamic point of view. From an economic perspective, GSF-ORC has the lowest LCOE of 0.028 $·kWh-1, implying that it is the best system. © 2022 Elsevier Ltd
Number of references: 31
Main heading: Rankine cycle
Controlled terms: Economic analysis - Exergy - Genetic algorithms - Geothermal energy - Liquefied natural gas - Multiobjective optimization - Thermoanalysis
Uncontrolled terms: Cold energy - Cost of energies - Economics analysis - Energy and exergy efficiency - Geothermal single flash cycle - Levelized costs - Liquefied natural gas cold energy - Organic rankine cycle - Organics - Thermo dynamic analysis
Classification code: 481.3.1 Geothermal Phenomena - 523 Liquid Fuels - 615.1 Geothermal Energy - 641.1 Thermodynamics - 801 Chemistry - 911.2 Industrial Economics - 921.5 Optimization Techniques
Numerical data indexing: Percentage 2.956E+01%, Percentage 3.48E+01%, Percentage 5.129E+01%, Percentage 5.261E+01%
DOI: 10.1016/j.renene.2022.12.021
Funding Details: Number: 51774237, Acronym: NSFC, Sponsor: National Natural Science Foundation of China; Number: 52274064, Acronym: NSFC, Sponsor: National Natural Science Foundation of China;
Funding text: This study was supported by the National Natural Science Foundation of China (Grant No. 52274064, 51774237).
Compendex references: YES
Database: Compendex
Data Provider: Engineering Village
Compilation and indexing terms, Copyright 2023 Elsevier Inc.

88. Class-wise Knowledge Distillation

ISBN-13: 9781510662964
Document type: Conference article (CA)
Conference name: 3rd International Seminar on Artificial Intelligence, Networking, and Information Technology, AINIT 2022
Conference date: September 23, 2022 - September 25, 2022
Conference location: Shanghai, China
Conference code: 187963
Sponsor: Academic Exchange Information Centre (AEIC); Shanghai Lixin University of Accounting and Finance
Publisher: SPIE

Abstract: Knowledge distillation (KD) transfers knowledge of a teacher model to improve the performance of a student model which is usually equipped with a lower capacity. The standard KD framework, however, neglects that the DNNs exhibit a wide range of class-wise accuracy and the performance of some classes is even decreased after distillation. Observing the above phenomena, we propose a novel Class-Wise Knowledge Distillation method to find the hard classes with a simple yet effective technique and then make the students take more effort to learn these hard classes. In the experiments on image classification tasks using CIFAR-100 dataset, we demonstrate that the proposed method outperforms the other KD methods and achieves excellent performance enhancement on various networks. © 2023 SPIE.

Number of references: 14
Main heading: Distillation
Controlled terms: Classification (of information) - Image enhancement
Uncontrolled terms: Class-wise accuracy - Distillation method - Images classification - Knowledge distillation - Learn+ - Model compression - Performance - Simple++ - Student Modeling - Teacher models
Classification code: 716.1 Information Theory and Signal Processing - 802.3 Chemical Operations - 903.1 Information Sources and Analysis
DOI: 10.1117/12.2667603
Compendex references: YES
Database: Compendex
Data Provider: Engineering Village

89. High-sensitivity Fiber-optic Humidity Sensor without Sensitizing Material Modification

Accession number: 20231713945700
Title of translation:
Authors: Li, Mi (1); Ma, Chengju (1); Li, Dongming (1); Zhang, Yuebin (1); Bao, Shiqian (1); Jin, Jiasheng (1); Zhang, Yao (1); Liu, Qianzhen (1); Liu, Ming (1); Zhang, Yixin (1)
Author affiliation: (1) School of Science, Xi'an Shiyou University, Xi'an; 710065, China
Corresponding author: Ma, Chengju(chengjuma@xsyu.edu.cn)
Source title: Guangzi Xuebao/Acta Photonica Sinica
Abbreviated source title: Guangzi Xuebao
Volume: 52
Issue: 2
Issue date: February 2023
Publication year: 2023
Article number: 0206002
Language: Chinese
ISSN: 10044213
CODEN: GUXUED
Document type: Journal article (JA)
Publisher: Chinese Optical Society

Abstract: Relative Humidity (RH) is a physical parameter which reflects the degree of atmospheric dryness. It has wide applications in agriculture, biology, petrochemical fields, food-processing, medical treatment and Internet of Things (IOT) technology. Fiber-optic humidity sensors have attracted widespread attention from scholars due to their high-measurement accuracy, anti-electromagnetic interference, multiplexing, and distributed sensing. Especially, humidity sensors based on Fabry-Pérot Interferometers (FPIs) have been widely valued for their high repeatability, compact size and high-sensitivity. Various humidity sensors based on silica fiber-optic have been reported. In the majority of fiber-optic humidity sensors, however, the sensitivity of RH detection can be improved by coating hygroscopic materials. At the same time, because they are fragile and inflexible, silica optical fibers must be treated carefully. This increases the cost and complexity of the fabrication process. Therefore, it has great research significance and application value to study new materials and structures. In order to simplify the manufacture of sensor and obtain excellent humidity sensitivity, a composite humidity sensor based on Polymethyl Methacrylate

(PMMA)-microsphere and Single-mode Fiber (SMF) is designed and fabricated. Since the Polymer Optical Fiber (POF) material is very easily heated to form a molten state. In this work, the proposed sensor can be fabricated with an electric soldering iron. When the soldering iron is heated to about 70°C, place it 1 cm below the POF to slightly attach the POF to the SMF. Slowly rotate the heating source (i. e., electric iron) to allow the POF to be evenly heated. A Fabry-Pérot (F-P) cavity is formed between PMMA-microsphere and the fiber endface. It should be noted that adjusting the heat source temperature and distance between fiber-optic and heat source, the temperature of heating can be controlled in the heating process. Compared with the alcohol lamp heating method, the electric soldering iron heating method can provide a stable heating source and high safety factor in the experiment. And then, the humidity sensing characteristics of the sensor are theoretily and experimentally studied. When the external ambient humidity rises, the volume of PMMA-microsphere can expand after absorbing moisture from the surrounding. It causes the length of the F-P microcavity to grow. Then, the peak (or valley) of the F-P reflection spectrum shift toward longer wavelengths (i.e., red-shift). Thus, the humidity sensing can be realized. To investigate the sensing performance of the designed sensor, a test system that includes a demodulator, a humidity box, and a personal computer is built. Firstly, humidity test experiments are performed when the RH increases from 30% to 80% at a step of 10%. The humidity experimental results show that the wavelength shifts approximately linearly with the humidity changing, and the linearity reaches 0.992 26. The sensitivity of the sensor is up to 173.36 pm/%RH in the humidity range of 30%~ 80%. Meanwhile, the sensor is placed in the temperature box (NBD-M1200-10IC, NOBODY. China). The reflection spectra of the sensor with different temperature are acquired by a spectral acquisition with the range of 1 520~1 580 nm. Experimental results demonstrate that the interference spectrum has a red-shifted about 3.15 nm in the temperature range from 35°C to 65 °C . The temperature sensitivity of the sensor is 105.07 pm/°C, and the linearity is 0.989 55. In the subsequent studies, we will consider cascading FBG in the proposed sensor to solve the problem that cross-sensitivity of temperature and humidity. Finally, the proposed sensor performs well, showing a superior stability and repeatability over the test cycles in the performance evaluation actualized. When relative humidity is 33%RH and 38%RH, the resonant wavelength of the reflection spectrum has a very small shift within 60 min. The maximum deviations are 0.08 nm and 0.09 nm, respectively. The results indicate that the proposed sensor can maintain good stability in a long-term working condition. In addition, the wavelength drift deviation of the three repeated experiments is small, and the sensitivities are 176.05 pm/% RH, 170.35 pm/% RH and 173.68 pm/%RH, respectively. The average humidity sensitivity of the three groups tests is 173.36 pm/% RH. The designed humidity sensor offers numerous advantages such as low cost, high-sensitivity, simple structure and easy fabrication, which has a wide application prospect in the field of biochemical, agriculture and environmental monitoring. © 2023 Chinese Optical Society. All rights reserved.

Number of references: 26
Main heading: Atmospheric humidity
Controlled terms: Curing - Electromagnetic pulse - Fabry-Perot interferometers - Fiber Bragg gratings - Fiber optic sensors - Fiber optics - Iron - Microspheres - Silica - Single mode fibers
Uncontrolled terms: Fabry-Perot cavity - Fiber-optics - Fibre-optic sensor - Heating method - Heating source - High sensitivity - Humidity sensitivity - Polymer optical fibre - Reflection spectrum - Single-mode fibers
Classification code: 443.1 Atmospheric Properties - 545.1 Iron - 701 Electricity and Magnetism - 741.1.2 Fiber Optics - 802.2 Chemical Reactions - 941.3 Optical Instruments
Numerical data indexing: Percentage 1.00E+01%, Percentage 3.00E+01%, Percentage 3.00E+01% to 8.00E+01%, Percentage 3.30E+01%, Percentage 3.80E+01%, Percentage 8.00E+01%, Size 1.00E-02m, Size 1.0507E-10m, Size 1.7035E-10m, Size 1.7336E-10m, Size 1.7368E-10m, Size 1.7605E-10m, Size 3.15E-09m, Size 5.80E-07m, Size 8.00E-11m, Size 9.00E-11m, Temperature 3.08E+02K to 3.38E+02K, Temperature 3.43E+02K, Time 3.60E+03s
DOI: 10.3788/gzxb20235202.0206002
Funding Details: Number: YCS20213213, Acronym: -, Sponsor: -; Number: 2018GY#062, Acronym: -, Sponsor: Shanxi Provincial Key Research and Development Project;
Funding text: The Key Research and Development Plan Program of Shaanxi Province(No. 2018GY062), the Innovation and Practice Ability Training Fund of Xian Shiyou University(No. YCS20213213)
Compendex references: YES
Database: Compendex
Data Provider: Engineering Village

90. A novel Cr-doped CdS/ZnO nanocomposite for efficient photocatalytic hydroxylation of benzene to phenol

Accession number: 20231814039338
Authors: Han, Weiwei (1); Xiang, Wei (1); Meng, Zuchao (1); Dong, Sanbao (1); Lv, Ying (2)

Author affiliation: (1) College of Chemistry and Chemical Engineering, Xi'an Shiyou University, Dianzi 2nd Road Dongduan#18, Shaanxi, Xi'an; 710065, China; (2) College of New Energy, Xi'an Shiyou University, Dianzi 2nd Road Dongduan#18, Shaanxi, Xi'an; 710065, China
Corresponding author: Han, Weiwei(hanweiwei@xsyu.edu.cn)

Abstract: In this study, Cr-doped CdS/ZnO (Cr-CdS/ZnO) nanocomposites were synthesized for the first time and systematically characterized using different physicochemical methods, such as XRD, SEM, HRTEM, UV-Vis DRS, XPS, PL, EIS and EPR, etc. The photocatalytic activity of the Cr-CdS/ZnO nanocomposites was evaluated for the hydroxylation of benzene to phenol using H_2O_2 as the oxidant under visible-light irradiation. The impacts of various reaction conditions, including the role of catalyst dosage, solvents and volume ratio of benzene to H_2O_2 were specifically investigated. Owing to the similar lattice structure and well-matched band positions of CdS and ZnO, generation of electrons and holes by CdS-captured photons, as well as separation and imigration of electrons to ZnO were all realized. Furthermore, Cr-doping favored the formation of a new trapping level in the band gap of the Cr-CdS/ZnO composite, which would not only enhance visible-light absorption capacity, but also inhibit the rapid recombination of photo-generated electron-hole pairs. As a result, an excellent phenol selectivity of 98% with a phenol yield of 11.1% was achieved, which was higher than those of the pristine Cr-CdS, Cr-ZnO and CdS/ZnO. In the end, a rational mechanism for enhanced photocatalytic activity of the synthesized composites under visible-light irradiation was also proposed. The visible-light absorption and remarkably improved photocatalytic performance for benzene hydroxylation enable the potential of Cr-CdS/ZnO nanocomposites for the application of photocatalytic green synthesis of fine chemicals. © 2023

Compendex references: YES
Database: Compendex
Data Provider: Engineering Village

91. Structural Design of Small-size At-bit Azimuthal Gamma Geosteering Tool Based on Axiomatic Design   (*Open Access*)

Accession number: 20232114111932
Authors: Xi, Wenkui (1); Sun, Dongxin (1); Jia, Chao (1)
Author affiliation: (1) School of Mechanical Engineering, Xi'An Shiyou University, Xi'an, China
Corresponding author: Xi, Wenkui(xiwenkui@xsyu.edu.cn)
Source title: Journal of Physics: Conference Series
Abbreviated source title: J. Phys. Conf. Ser.
Volume: 2477
Part number: 1 of 1
Issue: 1
Issue date: 2023
Publication year: 2023
Article number: 012018
Language: English
ISSN: 17426588
E-ISSN: 17426596
Document type: Conference article (CA)
Conference name: 2022 7th International Seminar on Computer Technology, Mechanical and Electrical Engineering, ISCME 2022
Conference date: November 25, 2022 - November 27, 2022
Conference location: Hangzhou, Virtual, China
Conference code: 188101
Publisher: Institute of Physics
Abstract: To revitalize old wells and reduce costs, sidetracking has become an effective technical means to excavate the remaining oil reservoirs of old wells. The small-size at-bit azimuthal gamma geosteering tool designed in this paper is used for sidetracking. First, according to axiomatic design, we determine each functional module. Second, according to the function module, we design the structure of the geosteering tool. Finally, we conduct finite element strength analysis on the geosteering tool. The results are as follows: the geosteering tool realizes the structural design under limited space; its maximum stress is lower than the yield strength of the non-magnetic drill collar under the actual working conditions. The structure meets the strength requirements. The research method based on the axiomatic design proposed in this paper makes a beneficial exploration of the structural design of geosteering tools in the petroleum industry. © Published under licence by IOP Publishing Ltd.
Number of references: 10
Main heading: Structural design
Controlled terms: Petroleum industry - Petroleum prospecting - Petroleum reservoir engineering - Petroleum reservoirs
Uncontrolled terms: Axiomatic design - Function module - Functional modules - Geosteering - Limited space - Oil reservoirs - Reduce costs - Remaining oil - Strength analysis - Well costs
Classification code: 408.1 Structural Design, General - 512.1.1 Oil Fields - 512.1.2 Petroleum Deposits : Development Operations
DOI: 10.1088/1742-6596/2477/1/012018
Compendex references: YES
Open Access type(s): All Open Access, Bronze
Database: Compendex
Data Provider: Engineering Village

92. State monadic residuated lattices and their corresponding filters

Accession number: 20230813602370
Authors: Wang, Juntao (1); Kang, Mengna (1); Fu, Xuesong (1); Li, Fei (1)
Author affiliation: (1) School of Science, Xi'an Shiyou University, Shaanxi, Xi'an, China

Corresponding author: Kang, Mengna(kangmengna0118@126.com)
Abstract: In this paper, we introduce the notion of state monadic residuated lattices and study some of their related properties. Then we prove that the relationship between state monadic algebras of substructural fuzzy logics completely maintains the relationship between corresponding monadic algebras. Moreover, we introduce state monadic filters of state monadic residuated lattice, giving a state monadic filter generated by a nonempty subset of a residuated lattice, and obtain some characterizations of maximal and prime state monadic filters. Finally, we give some characterization of special kinds of state monadic residuated lattices, including simple, semisimple and local state monadic residuated lattices by state monadic filters. © 2023 - IOS Press. All rights reserved.
Number of references: 32
Main heading: Algebra
Controlled terms: Fuzzy filters - Fuzzy logic
Uncontrolled terms: Fuzzy-Logic - Mathematical fuzzy logic - Mondaic residuated lattice - Nonempty subsets - Prime state - Property - Residuated lattices - State monadic filter - State monadic residuated lattice
Classification code: 721.1 Computer Theory, Includes Formal Logic, Automata Theory, Switching Theory, Programming Theory - 723 Computer Software, Data Handling and Applications - 921.1 Algebra
DOI: 10.3233/JIFS-213527
Compendex references: YES
Database: Compendex
Data Provider: Engineering Village

93. A Multiple-Kernel Based Subspace Clustering Method

Accession number: 20232014104141
Authors: Yang, Yifang (1); Li, Fei (1)
Author affiliation: (1) College of Science, Xi'an Shiyou University, Xi'an; 710065, China
Corresponding author: Yang, Yifang(yang-yifang@163.com)

ISBN-13: 9781510660298
Document type: Conference article (CA)
Conference name: 3rd International Symposium on Computer Engineering and Intelligent Communications, ISCEIC 2022
Conference date: September 16, 2022 - September 18, 2022
Conference location: Xi'an, China
Conference code: 187947
Sponsor: Academic Exchange Information Center; Dalian Maritime University
Publisher: SPIE

Abstract: Spectral clustering has been successfully used in the domain of pattern recognition and computer vision. Kernel subspace clustering has become a hot research topic because it can reveal the nonlinear structure. However, the performance of exiting single kernel subspace clustering relys heavily on the choice of kernel function. To address the problem, we propose a novel method called multiple-kernel based subspace clustering method (MKSC) by combining kernel block diagonal representation with multiple kernel learning. The proposed MKSC algorithm firstly obtains the optimal kernel matrix by using multiple kernel clustering method, then replace the kernel function in single kernel subspace clustering model with the optimized kernel matrix, finally the clustering result is got by optimizing the MKSC model. Experimental results on three datasets testify the effectiveness of our proposed MKSC method. © The Authors. Published under a Creative Commons Attribution CC-BY 3.0 License.
Number of references: 10
Main heading: Pattern recognition
Controlled terms: Cluster analysis - Clustering algorithms - Learning systems - Matrix algebra
Uncontrolled terms: Block diagonal - Block diagonal representation - Clustering methods - Kernel function - Kernel matrices - Multiple Kernel Learning - Multiple kernels - Single kernel - Spectral clustering - Subspace clustering
Classification code: 723 Computer Software, Data Handling and Applications - 903.1 Information Sources and Analysis - 921.1 Algebra
DOI: 10.1117/12.2661171
Funding Details: Number: 2020JM-543, Acronym: -, Sponsor: Natural Science Foundation of Shaanxi Province; Number: 2021GY-038, Acronym: -, Sponsor: Shanxi Provincial Key Research and Development Project;
Funding text: This work was supported by the Natural Science Basic Research Plan in Shaanxi Province (No.2020JM-543), and the Key Research and Development Project of Shaanxi Province (No.2021GY-038).
Compendex references: YES
Database: Compendex
Data Provider: Engineering Village
Compilation and indexing terms, Copyright 2023 Elsevier Inc.

94. Influence of welding parameters on the interface temperature field of TC4 titanium alloys/304 stainless steel friction stir lap joints

Accession number: 20231914056218
Authors: Lu, Yongxin (1, 2); Zhang, Binhua (1); Wen, Pengjun (1); Zhou, Yuwei (1); Feng, Hongfeng (1); Wang, Hongduo (1, 2); Xu, Xueli (1, 2); Li, Xiao (1, 2); Zhang, Xiaoyong (1, 2)
Author affiliation: (1) School of Materials Science and Engineering, Xi'An Shiyou University, Xi'an; 710065, China; (2) Xi'An Key Laboratory of High Performance Oil and Gas Field Materials, Xi'An Shiyou University, Xi'an; 710065, China
Corresponding author: Lu, Yongxin(luyongxin618@163.com)
Source title: Materialpruefung/Materials Testing
Abbreviated source title: Materialpruefung
Volume: 65
Issue: 4
Issue date: April 2023
Publication year: 2023
Pages: 479-493
Language: English
ISSN: 00255300
CODEN: MTPRAJ
Document type: Journal article (JA)
Publisher: Walter de Gruyter GmbH
Abstract: The welding parameters optimization of TC4 titanium alloys/304 stainless steel (TC4/304 SS) by friction stir lap welding (FSLW) based on orthogonal test was researched. The results show that when the rotating speed was constant, the area of the high temperature zone and the peak temperature decreased with the increase of the

traversing speed; when the traversing speed was constant, the area of the high temperature zone and the peak temperature increased with the increasing rotating speed. Among them, under the condition of low heat input, the interface temperature was about 912 °C, the material at the interface cannot fully react, and there was no formation of a large amount of brittle and hard intermetallic compounds; under the condition of medium heat input, the interface temperature was about 930 °C, this temperature caused a large amount of brittle and hard intermetallic compounds at the interface; under high heat input, the interface temperature was about 975 °C, a large number of intermetallic compounds were not formed at the interface. © 2023 Walter de Gruyter GmbH, Berlin/Boston.

Number of references: 27
Main heading: Intermetallics
Controlled terms: Austenitic stainless steel - Friction - Friction stir welding - Rotating machinery - Temperature - Titanium alloys
Uncontrolled terms: 304 stainless steel - Friction stir lap welding - High temperature zones - Interface temperatures - Intermetallics compounds - Peak temperatures - Rotating speed - TC4 titanium alloy - Traversing speed - Welding parameters
Classification code: 531.1 Metallurgy - 538.2.1 Welding Processes - 542.3 Titanium and Alloys - 545.3 Steel - 601.1 Mechanical Devices - 641.1 Thermodynamics
Numerical data indexing: Temperature 1.185E+03K, Temperature 1.203E+03K, Temperature 1.248E+03K
DOI: 10.1515/mt-2022-0290

Compendex references: YES
Database: Compendex
Data Provider: Engineering Village

95. Effect of pressure pulse stimulation on imbibition displacement within a tight sandstone reservoir with local variations in porosity

Accession number: 20232114136078

Authors: Gao, Hui (1, 2, 3); Wang, Chen (1, 2, 3); Cheng, Zhilin (1, 2, 3); Li, Teng (1, 2, 3); Dou, Liangbin (1, 2, 3); Zhao, Kai (1, 2, 3); Xue, Junjie (1, 2, 3); Luo, Kaiqing (1, 2, 3)
Author affiliation: (1) School of Petroleum Engineering, Xi'an Shiyou University, Shaanxi, Xi'an; 710065, China; (2) Western Low-Permeability-Ultra-Low Permeability Reservoir Development and Management Engineering Research Center, Ministry of Education, Xi'an Shiyou University, Shaanxi, Xi'an; 710065, China; (3) Xi'an Key Laboratory of Tight Oil (Shale Oil) Development, Xi'an Shiyou University, Shaanxi, Xi'an; 710065, China
Corresponding author: Gao, Hui(ghtopsun1@163.com)

Source title: Geoenergy Science and Engineering
Abbreviated source title: Geoenergy. Sci. Eng.
Volume: 226
Issue date: July 2023
Publication year: 2023
Article number: 211811
Language: English
E-ISSN: 29498910
Document type: Journal article (JA)
Publisher: Elsevier B.V.

Abstract: The pressure pulse technique has been suggested as a potential method to enhance oil recovery from tight oil reservoirs. To investigate the variations in the pore structure of tight sandstone samples from the Triassic Yanchang Formation in the Ordos Basin (China), a combination of casting thin sections, high-pressure mercury intrusion, and nuclear magnetic resonance was employed. Imbibition experiments combined with the imposed pressure pulse were performed to quantitively examine the effects of the primary parameter relevant to pressure pulse on displacement efficiency and oil recovery contribution of the various pore systems. By testing the effect of different pulse pressures, it was investigated which mechanisms controlled the oil recovery. It was thus found that a series of four pulses could enhance the oil recovery significantly, and that the pressure should be 2 MPa4 MPa and 6 MPa for the three investigated types of reservoirs, respectively. In these cases, their corresponding pulse times are 48 h, 96 h, and 144 h, respectively. The oil displacement efficiency increases with the increasing pressure and pulse cycles; however, the amplitude in oil recovery gradually diminishes. It was also found that an increasing pulse pressure is favorable for

mobilizing oil that is trapped in pore spaces, especially for the low-permeability samples, despite the longer pulse time. Employing the pressure pulse method could markedly improve the imbibition oil recovery, and the simultaneous pulse pressure with imbibition leads to a higher oil recovery than the approach that adopts the pulse pressure after imbibition experiments. The main cause is that the former method facilitates oil recovery, particularly from intermediate-sized pores in relatively porous media. Furthermore, there is a significant difference in oil displacement within the various pore systems for the various types of reservoirs. The developed microfractures greatly contribute to oil recovery during the early imbibition stage, and the pressure pulse method appears most suitable to tight reservoirs with a relatively uniform pore size distribution and a higher proportion of medium-large pores. © 2023 Elsevier B.V.

Number of references: 35

Main heading: Pore structure

Controlled terms: Efficiency - Petroleum reservoir engineering - Petroleum reservoirs - Pore size - Sandstone - Tight gas

Uncontrolled terms: Imbibition oil displacement - Oil displacement - Oil recoveries - Pore utilization law - Pressure pulse - Pressure stimulation - Pulse parameter - Pulse pressure - Pulse pressure stimulation - Tight sandstone reservoirs

Classification code: 482.2 Minerals - 512.1.1 Oil Fields - 512.1.2 Petroleum Deposits : Development Operations - 512.2 Natural Gas Deposits - 522 Gas Fuels - 913.1 Production Engineering - 931.2 Physical Properties of Gases, Liquids and Solids - 951 Materials Science

Numerical data indexing: Pressure 2.00E+06Pa, Pressure 4.00E+06Pa, Pressure 6.00E+06Pa, Time 1.728E+05s, Time 3.456E+05s, Time 5.184E+05s

DOI: 10.1016/j.geoen.2023.211811

Compendex references: YES

Database: Compendex

Data Provider: Engineering Village

96. A hot-wire flowmeter based on polymer-filled extrinsic-phase-shift fiber Bragg grating

Accession number: 20230413417098

Authors: Jia, Zhen'an (1); Ren, Jie (1); Liu, Yinggang (1); Gao, Hong (1); Fan, Wei (1); Bai, Yan (1); Wen, Junliang (1)

Author affiliation: (1) School of Science, Xi'an Shiyou University, Shaanxi, Xi'an; 710065, China

Corresponding author: Ren, Jie(jie_ren_cn@163.com)

Abstract: A polymer-filled extrinsic-phase-shift fiber Bragg grating (EPS-FBG) sensor for flow measurement is proposed. The EPS-FBG is obtained by cutting a common FBG to form a micron gap and filling it with epoxy resin polymer, and the reflection spectrum shows a phase shift peak with a very narrow bandwidth different from that of FBG. The phase shift peak of the EPS-FBG has a high-temperature sensitivity of 28.3 pm/°C, and the linearity of temperature is 0.996, which makes it possible to exhibit excellent for measuring temperature and improve any sensor that takes temperature measurements. The phase shift peak of the proposed flowmeter with active heating shifts with variations in flow, the flow measurement is realized by monitoring the wavelength change of the phase shift peak. Experiments have been conducted in the range of 300–4000 L/h and confirmed that the flowmeter exhibits compliance of more than 0.998 for specific non-linear functions at different powers, which enables an accurate theoretical calculation. At a heating power of 33 W, the average sensitivity of the flowmeter was measured to be 12 L/h/pm, and at lower flow rates the sensitivity was up to 1 pm/L/h, which indicates that the EPS-FBG hot-wire flowmeter

has potential for micro-flow measurement applications. Moreover, the proposed flowmeter has the merits of easy fabrication and low cost, and is expected to be widely used in the industry. © 2023 Elsevier GmbH

Number of references: 17
Main heading: Fiber Bragg gratings
Controlled terms: Costs - Epoxy resins - Filled polymers - Flow measurement - Flow rate - Flowmeters - Temperature measurement
Uncontrolled terms: Active heating - Extrinsic-phase-shift fiber bragg grating - Fiber Bragg Grating Sensors - High temperature sensitivity - Hot wires - Measuring temperature - Narrow bandwidth - Reflection spectrum - Resins/polymers - Sensitivity
Classification code: 631 Fluid Flow - 631.1 Fluid Flow, General - 815.1.1 Organic Polymers - 911 Cost and Value Engineering; Industrial Economics - 943.1 Mechanical Instruments - 943.2 Mechanical Variables Measurements - 944.6 Temperature Measurements - 951 Materials Science
Numerical data indexing: Power 3.30E+01W, Size 1.00E-12m, Size 2.83E-11m, Volume 1.20E-02m3, Volume 3.00E-01m3 to 4.00E+00m3
DOI: 10.1016/j.ijleo.2023.170571
Funding Details: Number: YCS22112076, Acronym: -, Sponsor: -; Number: 18JS093, Acronym: -, Sponsor: Education Department of Shaanxi Province;
Funding text: This work was supported by the Scientific Research Program Funded by the Shaanxi Provincial Education Department of China (18JS093) and the Graduate Student Innovation Fund of Xi'an Shiyou University , China (YCS22112076).This work was supported by the Scientific Research Program Funded by the Shaanxi Provincial Education Department of China (18JS093) and the Graduate Student Innovation Fund of Xi'an Shiyou University, China (YCS22112076).
Compendex references: YES
Database: Compendex
Data Provider: Engineering Village
Compilation and indexing terms, Copyright 2023 Elsevier Inc.

97. Effect of Janus Nanoparticles on Foam Stability   (*Open Access*)

Accession number: 20230913637782
Authors: Du, Ruotong (1); Li, Ning (2); Cui, Zijing (1); He, Zongli (1); Zhou, Likang (1); Tang, Zixiang (1); Wang, Yang (1)
Author affiliation: (1) Xi'An Shiyou University, China; (2) Dagang Oilfield Down-hole Service Corporation, China
Source title: Journal of Physics: Conference Series
Abbreviated source title: J. Phys. Conf. Ser.
Volume: 2418
Part number: 1 of 1
Issue: 1
Issue date: 2023
Publication year: 2023
Article number: 012027
Language: English
ISSN: 17426588
E-ISSN: 17426596
Document type: Conference article (CA)
Conference name: 2022 2nd International Conference on Energy, Power and Electrical Engineering, EPEE 2022
Conference date: September 23, 2022 - September 25, 2022
Conference location: Hangzhou, Virtual, China
Conference code: 186685
Publisher: Institute of Physics
Abstract: The foam properties of different surfactants were evaluated by the stirring method. The synergistic foam stabilizing effect was formed by the combination of lauryl glucoside and hydrophilic nanoparticles, but the result was feeble. The blend of Janus nanoparticles and surfactants significantly improves foam stability, and the two have a strong synergistic effect on foam stability. The compound system has a specific temperature resistance. Kruss dynamic surface tensiometer and surface dilatation rheometer were used to measure the gas-liquid interface properties of the hydrophilic nanoparticles compound system, Janus nanoparticles compound system, and surfactant system, respectively. The effects of Janus nanoparticles on the surface tension and surface dilatation modulus of the compound system were analyzed, which were correlated with the stability of the foam. © Published under licence by IOP Publishing Ltd.
Number of references: 11
Main heading: Surface active agents

Engineering Village™

98. Research on oil-water two-phase water content detection model based on near-infrared spectroscopy   (*Open Access*)

Authors: Liu, Ke-Ke (1); Gao, Guo-Wang (1); Wang, Fei (1); Wu, Dan (1); Wu, Zhao-Xue (1); Gong, Yu (1)
Author affiliation: (1) School of Electronic Engineering, Xi'an Shiyou University, Xi'an; 710065, China
Corresponding author: Gao, Guo-Wang(wwgao1205@163.com)

Abstract: Crude oil water content is an important technical indicator in oil extraction, transportation and oil trading. Real-time online testing of crude oil water content is extremely important in estimating crude oil production and evaluating the extraction value of oil wells. At present, most of the wells at home and abroad are in the middle and late stage of development, it is difficult and inaccurate to measure under the high water content condition of crude oil, so it is necessary to adopt new detection means to improve the detection accuracy. In this paper, a study on the method of water content measurement using infrared spectroscopy was carried out. This study used S-G smoothing and normalization as the method of data pre-processing, selected the characteristic wavelengths using the continuous projection method (SPA) with a root mean square error of 4.4702, and then used partial least squares (PLS) to establish a water content detection model, and obtained a prediction root mean square error of 9.7131 and a correlation coefficient of 0.98527, which obtained a good accuracy. The feasibility of using spectroscopic detection technology to measure the water content of crude oil was demonstrated, providing a new method for oil extraction exploration and production processing. © The Authors. Published under a Creative Commons Attribution CC-BY 3.0 License.

Controlled terms: Data handling - Extraction - Infrared devices - Infrared spectroscopy - Least squares approximations - Mean square error - Near infrared spectroscopy - Oil wells - Petroleum transportation - Well testing
Uncontrolled terms: Content detection - Continuous projection algorithm - Crude oil water content - Detection models - Oil extraction - Oil-water two-phase - Oil/water - Partial least-squares - Projection algorithms - Root mean square errors
Classification code: 512.1 Petroleum Deposits - 512.1.1 Oil Fields - 723.2 Data Processing and Image Processing - 802.3 Chemical Operations - 921.6 Numerical Methods - 922.2 Mathematical Statistics
DOI: 10.1117/12.2660957
Funding Details: Number: YCS21113132, Acronym: -, Sponsor: -; Number: 2022GY-435, Acronym: -, Sponsor: Natural Science Foundation of Shaanxi Province;
Funding text: This project is supported by the Innovation and Practical Ability Cultivation Program for Postgraduates of Xi 'an Shiyou University (YCS21113132), Natural Science Foundation of Shaanxi Province (2022GY-435).
Compendex references: YES
Open Access type(s): All Open Access, Bronze
Database: Compendex
Data Provider: Engineering Village
Compilation and indexing terms, Copyright 2023 Elsevier Inc.

99. Dual-parameter optical fiber sensor for temperature and humidity based on PMMA-microsphere and FBG composite structure

Accession number: 20231113709209
Authors: Li, Mi (1); Ma, Chengju (1); Li, Dongming (1); Bao, Shiqian (1); Jin, Jiasheng (1); Zhang, Yao (1); Liu, Qianzhen (1); Liu, Ming (1); Zhang, Yixin (1); Li, Tingyu (1); Hu, Hui (1); Wu, Jirui (1)
Author affiliation: (1) School of Science, Xi'an Shiyou University, Shaanxi, Xi'an; 710065, China
Corresponding author: Ma, Chengju(chengjuma@xsyu.edu.cn)
Source title: Optical Fiber Technology
Abbreviated source title: Opt. Fiber Technol.
Volume: 78
Issue date: July 2023
Publication year: 2023
Article number: 103292
Language: English
ISSN: 10685200
CODEN: OFTEFV
Document type: Journal article (JA)
Publisher: Academic Press Inc.
Abstract: In this work, we proposed and experimentally demonstrated an optical fiber temperature and humidity sensor composed of a polymethyl methacrylate (PMMA)-microsphere and a fiber Bragg grating (FBG), and realize monitoring the environment temperature and humidity simultaneously. The experimental results show that when the relative humidity (RH) change from 35% to 85%, the response sensitivity of the Fabry-Pérot (F-P), which is formed between PMMA-microsphere and the fiber end-face, is about 127 pm/%RH. However, the FBG in the structure is not sensitive to humidity. When temperature changes from 33 °C to 58 °C, the response sensitivity of the F-P and FBG are about 45.68 pm/°C and 10 pm/°C, respectively. When temperature and humidity change simultaneously, these two-parameters can be monitored simultaneously by using the dual-parameter measurement matrix method. The optical fiber dual-parameter sensor offers numerous advantages, such as low cost, high sensitivity, and easy fabrication. © 2023 Elsevier Inc.
Number of references: 35
Main heading: Fiber Bragg gratings
Controlled terms: Fabry-Perot interferometers - Humidity sensors - Microspheres - Polymethyl methacrylates
Uncontrolled terms: A.Fibres - Composites structures - Environment temperature - Fabry-Perot - Humidity sensing - Polymethyl methacrylate microsphere - Response sensitivity - Temperature and humidities - Temperature and humidity sensor - Temperature changes
Classification code: 443.2 Meteorological Instrumentation - 815.1.1 Organic Polymers - 941.3 Optical Instruments
Numerical data indexing: Percentage 3.50E+01% to 8.50E+01%, Size 1.00E-11m, Size 1.27E-10m, Size 4.568E-11m, Temperature 3.06E+02K to 3.31E+02K
DOI: 10.1016/j.yofte.2023.103292
Funding Details: Number: 2018GY-062, Acronym: -, Sponsor: -; Number: YCS20213213, Acronym: -, Sponsor: -;

Compendex references: YES
Database: Compendex
Data Provider: Engineering Village

100. Denoising research of petrographic thin section images with the global residual generative adversarial network

Accession number: 20231113729896
Authors: Pan, Shaowei (1); Ma, Jincai (1); Fu, Xiaomei (2); Chen, Dou (2); Xu, Ning (2); Qin, Guowei (3)
Author affiliation: (1) School of Computer Science, Xi'an Shiyou University, Shaanxi, 710065, China; (2) Changqing Business Division of CNPC Logging Co. Ltd, Shaanxi, 710201, China; (3) College of Petroleum Engineering, Xi'an Shiyou University, Shaanxi, 710065, China
Corresponding author: Pan, Shaowei(swpan@xsyu.edu.cn)
Source title: Journal of Petroleum Science and Engineering
Abbreviated source title: J. Pet. Sci. Eng.
Volume: 220
Issue date: January 2023
Publication year: 2023
Article number: 111204
Language: English
ISSN: 09204105
Document type: Journal article (JA)
Publisher: Elsevier B.V.
Abstract: Petrographic thin section images have an important role in depositional environment inference, prediction of reservoir physical properties, and oil and gas analysis. To overcome the current challenges in thin section image denoising, we propose the global residual generative adversarial network (GR-GAN). Compared with the classical generative adversarial network (GAN), the residual network structure of the GR-GAN is reconstructed, and the loss function is redefined. The GR-GAN is then applied to denoise the thin section images in two different oilfields. The final denoising results confirmed that the GR-GAN achieves the best denoising effects on both visual evaluation metrics and objective evaluation metrics compared with colour block-matching 3D filtering (CBM3D), K-singular value decomposition (K-SVD), the GAN and a fast and flexible denoising network (FFDNet). Specifically, the peak signal-to-noise ratio (PSNR) and structural similarity (SSIM) generated by the GR-GAN on the test set are 28.2410 and 0.9674, 28.1075 and 0.9443, and 27.9919 and 0.9399, respectively, when the Gaussian noise is 15 dB, 25 dB and 35 dB, respectively, in the thin section image of the small-pore and fine-throat-type structures of J Oilfield; however, the data become 27.2841 and 0.9228, 26.8177 and 0.9162, and 26.3043 and 0.9068 for CBM3D, respectively, and these data generated by other methods are between the aforementioned two sets of data. The normalized root mean squared error (NRMSE) generated by the GR-GAN and CBM3D with the test set are 0.0327 and 0.1382, 0.0584 and 0.1341, and 0.0786 and 0.1382, respectively, when the Gaussian noise is 15 dB, 25 dB and 35 dB, respectively, and the NRMSE generated by the other methods is also between the aforementioned two sets of data. For other types of thin section images, when the Gaussian noise is 15 dB, 25 dB and 35 dB, respectively, CBM3D, K-SVD, the GAN, FFDNet and the GR-GAN show similar denoising effects as previously described. Moreover, in a denoising experiment repeated more than 10 times with the above methods, the GR-GAN has the shortest mean running time of 1.0589 s, and the mean running times of CBM3D, K-SVD, the GAN and FFDNet are 6.4609 s, 155.3158 s, 1.9394 s and 1.0622 s, respectively. © 2022
Number of references: 34
Main heading: Generative adversarial networks
Controlled terms: Gaussian distribution - Gaussian noise (electronic) - Image denoising - Mean square error - Signal to noise ratio - Singular value decomposition
Uncontrolled terms: Block Matching - De-noising - Evaluation metrics - Gaussians - Global residual generative adversarial network - Root mean squared errors - Section image - Test sets - Thin section image - Thin-sections
Classification code: 716.1 Information Theory and Signal Processing - 723.2 Data Processing and Image Processing - 723.4 Artificial Intelligence - 921 Mathematics - 922.1 Probability Theory - 922.2 Mathematical Statistics
Numerical data indexing: Decibel 1.50E+01dB, Decibel 2.50E+01dB, Decibel 3.50E+01dB, Time 1.0589E+00s, Time 1.0622E+00s, Time 1.553158E+02s, Time 1.9394E+00s, Time 6.4609E+00s

101. A novel strengthening mechanism in crystalline/amorphous dual-phase Mg alloys: A molecular dynamics study

Authors: Han, L. (1, 2); Song, H.Y. (1, 3); An, M.R. (1); Shen, T.Z. (1); Li, Y.L. (3)
Author affiliation: (1) College of New Energy, Xi'an Shiyou University, Xi'an; 710065, China; (2) College of Material Science and Engineering, Xi'an Shiyou University, Xi'an; 710065, China; (3) School of Aeronautics, Northwestern Polytechnical University, Xi'an; 710072, China
Corresponding authors: An, M.R.(anminrong@xsyu.edu.cn); Song, H.Y.(hysong@xsyu.edu.cn)

Abstract: The crystalline/amorphous dual-phase structure is a novel and advanced strategy to improve the mechanical properties of Mg alloys. Here, molecular dynamics simulation is employed to investigate the effect of the amorphous nanopillar size and the content of rare earth element Y on the interaction mechanism between prismatic $\langle\#\rangle$ dislocation and amorphous nanopillar in the Mg alloys. The results show that the strengthening effect of amorphous nanopillar on the Mg alloys is significantly dependent on the size of the amorphous nanopillar. It is worth noting that an unconventional mechanism caused by extended dislocations appears when dislocation interacts with amorphous nanopillar, which is different from the traditional shear mechanism and Orowan mechanism of the interaction between dislocation and crystalline precipitates. The results also indicate that Y atoms can increase the difficulty of the $\langle\#\rangle$ basal slip, thus preventing the perfect prismatic dislocation from decomposing into extended dislocation on basal plane. © 2023

102. Role of natural fractures with topology structure for hydraulic fracture propagation in continental shale reservoir

Authors: Wang, Xiaoming (1, 2); Chen, Junbin (1, 2); Ren, Dazhong (1, 2); Zhu, Jianhong (1, 2)
Author affiliation: (1) Shaanxi Key Laboratory of Well Stability and Fluid & Rock Mechanics in Oil and Gas Reservoirs, Xi'an Shiyou University, Shaanxi, Xi'an; 710065, China; (2) College of Petroleum Engineering, Xi'an Shiyou University, Shaanxi, Xi'an; 710065, China
Corresponding author: Chen, Junbin(chenjbxu@126.com)
Abstract: Natural fractures tend to further promote fracture network which is initiated by hydraulic fracturing. However, how natural fractures with various topology structures impact hydraulic fracture propagation in continental shale reservoir is still unclear. With Fullbore Microscan Imager (FMI) and geo-statistics of Chang 7 reservoir in Yanchang Formation, typical natural fractures are classified into three topology structures, which are natural fractures with type I, type II and type III nodes respectively, and the average occurrence strikes of natural fractures with type I, type II and type III nodes are SW260°, SW255° and SW255°. Coupling with seepage field and stress field, a model simulating fracture initiation and propagation is established considering the transversely isotropic property of continental shale reservoir. On this basis, the role of typical natural fractures with topology structure for hydraulic fracture propagation is studied qualitatively and quantitatively by Finite Element Method (FEM) with globally embedded cohesive element. Natural fractures with type II nodes have largest effect on inducing hydraulic fracture propagation, hydraulic fractures can communicate most easily with them, and also the length and velocity of hydraulic fracture propagation are the longest and fastest, so fracture network is the most complex after fracturing in naturally fractured continental shale reservoir with type II nodes, which follows by the effect of hydraulic fracture propagation in naturally fractured continental shale reservoir with type III nodes. In comparison, natural fractures with type I nodes have insignificant impacts on hydraulic fracture propagation. The research results are conductive to fracturing design in continental shale reservoir. © 2023 Elsevier Ltd

103. Angle of Arrival Localization in Wireless Sensor Networks With Inaccurate Anchor Positions

Authors: Wang, Qi (1); Hu, Guang (1); Li, Fei (1)
Author affiliation: (1) School of Electronic Engineering, Xi'an Shiyou University, Shaanxi, Xi'an; 710065, China
Corresponding author: Wang, Qi(wangqi@xsyu.edu.cn)

Abbreviated source title: Proc SPIE Int Soc Opt Eng
Volume: 12610
Part number: 1 of 1
Issue title: Third International Conference on Artificial Intelligence and Computer Engineering, ICAICE 2022
Issue date: 2023
Publication year: 2023
Article number: 126104H
Language: English
ISSN: 0277786X
E-ISSN: 1996756X
CODEN: PSISDG
ISBN-13: 9781510663473
Document type: Conference article (CA)
Conference name: 3rd International Conference on Artificial Intelligence and Computer Engineering, ICAICE 2022
Conference date: November 11, 2022 - November 13, 2022
Conference location: Wuhan, China
Conference code: 188293
Sponsor: Academic Exchange Information Centre (AEIC); Dalian Minzu University; Dalian Ocean University; Nanjing University of Aeronautics and Astronautics
Publisher: SPIE

Abstract: Angle of arrival based localization has been widely applied in wireless sensor network due to its easy access of measurements and simple system structure. In previous work, the positions of anchor nodes are generally assumed precisely known, which is an important condition in addition to the angle of arrival measurements. However, in practice, anchor positions are obtained by Global Positioning System or other localization methods, which inevitably suffer from errors. These errors, leading to inaccurate anchor positions, have heavy impact on the localization result. Although there are a few studies on the errors of anchor position in wireless localization, they mainly focus on range based measurements. In this paper, we study angle of arrival based localization with inaccurate anchor positions. Stemming from the maximum likelihood estimation, a novel semidefinite programming method is proposed by using tight approximation and proper relaxation. Numerical examples demonstrate that the proposed method provides much better performance in terms of localization accuracy, compared to some existing methods. © 2023 SPIE.
Number of references: 10
Main heading: Errors
Controlled terms: Direction of arrival - Maximum likelihood estimation - Numerical methods - Wireless sensor networks
Uncontrolled terms: Anchor nodes - AOA - Aoa (angleof-arrival) - Inaccurate position - Localisation - Measurement system - SDP - Simple system - Systems Structure - WSN
Classification code: 716.1 Information Theory and Signal Processing - 716.3 Radio Systems and Equipment - 722.3 Data Communication, Equipment and Techniques - 921.6 Numerical Methods - 922 Statistical Methods
DOI: 10.1117/12.2671085

Compendex references: YES
Database: Compendex
Data Provider: Engineering Village

104. Weighted Schatten p -norm and Laplacian scale mixture-based low-rank and sparse decomposition for foreground-background separation

Accession number: 20232014109127
Authors: Fan, Ruibo (1); Jing, Mingli (1); Li, Lan (2); Shi, Jingang (3); Wei, Yufeng (4)
Author affiliation: (1) Xi'an Shiyou University, School of Electronics Engineering, Xi'an, China; (2) Xi'an Shiyou University, School of Science, Xi'an, China; (3) Xi'an Jiaotong University, School of Software Engineering, Xi'an, China; (4) Northwestern Polytechnical University, School of Computer Science, Xi'an, China
Corresponding author: Jing, Mingli(mljingsy@xsyu.edu.cn)

Source title: Journal of Electronic Imaging
Abbreviated source title: J. Electron. Imaging
Volume: 32
Issue: 2
Issue date: March 1, 2023
Publication year: 2023
Report number: 221268G
Article number: 023021
Language: English
ISSN: 10179909
E-ISSN: 1560229X
CODEN: JEIME5
Document type: Journal article (JA)
Publisher: SPIE

Abstract: Low-rank and sparse decomposition (LRSD) plays a vital role in foreground-background separation. The existing LRSD methods have the drawback: imprecise surrogate functions of rank and sparsity. We propose the weighted Schatten p-norm (WSN) and Laplacian scale mixture (LSM) method based on LRSD for foreground-background separation, which introduces the WSN and LSM to improve this drawback. To demonstrate the performance of the proposed method, it is applied to foreground-background separation and gets the highest average F-measure score. © 2023 SPIE and IS&T.

Number of references: 46
Main heading: Laplace transforms
Controlled terms: Approximation theory
Uncontrolled terms: Background separation - Foreground-background separation - Foreground/background - Laplacian scale mixture - Laplacians - Low rank approximations - P -norm - Scale mixtures - Sparse representation - Weighted schatten
Classification code: 921.3 Mathematical Transformations - 921.6 Numerical Methods
DOI: 10.1117/1.JEI.32.2.023021
Funding Details: Number: 290088266, Acronym: -, Sponsor: -; Number: YCS22112056, Acronym: -, Sponsor: -; Number: 62002283, Acronym: NSFC, Sponsor: National Natural Science Foundation of China;
Funding text: This work was supported in part by the National Natural Science Foundation of China (Grant No. 62002283), the Doctoral Innovation Fund of Xi'an Shiyou University (Grant No. 290088266), and the Postgraduate Innovation and Practical Ability Training Program of Xi'an Shiyou University (Grant No. YCS22112056).
Compendex references: YES
Database: Compendex
Data Provider: Engineering Village

105. E-Learning Teaching System in Augmentative and Alternative Communication Using Big Data Analytics (*Open Access*)

Accession number: 20231013693533
Authors: Lei, Lei (1); Hsu, Ching-Hsien (2); Kadry, Seifedine Nimer (3)
Author affiliation: (1) Xi'an Shiyou University, China; (2) Asia University, Taiwan; (3) Beirut Arab University, Lebanon
Corresponding author: Lei, Lei
Source title: International Journal of e-Collaboration
Abbreviated source title: Int. J. e-Collab.
Volume: 19
Issue: 4
Issue date: 2023
Publication year: 2023
Language: English
ISSN: 15483673
E-ISSN: 15483681
Document type: Journal article (JA)
Publisher: IGI Global

Abstract: The key barriers to children with special needs to contact individuals are to sustain them alertly and efficiently for learning languages. As the first step for students with disabilities is language development. The report contributes to the sector by identifying the obstacles and opportunities. The research proposed an English language teaching in augmentative and alternative communication (ELT-AAC) and was performed using a qualitative approach

by extracting evidence from several independent schools with particular students. The results showed the educators were faced with great difficulty in educating advanced students on the language: limited comprehension, classroom equipment, unawareness, and inappropriate language instruction. The research further showed that the problems were mitigated and language instruction improved by special education, another welldesigned class, daily psychological counseling, and various viewpoints. © 2023 IGI Global. All rights reserved.

Number of references: 39
Main heading: Students
Controlled terms: Big data - Data Analytics - E-learning - Learning systems
Uncontrolled terms: Analytic - Augmentative-and-alternative communication - Data analytics - E - learning - E-learning teaching - Language development - Language proficiency - Special education - Special needs - Teaching systems
Classification code: 723.2 Data Processing and Image Processing
DOI: 10.4018/ijec.316826
Compendex references: YES
Open Access type(s): All Open Access, Hybrid Gold
Database: Compendex
Data Provider: Engineering Village
Compilation and indexing terms, Copyright 2023 Elsevier Inc.

106. Highway traffic accident duration prediction based on ensemble learning and data augmentation

Accession number: 20232014107859
Authors: Chen, Jiaona (1); Li, Daofeng (1); Tao, Weijun (1); Zhang, Jing (1); Wang, Peng (1)
Author affiliation: (1) School of Electronic Engineering, Xi'an Shiyou University, Shaanxi, Xi'an; 710061, China
Corresponding author: Chen, Jiaona(chenjn@xsyu.edu.cn)
Source title: Proceedings of SPIE - The International Society for Optical Engineering
Abbreviated source title: Proc SPIE Int Soc Opt Eng
Volume: 12609
Part number: 1 of 1
Issue title: International Conference on Computer Application and Information Security, ICCAIS 2022
Issue date: 2023
Publication year: 2023
Article number: 126091B
Language: English
ISSN: 0277786X
E-ISSN: 1996756X
CODEN: PSISDG
ISBN-13: 9781510663459
Document type: Conference article (CA)
Conference name: 2022 International Conference on Computer Application and Information Security, ICCAIS 2022
Conference date: December 23, 2022 - December 24, 2022
Conference location: Wuhan, China
Conference code: 187975
Sponsor: The Society of Photo-Optical Instrumentation Engineers (SPIE)
Publisher: SPIE
Abstract: Predicting the duration of traffic accidents is an important part of emergency safety management, which can provide theoretical basis for road diversion and rescue. The validity of long-term forecasts depends largely on the quality of the data. Due to the discreteness, randomness and complexity of traffic accidents, the unbalanced samples is a common problem in traditional prediction models. The generalization ability of the model is insufficient. Based on the Mixup and ensemble learning, the accident duration prediction model is designed. The new datasets are created and extended. Several machine learning techniques are compared and analyzed with RMSE, MAPE and R2, including K Nearest Neighbor (KNN), decision trees (DT), random forests (RF), gradient-based trees (GBDT), AdaBoost, extreme random trees, and XGBoost. The results show that the Mixup-PSO-XGBoost performs the best as well as the training time. Furthermore, data augmentation is an effective technique to strengthen the ensemble algorithms in prediction. © 2023 SPIE.

Number of references: 10
Main heading: Learning systems
Controlled terms: Adaptive boosting - Decision trees - Forecasting - Highway accidents - Nearest neighbor search

Uncontrolled terms: Data augmentation - Duration predictions - Duration time - Ensemble learning - Highway traffic accidents - Long-term forecast - Prediction modelling - Prediction-based - Safety management - Unbalanced data

Classification code: 432.1 Highway Transportation, General - 723 Computer Software, Data Handling and Applications - 914.1 Accidents and Accident Prevention - 921.4 Combinatorial Mathematics, Includes Graph Theory, Set Theory - 921.5 Optimization Techniques - 961 Systems Science

DOI: 10.1117/12.2671822

Compendex references: YES
Database: Compendex
Data Provider: Engineering Village

107. A one-pot strategy for the preparation of fire-retardant poly(propylene carbonate) by terpolymerization of CO2, propylene oxide and chlorendic anhydride

Accession number: 20230113330679

Authors: Wang, Wenzhen (1); Zhang, Xiangmin (1); Han, Weiwei (1); Huang, Jian (1); Zhang, Yile (1); Zhao, Chen (1); Li, Leilei (1)
Author affiliation: (1) College of Chemistry and Chemical Engineering, Xi'an Shiyou University, Xi'an; 710065, China
Corresponding author: Wang, Wenzhen(wzwang@xsyu.edu.cn)

Source title: Materials Today Communications
Abbreviated source title: Mater. Today Commun.
Volume: 34
Issue date: March 2023
Publication year: 2023
Article number: 105179
Language: English
E-ISSN: 23524928
Document type: Journal article (JA)
Publisher: Elsevier Ltd

Abstract: A functional monomer chlorendic anhydride (CA) with flame retardancy was added to the polymerization reaction between CO_2 and propylene oxide (PO) to form a terpolymer plastic polycarbonates (PPCCA) for the first time. Compared with conventional poly(propylene carbonate) (PPC), the synthesized PPCCA exhibited excellent thermal properties, mechanical properties, dimensional stability, high degradation and flame retardant (FR) properties. When the CA content was increased to 5 mol% (with respect to PO, except specially stated), the 5% weight-loss degradation temperatures (T_d, -5%), the maximum weight-loss degradation temperatures (T_d, max) and the glass transition temperature (T_g) of PPCCA were increased to 235 , 345 and 44 , respectively. Additionally, in the CA content range of 0–5 mol%, the tensile strength of PPCCA increased to 26.7 ± 1.4 MPa and the elongation at break decreased to 144.4 ± 1.2%. Furthermore, within the same content range (0–5 mol%) of CA, the hot-set elongation (#Lh) and permanent deformation (#Lp) were reduced to 95% and 50%, respectively. The PPCCA exhibited good degradability as well. In terms of FR properties, the limiting oxygen index (LOI) of PPCCA (with 5 mol% CA, PPCCA5) was 33.5%, with which the vertical combustion test level turned out to be at the highest level (V-0), which truly improved the flame retardancy of the polymer. © 2022 Elsevier Ltd

Number of references: 55
Main heading: Carbon dioxide
Controlled terms: Carbonation - Combustion - Glass transition - Propylene - Tensile strength
Uncontrolled terms: Chlorendic anhydride - Degradation temperatures - Flame retardant properties - Flame-retardancy - One pot - Poly(propylene carbonate) - Polypropylene carbonate - Propylene oxide - Weight loss
Classification code: 802.2 Chemical Reactions - 802.3 Chemical Operations - 804.1 Organic Compounds - 804.2 Inorganic Compounds

Compendex references: YES
Database: Compendex
Data Provider: Engineering Village

108. Direct Mass Spectrometric Analysis of Hydrogen Sulfide in Complex Oil Samples

Accession number: 20231013663125
Title of translation:
Authors: Zhang, Yuan (1); Zheng, Ya-Jun (1); Lu, Fang-Fang (1); Zhang, Zhi-Ping (1)
Author affiliation: (1) School of Chemistry and Chemical Engineering, Xi'an Shiyou University, Xi'an; 710065, China
Corresponding author: Zhang, Zhi-Ping
Source title: Journal of Chinese Mass Spectrometry Society
Abbreviated source title: J. Chin. Mass Spectrom. Soc.
Volume: 44
Issue: 1
Issue date: January 1, 2023
Publication year: 2023
Pages: 46-54
Language: Chinese
ISSN: 10042997
Document type: Journal article (JA)
Publisher: Chinese Society for Mass Spectrometry
Abstract: Due to the high viscosity and bulk complexity of crude oil samples, it poses a grand challenge to determine hydrogen sulfide (H2S) in them. Although many methods have been developed for the analysis of H2S in complex systems, these methods generally have complex processes, large analysis error and low sensitivity. In the study, based on the reaction between triazine and H2S by generating thiadiazine, a small volume of complex crude oil sample was introduced directly into a triazine solution using acetonitrile as solvent for transferring H2S into detectable species by organic mass spectrometry. The experimental parameters of solution composition, acetic acid content, reaction time and reaction temperature were optimized, and the method of paper spray ionization-mass spectrometry (PSI-MS) was established for rapid analysis of H2S in complex crude oil samples. An optimal performance was achieved when the reaction of triazine and H2S was carried out at 30 °C for 2 h with acetonitrile containing 0. 1 % acetic acid as solvent. The standard curve for the quantitative analysis of H2S was constructed according to the linear relationship between MS signal intensity of resulting thiadiazine and the concentration of H 2 S, which was applied for actual crude oil samples from different sources. The results showed that the linear range and the limit of detection (LOD) were 0. 1-1000 μg/L and 0. 041 μg/L with intra-day precision of 3. 04% and inter-day precision of 3.18%, respectively. The PSI-MS was also employed to determine H2S in different actual crude oil samples, and the spiked recovery was 91.7%-103.5% with relative standard deviation (RSD) of 1.2%-4.5%. This method has the advantages of easy operation, low cost, high sensitivity and less contamination to mass spectrometer, which is promising for the direct and fast analysis of ITS in complex crude oil samples. © 2023 Chinese Society for Mass Spectrometry. All rights reserved.
Number of references: 28
Main heading: Hydrogen sulfide
Controlled terms: Acetic acid - Acetonitrile - Crude oil - Mass spectrometry - Organic solvents - pH - Sulfur determination
Uncontrolled terms: Complex Processes - Error sensitivity - Grand Challenge - High viscosities - Ionization mass spectrometry - Mass spectrometric analysis - Oil samples - Paper spray - Spray ionization - Triazine
Classification code: 512.1 Petroleum Deposits - 801 Chemistry - 801.1 Chemistry, General - 803 Chemical Agents and Basic Industrial Chemicals - 804.1 Organic Compounds - 804.2 Inorganic Compounds

109. Long lifespan thermal barrier coatings overview: Materials, manufacturing, failure mechanisms, and multiscale structural design

Authors: Song, Jin-Bao (1); Wang, Li-Shuang (1); Dong, Hui (1); Yao, Jian-Tao (1)
Author affiliation: (1) School of Materials Science and Engineering, Xi'an Shiyou University, Xi'an; 710065, China
Corresponding author: Wang, Li-Shuang(lswang@xsyu.edu.cn)

Abstract: A long lifespan is a basic support for the thermal protection of thermal barrier coatings (TBCs). Plasma-sprayed TBCs provide high thermal insulation and cost-effective advantages; thus, they are used in cutting-edge areas, such as land-based gas turbines. However, following thermal exposure, sintering causes structural changes and significant degradation in thermal insulation and strain tolerance. Thus, plasma-sprayed TBCs often show poor performance in thermal cycling tests. Therefore, extending the lifespan of plasma-sprayed TBCs is crucial. This study reviews the structural design of TBCs for a long lifespan. The main contents reviewed include the following aspects: (1) the basic structural features of plasma-sprayed TBCs with high thermal insulation and strain tolerance in an as-deposited state; (2) the dynamic structural evolution during thermal exposure to reveal the degradation mechanism in thermal and mechanical properties; and (3) multiscale structural design of TBCs to achieve a long lifespan. This review aims to contribute to the development of advanced gas turbines. © 2022 Elsevier Ltd and Techna Group S.r.l.

Compendex references: YES
Database: Compendex
Data Provider: Engineering Village

110. Evaluation of Spatial Spillover Effect of Multidimensional Hybrid Financial Risk Contagion Based on the DAI Spatial Econometric Model

Accession number: 20231714006169
Authors: Li, Shanshen (1); Dong, Zhonghui (1)
Author affiliation: (1) School of Economics and Management, Xi'An Shiyou University, Shaanxi, Xi'an; 710065, China
Corresponding author: Li, Shanshen(ssli@xsyu.edu.cn)
Source title: Advances in Multimedia
Abbreviated source title: Adv. Multimedia
Volume: 2023
Issue date: 2023
Publication year: 2023
Article number: 5167499
Language: English
ISSN: 16875680
E-ISSN: 16875699
Document type: Journal article (JA)
Publisher: Hindawi Limited
Abstract: The process of global integration has accelerated, and the international financial market has become increasingly closely linked. The financial risks that come with them are becoming more complex and difficult to guard against. Multimedia modeling in Health Cloud biometric authentication and data management systems can be applied to the analysis of financial markets. Most of the current financial risk analysis models are based on a single time, and the models are relatively simple and cannot adapt to the current complex multidimensional mixed financial risk environment. Therefore, this paper aimed to analyze the spatial spillover effect of financial risk contagion based on the directed asymmetric (DAI) spatial econometric model. This paper proposed to transfer entropy information weight information and introduce the GARCH (generalized auto-regressive conditional heteroskedasticity) model to improve the traditional econometric model. By constructing a DAI measurement model, the spatial contagion of multidimensional mixed financial risks was analyzed, and on this basis, a generalized multidimensional economic space was established to analyze spatial spillover effects and analyze the specific path of spatial spillover effects. The model results in this paper showed that the degree of correlation between the stock and bond market varied greatly between countries. Among them, the change coefficient Ws#brsD of the event period was judged to have a large degree of negative change in the United Kingdom, Germany, and France in the European Union, which were -0.9885, -0.9876, and -0.9748, respectively. This showed that the model in this paper had a good and reliable ability to cope with the current multidimensional mixed complex financial risk environment and could be used as a reference for financial risk-related research. At the same time, it also proved that multimedia modeling in health cloud biometric authentication and data management system could provide a role in financial risk contagion analysis. © 2023 Shanshen Li and Zhonghui Dong.
Number of references: 18
Main heading: Financial markets
Controlled terms: Authentication - Biometrics - Commerce - Health risks - Information management - Risk analysis - Risk assessment - Spatial variables measurement
Uncontrolled terms: 'current - Biometric authentication - Biometric data - Data management system - Financial risks - Health clouds - Multimedia modeling - Risk environment - Spatial econometric models - Spillover effects
Classification code: 461 Bioengineering and Biology - 461.7 Health Care - 723 Computer Software, Data Handling and Applications - 914.1 Accidents and Accident Prevention - 922 Statistical Methods - 943.2 Mechanical Variables Measurements
DOI: 10.1155/2023/5167499
Compendex references: YES
Database: Compendex
Data Provider: Engineering Village

111. Molecular dynamics-based analysis of the factors influencing the CO2 replacement of methane hydrate

Authors: Li, Weirong (1); Xu, Haobin (1); Ma, Xinle (1); Dong, Zhenzhen (1); Lei, Gang (2); Qian, Shihao (1); Wei, Xin (1); Pan, Xu (1)
Author affiliation: (1) Xi'an Shiyou University, Xi'an; 710065, China; (2) China University of Geoscience, Wuhan; 430074, China
Corresponding author: Dong, Zhenzhen(zzdong@xsyu.edu.cn)
Abstract: The benefits of large reserves, wide distribution, and high combustion energy density of natural gas hydrates are of great practical importance to alleviate the energy tension, enhance the existing energy system in China and reduce the greenhouse effect. The CO2 replacement method is a critical way to develop natural gas hydrate, while traditional experimental methods are difficult to reveal the microscopic mechanism of the replacement system. An MD (molecular dynamics) technique was utilized in this work to simulate the process of carbon dioxide replacement of gas hydrates. This simulation investigates the effects of temperature, pressure, and CO2 purity during the CO2 replacement process. CO2, different concentrations of CO2/H2O, and CO2/NH3 are used as the injected fluid. The simulation results show that the influence of temperature on the CO2 replacement of natural gas hydrate is more significant than that of pressure. Within the temperature and pressure range specified in the simulation, H2O inhibits the replacement of CO2, owing to the inhibitory effect increasing as the concentration of H2O increases; NH3 promotes the process of CO2 replacement under the temperature conditions of 250 K and 260 K, and the promotion effect becomes more significant as the concentration of NH3 increases. However, adding NH3 inhibits the CO2 replacement process with hydrate when the temperature lifts to 270 K. These findings provide new ideas to improve the efficiency of the CO2 replacement method and provide theoretical insight for the engineering exploitation of hydrates. © 2022 Elsevier Inc.
Number of references: 36
Main heading: Carbon dioxide
Controlled terms: Ammonia - Density of gases - Gas hydrates - Gases - Greenhouse effect - Hydration - Methane - Molecular dynamics - Natural gas - Proven reserves - Temperature
Uncontrolled terms: CO2 replacement - Combustion energies - Energy density - Existing energies - Methane hydrates - Natural gas hydrates - Natural gas-hydrates - Practical importance - Replacement methods
Classification code: 443.1 Atmospheric Properties - 451 Air Pollution - 512.1.2 Petroleum Deposits : Development Operations - 512.2 Natural Gas Deposits - 522 Gas Fuels - 641.1 Thermodynamics - 801.4 Physical Chemistry - 804.1 Organic Compounds - 804.2 Inorganic Compounds - 931.2 Physical Properties of Gases, Liquids and Solids
Numerical data indexing: Temperature 2.50E+02K, Temperature 2.60E+02K, Temperature 2.70E+02K
DOI: 10.1016/j.jmgm.2022.108394
Compendex references: YES
Database: Compendex
Data Provider: Engineering Village

112. Elastic-net based robust extreme learning machine for one-class classification

Authors: Zhan, Weicheng (1); Wang, Kuaini (2, 3); Cao, Jinde (3, 4)

Author affiliation: (1) School of Computer Science, Xi'an Shiyou University, Shaanxi, 710065, China; (2) College of Science, Xi'an Shiyou University, Shaanxi, 710065, China; (3) School of Mathematics, Southeast University, Nanjing; 210096, China; (4) Yonsei Frontier Lab, Yonsei University, Seoul; 03722, Korea, Republic of
Corresponding author: Wang, Kuaini(wangkuaini1219@sina.com)
Abstract: The one-class extreme learning machine (OC-ELM) builds a classification model by learning samples of the known class to detect abnormal samples, and has the advantages of high learning speed and good generalization performance. However, OC-ELM with the square loss function is sensitive to outliers, which leads to poor robustness. To address this issue, an elastic-net based robust extreme learning machine for one-class classification (ER-OCELM) is proposed to achieve both excellent robustness and comparable sparsity. Correntropy loss function is utilized to limit the negative effects of outliers due to its property of bounded. With an elastic-net regularizer, automatic variable selection and continuous shrinkage can be performed simultaneously, and groups of correlated variables can be selected to make the model sparse. The corresponding optimization can be transformed into the linear equation system. We employ an iterative reweighted algorithm to obtain the optimal solution. In each iteration, the solution form of ER-OCELM is similar to that of ELM. Experiments on artificial and benchmark datasets verify that ER-OCELM has superior robustness and sparsity compared to many state-of-the-art methods. © 2023
Number of references: 37
Main heading: Iterative methods
Controlled terms: Knowledge acquisition - Linear equations - Machine learning - Statistics
Uncontrolled terms: Abnormal samples - Classification models - Correntropy - Correntropy loss function - Elastic net - Learning machines - Learning samples - Loss functions - One-class Classification - One-class extreme learning machine
Classification code: 723.4 Artificial Intelligence - 921.6 Numerical Methods - 922.2 Mathematical Statistics
DOI: 10.1016/j.sigpro.2023.109101
Compendex references: YES
Database: Compendex
Data Provider: Engineering Village

113. Design and Test of Flexible Drill Pipe for Sidetracking Horizontal Well in Digital Oilfield (*Open Access*)

Accession number: 20231713946704
Authors: Xue, Xianbo (1); Wang, Tianqi (2); Zhang, Wenbo (1); Liu, Xiaomin (1); Qu, Yue (1); Liu, Haijun (1); Feng, Yao (3)
Author affiliation: (1) China Oilfield Services Co., Ltd., Tianjin; 300459, China; (2) Mechanical Engineering College, Xi'an Shiyou University, Shaanxi, Xi'an; 710065, China; (3) Shaanxi Key Laboratory of Measurement and Control Technology for Oil and Gas Wells, Xi'an Shiyou University, Xi'an; 710065, China
Corresponding author: Wang, Tianqi(wangtianqi@xsyu.edu.cn)
Source title: Frontiers in Artificial Intelligence and Applications
Abbreviated source title: Front. Artif. Intell. Appl.

Abstract: Digital oilfield is the main means to increase production and income. Developing ultra-short radius sidetracking horizontal wells in old wells requires high-performance well trajectory control. In this paper, the ultra-short radius flexible drill pipe is designed by bionics principle, and logging tool is designed to monitor borehole trajectory in real time by using gamma ray technology. The combination of the flexible drill pipe and logging tool can realize the remaining oil recovery between dense well patterns. The dense well network determines that the drill pipe has a certain bending angle during drilling, and the remaining oil reservoir can be drilled in the shortest distance. The design of drilling tools for ultra-short radius horizontal wells for 7 'and 9-5/8' old well casings is the basis of this paper, the key is to verify the rationality of the design through experiments. The test research shows that, the strength of flexible drill pipe meets the design requirements and importing the monitoring data of gamma logging tool simulating the drilling process of the experimental well into LANDMARK software to describe the well trajectory, the radius of curvature of the deflecting section is 1.5m-2m, meeting the design expectation. © 2023 The authors and IOS Press.

Number of references: 19
Main heading: Infill drilling
Controlled terms: Boreholes - Drill pipe - Drills - Gamma rays - Horizontal wells - Oil well drilling - Oil well logging - Petroleum reservoir engineering - Software testing - Trajectories
Uncontrolled terms: Design and tests - Digital oilfield - Flexible drill pipe - Increase productions - Logging tools - Remaining oil - Sidetracking - Test - Well - Well trajectory
Classification code: 511.1 Oil Field Production Operations - 511.2 Oil Field Equipment - 512.1.1 Oil Fields - 512.1.2 Petroleum Deposits : Development Operations - 603.2 Machine Tool Accessories - 723.5 Computer Applications - 931.3 Atomic and Molecular Physics - 932.1 High Energy Physics
Numerical data indexing: Size 1.50E+00m to 2.00E+00m
DOI: 10.3233/FAIA230064
Compendex references: YES
Open Access type(s): All Open Access, Hybrid Gold
Database: Compendex
Data Provider: Engineering Village

114. Hologram quantitative structure-activity relationship guided in silicon molecular design of phenothiazine dye sensitizers for dye-sensitized solar cells

Accession number: 20225213319305
Authors: Jiao, Long (1); Liu, Pengfei (1); Yan, Chunhua (1); Qu, Le (2); Wang, Qin (3); Li, Hua (1)
Author affiliation: (1) College of Chemistry and Chemical Engineering, Xi'an Shiyou University, Xi' an; 710065, China; (2) College of Petroleum Engineering, Xi'an Shiyou University, Xi' an; 710065, China; (3) Shaanxi Key Laboratory of Catalysis, School of Chemistry and Environment Science, Shaanxi University of Technology, Shaanxi, Hanzhong; 723000, China
Corresponding author: Jiao, Long(mop@xsyu.edu.cn)

Abstract: Hologram quantitative structure–activity relationship (HQSAR) method was successfully introduced into the structure-performance study on the phenothiazine dye sensitizers of dye-sensitized solar cells. A total of 79 phenothiazine derivatives were investigated to build the HQSAR model of power conversion efficiency. The fragment parameters of the established optimal HQSAR model are fragment size: "4 ⌣ 7", hologram length: "353", and fragment distinction: "bonds, connections, chirality, donor and acceptor atoms". The predictive performance of the HQSAR model was evaluated with external test set validation and leave-one-out cross-validation. The validation results demonstrate that the developed model possesses high prediction ability and stability. The molecular contribution map of this model was analyzed to reveal the key structures and modification positions for improving the power conversion efficiency, and was used to guide the molecular design of high performance dye sensitizers. The theoretical prediction result of several literature reported phenothiazine compounds indicates that the developed model is an effective and important guidance to the molecular design of dye sensitizers. Therefore, several new phenothiazine derivatives with theoretically improved power conversion efficiency were designed by the proposed HQSAR-based strategy. © 2022 International Solar Energy Society

Number of references: 42
Main heading: Conversion efficiency
Controlled terms: Dye-sensitized solar cells - Holograms - Insecticides - Silicon - Structural design
Uncontrolled terms: Developed model - Dye sensitizers - Dye- sensitized solar cells - Hologram quantitative structure–activity relationship - Molecular design - Phenothiazine derivatives - Power conversion efficiencies - Quantitative structure activity relationship - Quantitative structure-activity relationship methods - Quantitative structure-activity relationship modeling
Classification code: 408.1 Structural Design, General - 525.5 Energy Conversion Issues - 549.3 Nonferrous Metals and Alloys excluding Alkali and Alkaline Earth Metals - 702.3 Solar Cells - 743 Holography - 801.4.1 Electrochemistry - 803 Chemical Agents and Basic Industrial Chemicals
DOI: 10.1016/j.solener.2022.12.021

Compendex references: YES
Database: Compendex
Data Provider: Engineering Village

115. Study on the influence law of well location and water injection displacement on heat extraction performance of EGS   (*Open Access*)

Accession number: 20232414214413
Authors: Zhao, Kai (1, 2, 3); Song, Wenjie (1); Wang, Xiaoyun (1); Xu, Zhihui (1); Shi, Shuyi (1)
Author affiliation: (1) College of Petroleum Engineering, Xi'an Shiyou University, Shaanxi, Xi'an, China; (2) State Key Laboratory of Oil and Gas Reservoir Geology and Exploitation, Chengdu University of Technology, Chengdu, China; (3) Xi'an Key Laboratory of Tight Oil (Shale oil) Development (Xi'an Shiyou University), Shaanxi, Xi'an, China
Corresponding author: Zhao, Kai(zkaiup@126.com)
Source title: Energy Science and Engineering
Abbreviated source title: Energy Sci. Eng.
Issue date: 2023
Publication year: 2023
Language: English
E-ISSN: 20500505
Document type: Article in Press

Publisher: John Wiley and Sons Ltd

Abstract: The enhanced geothermal system (EGS) is the key to improving the heat production efficiency of hot dry rock (HDR). Due to the existence of EGS, the reservoir produces significant heterogeneity, so the optimal design of well location and injection rate has an important influence on the heat recovery effect of an EGS. To solve this problem, a calculation model for the heat output of an EGS under multifield coupling is established in this paper, and the influence of well location and injection rate on the heat recovery effect under different scales of EGS is deeply analyzed. The results show that the production well location and injection well displacement have a great influence on the heat recovery effect under different fracture-network scales. The larger the size of the fracture network, the larger the effective utilization area of reservoir heat recovery and the better the effect of heat recovery. The closer the production well is to the fracture network and in the direction of the fracture network, the larger the effective utilization area of reservoir heat recovery is, and the better the effect of heat recovery is. The higher the injection well displacement is, the larger the effective utilization area of reservoir heat recovery is, and the better the heat recovery effect is. The research results have important guiding significance for the optimization of the scale, well placement, and water injection displacement of the EGS in the HDR reservoir. © 2023 The Authors. Energy Science & Engineering published by Society of Chemical Industry and John Wiley & Sons Ltd.

Number of references: 19

Main heading: Extraction

Controlled terms: Fracture - Geothermal fields - Geothermal wells - Injection (oil wells) - Location - Production efficiency - Waste heat - Water injection

Uncontrolled terms: Enhanced geothermal systems - Fracture network - Heat extraction - Heat extraction effect - Hot dry rock - Placement of well - Recovery effects - Water injection rate - Well injections - Well location

Classification code: 481.3.1 Geothermal Phenomena - 511.1 Oil Field Production Operations - 525.4 Energy Losses (industrial and residential) - 612.1 Internal Combustion Engines, General - 615.1 Geothermal Energy - 802.3 Chemical Operations - 913 Production Planning and Control; Manufacturing - 913.4 Manufacturing - 951 Materials Science

DOI: 10.1002/ese3.1474

Compendex references: YES

Open Access type(s): All Open Access, Gold

Database: Compendex

Data Provider: Engineering Village

116. Self-Attention Mechanism for Dynamic Multi-Step Rop Prediction Under Continuous Learning Structure

Accession number: 20230086164

Authors: Liu, Ye (1); Zhang, Fuqiang (1); Yang, Shuopeng (1); Cao, Jie (2)

Author affiliation: (1) School of Computer Science, Xi'an Shiyou University, Shaanxi, Xi'An; 710065, China; (2) eDrilling AS, Rogaland, Stavanger, Norway

Corresponding author: Cao, Jie

Source title: SSRN

Issue date: March 14, 2023

Publication year: 2023

Language: English

ISSN: 15565068

Document type: Preprint (PP)

Publisher: SSRN

Abstract: The evaluation and prediction of the rate of penetration in real-time drilling operations have been long-term challenging due to, for example, the complexity of influence parameters and uncertainties from the subsurface. In this paper, to further improve the practical ROP prediction, we propose a machine learning structure combining with a conceptual framework of continuous learning and a deep learning network with the self-attention mechanism. The self-attention mechanism presents a more powerful ability to capture the long-dependence relation within the sequential data. Compared with the other commonly used recurrent neural networks, the proposed self-attention

network model shows significant improvement in reliability and accuracy, especially when one tries to forward predict a long sequence of ROPThis newly presented model can predict the real-time long-term ROP value and can further improve its efficiency by adjusting the controllable drilling parameters. Case studies demonstrate the effectiveness and stability of the proposed model, which reaches a higher prediction accuracy than 90% for three testing wells. Hence, the proposed structure and networt can help with predictive analysis for real-tme drilling performance an accurate and stable model. © 2023, The Authors. All rights reserved.

Number of references: 24
Main heading: Recurrent neural networks
Controlled terms: Infill drilling - Learning systems - Predictive analytics - Well testing
Uncontrolled terms: Attention mechanisms - Continuous learning - Drilling operation - Evaluation and predictions - Influence parameter - Learning structure - Multisteps - Rate of penetration - Real time drilling - Self-attention network
Classification code: 511.1 Oil Field Production Operations
Numerical data indexing: Percentage 9.00E+01%
DOI: 10.2139/ssrn.4388304
Compendex references: YES
Preprint ID: 4388304
Preprint source website: https://papers.ssrn.com/sol3/papers.cfm
Preprint ID type: SSRN
Database: Compendex
Data Provider: Engineering Village

117. Trajectory tracking control of remotely operated vehicle based on thruster dynamics (*Open Access*)

Accession number: 20231914065919
Authors: Zhou, Huadong (1, 2)
Author affiliation: (1) School of Electronic Engineering, Xi'An Shiyou University, Shaanxi, Xi'an; 710065, China; (2) Shanghai Salvage, Shanghai; 201914, China
Corresponding author: Zhou, Huadong(bjhs2012zhd@126.com)
Source title: Applied Mathematics and Nonlinear Sciences
Abbreviated source title: Appl. Math. Nonlinear Sci.
Issue date: 2023
Publication year: 2023
Language: English
E-ISSN: 24448656
Document type: Article in Press
Publisher: Sciendo
Abstract: In order to reduce the impact of thruster dead zone on remotely operated vehicle (ROV) motion performance and ensure that it can complete trajectory tracking control under external interference. In this paper, the adaptive backstepping sliding mode control(ABSMC) method based on improved rapid power-to-power approximation law is proposed. Under the influence of external interference; ABSMC can quickly reduce the position error of the system, namely, shorten the approaching time. When the position error is small, the system can smoothly enter the sliding surface to eliminate chattering. A new thrust distribution method based on the pseudo-inverse method is proposed for the dead zone of a thruster. This method uses the pseudo-inverse method when the thrust is saturated. When all thruster thrusts are unsaturated, the thrust will remain outside the dead zone for a long time. Combined with the ABSMC method, the thrust output of the thruster is more smooth and more stable with small position errors. Finally, the effectiveness of the ABSMC method and the superiority of the new thrust distribution method is verified by simulation experiments. © 2023 Huadong Zhou, published by Sciendo 2023.
Number of references: 21
Main heading: Trajectories
Controlled terms: Backstepping - Errors - Inverse problems - Navigation - Remote control - Remotely operated vehicles - Sliding mode control
Uncontrolled terms: Adaptive backstepping sliding mode controls - Control methods - Dead zones - External interference - Position errors - Power - Pseudo-inverse method - Thrust distribution - Thrust saturation - Trajectory tracking control
Classification code: 731.1 Control Systems - 921 Mathematics - 961 Systems Science
DOI: 10.2478/amns.2023.1.00018
Compendex references: YES

118. Experimental study on the drainage gas recovery of an environmentally friendly nanofluid in tight gas reservoirs

Authors: Guowei, Qin (1, 2); Qingping, Liu (1); Xiaohui, Li (3); Saisai, Sun (1); Wenlong, Qin (1); Mei, Wu (4)
Author affiliation: (1) College of Petroleum Engineering, Xi'an Shiyou University, Xi'an, China; (2) Provincial Key Laboratory of Unusual Well Stimulation, Xi'an Shiyou University, Xi'an, China; (3) No. 3 Gas Production Plant of Changqing Oilfield Company, Inner Mongolia, China; (4) PetroChina Research Institute of Petroleum Exploration and Development, Beijing, China
Corresponding author: Guowei, Qin(qgw126@126.com)
Abstract: The efficiency of gas recovery in tight gas reservoirs has been a challenge in the oil and gas industry for the past decade because conventional drainage or water-controlled gas recovery technologies typically have poor performance in low-permeability reservoirs. To solve this problem, self-made nanofluid was introduced to enhance drainage gas recovery in a tight gas reservoir. In this paper, nanofluid was prepared by phase reversal technology for application in a tight gas reservoir. Its thermal, acidic, alkaline, and salty stabilities were systematically investigated by using light transmittance as a shortcut index. At the same time, its biodegradability and biotoxicity were evaluated based on the industry/national standard, and the effectiveness of its drainage gas recovery was studied by dynamic gas–water percolation. The results showed that the self-made nanofluid can be effectively used for drainage gas recovery in tight gas reservoirs. The nanofluid has chemical stability and is environmentally friendly, which fully conforms to the contemporary development trend of the oil and gas industry. The nanofluid can shift the isotonic point of the gas–water relative permeability to the left (its minimum is 1.83% at 6.25 wt.% and maximum is 4.78% at 100 wt.%) and reduce the irreducible water saturation (its minimum is 8.84% at 6.25 wt.% and maximum is 4.28% at 100 wt.%), achieving the purpose of the enhancement of drainage gas recovery. The research results provide technical support for the application of nanofluid to improve the gas production in tight gas reservoirs. © 2022 Canadian Society for Chemical Engineering.

Compendex references: YES
Database: Compendex
Data Provider: Engineering Village

119. Low-frequency temperature compensation fiber Bragg grating accelerometer based on double-arched beam

Accession number: 20224413026047
Authors: Fan, Wei (1, 2); Zhou, Rui (1); Li, Huidong (1, 2); Yu, Dakuan (2); Qiao, Xueguang (1)
Author affiliation: (1) School of Physics, Northwest University, Xi'an; 710072, China; (2) School of Science, Xi'an Shiyou University, Xi'an; 710065, China
Corresponding authors: Fan, Wei(fanwei@xsyu.edu.cn); Qiao, Xueguang(xgqiao@nwu.edu.cn)
Source title: Optics Communications
Abbreviated source title: Opt Commun
Volume: 528
Issue date: February 1, 2023
Publication year: 2023
Article number: 129058
Language: English
ISSN: 00304018
CODEN: OPCOB8
Document type: Journal article (JA)
Publisher: Elsevier B.V.
Abstract: To address the difficulty of existing optical sensors in meeting the requirements of low-frequency vibration monitoring in large structures, a dual-fiber Bragg grating acceleration sensor based on a double-arched beam was proposed. The difference in a wavelength shift of the two fiber gratings is used as the output signal of the accelerometer to realize the measurement of acceleration and temperature compensation in the low-frequency band. The sensitivity and resonant frequency of the accelerometer were analyzed based on the theoretical model of the sensor, and the sensitivity calibration experiment was carried out. The results show that the resonant frequency of the accelerometer is about 30Hz, the sensitivity is about 1158.6pm/g, and the temperature sensitivity can be reduced to 1.3 pm/C. The accelerometer can be used for real-time monitoring of vibration signals between 0.05 and 20 Hz. © 2022 Elsevier B.V.
Number of references: 24
Main heading: Accelerometers
Controlled terms: Arches - Fiber Bragg gratings - Natural frequencies - Temperature distribution
Uncontrolled terms: Acceleration sensors - Double-arched beam - Dual-fibre Bragg gratings - Fiber bragg grating accelerometer - Frequency-temperature compensations - Large structures - Low-frequency vibration - Lower frequencies - Temperature compensation - Vibration monitoring
Classification code: 408.2 Structural Members and Shapes - 641.1 Thermodynamics - 943.1 Mechanical Instruments
Numerical data indexing: Frequency 3.00E+01Hz, Frequency 5.00E-02Hz to 2.00E+01Hz, Size 1.1586E-09m, Size 1.30E-12m
DOI: 10.1016/j.optcom.2022.129058
Compendex references: YES
Database: Compendex
Data Provider: Engineering Village

120. The propagation behavior of hydraulic fracture network in a reservoir with cemented natural fractures (*Open Access*)

Accession number: 20231313812137
Authors: Zhang, Haoyu (1); Chen, Junbin (1); Zhao, Zhengyan (2); Li, Ziyan (1); Nie, Xiangrong (1)
Author affiliation: (1) College of Petroleum Engineering, Xi'an Shiyou University, Shaanxi, Xi'an, China; (2) Changqing Oilfield Oil & Gas Technology Research Institute, PetroChina, Shaanxi, Xi'an, China
Corresponding authors: Zhang, Haoyu(20111010006@stumail.xsyu.edu.cn); Chen, Junbin(chenjb@xsyu.edu.cn)
Source title: Energy Science and Engineering
Abbreviated source title: Energy Sci. Eng.
Volume: 11
Issue: 5
Issue date: May 2023
Publication year: 2023
Pages: 1643-1661
Language: English
E-ISSN: 20500505
Document type: Journal article (JA)
Publisher: John Wiley and Sons Ltd
Abstract: There are still some problems in the study of hydraulic fracture (HF) network evolution in cemented naturally fractured reservoirs, such as microseismic mapping showing exaggerated stimulated reservoir volume in some cases. In addition, the dominant role of natural fracture (NF) cementation strength, injection rate, in situ stress difference, NF distribution, and fracture initiation sequence of perforations in synthetically influencing fracture network formation needs to be further studied. For this purpose, a three-dimensional matrix hexahedral element global coupled 0-thickness cohesive element hydraulic fracturing model was developed. Results show that each interaction between HF and NF causes HF diameter shrinkage, which increases the propagation pressure of HF. When the cementation strength of the NF is low, the HF tends to deviate toward the tip of the NF to form a complex fracture network. Increasing the injection rate and the number of NFs can significantly enhance the complexity of the HF network, but does not change the HF and NF interaction pattern. The in situ stress differences dominate the morphology of the HF network when the cementation strength of NFs is constant. The stress interference of multiple fractures under segmented fracturing may form "S"-shaped HFs, and the HFs are difficult to maintain a symmetrical morphology in the direction of the well axis. In addition, some NFs in inactivated damaged zones have developed a certain width geometrically due to the induced effect of HF, but they are still isolated by the low permeability matrix and might only generate some microseismic events. © 2023 The Authors. Energy Science & Engineering published by the Society of Chemical Industry and John Wiley & Sons Ltd.
Number of references: 52
Main heading: Fracture
Controlled terms: Cementing (shafts) - Complex networks - Hydraulic fracturing - Morphology - Seismology - Stresses
Uncontrolled terms: Cementation strength - Energy - Fracture network - Hydraulic fracture network - Injection rates - Insitu stress - Natural fracture - Networks evolutions - Propagation behavior - Stress difference
Classification code: 484.1 Earthquake Measurements and Analysis - 512.1.2 Petroleum Deposits : Development Operations - 722 Computer Systems and Equipment - 931.2 Physical Properties of Gases, Liquids and Solids - 951 Materials Science
DOI: 10.1002/ese3.1410
Funding Details: Number: YCS22111002, Acronym: -, Sponsor: -; Number: 51874239, Acronym: NSFC, Sponsor: National Natural Science Foundation of China;
Funding text: The authors gratefully acknowledge the study presented in this paper was supported by the National Natural Science Foundation of China (No. 51874239), and the Postgraduate Innovation and Practice Ability Training Program of Xi'an Shiyou University (YCS22111002).
Compendex references: YES
Open Access type(s): All Open Access, Gold
Database: Compendex
Data Provider: Engineering Village
Compilation and indexing terms, Copyright 2023 Elsevier Inc.

121. Corrigendum to "SVR-based weighted processing method for electrical imaging logging in oil-based mud" [Journal of Applied Geophysics 209 (2023) 104911] (Journal of Applied Geophysics (2023) 209, (S0926985122003822), (10.1016/j.jappgeo.2022.104911))

Accession number: 20231313810289

Authors: Gao, Jianshen (1); Li, Dan (1); Jiang, Liming (2); Lu, Chunli (2); Zhu, Kairan (1); Xue, Fei (1)
Author affiliation: (1) School of Electronic Engineering, Xi'an Shiyou University, Xi'an; 710065, China; (2) China Petroleum Logging CO. LTD., Xi'an; 710077, China
Corresponding author: Gao, Jianshen(gjs1109@126.com)
Source title: Journal of Applied Geophysics
Abbreviated source title: J. Appl. Geophys.
Volume: 211
Issue date: April 2023
Publication year: 2023
Article number: 104984
Language: English
ISSN: 09269851
Document type: Erratum (ER)
Publisher: Elsevier B.V.
Abstract: The authors regret to inform that The authors would like to apologise for any inconvenience caused. © 2023 Elsevier B.V.
DOI: 10.1016/j.jappgeo.2023.104984
ErratuFlg: 2021691925
Database: Compendex
Data Provider: Engineering Village

122. SVR-based weighted processing method for electrical imaging logging in oil-based mud

Accession number: 20225013239118
Authors: Gao, Jianshen (1); Li, Dan (1); Jiang, Liming (2); Lu, Chunli (2); Zhu, Kairan (1); Xue, Fei (1)
Author affiliation: (1) School of Electronic Engineering, Xi'an Shiyou University, Xi'an; 710065, China; (2) China Petroleum Logging CO. LTD., Xi'an; 710077, China
Corresponding author: Gao, Jianshen(gjs1109@126.com)
Source title: Journal of Applied Geophysics
Abbreviated source title: J. Appl. Geophys.
Volume: 209
Issue date: February 2023
Publication year: 2023
Article number: 104911
Language: English
ISSN: 09269851
Document type: Journal article (JA)
Publisher: Elsevier B.V.
Abstract: Electrical imaging logging in high-resistivity oil-based mud (OBM) has been one of the hotspots in petroleum exploration and development recently. Compared with the traditional electrical imaging logging in water-based mud (WBM), the core issue restricting the application of electrical imaging logging in OBM is that the mud-layer with high impedance prevents the emitted current from flowing into the formation and seriously disturbs the measurement of formation properties. Here, a SVR (support vector machine regression)-based weighted processing method is proposed to resolve the intractable problem and three key parameters are obtained simultaneously. First, the equivalent circuit model of electrical imaging logging in OBM is established and the drawback especially occurring in low-resistivity formation is analyzed. Then, a weighted coefficient applied to the mud-layer impedance is introduced for the quantitative calculation of formation resistivity, and the change of relative formation permittivity and mud-layer thickness can also be depicted with weighted processing. Next, a SVR model is established to inverse the weighted coefficient and then figure out the inversed parameters including the formation resistivity, the relative formation permittivity, and the mud-layer thickness. A stochastic parameter model is adopted to verify the validity of SVR model. Finally, two deviated formation models further test the advantage and robustness of SVR model. The results demonstrate that the SVR-based weighted processing method possesses a terrific performance and all the three parameters can be calculated simultaneously regardless of the borehole wall condition. This study will provide a new approach to the data processing and interpretation of electrical imaging logging in OBM. © 2022 Elsevier B.V.

Number of references: 27
Main heading: Permittivity
Controlled terms: Boreholes - Data handling - Equivalent circuits - Gasoline - Image processing - Inverse problems - Oil field equipment - Petroleum prospecting - Stochastic models - Stochastic systems - Support vector machines
Uncontrolled terms: Electrical imaging - Electrical imaging logging - Formation permittivity - Formation resistivity - Imaging logging - Layer thickness - Mud layer - Mud-layer thickness - Oil-based mud - Support vector machine regression-based weighted processing - Support vector machine regressions
Classification code: 511.2 Oil Field Equipment - 512.1.2 Petroleum Deposits : Development Operations - 523 Liquid Fuels - 723 Computer Software, Data Handling and Applications - 723.2 Data Processing and Image Processing - 731.1 Control Systems - 922.1 Probability Theory - 961 Systems Science
DOI: 10.1016/j.jappgeo.2022.104911
Compendex references: YES
ErratuFlg: 2023182897
Database: Compendex
Data Provider: Engineering Village

123. Active and Reactive Power Coordination Optimization of the Active Distribution Network   (*Open Access*)

Accession number: 20231413833139
Authors: Deng, Guohao (1); Wang, Dang (2); Gao, Weixin (1)
Author affiliation: (1) School of Electronic Engineering, Xi'An Shiyou University, Shaanxi, Xian, China; (2) PipeChina West East Gas Pipeline Company, Shanghai, China
Corresponding author: Gao, Weixin(544778455@qq.com)
Source title: Journal of Physics: Conference Series
Abbreviated source title: J. Phys. Conf. Ser.
Volume: 2450
Part number: 1 of 1
Issue: 1
Issue date: 2023
Publication year: 2023
Article number: 012023
Language: English
ISSN: 17426588
E-ISSN: 17426596
Document type: Conference article (CA)
Conference name: 2022 6th International Conference on Electrical, Mechanical and Computer Engineering, ICEMCE 2022
Conference date: October 28, 2022 - October 30, 2022
Conference location: Xi'an, Virtual, China
Conference code: 187125
Publisher: Institute of Physics
Abstract: The operation and control of the active distribution network are faced with great challenges due to a mass of tunable and controllable devices connected to the network, resulting in large active power loss and voltage deviation. In this paper, a method of active and reactive power coordination optimization for the active distribution network based on a one-dimensional convolutional neural network (1D-CNN) is proposed. This method can mine valuable information from the historical data of distribution networks, and use one-dimensional convolutional neural networks to map the complex nonlinear relationship between node load and optimization strategy. The simulation results of the modified IEEE33 node distribution network system show that the active power loss and the node voltage deviation of the proposed method are significantly reduced. © Published under licence by IOP Publishing Ltd.
Number of references: 5

Main heading: Electric power distribution
Controlled terms: Convolution - Electric loads - Neural networks - Reactive power
Uncontrolled terms: Active and Reactive Power - Active distributions - Active power loss - Convolutional neural network - Coordination optimization - One-dimensional - Operations and control - Reactive power coordination - Tunables - Voltage deviations
Classification code: 706.1 Electric Power Systems - 706.1.2 Electric Power Distribution - 716.1 Information Theory and Signal Processing
DOI: 10.1088/1742-6596/2450/1/012023

Compendex references: YES
Open Access type(s): All Open Access, Gold
Database: Compendex
Data Provider: Engineering Village

124. Pore scale insights into the role of inertial effect during the two-phase forced imbibition

Accession number: 20232214165093
Authors: Cheng, Zhilin (1, 2); Gao, Hui (1); Tong, Shaokai (3); Zhang, Wentong (4); Ning, Zhengfu (2)
Author affiliation: (1) School of Petroleum Engineering, Xi'an Shiyou University, Shaanxi, Xi'an; 710065, China; (2) State Key Laboratory of Petroleum Resources and Prospecting in China University of Petroleum, Beijing; 102249, China; (3) Changqing Downhole Technology Company, CNPC Chuanqing Drilling Engineering Company, Xi'an, China; (4) School of New Energy, Xi'an Shiyou University, Shaanxi, Xi'an; 710065, China
Corresponding author: Cheng, Zhilin(zhilin_cheng1992@163.com)
Source title: Chemical Engineering Science
Abbreviated source title: Chem. Eng. Sci.
Volume: 278
Issue date: August 15, 2023
Publication year: 2023
Article number: 118921
Language: English
ISSN: 00092509
CODEN: CESCAC
Document type: Journal article (JA)
Publisher: Elsevier Ltd
Abstract: Fluid inertia could significantly alter the flow paths of fluids in multiphase flow. This study aims to quantify the role of the inertia effect in fluid flow through porous media using the modified color-gradient lattice Boltzmann method. Specifically, we focused on understanding the effects of fluid inertia on two-phase distribution, pore scale events, displacement patterns, transient behaviors of fluids, and the consumption of thermodynamic energy. Results show that the effect of fluid inertia on the two-phase distribution and the final invading wetting saturation is trivial under a low viscosity ratio. However, as the viscosity ratio increases, the inertia effect becomes more pronounced and cannot be ignored in the displacement process. This observation can also be found from the dependence of the invading saturation on the injected volume when the viscosity ratio and the Ohnesorge (Oh) number are varied. In

addition, we found that the contribution from the post-breakthrough stage to the total invading saturation is increasingly significant with the increasing viscosity ratio, and its contribution varies depending on the fluid inertia for a given viscosity ratio. We also used the pressure difference between the inlet and outlet to identify the direction of energy conversion in multiphase flow. It is found that for the high viscosity ratio, there is a positive relationship between the dissipated energy and the invading saturation, and both exhibit a non-monotonic change with increasing Oh. However, for low viscosity ratios, fluid inertia does not significantly affect forced imbibition. In addition, the nonwetting phase becomes less connected with the injected wetting fluid, and there exists an almost linear relationship between the invading wetting saturation and the Euler characteristic, irrespective of the Oh numbers for a given viscosity ratio. The mechanism of inertial effect is that the local fluid velocity can be several orders of magnitude larger than the mean velocity despite the low capillary number, which leads to frequent release of surface energy and notably alters the flow paths, particularly under the unfavorable displacement pattern. © 2023 Elsevier Ltd

125. Study of a high efficient composite foam drainage surfactant for gas production

Authors: Dong, Jie (1, 2); Tao, Rongde (3); Xu, Jun (4); Li, Yongfei (1); Dong, Sanbao (1, 2); Chen, Gang (1, 2)
Author affiliation: (1) State Key Laboratory of Petroleum Pollution Control, Xi'An Shiyou University, Xi'an; 710065, China; (2) Shaanxi Prov. Key Lab. of Environ. Poll. Control and Reservoir Protection Technology of Oilfields, Xi'An Shiyou University, Xi'an; 710065, China; (3) No 8 Production Plant, Changqing Oilfield Company Oil, Xi'an; 710068, China; (4) CCDC Drilling & Production Technology Research Institute, Xi'an; 710068, China
Corresponding authors: Dong, Sanbao(772788077@qq.com); Chen, Gang(gangchen@xsyu.edu.cn)

Abstract: The foam drainage technique for gas production has the disadvantage of requiring a large amount of surfactant and having low resistance to salt and oil. In this study, a new surfactant mixture (composite surfactant) of lauramidopropyl betaine (LAB-35), α-olefin sulfonate (AOST), sodium alkyl sulfonate (SASE) and cetyltrimethylammonium bromide (CTAB) was tested and its foaming properties were investigated in detail. The foaming properties were determined using high-speed measurements and the Ross-Miles method. The results show that the foaming volume of the composite surfactant can reach 563 mL, indicating that the foaming behaviour of the composite surfactant is more effective than that of the individual surfactants used for the mixture. In addition, the results show that the composite surfactant has a resistance to salt, methanol and condensate oil that most foam drainage agents do not have. However, the stability of the composite surfactant gradually decreases with increasing

temperature and concentration. The surface tension was measured and the critical micelle concentration of the composite surfactant is 0.023 g/L. © 2022 Walter de Gruyter GmbH, Berlin/Boston.

Number of references: 30
Main heading: Surface tension
Controlled terms: Critical micelle concentration - Foams - Micelles
Uncontrolled terms: Composite foams - Foam drainage - Foaming properties - Gas productions - High efficient - Highly efficient surfactant mixture - Oil resistant - Salt resistance - Surfactant mixture - Temperature resistances
Classification code: 801.3 Colloid Chemistry - 931.2 Physical Properties of Gases, Liquids and Solids
Numerical data indexing: Mass density 2.30E-02kg/m3, Volume 5.63E-04m3
DOI: 10.1515/tsd-2022-2462
Funding Details: Number: 21JP094, Acronym: -, Sponsor: Education Department of Shaanxi Province; Number: 2020JQ-775, Acronym: -, Sponsor: Natural Science Basic Research Program of Shaanxi Province;
Funding text: Research funding: The work was supported financially by the Natural Science Basic Research Program of Shaanxi (2020JQ-775), Scientific Research Program Funded by Shaanxi Provincial Education Department (21JP094) and The Youth Innovation Team of Shaanxi Universities. And we thank the work of the Modern Analysis and Testing Center of Xi'an Shiyou University.
Compendex references: YES
Database: Compendex
Data Provider: Engineering Village

Compilation and indexing terms, Copyright 2023 Elsevier Inc.

126. An FBG Temperature-Pressure Sensor Based on Diaphragm and Special-Shaped Bracket Structure

Accession number: 20230613541752
Authors: Feng, Dequan (1, 2); Xu, Dongpo (3); Chen, Fengyi (1); Chen, Qiang (4); Qiao, Xueguang (1)
Author affiliation: (1) Northwest University, School of Physics, Xi'an; 710127, China; (2) Xi'an Shiyou University, School of Science, Xi'an; 710065, China; (3) Xi'an Shiyou University, Ministry of Education Key Laboratory on Photoelectric Oil-Gas Logging and Detecting, School of Science, Xi'an; 710065, China; (4) Logging Technology Research Institute, China Petroleum Logging Company Ltd., Xi'an; 710005, China
Corresponding author: Qiao, Xueguang(xgqiao@nwu.edu.cn)
Source title: IEEE Sensors Journal
Abbreviated source title: IEEE Sensors J.
Volume: 23
Issue: 4
Issue date: February 15, 2023
Publication year: 2023
Pages: 3589-3596
Language: English
ISSN: 1530437X
E-ISSN: 15581748
Document type: Journal article (JA)
Publisher: Institute of Electrical and Electronics Engineers Inc.
Abstract: A fiber Bragg grating (FBG) sensor capable of simultaneous temperature-pressure measurement is presented and experimentally verified, which consists of a diaphragm, a special-shaped bracket, dual FBGs, and protective housing. The principle of simultaneous temperature and pressure measurement with dual FBGs is theoretically illustrated and simulated by a finite-element analysis. The experimentally investigated results demonstrate that the sensor can be employed to measure temperature and pressure in environments where the temperature ranges from 50 °C to 200 °C and the pressure ranges from 0 to 40 MPa. The temperature sensitivity of the sensor is 31.8 pm/°C with a linear correlation coefficient of 0.9997; the pressure sensitivity is 50.6 pm/MPa, the linearity is 0.21%, and the repeatability and hysteresis error are 0.024% and 0.16%, respectively. The sensor exhibits a large measuring range, high-temperature resistance, miniaturized structure, and easily multiplexed, which allows it for temperature and pressure dual parametric measurements in high-temperature and high-pressure environments such as oil and gas wells. © 2001-2012 IEEE.
Number of references: 21
Main heading: Diaphragms
Controlled terms: Fiber Bragg gratings - Finite element method - Pressure measurement
Uncontrolled terms: A.Fibres - Fiber Bragg Grating Sensors - Finite element analyse - Linear correlation coefficient - Pressure ranges - Pressure sensitivities - Sensitivity - Temperature and pressures - Temperature range - Temperature sensitivity

127. Synthesis of Castor Oil-Maleic Anhydride-Styrene Bifunctional Lubricant Additive

Authors: Ding, Liqin (1, 2, 3); Guo, Xiao (1); Su, Biyun (1, 2); Lu, Suhong (1); Liang, Shengrong (3, 4)
Author affiliation: (1) College of Chemistry and Chemical Engineering, Xi'an Shiyou University, Xi'an; 710065, China; (2) Green and Low-Carbon Energy Materials and Process Engineering Technology Research Center of Shaanxi Province, Xi'an; 710065, China; (3) Xi'an Key Laboratory of Low-Carbon Utilization for High-Carbon Resources, Xi'an; 710065, China; (4) Modern Analysis and Testing Center, Xi'an Shiyou University, Xi'an; 710065, China
Abstract: The adverse effect of traditional petroleum-based lubricant additives on the environment has made the biodegradable lubricant additives become a research hotspot. In the work, poly (castor oil(CO)-maleic anhydride(MAH)styrene(ST)) (PCMAS) was synthesized with azodiisobutyronitrile (AIBN) as the initiator in toluene through Schlenk technology. The structure of PCMAS was characterized by Fourier Transform Infrared spectroscopy (FT-IR) and 1H nuclear magnetic resonance (1H NMR). The relative molecular mass and its polydispersity index of PCMAS were determined by gel permeation chromatography (GPC). Thermo gravimetric analysis method was used to study the thermal stability of the prepared polymers. Performance of the synthesized polymers was evaluated as pour point depressant and viscosity index improver. Experimental results show that the optimum process conditions are as follows: m(CO)m(MAH)m(ST)is equal to 1.00.21.2, AIBN mass fraction is 0.5% (based on the total mass of monomers), reaction temperature is 90 , and reaction time is 4 h. Under the above conditions, the copolymer has a yield of 68.39%, the number average relative molecular mass is $0.348{\times}10^5$, and the polydispersity index is 4.77. When the synthesized PCMAS copolymer was added, pour point of lubricant fraction (350—395) was decreased and its viscosity index was increased. Therefore, the synthesized PCMAS copolymer could be used as a lubricant additive with double functions of reducing pour point and increasing viscosity index. © 2023 Science Press. All rights reserved.
Number of references: 21
Main heading: Styrene
Controlled terms: Additives - Fourier transform infrared spectroscopy - Gel permeation chromatography - Maleic anhydride - Molecular mass - Nuclear magnetic resonance - Nuclear magnetic resonance spectroscopy - Thermodynamic stability - Thermogravimetric analysis - Viscosity
Uncontrolled terms: Bi-functional˙ - Castor oil - Copolymerisation - Lubricant additives - Maleic anhydride/ styrenes - Polydispersity indices - Pour points - Relative molecular mass - Synthesised - Viscosity index
Classification code: 631.1 Fluid Flow, General - 641.1 Thermodynamics - 801 Chemistry - 802.3 Chemical Operations - 803 Chemical Agents and Basic Industrial Chemicals - 804.1 Organic Compounds - 931.2 Physical Properties of Gases, Liquids and Solids
Numerical data indexing: Inductance 1.00E00H, Percentage 5.00E-01%, Percentage 6.839E+01%, Time 1.44E+04s

128. Preparation of ZrW2O8-Cf/E51 low/negative CTE composites and effect of ultrasonic time on its thermal and mechanical property

Accession number: 20230413428558
Title of translation: ZrW2O8-Cf/E51/
Authors: Ju, Luyan (1); Zhang, Jianbing (1); Ma, Yuqin (2); Zhang, Zhaoyuan (1); Wei, Wenlan (1)
Author affiliation: (1) Mechanical Engineering College, Xi'an Shiyou University, Xi'an; 710065, China; (2) School of Mechano-Electronic Engineering, Xidian University, Xi'an; 710071, China
Corresponding author: Ju, Luyan(yan885858@163.com)
Abstract: In order to prepare low expansion, high strength and light weight composites, ZrW2O8-Cf/E51 composites were prepared by compression molding method, and the effects of ultrasonic time on its microstructure, thermal expansion behavior and ultimate tensile strength were studied. The results show that the agglomerated particles will be blocked by the fibers and gather on the surface of fiber bundles during the preparation. Within 20 minutes, the agglomeration of ZrW2O8 particles can be reduced by prolonging the ultrasonic time. With the decrease of particle agglomeration, the fracture surface of the composites will be changed from plane without fiber pull-out to uneven with fiber pull-out. During the thermal expansion process, the dL/L0of ZrW2O8-Cf/E51 composites show three stages:increase, decrease and slow increase under the combined action of carbon fiber and ZrW2O8 particles. When ultrasonic time increases from 5 min to 20 min, the average thermal expansion coefficient of ZrW2O8-Cf/ E51 composites decreases by about 130%, and the ultimate tensile strength increases by about 8%. © 2023 Beijing Institute of Aeronautical Materials (BIAM). All rights reserved.
Number of references: 19
Main heading: Carbon fibers
Controlled terms: Agglomeration - Compression molding - Tensile strength - Thermal expansion - Tungsten compounds - Zirconium compounds
Uncontrolled terms: Fiber pull out - High lights - High-strength - Light weight - Low expansion - Low/ negative thermal expansion - Molding methods - Thermal and mechanical properties - Ultimate tensile strength - ZrW2O8particle
Classification code: 641.1 Thermodynamics - 802.3 Chemical Operations - 804 Chemical Products Generally - 951 Materials Science
Numerical data indexing: Percentage 1.30E+02%, Percentage 8.00E+00%, Time 1.20E+03s, Time 3.00E+02s to 1.20E+03s
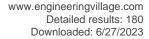
129. A high-efficiency spaceborne processor for hybrid neural networks

Accession number: 20231814048714
Authors: Wang, Shiyu (1); Zhang, Shengbing (2); Huang, Xiaoping (2); Chang, Libo (2)
Author affiliation: (1) School of Computer Science, Xi'an Shiyou University, Xi'an; 710065, China; (2) School of Computer Science, Northwestern Polytechnical University, Xi'an; 710072, China

Corresponding author: Wang, Shiyu(wangshiyu@xsyu.edu.cn)
Abstract: Featuring with characteristics of convolutional neural network (CNN) and recurrent neural network (RNN), hybrid neural network (H-NN) has been widely applied within the field of remote sensing. In order to satisfy de mands of on-orbit processing that requires high throughput with restriction on power consumption, designing specific heterogeneous array processor therefore becomes one of the most effective ways fulfilling various tasks engaged in the above field. In this paper, a heterogeneous array architecture is proposed to support the hybrid neural network, based on the characteristics of various computation types in between different neural network module types and of dynamic computation burden among different layers. Firstly, a heterogeneous array structure consisting of different PE, PPE, RPE and LPE units is proposed, enabling strong flexibility and high throughput. Four types of operation units are used for operations of MAC, ReLU, pooling and nonlinear lookup-table. Secondly, a multi-level on-chip memory structure and access strategy supporting different access modes are proposed to reduce the bandwidth requirements of off-chip data access and to improve the computation efficiency. Thirdly, a management strategy of heterogeneous computing array is designed, which combines pipelining and parallel processing to support efficient mapping of different types of hybrid neural networks. The hybrid neural network processor based on 65 nm CMOS technique has a peak throughput of up to 1.96 TOPS. The implementation on models of AlexNet, LRCN, VGG19-LSTM and CLDNN can achieve the throughput of 1.92 TOPS, 1.89 TOPS, 1.93 TOPS and 1.84 TOPS, respectively. Compared with the similar neural network processor that is based on the same technology, the throughput of AlexNet model is increased by 76.4%. The peak power consumption of a single processor core is 824mW, to which the power consumption restriction of on-orbit AI platform is satisfied. © 2023 Elsevier B.V.
Number of references: 40
Main heading: Electric power utilization
Controlled terms: Convolutional neural networks - Energy efficiency - Long short-term memory - Memory architecture - Multilayer neural networks - Network architecture - Orbits - Remote sensing - Table lookup
Uncontrolled terms: Domain specific architectures - Heterogeneous array - High energy efficiency - High-throughput - Higher efficiency - Hybrid neural networks - Network processor - Neural-networks - On orbit - Space-borne
Classification code: 525.2 Energy Conservation - 706.1 Electric Power Systems - 722 Computer Systems and Equipment - 723.1 Computer Programming
Numerical data indexing: Percentage 7.64E+01%, Power 8.24E-01W, Size 6.50E-08m
DOI: 10.1016/j.neucom.2023.126230
Compendex references: YES
Database: Compendex
Data Provider: Engineering Village

130. Sedimentary Microfacies and Depositional Model of Fine-Grained Rocks in the middle Ordos Basin

Accession number: 20232014106798
Authors: Guo, Feng (1); Pan, Qi (1); Zhao, Qilin (1); Chen, Xiaoyi (1); Xu, Qiang (1); Huang, Shuoyang (1); Aike, Ikram (1)
Author affiliation: (1) School of Earth Sciences and Engineering, Shaanxi Key Lab of Oil and Gas Accumulation, Xi'an Shiyou University, Xi'an; 710065, China
Corresponding author: Guo, Feng(guofeng@xsyu.edu.cn)

Abstract: Detailed sedimentary microfacies research is important to determine favorable target areas for oil and gas exploration. In order to clarify the sedimentary microfacies characteristics of Chang 7 in the Ordos Basin, the types and distribution of Chang 7 sedimentary microfacies were studied using logging, core, analysis and testing data. The results show that delta facies is developed in the Chang 7, mainly in the delta front subfacies, including distributary channel, natural levee, interdistributary bay and mouth bar. The underwater distributary channel sand body, as the skeleton sand body, is relatively well developed and is the main place for oil and gas accumulation. The thick fine sediments in Chang 7 sedimentary period are mainly mudstone and silty mudstone. Multi channel sand bodies and extremely thick fine-grained rocks form a high-quality source reservoir cap rock association. © 2023 SPIE.

Number of references: 17
Main heading: Sedimentology
Controlled terms: Metamorphic rocks - Petroleum prospecting - Sedimentary rocks
Uncontrolled terms: Chang7 - Channel sand body - Core datum - Depositional models - Favorable targets - Fine grained - Logging data - Oil and gas exploration - Ordos Basin - Sedimentary micro-facies
Classification code: 481.1 Geology - 482.2 Minerals - 512.1.2 Petroleum Deposits : Development Operations
Numerical data indexing: Size 1.778E-01m
DOI: 10.1117/12.2668298

Compendex references: YES
Database: Compendex
Data Provider: Engineering Village

131. Seismic Sedimentological Interpretation Method Under Coal Seam Interference: A Case Study of Shan2 in the Southeast Ordos Basin

Accession number: 20232014106775

Authors: Guo, Feng (1); Zhang, Lei (1); Lai, Shenghua (1)
Author affiliation: (1) School of Earth Sciences and Engineering, Shaanxi Key Lab of Oil and Gas Accumulation, Xi'an Shiyou University, Xi'an; 710065, China
Corresponding author: Guo, Feng(guofeng@xsyu.edu.cn)

Abstract: In order to clarify the seismic sedimentology interpretation method under coal seam interference, time-frequency analysis technology was used to analyze the seismic reflection frequency of the coal seam. Combined with seismic filtering, the seismic interference of the coal seam is suppressed through the sedimentological interpretation of stratigraphic slices with different dominant frequencies. The spatial distribution characteristics of the sedimentary system are determined by comprehensive mixed display technology. The results show that the delta plain subfacies are developed, which are composed of four distributary channels, crevasse splays, and swamps in the near north-south direction, and a large-scale channel migration zone is formed in the southwest. © 2023 SPIE.

Number of references: 21
Main heading: Coal
Controlled terms: Coal deposits - Metamorphic rocks - Sedimentology - Seismology - Stratigraphy
Uncontrolled terms: Case-studies - Coal seams - Frequency mixing - Frequency mixing display - Interference time - Interpretation methods - Ordos Basin - Sedimentological interpretations - Seismic sedimentology - Time-frequency Analysis
Classification code: 481.1 Geology - 484.1 Earthquake Measurements and Analysis - 503 Mines and Mining, Coal - 524 Solid Fuels
DOI: 10.1117/12.2668321

Compendex references: YES
Database: Compendex
Data Provider: Engineering Village

132. Seven-core fiber based in-fiber Mach–Zehnder interferometer for temperature-immune curvature sensing

Accession number: 20224313000488

Authors: Shao, Min (1); Liang, Junjun (1); Gao, Hong (1); Wang, Chun (1); Liu, Yinggang (1)
Author affiliation: (1) School of Science, Ministry of Education Key Laboratory on Photoelectric Oil-gas Logging and Detecting, Xi'an Shiyou University, Xi'an; 710065, China
Corresponding author: Shao, Min(shaomin@xsyu.edu.cn)

Abstract: An in-fiber Mach–Zehnder interferometer (MZI) based on a brief coreless fiber (CLF) and a section of seven-core fiber (SCF) sandwiched in single mode fiber (SMF) is proposed and demonstrated. A supermode interference is created in the SCF that forms interference spectrum to perceive external curvature changes. A linear enhanced sensitivity of -26.5517 dB/m-1 for temperature-immune curvature measurement within the curvature range of 0.527–

1.395 m-1 is experimentally achieved. Moreover, the strain response of the MZI is experimentally investigated. This MZI exhibits accurate and high sensitivity for curvature detection by economic intensity detection, which indicates its potential applications in the engineering field. © 2022 Elsevier B.V.

Number of references: 20
Main heading: Single mode fibers
Controlled terms: Fiber optic sensors - Interferometers
Uncontrolled terms: Core fibre - Coreless - Curvature sensing - Curvature sensor - Fiber Mach-Zehnder interferometers - In-fiber - Interference spectrum - Seven-core fiber - Single-mode fibers - Supermodes
Classification code: 741.1.2 Fiber Optics - 941.3 Optical Instruments
Numerical data indexing: Decibel -2.65517E+01dB, Size 5.27E-01m to 1.395E+00m
DOI: 10.1016/j.optcom.2022.128989
Funding Details: Number: YCS20111007, Acronym: -, Sponsor: -; Number: 61805197, Acronym: NSFC, Sponsor: National Natural Science Foundation of China;
Funding text: This work is supported by the National Natural Science Foundation of China under Grant (61805197) and Graduate Student Innovation Fund of Xi'an Shiyou University (YCS20111007).This work is supported by the National Natural Science Foundation of China under Grant (61805197) and Graduate Student Innovation Fund of Xi'an Shiyou University (YCS20111007).
Compendex references: YES
Database: Compendex
Data Provider: Engineering Village
Compilation and indexing terms, Copyright 2023 Elsevier Inc.

133. Preparation and the foaming activity of hydroxymethyl octadecyltrimethyl ammonium chloride

Accession number: 20231113727635
Authors: Lv, Shiyi (1); Liu, Qiaona (1); Dong, Sanbao (1); Li, Jinling (1); Zhang, Jie (1); Wang, Manxue (1, 2); Chen, Gang (1, 2, 3)
Author affiliation: (1) Shaanxi Prov. Key Lab. of Environ. Poll. Control and Reservoir Protection Technology of Oilfields, Xi'An Shiyou University, Xi'an; 710065, China; (2) Shaanxi Key Laboratory of Lacustrine Shale Gas Accumulation and Exploitation (Under Planning), Xi'an; 710060, China; (3) College of Chemistry and Chemical Engineering, Xi'An Shiyou University, Shannxi Province, Xi'an; 710065, China
Corresponding author: Chen, Gang(gangchen@xsyu.edu.cn)
Source title: Tenside, Surfactants, Detergents
Abbreviated source title: Tenside Surfactants Deterg
Volume: 60
Issue: 2
Issue date: March 2023
Publication year: 2023
Pages: 182-189
Language: English
ISSN: 09323414
CODEN: TSDEES
Document type: Journal article (JA)
Publisher: Walter de Gruyter GmbH
Abstract: In this work, hydroxymethyl octadecyltrimethyl ammonium chloride (HM-OTAC) was obtained from the reaction between octadecyltrimethyl ammonium chloride (OTAC) and formaldehyde in different molar ratios. The effects of the reaction conditions (different molar ratios) on the properties of the product (surface tension, foaming, high temperature resistance, methanol resistance and salt resistance) were investigated. The results showed that the HM-OTAC produced under different molar ratios could lower the surface tension of water solutions more than the surfactant OTAC. The HM-OTAC (1:2) reduced the surface tension to 28.29 mN m-1. The HM-OTAC produced under other molar ratios gave higher interfacial tensions than HM-OTAC (1:2). With increasing surfactant concentration, the foam volume first increased and then gradually decreased. At a concentration of 0.3 wt.%, the highest foam volume (460 mL) was produced with HM-OTAC (1:3). Compared to OTAC, the foams produced by each HM-OTAC surfactant exhibited higher temperature stability. In the presence of 30 mL methanol, the initial foam volume of all HM-OTAC surfactants (0.3 wt.%) was generally higher than that of OTAC. With 300 mL HM-OTAC (1:4) solution, the highest foam volume of 20.2 mL could be produced. HM-OTAC (1:3) showed the highest salt resistance. © 2023 Walter de Gruyter GmbH, Berlin/Boston.
Number of references: 25
Main heading: Surface tension

Controlled terms: Chlorine compounds - Methanol - Molar ratio - Surface active agents
Uncontrolled terms: Ammonium chloride - Foaming ability - Foaming stabilities - High-temperature resistance - Hydroxymethyl octadecyltrimethyl ammonium chloride - Molar ratio - Product surface - Property - Reaction conditions - Salt resistance
Classification code: 801.4 Physical Chemistry - 803 Chemical Agents and Basic Industrial Chemicals - 804.1 Organic Compounds - 931.2 Physical Properties of Gases, Liquids and Solids
Numerical data indexing: Surface tension 2.829E-02N/m, Volume 2.02E-05m3, Volume 3.00E-04m3, Volume 3.00E-05m3, Volume 4.60E-04m3
DOI: 10.1515/tsd-2020-2259
Funding Details: Number: 41202214,51774184, Acronym: NSFC, Sponsor: National Natural Science Foundation of China; Number: 2020JQ-775, Acronym: -, Sponsor: Natural Science Foundation of Shaanxi Province;
Funding text: Research funding: This work was financially supported by the grants from National Science Foundation of China (41202214, 51774184), Natural Science Basic Research Plan in Shaanxi Province of China (Program No. 2020JQ-775) and Open Foundation of Shaanxi Key Laboratory of Lacustrine Shale Gas Accumulation and Exploitation (Under planning). And we thank the work of Modern Analysis and Testing Center of Xi'an Shiyou University.
Compendex references: YES
Database: Compendex
Data Provider: Engineering Village

134. Prediction of instantaneous yield of bio-oil in fluidized biomass pyrolysis using long short-term memory network based on computational fluid dynamics data

Accession number: 20230513493388
Authors: Zhong, Hanbin (1, 2); Wei, Zhenyu (1); Man, Yi (3); Pan, Shaowei (4); Zhang, Juntao (1); Niu, Ben (1, 2); Yu, Xi (5); Ouyang, Yi (6); Xiong, Qingang (3)
Author affiliation: (1) Xi'an Key Laboratory of Low-carbon Utilization for High-carbon Resources, Xi'an Shiyou University, Shaanxi, Xi'an; 710065, China; (2) Shaanxi Engineering Research Center of Green Low-carbon Energy Materials and Processes, Xi'an Shiyou University, Shaanxi, Xi'an; 710065, China; (3) State Key Laboratory of Pulp and Paper Engineering, South China University of Technology, Guangzhou; 510641, China; (4) School of Computer Science, Xi'an Shiyou University, Shaanxi, Xi'an; 710065, China; (5) College of Engineering and Physical Sciences, Aston University, Birmingham; B4 7ET, United Kingdom; (6) Laboratory for Chemical Technology, Ghent University, Ghent; 9052, Belgium
Corresponding author: Xiong, Qingang(qingangxiong@scut.edu.cn)
Source title: Journal of Cleaner Production
Abbreviated source title: J. Clean. Prod.
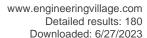**Volume:** 391
Issue date: March 10, 2023
Publication year: 2023
Article number: 136192
Language: English
ISSN: 09596526
CODEN: JCROE8
Document type: Journal article (JA)
Publisher: Elsevier Ltd
Abstract: Computational fluid dynamics (CFD) is an effective tool to investigate biomass fast pyrolysis in fluidized bed reactor for bio-oil production, while it requires huge computational time when optimizing operating conditions or simulating large/industrial units. Machine learning (ML) is a promising approach to achieving both accuracy and efficiency. In this work, a reduced-order model including long short-term memory (LSTM) layer, pooling layer, and fully connected layer was established to predict future mass flow rates by training the historical CFD data. Unsteady mass flow rates, which are normally used to determine product yields, were treated as data of time series in ML. Influencing factors, such as sequence length, number of neurons, learning rate, subsequences order (shuffle or not), number of LSTM layers, and ratio of testing set, were evaluated to obtain their optimal values. The developed LSTM model framework and training process showed good applicability for the dataset of different species and temperatures. Product yields predicted by the derived LSTM were in good agreement with those obtained by CFD, while nearly 30% computational effort was saved. Thus, it is clearly seen that the well-predicted fluctuating characteristics and final product yields are helpful to improve accuracy of process simulation for digitalizing key reactors and building smart factories. © 2023 Elsevier Ltd
Number of references: 35
Main heading: Fluidized beds

Controlled terms: Biomass - Brain - Chemical reactors - Computational fluid dynamics - Long short-term memory - Mass transfer
Uncontrolled terms: Bio-oils - Biomass fast pyrolyse - Biomass pyrolysis - Dynamic data - Fast pyrolysis - Machine-learning - Mass-flow rate - Memory layers - Memory network - Product yields
Classification code: 461.1 Biomedical Engineering - 641.3 Mass Transfer - 723.5 Computer Applications - 802.1 Chemical Plants and Equipment - 931.1 Mechanics
Numerical data indexing: Percentage 3.00E+01%
DOI: 10.1016/j.jclepro.2023.136192

Compendex references: YES
Database: Compendex
Data Provider: Engineering Village

135. Assessment of optimal specimen to measure the compressive strength of earthen-based masonry

Authors: Lan, Guanqi (1, 2); Weng, Guangyuan (1); Zhang, Kun (1)
Author affiliation: (1) School of Mechanical Engineering, Xi'an Shiyou University, China; (2) State Key Laboratory of Green Building in Western China, Xian University of Architecture & Technology, China
Corresponding author: Lan, Guanqi(langq@xsyu.edu.cn)
Abstract: The compressive strength of masonry is regarded as an essential primary mechanical parameter of this kind of structure. However, standard specimens used to test compressive strength of earthen-based masonry vary considerably in issued codes, which hinders the intercomparison of experimental results. In this study, two kinds of adobe and two kinds of new earthen bricks were selected for preparing masonry specimens. A series of uniaxial compression tests were performed to reveal the compression behaviors of several types of earthen-based masonry, while considering the influence of the specimen bonding arrangement and h/t ratio. Analytic hierarchical processes were used to evaluate the bonding arrangement and h/t ratio of earthen-based masonry specimens from operability, reproducibility, instrument, and equipment requirements for determining an optimal specimen with excellent comprehensive performance. The results showed that optimal specimens for compressive strength tests of different earthen-based masonry can use the same bonding arrangement and h/t ratio. The stretcher bonded specimen with a h/t ratio of 3/1–4/1 should be used as the optimal specimen for compressive strength testing of earthen-based masonry. The results can be used as a reference for establishing a simple and general compressive test method for earthen-based masonry. © 2023 Elsevier Ltd
Number of references: 44
Main heading: Compressive strength
Controlled terms: Compression testing - Masonry materials
Uncontrolled terms: Bonding arrangement - Compression behaviours - Earthen-based masonry - Experimental methods - Height to thickness ratio - Intercomparisons - Mechanical parameters - Standard specimens - Thickness ratio - Uni-axial compression tests
Classification code: 414 Masonry Materials
DOI: 10.1016/j.measurement.2023.112484

Compendex references: YES
Database: Compendex
Data Provider: Engineering Village

136. ANALYSIS OF ABNORMAL VIBRATIONS OF CRUDE OIL EFFLUX PUMPS USING ANSYS (*Open Access*)

Accession number: 20232314185687
Authors: Wang, Tianqi (1, 2); Xie, Lei (3); Yu, Hongsheng (4); Wei, Xiuliang (4); Dong, Pengmin (1); Zhao, Tianyi (1)
Author affiliation: (1) Xian Shiyou University, Mechanical Engineering College, Xi'an, China; (2) Xidian University, The School of Mechano-Electronic Engineering, Xi'an, China; (3) Cementing Company Downhole Service Company CCDC, Chengdu, China; (4) Changqing Oilfield Second Oil Transmission Office, Xianyang, China
Corresponding author: Wang, Tianqi(wangtianqi@xsyu.edu.cn)
Source title: Journal of Theoretical and Applied Mechanics (Poland)
Abbreviated source title: J. Theor. Appl. Mech.
Volume: 61
Issue: 1
Issue date: 2023
Publication year: 2023
Pages: 23-36
Language: English
ISSN: 14292955
Document type: Journal article (JA)
Publisher: Polish Society of Theoretical and Allied Mechanics
Abstract: In this study, abnormal vibrations of 1 pump fluid in a crude oil efflux station in the Changqing Oilfield was investigated. Kinetic simulation was applied to flow fields in the crude oil efflux pump using Ansys to determine trends of the impeller static pressure, speed, total pressure, wall pressure of the impeller, outlet pressure and pressure on the pump shell and to identify the reasons behind the abnormal vibrations. The results indicated that the axial vibration amplitude of the pump could be reduced from 1.3mm down to 0.68mm if the operation parameters of the external control oil pump were set as 2500-2550r/min and 325-335m3/h, respectively. © 2023 Polish Society of Theoretical and Allied Mechanics. All rights reserved.
Number of references: 20
Main heading: Crude oil
Controlled terms: Flow fields - Impellers - Vibration analysis
Uncontrolled terms: Abnormal vibration - Ansys - Changqing oilfields - Efflux pumps - Impeller outlet - Internal flow field - Kinetics simulations - Static pressure - Total pressure - Wall pressure
Classification code: 512.1 Petroleum Deposits - 601.2 Machine Components - 631.1 Fluid Flow, General
Numerical data indexing: Angular velocity 4.175E+01rad/s to 4.2585E+01rad/s, Size 1.30E-03m to 6.80E-04m, Volume 3.25E+02m3 to 3.35E+02m3
DOI: 10.15632/jtam-pl/157464
Compendex references: YES
Open Access type(s): All Open Access, Gold
Database: Compendex
Data Provider: Engineering Village

137. One-cycle controllability of high step-up Boost converter with coupled inductor

Authors: Song, Jiuxu (1); Chang, Zhiwei (1); Liu, Hongxia (2); Ding, Shuai (3)
Author affiliation: (1) School of Electronic Engineering, Xi'an Shiyou University, Xi'an, China; (2) Xi'an Microelectronics Technology Institute, Xi'an, China; (3) Department of Engineering, University of Leicester, Leicester, United Kingdom
Corresponding author: Liu, Hongxia(liuhx@mail.xidian.edu.cn)
Abstract: Comparing with traditional pulse width modulation technique, the transient performances of the high step-up DC/DC converters can be significantly improved by one-cycle control (OCC) technique, which is an appropriate control strategy for interface converters directly connecting the renewable energies to the DC microgrid. However, the suitability of OCC for these converters is rarely studied. One-cycle controllability of the high step-up DC/DC Boost converter with coupled inductor is studied with theoretical researches and experimental verifications. First, with the analysis on the operating modes of the converter, its periodic switched linear system model and the criterion for OCC are established. Furthermore, one-cycle controllability of the converter is calculated in detail. Final, a prototype of the high step-up converter from 48 to 380 V is prepared. Experimental results indicate that the disturbances in the input of the high step-up converter can be depressed within only one switching cycle. Ideal dynamic characteristic for the converter under disturbance in the output is also achieved. Results of this paper are meaningful for investigations on the transient characteristics of high step-up DC/DC converters applied to DC microgrid. © 2023 John Wiley & Sons Ltd.
Number of references: 37
Main heading: Controllability
Controlled terms: Boost converter - Electric inductors - Linear systems
Uncontrolled terms: BOOST converter - Coupled inductor - High step-up converters - High step-up DC/DC converter - High step-ups - Microgrid - One cycle control - One-cycle controllability - Periodic switched linear system - Switched linear system
Classification code: 704.1 Electric Components - 731.1 Control Systems - 961 Systems Science
Numerical data indexing: Voltage 4.80E+01V to 3.80E+02V
DOI: 10.1002/cta.3532
Compendex references: YES
Database: Compendex
Data Provider: Engineering Village

138. Investigation of silica nanoparticles grafted with sulphonated polymer for enhanced oil recovery at high temperature and high salt

Authors: Wenlong, Qin (1, 2); Guoqing, Li (1); Lu, Li (1); Hanxi, Li (1); Ruixuan, Li (1); Guowei, Qin (1); Jiang, Yang (1)
Author affiliation: (1) Shaanxi Key Laboratory of Advanced Stimulation Technology for Oil &Gas Reservoirs, Xi'an Petroleum University, Xi'an, China; (2) College of Petroleum Engineering, Xi'an Petroleum University, Xi'an, China
Corresponding author: Wenlong, Qin(wlqin@xsyu.edu.cn)

Language: English
ISSN: 00084034
E-ISSN: 1939019X
CODEN: CJCEA7
Document type: Article in Press
Publisher: John Wiley and Sons Inc

Abstract: Nano-fluids' application for enhanced oil recovery (EOR) has attracted noticeable attention and formed a new research area in recent years. Currently, the greatest challenge in this area is to formulate stable nano-fluids for oil reservoirs with high temperatures and salinity. To overcome the limitations of its application in high-temperature drilling, polymer-coated nanoparticles (SiO2-PAMPS NPs) were prepared via solution polymerization of 2-acrylamide-2-methyl-1-propane sulphonic acid (AMPS) from the surface of aminopropyl-functionalized silica nanoparticles. The SiO2-PAMPS NPs were characterized by Fourier-transform infrared spectroscopy (FTIR), thermogravimetric analysis (TGA), scanning electron microscopy (SEM), and dynamic light scattering (DLS). The results indicated that the AMPS was successfully grafted onto the surface of silica nanoparticles, and the average diameter of SiO2-PAMPS NPs was about 16 nm. The nano-fluids showed noticeable stability in American Petroleum Institute (API) brine (2 wt.% CaCl2 and 8 wt.% NaCl) at 90°C beyond 46 days. When amphipathic nanoparticles were introduced to brine at 90°C, the potential of the nano-fluids in recovering oil was evaluated by investigating the interfacial tension with kerosene oil and the oil contact angle in the nano-fluids. The contact angle of the glass sheet surface before treatment was about 144°, while after SiO2-PAMPS NPs treatment for 72 h, it became about 92°. Meanwhile, the nano-fluids showed an excellent enhancing emulsibility property, which plays a vital role in promoting the development of EOR in high-temperature and high-salt environments. © 2023 Canadian Society for Chemical Engineering.

Number of references: 24
Main heading: Contact angle
Controlled terms: Amides - Dynamic light scattering - Emulsification - Enhanced recovery - Fourier transform infrared spectroscopy - Grafting (chemical) - Petroleum reservoir engineering - Petroleum reservoirs - Scanning electron microscopy - Silica nanoparticles - SiO2 nanoparticles - Sodium chloride - Thermogravimetric analysis
Uncontrolled terms: Acrylamides - Enhanced-oil recoveries - High salts - Highest temperature - Nanofluids - Oil reservoirs - Research areas - Silica nanoparticles - Sulphonated polymers - Sulphonic acids
Classification code: 511.1 Oil Field Production Operations - 512.1.1 Oil Fields - 512.1.2 Petroleum Deposits : Development Operations - 741.1 Light/Optics - 761 Nanotechnology - 801 Chemistry - 802.2 Chemical Reactions - 802.3 Chemical Operations - 804.1 Organic Compounds - 931.2 Physical Properties of Gases, Liquids and Solids
Numerical data indexing: Age 1.2604E-01yr, Size 1.60E-08m, Temperature 3.63E+02K, Time 2.592E+05s
DOI: 10.1002/cjce.24841

Compendex references: YES
Database: Compendex
Data Provider: Engineering Village

139. An Adaptive Grid Refinement Method for Flow-Based Embedded Discrete Fracture Models

Accession number: 20231513867126

Authors: Li, Junchao (1); Tang, Huiying (2); Zhang, Yongbin (3); Li, Xin (4)
Author affiliation: (1) Xi'an Shiyou University, China; (2) Southwest Petroleum University, China; (3) Research Institute of the Tarim Oilfield, CNPC; (4) Research Institute of Petroleum Exploration and Development, CNPC

Source title: Society of Petroleum Engineers - SPE Reservoir Simulation Conference, RSC 2023
Abbreviated source title: Soc. Pet. Eng. - SPE Reserv. Simul. Conf., RSC
Part number: 1 of 1
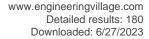**Issue title:** Society of Petroleum Engineers - SPE Reservoir Simulation Conference, RSC 2023
Issue date: 2023
Publication year: 2023
Report number: SPE-212194-MS
Language: English
ISBN-13: 9781613998717

Document type: Conference article (CA)
Conference name: 2023 SPE Reservoir Simulation Conference, RSC 2023
Conference date: March 28, 2023 - March 30, 2023
Conference location: Galveston, TX, United states
Conference code: 187391
Publisher: Society of Petroleum Engineers
Abstract: Projection-based embedded discrete fracture models (pEDFMs) are proven effective for modeling flow barrier effects of high-conductivity or impermeable fractures. However, local grid refinements are still needed to improve the accuracy of simulation in flow areas near fractures. In recent years, adaptive grid refinement techniques have received a lot of attention for dealing with highly heterogeneous and fractured models. But few of them are capable of EDFMs. In this paper, an adaptive grid refinement method under flow-based EDFMs (fEDFMs) is proposed for fractured models. The method starts from an fEDFM model which is built by a new technique of transmissibility modification by introducing an artificial pseudo-steady flow near fractures. Adaptive grid refinement and coarsening procedures are designed under an adaptive criterion based on both the fracture distribution and flow solutions. A flow-based upscaling procedure is adopted to form transmissibilities of the hybrid grids and the solution is mapped from the former grid system. The adaptive grid refinement method is applied in a validation case and a real field case, respectively. In each case, comparisons are made between the simulation results of the proposed adaptive grid refinement models and traditional uniform pEDFMs. Besides, comparisons are also made with the overall fine-scale models which serve as the reference models. The comparisons show that the numerical results of the proposed models have a better match to that of the reference models. And it is proven that the approach is more robust when applied to more general flow scenarios with extremely high or completely sealed fractures which could have a great impact on the flow. The proposed method aims to improve the accuracy of numerical simulation for fractured reservoirs. Copyright 2023, Society of Petroleum Engineers.
Number of references: 24
Main heading: Fracture
Controlled terms: Coarsening - Numerical methods - Petroleum reservoirs
Uncontrolled terms: Adaptive grid refinement - Barrier effects - Discrete-fracture models - Flow area - Flow barriers - Flow based - High conductivity - Local grid refinement - Reference modeling - Refinement methods
Classification code: 512.1.1 Oil Fields - 921.6 Numerical Methods - 951 Materials Science
DOI: 10.2118/212194-MS
Compendex references: YES
Database: Compendex
Data Provider: Engineering Village

140. Improvement of ethanolamine sensing performance based on Au-modified ZnO rod-like nanoflowers

Accession number: 20231113709237
Authors: Dai, Hangfei (1); Ding, Jijun (1); Chen, Haixia (1); Fu, Haiwei (1)
Author affiliation: (1) Shaanxi Key Laboratory of Measurement and Control Technology for Oil and Gas Wells, College of Science, Xi'an Shiyou University, Xi'an; 710065, China
Corresponding author: Ding, Jijun(jjding@xsyu.edu.cn)
Source title: Materials Letters
Abbreviated source title: Mater Lett
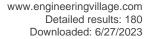**Volume:** 340
Issue date: June 1, 2023
Publication year: 2023
Article number: 134183
Language: English
ISSN: 0167577X
E-ISSN: 18734979
CODEN: MLETDJ
Document type: Journal article (JA)
Publisher: Elsevier B.V.

Abstract: Au-modified ZnO rod-like nanoflowers are fabricated. As prepared Au-ZnO nanoflower based gas sensor exhibits excellent gas sensing performance for 100 ppm ethanolamine (EA) gas at 210 °C, including high response (138.27), fast response/recovery time (15 s/34 s), good linearity between response and gas concentration, low detection limit down to 1 ppm, and good stability and repeatability. We propose that these excellent sensing properties come from the fact that Au-ZnO nanoflowers are assembled from one-dimensional nanorods into a regular and ordered three-dimensional flower-like structures, the open space in which provides more active sites with a larger specific surface area. Therefore, Au-ZnO nanoflowers can be used as candidate materials in efficient gas sensors in the future. © 2023 Elsevier B.V.

Number of references: 19
Main heading: Zinc oxide
Controlled terms: Chemical sensors - Ethanolamines - Gas detectors - Gases - Gold compounds - II-VI semiconductors - Nanoflowers - Nanorods
Uncontrolled terms: Au-ZnO nanoflower - Fast response - Gas sensing - Gas-sensors - High response - Hydrothermal methods - Ion sputtering - Performance based - Sensing performance - ZnO rod
Classification code: 712.1 Semiconducting Materials - 761 Nanotechnology - 801 Chemistry - 804.1 Organic Compounds - 804.2 Inorganic Compounds - 914.1 Accidents and Accident Prevention - 933 Solid State Physics - 943.3 Special Purpose Instruments
Numerical data indexing: Temperature 4.83E+02K, Time 1.50E+01s, Time 3.40E+01s
DOI: 10.1016/j.matlet.2023.134183
Funding Details: Number: YCS22213171, Acronym: -, Sponsor: -; Number: 11804273, Acronym: NSFC, Sponsor: National Natural Science Foundation of China; Number: 2019GY-170, Acronym: -, Sponsor: Key Research and Development Projects of Shaanxi Province;
Funding text: This work was supported by the National Natural Science Foundations of China (Grant No. 11804273), Key Research and Development Projects of Shaanxi Province (Grant No. 2019GY-170), Graduate Student Innovative and Practical Ability Training Program of Xi'an Shiyou University (Grant No. YCS22213171).This work was supported by the National Natural Science Foundations of China (Grant No. 11804273), Key Research and Development Projects of Shaanxi Province (Grant No. 2019GY-170), Graduate Student Innovative and Practical Ability Training Program of Xi'an Shiyou University (Grant No. YCS22213171).
Compendex references: YES
Database: Compendex
Data Provider: Engineering Village

141. A numerical investigation of wavy microchannels with secondary branches under non-uniform heating

Accession number: 20230813621801
Authors: Gao, Zhigang (1); Zheng, Dawen (1); Bai, Junhua (2); Shang, Xiaolong (1); Li, Peng (1)
Author affiliation: (1) Institute of Precision Guidance and Control, Northwestern Polytechnical University, Xi'an; 710072, China; (2) College of Petroleum Engineering, Xi'an Shiyou University, Xi'an; 710065, China
Corresponding author: Gao, Zhigang(gaozhigang@nwpu.edu.cn)

Source title: Physics of Fluids
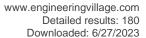**Abbreviated source title:** Phys. Fluids
Volume: 35
Issue: 2
Issue date: February 2023
Publication year: 2023
Article number: 023610
Language: English
ISSN: 10706631
E-ISSN: 10897666
CODEN: PHFLE6
Document type: Journal article (JA)
Publisher: American Institute of Physics Inc.

Abstract: The maneuverability of flight vehicles and their significant working power cause high non-uniform heat flux in their electrical components. Meanwhile, the package structure of components leads to a hostile heat dissipation environment in which air cooling cannot be realized, and a heat sink with conventional dimensions cannot meet the strong heat dissipation requirement, so the microchannel heat sink (MCHS) has been proposed instead. The mode of secondary branches of microchannel heat sink on the current research was full-opening one crossing the channel wall, the semi-opening secondary branch has rarely been studied yet. Meanwhile, the influences of secondary

branches on the flow and heat transfer performance and temperature uniformity of an MCHS under non-uniform heat flux have not been mentioned. Hence, in this paper, a numerical model for a MCHS with secondary branches is proposed to enhance the thermal performance of heat sinks and to improve the temperature uniformity of the substrates. Considering the symmetry structure of the heat sinks, the computational domain is constructed by two parallel sinusoidal channels with secondary branches on the adjacent channel wall. The effects of geometric factors, such as the cross-sectional opening degree and the arrangement of branches on the thermal performance of the heat sinks, are studied. The results show that compared with the conventional wavy MCHS, the secondary branches promote fluid mixing efficiency, enhance thermal performance, and provide dynamic adjustment of the flow distribution. Furthermore, a heat sink with middle semi-opening branches shows superior thermal performance, while the one with interlaced semi-opening branches shows better temperature uniformity of substrate. Meanwhile, an MCHS with secondary branches has a much larger F_c and a smaller $S_{gen}/S_{gen,0}$ than those of a heat sink with no branches. © 2023 Author(s).

Number of references: 42
Main heading: Heat sinks
Controlled terms: Heat flux - Heat transfer - Maneuverability - Microchannels - Substrates
Uncontrolled terms: Channel wall - Flight vehicles - Manoeuvrability - Micro channel heat sinks - Non-uniform heat fluxes - Nonuniform heating - Numerical investigations - Power - Temperature uniformity - Thermal Performance
Classification code: 616.1 Heat Exchange Equipment and Components - 641.2 Heat Transfer
DOI: 10.1063/5.0140456
Funding Details: Number: 52007153,52106112, Acronym: NSFC, Sponsor: National Natural Science Foundation of China; Number: 2022JM-185, Acronym: -, Sponsor: Natural Science Basic Research Program of Shaanxi Province;
Funding text: This study was supported by the National Natural Science Foundation of China (Grant Nos. 52106112 and 52007153) and Natural Science Basic Research Program of Shaanxi Province in China (Program No. 2022JM-185).
Compendex references: YES
Database: Compendex
Data Provider: Engineering Village
Compilation and indexing terms, Copyright 2023 Elsevier Inc.

142. Fracture Analysis on the Double-head Bolt of Wind Farm

Authors: Xu, Yan (1); Bi, Liuhan (2); Liu, Yinglai (1); Xu, Tianhan (2); Feng, Zhenjun (1); Bai, Qiang (1); Lv, Neng (1); Shen, Chen (1); Yang, Fengping (1)
Author affiliation: (1) Tubular Goods Research Institute of CNPC, Shaanxi, Xi'an; 710077, China; (2) School of Materials Science and Engineering, Xi'an Shiyou University, Xi'an; 710065, China
Corresponding author: Xu, Yan(xuyan008@cnpc.com.cn)
Abstract: The bolts of wind farm are prone to fatigue failure during service. Generally, the fatigue stress does not require too much external force. Sometimes the stress generated by bolts is much lower than the yield strength of bolts. In view of the failure problem of connecting bolts used in wind farms, the failure causes of the double-head

bolt were studied by macroscopic inspection, chemical composition analysis, metallographic analysis, and scanning electron microscopy. The results showed that the fracture was a fatigue fracture, and the fatigue source area was located at the bottom of the thread tooth. Under the action of long-term alternating stress, the single source crack evolved into multi-source fatigue cracks, where the fracture was related to the larger stress in the process of installation and service. This paper analysed the causes of bolt failure, and put forward effective suggestions for the service environment of wind turbine bolts. © 2023 SPIE.

Number of references: 7
Main heading: Scanning electron microscopy
Controlled terms: Bolts - Fatigue crack propagation - Fracture - Wind power
Uncontrolled terms: Double-head bolt - External force - Fatigue cracks - Fatigue failures - Fatigue fracture - Fatigue stress - Fracture analysis - Multi-source fatigue crack - Multi-Sources - Wind farm
Classification code: 605 Small Tools and Hardware - 615.8 Wind Power (Before 1993, use code 611) - 951 Materials Science
DOI: 10.1117/12.2672866
Compendex references: YES
Database: Compendex
Data Provider: Engineering Village
Compilation and indexing terms, Copyright 2023 Elsevier Inc.

143. Advantages of the aerodynamic performance of micro-Tesla turbines (*Open Access*)

Authors: Qi, Wenjiao (1); Deng, Qinghua (2); Yuan, Shuxia (1); Chen, Bing (1)
Author affiliation: (1) School of Mechanical Engineering, Xi'an Shiyou University, Xi'an, China; (2) Shaanxi Engineering Laboratory of Turbomachinery and Power Equipment, Institute of Turbomachinery, Xi'an Jiaotong University, Xi'an, China
Corresponding author: Qi, Wenjiao(wenjiaoqi@xsyu.edu.cn)
Abstract: Tesla turbines, featuring bladeless turbomachinery and energy transformation using the viscosity of the working medium, have wide application prospects in renewable energy utilization as micropower equipment and portable power units and show better aerodynamic performance with a smaller turbine size. In this paper, a miniaturization method of Tesla turbines, including the stator and rotor, was proposed based on its sensitivity analysis results and flow similitude law. A typical Tesla turbine with a disc outer diameter of 100 mm was miniaturized to 50, 20, and 10 mm, respectively. In addition, the miniaturized Tesla turbines, including both the simplified single-channel turbine model and the multichannel turbine model used in practical applications, were simulated numerically. The results show that the miniaturization method that maintains the two high-impact dimensionless parameters at their optimal values is simple, reasonable, and effective. The isentropic efficiency of the single-channel Tesla turbine decreases slightly with its scaling down. However, for the multichannel Tesla turbine in practical applications, the isentropic efficiency increases significantly with a decrease in turbine size, due to a decrease in the impact of the outermost disc channel on the flow fields of the inner disc channels (called the casing wall effect). This is embodied by the phenomenon that part of the working medium in the inner disc channels flows into the outermost disc channel through the nozzle-rotor chamber, and the proportion of this part of the working medium decreases significantly with a decrease in turbine size. In conclusion, the Tesla turbine with a smaller turbine size exhibits better aerodynamic performance and has great potential in the field of microturbomachinery. © 2023 The Authors. Energy Science & Engineering published by Society of Chemical Industry and John Wiley & Sons Ltd.
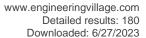**Number of references:** 27
Main heading: Sensitivity analysis
Controlled terms: Aerodynamics - Energy utilization - Miniature instruments - Turbines
Uncontrolled terms: Aero-dynamic performance - Flow characteristic - Micro-tesla turbine - Miniaturisation - Miniaturization method - Multi channel - Single channels - Tesla turbines - Turbine models - Working medium
Classification code: 525.3 Energy Utilization - 651.1 Aerodynamics, General - 921 Mathematics

Compendex references: YES
Open Access type(s): All Open Access, Gold
Database: Compendex
Data Provider: Engineering Village

144. Synergistic effect of ferrous ion-activated hydrogen peroxide and persulfate on the degradation of phthalates in aquatic environments by non-target analysis

Accession number: 20223712727755
Authors: Wu, Ya (1, 2); Fang, Rongmiao (1); Li, Hao (1); Li, Jingyao (1); Zhao, Dan (1); Chang, NaNa (1); Sun, Huaming (2); Shi, Jun (1)
Author affiliation: (1) College of Chemistry and Chemical Engineering, Xi'an Shiyou University, Xi'an; 710065, China; (2) School of Chemistry and Chemical Engineering, Shaanxi Normal University, Xi'an; 710119, China
Corresponding author: Wu, Ya(wuya@xsyu.edu.cn)
Source title: Chemical Engineering Journal
Abbreviated source title: Chem. Eng. J.
Volume: 451
Issue date: January 1, 2023
Publication year: 2023
Article number: 139100
Language: English
ISSN: 13858947
CODEN: CMEJAJ
Document type: Journal article (JA)
Publisher: Elsevier B.V.
Abstract: Oxidative degradation of most recalcitrant organics in the wastewater by exciting the oxidative potential and high efficacy of economic and environmental compatible oxidants is currently an extensively studied field of research. In this study, an efficient phthalate esters (PAEs) degradation method utilizing dual oxidants persulfate (PS) and hydrogen peroxide in the presence of ferrous ions was developed with high removal efficiency, small oxidant dosage and wide pH range. Compared with the degradation efficiency of single systems including Fe^{2+}/ H_2O_2 (40 %), PS (24 %) and Fe^{2+}/PS (49 %) for dimethyl phthalate (DMP) degradation, the combining PS and H_2O_2 activated by Fe^{2+} is more effective, with the removal efficiency of 95 %. The synergistic effect of PS and H_2O_2 in the Fe^{2+}-containing system on PAEs degradation was reflected by the degradation products determined by non-target analysis of various oxidation processes. The results showed that the degradation of DMP in two single oxidant systems was dominated by aromatic compounds via dealkylation, hydroxyl addition and decarboxylation, while DMP in the PS/H_2O_2/$FeSO_4$ system was mainly deeply oxidized to aliphatic molecules through further dearomatization, which was vulnerable for the mineralization of DMP to CO_2 and H_2O. In addition, the EPR technique combined with DMPO captured $SO_4^{•-}$ and $•OH$ signals in the presence of the same Fe^{2+} and oxidant dosage, revealing that a higher intensity of $·OH$ and $SO_4^{•-}$ generated in the combined oxidative process resulted in a high removal of DMP. This work lays the groundwork for recalcitrant organics removal to apply synergistic activation mode in the AOPs system. © 2022 Elsevier B.V.
Number of references: 68
Main heading: Oxidation
Controlled terms: Aromatization - Carboxylation - Degradation - Efficiency - Esters - Hydrogen peroxide - Iron compounds - Oxidants
Uncontrolled terms: Dearomatization - Dimethyl phthalate - Ferrous ion - Non-target analysis - Persulphate - Phthalate ester - Phthalates - Recalcitrant organics - Synergistic effect - Synergistic oxidation
Classification code: 802.2 Chemical Reactions - 803 Chemical Agents and Basic Industrial Chemicals - 804.1 Organic Compounds - 804.2 Inorganic Compounds - 913.1 Production Engineering
Numerical data indexing: Percentage 2.40E+01%, Percentage 4.00E+01%, Percentage 4.90E+01%, Percentage 9.50E+01%, Size 5.08E-02m

145. A novel FPI with hollow core taper structure for strain and inclination measurements

Accession number: 20224913218174
Authors: Gang, Tingting (1); Wang, Dunwei (1); Bian, Ce (2, 3); Zhang, Chun (1); Zheng, Zhihao (1); Fu, Binghan (1); Wei, Hongyan (1); Sun, Ruijuan (1)
Author affiliation: (1) School of Science, Xi'an Shiyou University, Xi'an; 710065, China; (2) Xi'an Institute of Electromechanical Information Technology, Xi'an; 710065, China; (3) Science and Technology on Electromechanical Dynamic Control Laboratory, China
Corresponding author: Gang, Tingting(tingtinggang1@163.com)
Abstract: A novel strain and inclination sensor based on a Fabry-Perot interferometer (FPI) using a Hollow Core Taper (HCT) structure is proposed and demonstrated experimentally. The Hollow Core Fiber (HCF) is sandwiched between the two sections of single mode fiber (SMF) via a taper operation to improve sensitivity to strain and inclination. The interfaces of SMF-HCF and HCF-SMF can be seen as two surfaces of a FP cavity. Partials of light are reflected to the SMF off of the reflective surfaces and eventually recoupled to the leading-in SMF, resulting in a well-defined interference spectrum. Experimental results show that the strain response sensitivity of the sensor is 3.7 pm/$_{\mu E}$, 3.59 pm/$_{\mu E}$ and 3.67 pm/$_{\mu E}$ with ranges of 1525–1535 nm, 1545–1555 nm, and 1570–1580 nm respectively. The intensity in the reflected interference spectrum increases at an exponential rate with a rotation angle of 0° to 3°. In addition, the spectral dips display a negligible change in wavelength in ambient temperature. Therefore, the proposed sensor performs well in terms of repeatability, stability, as well as low temperature sensitivity, and may potentially be useful in the structural health monitoring field. © 2022 Elsevier GmbH
Number of references: 21
Main heading: Single mode fibers
Controlled terms: Fabry-Perot interferometers - Structural health monitoring - Temperature
Uncontrolled terms: Fiber strain sensors - Hollow core fiber - Hollow-core - Inclination measurement - Inclination sensors - Interference spectrum - Novel strains - Single-mode fibers - Strain sensors - Taper structure
Classification code: 422 Strength of Building Materials; Test Equipment and Methods - 641.1 Thermodynamics - 741.1.2 Fiber Optics - 941.3 Optical Instruments
Numerical data indexing: Size 1.525E-06m to 1.535E-06m, Size 1.545E-06m to 1.555E-06m, Size 1.57E-06m to 1.58E-06m, Size 3.59E-12m, Size 3.67E-12m, Size 3.70E-12m

Compendex references: YES
Database: Compendex
Data Provider: Engineering Village

146. Effects of fracturing parameters on fracture network evolution during multicluster fracturing in a heterogeneous reservoir

Accession number: 20231714006920
Authors: Zhang, Haoyu (1); Chen, Junbin (1); Gong, Diguang (1); Liu, Huanmei (2); Ouyang, Wen (1)
Author affiliation: (1) College of Petroleum Engineering, Xi'an Shiyou University, Shaanxi, Xi'an; 710065, China; (2) No.1 Oil Production Plant, PetroChina Changqing Oilfield Company, Shaanxi, Yan'an; 716009, China
Corresponding author: Zhang, Haoyu(20111010006@stumail.xsyu.edu.cn)
Source title: Computers and Geotechnics
Abbreviated source title: Comput. Geotech.
Volume: 159
Issue date: July 2023
Publication year: 2023
Article number: 105474
Language: English
ISSN: 0266352X
E-ISSN: 18737633
CODEN: CGEOEU
Document type: Journal article (JA)
Publisher: Elsevier Ltd
Abstract: There are some major problems in the study of fracture network evolution during multicluster fracturing, such as the simple assumption that the reservoir is homogeneous, without considering the heterogeneity of rock mineral particles. In addition, different viscosities used in fracturing fluid and fluid injection methods can affect fracture propagation. As reservoir stimulation enters the 2.0 era, it is important to study the evolution of multicluster fracture networks based on reservoir heterogeneity to improve the stimulated reservoir volume. For this purpose, a 2D, coupled stress-seepage-damage field multicluster fracturing numerical model was developed in this study, and a globally embedded 0-thickness cohesive element was used to simulate the random propagation of hydraulic fractures. Moreover, the elastic modulus, tensile strength and mixed fracture energy of the cohesive element mesh were randomly assigned using the Weibull distribution probability density function to simulate the reservoir heterogeneity. In addition, the dynamic distribution of the injected fluid rate during multicluster fracturing was implemented based on the Bernoulli equation. The capability of the model was validated with analytical solutions of the Khristianovich-Geertsma-de Klerk (KGD) problem and similar numerical modeling criteria of multicluster fracturing and was used to investigate the geological and engineering factors that influence the evolution of the fracture network. The results show that the fracture network formed by hydraulic fracturing is more complex when the reservoir has significant heterogeneity and the injection pressure has a larger extreme value. As the reservoir becomes increasingly homogeneous, using low-viscosity fracturing fluid does not significantly contribute to fracture network complexity or effectively reduce the extreme value of the injection pressure. Shortening the pad fluid injection time can significantly increase the fracture network complexity, but it increases the extreme value of the injection pressure, which requires a higher pressure tolerance for fracturing equipment. The results of this study have important significance for the parameter optimization of multicluster fracturing. © 2023 Elsevier Ltd
Number of references: 56
Main heading: Fracturing fluids
Controlled terms: Complex networks - Ductile fracture - Hydraulic fracturing - Minerals - Numerical models - Probability density function - Tensile strength - Viscosity - Weibull distribution
Uncontrolled terms: Cohesive element - Extreme value - Fluid injections - Fracture network - Hydraulic fracture network - Injection pressures - Multicluster fracturing - Multiclusters - Networks evolutions - Reservoir heterogeneity
Classification code: 482.2 Minerals - 512.1.2 Petroleum Deposits : Development Operations - 631.1 Fluid Flow, General - 722 Computer Systems and Equipment - 921 Mathematics - 922.1 Probability Theory - 922.2 Mathematical Statistics - 931.2 Physical Properties of Gases, Liquids and Solids
DOI: 10.1016/j.compgeo.2023.105474

Compendex references: YES
Database: Compendex
Data Provider: Engineering Village

147. Prospecting for ophiolite-type chromite deposit in Sartohay, West Junggar (NW China): Constraints from geological and geophysical data

Accession number: 20231213748827
Authors: Li, Hai (1, 2); Li, Yongjun (3); Yang, Gaoxue (3); Philemon, Lindagato (3); Wan, Yu (4); Zhao, Qiang (4); Wang, Panlong (3)
Author affiliation: (1) School of Earth Sciences and Engineering, Xi'an Shiyou University, Xi'an; 710065, China; (2) Shaanxi Key Laboratory of Petroleum Accumulation Geology, Xi'an Shiyou University, Xi'an; 710065, China; (3) Key Laboratory of Western China's Mineral Resources and Geological Engineering. Ministry of Education, Chang'an University, Xi'an; 710054, China; (4) Seventh Geological Survey Team, Xinjiang Bureau of Geology and Mineral Resource Exploration, Urumqi, Wusu; 833099, China
Corresponding author: Li, Yongjun(yongjunl@chd.edu.cn)
Source title: Ore Geology Reviews
Abbreviated source title: Ore Geol. Rev.
Volume: 156
Issue date: May 2023
Publication year: 2023
Article number: 105379
Language: English
ISSN: 01691368
Document type: Journal article (JA)
Publisher: Elsevier B.V.
Abstract: Chromite is a critical mineral that is of great significance for the development of metallurgical, chemical, and other industries. In order to study the deep ore prospecting methods of ophiolite-type chromitite, we have carried out plane-profile geological and mineral surveys, as well as high-precision gravity, magnetic, and controlled source audio-frequency magnetotelluric (CSAMT) measurements in the Sartohay, West Junggar. Based on the analysis, interpretation, and inference of multi-source geological information, a three-dimensional (3D) geological model of the typical mining area in Sartohay District was established. The results show that Sartohay ophiolite was occurred in the form of rootless tectonic blocks and generally displayed deformation and metamorphism (e.g., oblique thrust, transverse extrusion, and lateral strike slip). Sartohay ophiolite is in tectonic contact with surrounding strata. Several northwest dipping high-angle thrust faults are developed at the contact sites and inside the ophiolite rock mass, showing a thrust imbricated structure. Meanwhile, ophiolite in the modeling area is a NW-trending monoclinic rock mass. The base surface of the ophiolite is obliquely distributed in an "N-like" shape, and the chromitite bearing lithofacies zones also have a NW-trending distribution. Geophysical data reveal that the studied mining area is characterized by a layered electrical structure in the vertical direction. The upper layer displays a high-resistivity agglomerate and a low-resistivity band distributed alternately, while the lower layer is a complete high-resistivity block. Combined with the deposit characteristics in Sartohay, it is considered that the morphological occurrence, geological structure, lithology, and lithofacies of ophiolite control the spatial distribution of related chromitites. The dunite-harzburgite lithofacies belts, highly strain zones, and strong tectonic alteration belts of the ophiolite rock mass are significant sites for the chromite ore bodies/groups occurrence. This study provides approaches for researching on the production laws of ophiolite-type chromitite and supplys a prospecting pattern for deep concealed orebodies. © 2023 The Author(s)
Number of references: 107
Main heading: Deposits
Controlled terms: Fault slips - Lithology - Mineral exploration - Mining - Ore deposits - Rock mechanics - Rocks - Strike-slip faults - Structural geology
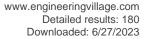**Uncontrolled terms:** Chromite deposit prospecting - Chromitites - Geophysical data - Geophysical methods - Lithofacies - Mining areas - Ophiolite-type chromitite - Rock-mass - Sartohay - West Junggar
Classification code: 481.1 Geology - 483.1 Soils and Soil Mechanics - 484.1 Earthquake Measurements and Analysis - 501.1 Exploration and Prospecting Methods - 502.1 Mine and Quarry Operations
DOI: 10.1016/j.oregeorev.2023.105379

Compendex references: YES
Database: Compendex
Data Provider: Engineering Village

148. Establishment of a Reynolds average simulation method and study of a drag reduction mechanism for viscoelastic fluid turbulence

Accession number: 20230513461323
Authors: Yuan, Ying (1, 2); Yin, Ran (3); Jing, Jiaqiang (4); Du, Shejiao (1); Pan, Jie (1, 2)
Author affiliation: (1) College of Petroleum Engineering, Xi'An Shiyou University, Xi'an; 710065, China; (2) Engineering Research Center of Safety and Energy Saving in Oil and Gas Storage and Transportation, Universities of Shaanxi Province, Xi'An Shiyou University, Xi'an; 710065, China; (3) Changqing Engineering Design Co., Ltd., Xi'an; 710018, China; (4) Oil and Gas Fire Protection Key Laboratory of Sichuan Province, Southwest Petroleum University, Sichuan, Chengdu; 611731, China
Corresponding author: Yuan, Ying(yyuan@xsyu.edu.cn)
Source title: Physics of Fluids
Abbreviated source title: Phys. Fluids
Volume: 35
Issue: 1
Issue date: January 1, 2023
Publication year: 2023
Article number: 015146
Language: English
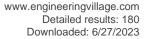**ISSN:** 10706631
E-ISSN: 10897666
CODEN: PHFLE6
Document type: Journal article (JA)
Publisher: American Institute of Physics Inc.
Abstract: Reynolds average simulation governing equations are derived for viscoelastic fluid turbulence using the Reynolds time-averaged method combined with the Navier-Stokes equations, the viscoelastic fluid finitely extensible nonlinear elastic-Peterlin constitutive equation, the viscoelastic fluid molecular conformation tensor transport equation, and the $k - \overline{v'2} - f$ turbulence model. To identify the relevant viscoelastic terms, user-defined functions and the programing language C are used to write a simulation subroutine for the Reynolds average of viscoelastic fluid turbulence; this subroutine is embedded into computational fluid dynamics software to establish a simulation method for Reynolds average of viscoelastic fluid turbulence. Then, the flow field structure of viscoelastic fluid turbulence is analyzed. Using energy transport theory, expressions for the contribution of viscous, elastic, and Reynolds shear stress to the turbulent friction factor of viscoelastic fluid in a horizontal tube are established, and the turbulent drag reduction mechanism of the viscoelastic fluid is revealed. The simulated values for pressure drop, Fanning friction factor, and the drag reduction rate of viscoelastic fluid in tests are in good agreement with experimental values, and the average relative error is less than 12.37%. In addition, elastic shear stress is produced after the dissolution of drag reduction agents in water, which increases the turbulent friction factor; however, Reynolds shear stress is greatly reduced, and viscous shear stress is weakened by inhibiting the turbulence fluctuation, so the turbulent friction factor decreases; more importantly, the increase in the friction factor of the former is much smaller than that of the latter. © 2023 Author(s).
Number of references: 44
Main heading: Turbulence models

Controlled terms: C (programming language) - Computation theory - Computational fluid dynamics - Friction - Navier Stokes equations - Nonlinear equations - Shear stress - Statistical mechanics - Subroutines - Transport properties - Viscoelasticity
Uncontrolled terms: Drag reduction mechanism - Elastic shear stress - Fluid turbulence - Friction factors - Governing equations - Reynold shear stress - Reynolds - Time-averaged - Vis-coelastic fluids - Visco-elastic fluid
Classification code: 721.1 Computer Theory, Includes Formal Logic, Automata Theory, Switching Theory, Programming Theory - 723.1 Computer Programming - 723.1.1 Computer Programming Languages - 723.5 Computer Applications - 921.2 Calculus - 922.2 Mathematical Statistics - 931.1 Mechanics - 931.2 Physical Properties of Gases, Liquids and Solids
Numerical data indexing: Percentage 1.237E+01%
DOI: 10.1063/5.0138491
Funding Details: Number: 51779212,U19B2012, Acronym: NSFC, Sponsor: National Natural Science Foundation of China;
Funding text: The work was supported by the National Natural Science Foundation of China (Grant Nos. U19B2012 and 51779212).
Compendex references: YES
Database: Compendex
Data Provider: Engineering Village
Compilation and indexing terms, Copyright 2023 Elsevier Inc.

149. High-sensitive and temperature-immune curvature sensor based on bitaper sandwiching in SMS fiber structure

Accession number: 20231713948687
Authors: Shao, Min (1); Cao, Zhongwei (1); Gao, Hong (1); Fu, Haiwei (1); Qiao, Xueguang (2)
Author affiliation: (1) Key Laboratory of Photo Electricity Gas & Oil Logging and Detecting of Ministry of Education, Xi'an Shiyou University, Xi'an; 710065, China; (2) School of Physics, Northwest University, Xi'an; 710065, China
Corresponding author: Shao, Min(shaomin@xsyu.edu.cn)
Source title: Optics Communications
Abbreviated source title: Opt Commun
Volume: 540
Issue date: August 1, 2023
Publication year: 2023
Article number: 129501
Language: English
ISSN: 00304018
CODEN: OPCOB8
Document type: Journal article (JA)
Publisher: Elsevier B.V.
Abstract: A high-sensitive and temperature-immune curvature sensor based on all fiber Mach–Zehnder interferometer (MZI) is proposed and experimentally investigated. The sensor is constructed by sandwiching a short section of multimode fiber (MMF) between two single-mode fibers (SMFs) with two bitapers. Experimental results show that the sensor can achieve a maximum sensitivity of -34.3935 nm/m-1 in the curvature range of 2.96-4.19 m-1 and a low temperature cross-sensitivity of -0.0003 m-1/C in the temperature range of 30-100 °C. The stability test reveals that the standard error of instability is 0.0004 m-1, indicating the sensor's capacity of long-term operation. The sensor has advantages of low cost, easy fabrication, large curvature detection range, high curvature sensitivity and temperature immunity, makes it has broad application prospects in the curvature sensing field. © 2023 Elsevier B.V.
Number of references: 37
Main heading: Temperature
Controlled terms: Interferometers - Multimode fibers - Single mode fibers
Uncontrolled terms: All fiber - Curvature sensitivities - Curvature sensor - Fiber Mach-Zehnder interferometers - Fibre structure - Lows-temperatures - Maximum sensitivity - Single-mode fibers - SMS fibers - Temperature cross-sensitivity
Classification code: 641.1 Thermodynamics - 741.1.2 Fiber Optics - 941.3 Optical Instruments
Numerical data indexing: Size -3.00E-04m, Size -3.43935E-08m, Size 2.54E-02m, Size 2.96E+00m to 4.19E+00m, Size 4.00E-04m, Temperature 3.03E+02K to 3.73E+02K
DOI: 10.1016/j.optcom.2023.129501
Funding Details: Number: YCS21111025, Acronym: -, Sponsor: -; Number: 12105220,61927812, Acronym: NSFC, Sponsor: National Natural Science Foundation of China;

Compendex references: YES
Database: Compendex
Data Provider: Engineering Village

150. A hybrid framework for predicting the remaining useful life of battery using Gaussian process regression

Accession number: 20231714024447

Authors: Li, Jiabo (1, 2); Ye, Min (2); Wang, Yan (1); Wang, Qiao (2); Wei, Meng (2)
Author affiliation: (1) Mechanical Engineering College, Xi'an Shiyou University, Xi'an; 710065, China; (2) Engineering Research Center of Expressway Construction & Maintenance Equipment and Technology of MOE, Chang'an University, Xi'an; 710064, China
Corresponding authors: Li, Jiabo(ljb92_7@163.com); Ye, Min(mingye@chd.edu.cn)

Source title: Journal of Energy Storage
Abbreviated source title: J. Energy Storage
Volume: 66
Issue date: August 30, 2023
Publication year: 2023
Article number: 107513
Language: English
E-ISSN: 2352152X
Document type: Journal article (JA)
Publisher: Elsevier Ltd

Abstract: The battery will inevitably deteriorate in its service life. Therefore, accurate prediction of the remaining useful life (RUL) is critical to the durability of the battery energy storage systems (ESS). The RUL prediction framework of Gaussian process regression(GPR) based on automatic stack autoencoder (SAE) and improved whale optimization algorithm (WOA) is proposed in this research paper. Firstly, the SAE and gray relation analysis are proposed to extract indirect health indicators (HIs) from battery degradation data. Secondly, the Gaussian process regression (GPR) approach combined with the WOA method to establish the RUL prediction framework. Besides, aiming at the disadvantage that WOA is prone to fall into local optimization, the WOA based on the sine cosine algorithm of decentralized foraging strategy is proposed to optimize the prediction ability of the GPR. Finally, compared with the prediction results of existing approaches under the same conditions, the simulation results indicate that the RUL prediction errors based on the proposed algorithm are controlled within 2 %, which has good advantages and prediction ability. © 2023 Elsevier Ltd

Number of references: 33
Main heading: Forecasting
Controlled terms: Battery storage - Digital storage - Electric batteries - Gaussian distribution - Gaussian noise (electronic) - Learning systems - Optimization - Regression analysis
Uncontrolled terms: Auto encoders - Energy storage system - Gaussian process regression - Health indicators - Hybrid framework - Optimization algorithms - Remaining useful life predictions - Remaining useful lives - Storage systems - Whale optimization algorithm
Classification code: 525.7 Energy Storage - 702.1 Electric Batteries - 702.1.2 Secondary Batteries - 722.1 Data Storage, Equipment and Techniques - 921.5 Optimization Techniques - 922.1 Probability Theory - 922.2 Mathematical Statistics
Numerical data indexing: Percentage 2.00E+00%
DOI: 10.1016/j.est.2023.107513

151. Study on the Behavior and Mechanism of D-amino Acid Dispersing Biofilm

Authors: Xu, Congmin (1); Gao, Haoran (1); Zhu, Wensheng (2); Yang, Xing (1); Chen, Yueqing (1); Wang, Wenyuan (1)
Author affiliation: (1) School of Materials Science and Engineering, Xi'an Shiyou University, Xi'an; 710065, China; (2) CNOOC Changzhou Paint and Coating Industry Research Institute Co.,Ltd., Jiangsu, Changzhou; 213000, China
Corresponding author: Xu, Congmin(cmxu@xsyu.edu.cn)

Abstract: In order to clarify the biofilm dispersing effect and bactericidal mechanism of D-amino acid enhanced biocide,different D-amino acids were used in this work to form a compound biocides with traditional biocides tributyl tetradecyl phosphonium chloride(TTPC),tetramethyl-phosphate sulfate(THPS)and antimicrobial peptides. By means of weightloss experiment,electrochemical test and surface analysis,the bactericidal inhibition effect of compound biocide on sulfate reducing bacteria(SRB),iron oxidizing bacteria(IOB)and the mixture of SRB + IOB on the surface of carbon steel was studied,and the behavior and mechanism of dispersive biofilm by D-amino acid were determined. The results show that SRB and IOB cooperate to form dense biofilms on the surface of carbon steel samples,which not only provides an anaerobic environment suitable for the growth of SRB,but also plays a certain protective role on SRB,which will lead to the most serious corrosion caused by the mixed bacteria of SRB + IOB. The biofilm dispersal signal factor released by D-amino acid can change the peptidoglycan composition of bacterial cell wall and regulate the expression of cell genes,inhibit the formation of biofilm by binding with bacterial proteins,and make the existing biofilm actively disperse off the surface of carbon steel,and destroy the oxygen concentration difference environment formed by SRB and IOB. D-amino acid to a large extent inhibits the aggravation of metal corrosion caused by extracellular polymeric substances(EPS)produced by bacteria,and thus enables biocides to better kill bacteria under the biofilm. The biocidal rates of SRB and IOB in the mixed biofilm are up to 100% and 82. 60%,respec-tively. The results showed that D-amino acid had a good bactericidal enhancement effect on the biocide by dispersing the biofilm behavior. © 2023 Cailiao Daobaoshe/ Materials Review. All rights reserved.

Number of references: 20
Main heading: Biofilms
Controlled terms: Amino acids - Bacteria - Biocides - Cell membranes - Chlorine compounds - Corrosion inhibitors - Corrosion protection - Iron - Proteins - Sulfur compounds - Surface analysis
Uncontrolled terms: Antimicrobial peptide - Bactericidal enhancement effect - Bactericidal mechanisms - d-Amino acids - Effect mechanism - Enhancement effects - Iron oxidizing bacterium - Mixed bacteria - Sulphate reducing bacteria - Tetramethyl
Classification code: 461.2 Biological Materials and Tissue Engineering - 462.5 Biomaterials (including synthetics) - 539.2 Corrosion Protection - 539.2.1 Protection Methods - 545.1 Iron - 803 Chemical Agents and Basic Industrial Chemicals - 804.1 Organic Compounds - 951 Materials Science
Numerical data indexing: Percentage 1.00E+02%, Percentage 6.00E+01%
DOI: 10.11896/cldb.21050076

Compendex references: YES
Database: Compendex
Data Provider: Engineering Village

152. Slow magnetic relaxation in a 3D dysprosium(III)-fluoro-oxalate framework containing zig-zag [Dy–F]n chains   (*Open Access*)

Accession number: 20223912810141
Authors: Li, Leilei (1, 2); Fang, Yifan (1); Liu, Shuang (1, 2); Hu, Mingfei (1); Wang, Wenzhen (1)
Author affiliation: (1) College of Chemistry and Chemical Engineering, Xi'an Shiyou University, Xi'an; 710065, China; (2) Key Laboratory of Advanced Energy Materials Chemistry (Ministry of Education), Nankai University, Tianjin; 300071, China
Corresponding author: Liu, Shuang(liush@xsyu.edu.cn)
Source title: Journal of Rare Earths
Abbreviated source title: J Rare Earth
Volume: 41
Issue: 1
Issue date: January 2023
Publication year: 2023
Pages: 100-107
Language: English
ISSN: 10020721
CODEN: JREAE6
Document type: Journal article (JA)
Publisher: Editorial Office of Chinese Rare Earths
Abstract: Dysprosium complexes based on [F–Dy] or near-linear [F–Dy–F] unit are of great concern in the field of single-molecule magnets due to their large magnetic anisotropy. Here, the crystal structure and the magnetic relaxation dynamics were reported for a three-dimensional (3D) metal–organic framework (MOF): [DyF(C2O4)(H2O)2]n·2nH2O (1), which is the unique MOF containing zig-zag [Dy–F]n chains. Magnetic susceptibility characterization reveals that 1 is one of the few 3D MOFs which show slow magnetic relaxation under zero dc field. And the effective energy barrier of 72 K for 1 is also higher than most Dy-based 3D MOFs. The diamagnetic ion dilution study shows that the ferromagnetic exchange couplings mainly transmitted by F- bridges in 1 contribute little to the energy barrier, but effectively suppress the quantum tunneling process and result in a smooth hysteresis loop with no waist-restricted step. © 2022 Chinese Society of Rare Earths
Number of references: 75
Main heading: Magnetic susceptibility
Controlled terms: Crystal structure - Dysprosium compounds - Energy barriers - Exchange coupling - Fluorine compounds - Ion exchange - Magnetic anisotropy - Magnetic materials - Magnetic relaxation - Magnetism - Rare earths
Uncontrolled terms: 3d metals - Crystals structures - Dysprosium complexes - Fluoride - Metalorganic frameworks (MOFs) - Rare-earths - Relaxation dynamics - Single-molecule magnet - Slow magnetic relaxations - Zig-zag
Classification code: 641.1 Thermodynamics - 701.2 Magnetism: Basic Concepts and Phenomena - 708.4 Magnetic Materials - 801.4 Physical Chemistry - 802.2 Chemical Reactions - 804.2 Inorganic Compounds - 931.2 Physical Properties of Gases, Liquids and Solids - 933.1.1 Crystal Lattice
Numerical data indexing: Inductance 2.00E-09H, Temperature 7.20E+01K
DOI: 10.1016/j.jre.2022.02.019

153. The influence of CO2 huff and puff in tight oil reservoirs on pore structure characteristics and oil production from the microscopic scale

Accession number: 20230213350657

Authors: Huang, Xing (1, 2, 3); Wang, Xingyu (1); He, Mengqing (1, 4); Zhang, Yu (1); Su, Zezhong (1); Li, Xiang (5); Yang, Weipeng (5); Lu, Jun (5)
Author affiliation: (1) School of Petroleum Engineering, Xi'an Shiyou University, Shaanxi, Xi'an; 710065, China; (2) Shaanxi Key Laboratory of Carbon Dioxide Sequestration and Enhanced Oil Recovery, Shaanxi, Xi'an; 710065, China; (3) Cooperative Innovation Center of Unconventional Oil and Gas Exploration and Development, Xi'an Shiyou University, Shaanxi, Xi'an; 710065, China; (4) College of Petroleum Engineering, China University of Petroleum-Beijing, Beijing; 102249, China; (5) McDougall School of Petroleum Engineering, The University of Tulsa, Tulsa; OK; 74104, United States
Corresponding author: He, Mengqing(mqhexsyu@163.com)

Source title: Fuel
Abbreviated source title: Fuel
Volume: 335
Issue date: March 1, 2023
Publication year: 2023
Article number: 127000
Language: English
ISSN: 00162361
CODEN: FUELAC
Document type: Journal article (JA)
Publisher: Elsevier Ltd

Abstract: CO2 huff-n-puff can store CO2 and improve the recovery of tight oil reservoir. The asphaltene precipitation produced by the interaction of CO2 and oil causes damage to tight oil reservoirs. Based on the FE-SEM, CST, Nano-CT, HPMI and NMR, the microscopic classification standard is established. The experiments were carried out on different types of samples to quantitatively evaluate the influence of asphaltenes on pore structure and oil recovery. The results show that the asphaltene precipitation is positively correlated with huff-n-puff rounds and injection pressure. The asphaltene precipitation in type I sample is the highest. The asphaltene precipitation in type II sample is lower. The lowest asphaltene precipitation is in type III sample. In the CO2 immiscible state, asphaltenes are mainly deposited in larger pore throats. In the CO2 miscible state, the CO2 extraction effect is enhanced, the asphaltene deposits in the smaller pore throats. The overall oil recovery of the type II sample is the highest. The asphaltene precipitation, the blockage degree, the oil recovery interact and restrict each other. The oil recovery increases, the asphaltene increases, and the blockage degree of pore throats become more serious. Asphaltene precipitation causes damage to physical properties in reservoir, the porosity and permeability damage rates range from 1.35% to 3.17% and 2.17% to 8.24%, respectively. Asphaltene changes the wettability to lyophilic. The wettability reversal index ranges from 0.86% to 4.92%, which increases the seepage resistance of the oil phase. This research is novel for quantitative evaluation of reservoir microscopic pore throat characteristics and microscopic oil displacement mechanism by asphaltene precipitation formed during CO2 huff and puff in tight oil reservoirs. Also, the research results are of significance for optimizing the field development parameters. © 2022 Elsevier Ltd

Number of references: 92
Main heading: Carbon dioxide
Controlled terms: Asphaltenes - Petroleum reservoir engineering - Petroleum reservoirs - Pore structure - Wetting
Uncontrolled terms: Asphaltene precipitation - CO2 huff-n-puff - Microscopic pore throat characteristic - Oil recoveries - Oil reservoirs - Pore throat - Pores structure - Structure characteristic - Tight oil reservoir - Type II
Classification code: 512.1.1 Oil Fields - 512.1.2 Petroleum Deposits : Development Operations - 513 Petroleum Refining - 804.2 Inorganic Compounds - 931.2 Physical Properties of Gases, Liquids and Solids
Numerical data indexing: Percentage 1.35E+00% to 3.17E+00%, Percentage 2.17E+00% to 8.24E+00%, Percentage 8.60E-01% to 4.92E+00%
DOI: 10.1016/j.fuel.2022.127000

Compendex references: YES
Database: Compendex
Data Provider: Engineering Village

154. Study on synergistic catalysis of ex-situ catalyst and in-situ clay in aquathermolysis of water-heavy oil-ethanol at low temperature

Accession number: 20224413021302
Authors: Ma, Liwa (1, 2); Slaný, Michal (3, 4); Guo, Rui (1); Du, Weichao (1); Li, Yongfei (1, 2); Chen, Gang (1)
Author affiliation: (1) State Key Laboratory of Petroleum Pollution Control, Xi'an Shiyou University, Xi'an, China; (2) Shaanxi Province Key Laboratory of Environmental Pollution Control and Reservoir Protection Technology of Oilfields, Xi'an Shiyou University, Xi'an, China; (3) Institute of Inorganic Chemistry, Slovak Academy of Sciences, Dúbravská cesta 9, Bratislava; 845 36, Slovakia; (4) Institute of Construction and Architecture, Slovak Academy of Sciences, Dúbravská cesta 9, Bratislava; 845 03, Slovakia
Corresponding author: Slaný, Michal(michal.slany@savba.sk)
Source title: Chemical Engineering Journal
Abbreviated source title: Chem. Eng. J.
Volume: 453
Issue date: February 1, 2023
Publication year: 2023
Article number: 139872
Language: English
ISSN: 13858947
CODEN: CMEJAJ
Document type: Journal article (JA)
Publisher: Elsevier B.V.
Abstract: There are so many studies on aquathermolysis for enhancing heavy oil recovery, but almost all of them are limited to the catalytic effect of an external catalyst on the reaction, ignoring its possible interaction with in-situ inorganic minerals after entering the reservoir. Therefore, we prepared and characterized ex-situ and in-situ catalyst compounds using metal complexes prepared from salicylic acid and chloride salts as ex-situ catalysts and bentonite (B) as in-situ carrier catalyst. Their synergistic catalytic viscosity reduction performance in aquathermolysis was investigated. B@Cu(II)L appears to be the most effective synergistic combination of an ex-situ catalyst with copper ions and ligands Cu(II)L and in-situ compound bentonite. Under the optimized conditions, 0.2 wt% B@Cu(II)L with 30 wt% ethanol at 180 °C for 4 h, the viscosity was decreased by 91.5 %. The temperature was about 70 °C lower than the traditional reaction temperature. The results of TGA and DSC of the heavy oil show that the macromolecular substances in the heavy oil had cracked into small molecules with a low boiling point after the reaction. The amounts of resin and asphaltene decrease, and those of saturated and aromatic HC increase. In addition, GC–MS analysis of polar substances dissolved in water after reaction shows that B@Cu(II)L can help to decrease the polar substances in heavy oil and reduce the aromaticity of polar substances. In addition, model compounds were used to study the reaction mechanism. GC–MS analysis results showed that C[sbnd]C, C[sbnd]N and C[sbnd]S bonds were broken during the reaction, thereby reducing the viscosity of the heavy oil. © 2022 Elsevier B.V.
Number of references: 41
Main heading: Crude oil
Controlled terms: Catalysts - Chlorine compounds - Copper compounds - Ethanol - Heavy oil production - Metal complexes - Metal ions - Salicylic acid - Temperature - Viscosity
Uncontrolled terms: Aquathermolysis - Bentonite complex catalyst - Catalytic aquathermolyse - Complex catalysts - Ex situ - GC/MS analysis - Polar substances - Synergistic catalysis - Viscosity reduction -]+ catalyst
Classification code: 511.1 Oil Field Production Operations - 512.1 Petroleum Deposits - 531.1 Metallurgy - 631.1 Fluid Flow, General - 641.1 Thermodynamics - 803 Chemical Agents and Basic Industrial Chemicals - 804 Chemical Products Generally - 804.1 Organic Compounds - 804.2 Inorganic Compounds - 931.2 Physical Properties of Gases, Liquids and Solids

155. Lanthanide metal-organic frameworks containing ferromagnetically coupled metal-carboxylate chains showing slow magnetic relaxation behavior

Authors: Li, Lei-Lei (1, 2); Chen, Shuang-Shuang (1); Liu, Shuang (1, 2); Yong, Zhi-Hua (1); Zhang, Da-Ke (1); Zhang, Shuai-Shuai (1); Xin, Yi-Chen (1)
Author affiliation: (1) College of Chemistry and Chemical Engineering, Xi'an Shiyou University, Xi'an; 710065, China; (2) Key Laboratory of Advanced Energy Materials Chemistry (Ministry of Education), Nankai University, Tianjin; 300071, China
Corresponding author: Li, Lei-Lei(lll@xsyu.edu.cn)

Abstract: Lanthanide metal-organic frameworks (Ln-MOFs) with slow magnetic relaxation behavior are of great interest to scientists due to their rich and peculiar physical phenomena and spin-related applications. In this contribution, the syntheses, characterizations and magnetic properties of two new Ln-MOFs: {[Ln2(btpdc)3·DMF·2H2O]·2DMF·4H2O}n (Ln = Dy (1), Gd (2), H2btpdc = benzo[b]thiophene-2,6-dicarboxylic acid) are reported. Single crystal X-ray diffraction experiments show the two complexes are isostructural with three dimensional (3D) porous framework structure constructed by metal-carboxylate chains separated by long organic linkers. Direct-current (dc) magnetic susceptibilities recorded under 1000 Oe reveal the overall exchange couplings in both the two MOFs are ferromagnetic. Interestingly, the ferromagnetic coupled metal-carboxylate chains in 1 are sufficiently isolated by the long organic linkers that makes 1 exhibit slow magnetic relaxation behavior and Ising-like behavior which was rarely reported for lanthanide-carboxylate complexes. © 2022 Elsevier B.V.

Compendex references: YES
Database: Compendex
Data Provider: Engineering Village

156. Particle erosion behavior in viscoelastic surfactant abrasive slurry jetting

Accession number: 20230313382209

Authors: Wang, Zhiguo (1); Wang, Wenjuan (1); Ni, Jun (2); Sun, Xiao (2); Guo, Jiangru (1); Su, Xiaohui (1); Luo, Xiangrong (1)

Author affiliation: (1) Xi'an Key Laboratory of Wellbore Integrity Evaluation, New Energy College, Xi'an Shiyou University, Xi'an; 710065, China; (2) Shaanxi Province Key Laboratory of CO2 Sequestration and Enhanced Oil Recovery, Xi'an; 710065, China

Corresponding author: Wang, Zhiguo(zhgwang@xsyu.edu.cn)

Source title: Powder Technology
Abbreviated source title: Powder Technol.
Volume: 416
Issue date: February 15, 2023
Publication year: 2023
Article number: 118230
Language: English
ISSN: 00325910
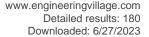**E-ISSN:** 1873328X
CODEN: POTEBX
Document type: Journal article (JA)
Publisher: Elsevier B.V.

Abstract: As a living polymer, Viscoelastic Surfactants (VES) fluids have the advantages of low friction, high sand arrying, environmental friendliness, and microstructures recoverability after mechanical degradation. It is better than common polymer as an abrasive slurries additive. In this work, Octadecyl Trimehyl Ammonium Chloride and NaSal are mixed as additives to form abrasive slurry. The erosion behavior of abrasive water jet (AWJ) and abrasive slurry jet (ASJ) was comparatively investigated using a submerged jet erosion experimental facility. The results showed that the addition of VES enhanced the erosion rate of the target specimen by the jet. Profile Scanning with a Laser Scanning Confocal Microscope (LSCM) showed that the surface morphology of ASJ eroded specimens is a deeper and more focused W-shape than that of AWJ. The micro-morphology of the specimens eroded by abrasive water jet and abrasive slurry jet was analyzed by Scanning Electron Microscope (SEM). In addition, we also found that the velocity of the VES abrasive slurry jet was significantly higher than that of the abrasive water jet on the condition of same pump power. At the same flow rate, the sand-carrying ability of VES is better than that of water, and the higher the flow rate, the stronger the sand-carrying ability of VES. Finally, considering the drag reducing and the sand-carrying ability of VES fluid, an erosion prediction model suitable for VES abrasive slurry jet is established. Furthermore, the accuracy of the model is verified by experiments. This work would provide a basis for the application of VES-ASJ in oil and gas fields such as rock-breaking drilling and fracturing perforation. © 2023 Elsevier B.V.

Number of references: 33
Main heading: Scanning electron microscopy

Controlled terms: Additives - Chlorine compounds - Drag reduction - Erosion - Gas industry - Morphology - Sand - Surface active agents - Surface morphology - Viscoelasticity
Uncontrolled terms: Abrasive slurries - Abrasive slurry jet - Abrasive waterjets - Drag reducing - Erosion behavior - Erosion modeling - Particle erosion - Sand-carrying ability - Slurry jets - Viscoelastic surfactants
Classification code: 483.1 Soils and Soil Mechanics - 522 Gas Fuels - 803 Chemical Agents and Basic Industrial Chemicals - 931.2 Physical Properties of Gases, Liquids and Solids - 951 Materials Science
DOI: 10.1016/j.powtec.2023.118230

Compendex references: YES
Database: Compendex
Data Provider: Engineering Village

157. Pseudointerpenetrating network nanocomposite hydrogel for temporary plugging in fractured reservoirs

Accession number: 20224413034478
Authors: Yang, Yang (1, 2); He, Xiaoxuan (1); Sun, Dalong (1); Zhang, Hao (1); Zhong, Ying (1); She, Jiping (1)
Author affiliation: (1) College of Energy, Chengdu University of Technology, Chengdu; 610059, China; (2) Shaanxi Key Laboratory of Advanced Stimulation Technology for Oil & Gas Reservoirs, Xi'an Shiyou University, Xi'an; 710015, China
Corresponding author: Yang, Yang(yangyang19@cdut.edu.cn)
Source title: Colloids and Surfaces A: Physicochemical and Engineering Aspects
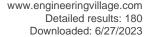**Abbreviated source title:** Colloids Surf. A Physicochem. Eng. Asp.
Volume: 656
Issue date: January 5, 2023
Publication year: 2023
Article number: 130369
Language: English
ISSN: 09277757
E-ISSN: 18734359
CODEN: CPEAEH
Document type: Journal article (JA)
Publisher: Elsevier B.V.

Abstract: Nanomaterial-enhanced hydrogels have attracted considerable attention as temporary plugging agents for lost circulation control due to their improved strength under high temperature and high pressure (HTHP) conditions compared to conventional hydrogels. In this study, a pseudointerpenetrating network nanocomposite hydrogel (PINNG), which was composed of temperature-resistant polyacrylamide (TSPAM), polyethyleneimine (PEI) and cellulose nanofibrils (CNFs), was proposed. CNF with a fibrous structure exhibited a more significant effect on the rheological behavior and mechanical strength of the hydrogel than nanosilica (nano-SiO2). The reversible CNF network endowed the gelant with increased zero-shear viscosity and significant thixotropy. Furthermore, the presence of CNF noticeably improved the strength of PINNG, and the elastic modulus of PINNG was 1232% greater than that of the blank sample. According to analyses of Fourier transform infrared spectroscopy (FTIR), thermogravimetry-derivative thermogravimetry (TG–DTG) and scanning electron microscopy (SEM), it can be deduced that the strengthening mechanism of CNF was mainly related to physical filling, physical crosslinking, and especially the formation of a pseudointerpenetrating network structure with the crosslinked polymer chains. Due to the strengthening effect of CNF, PINNG exhibited a better pressure-bearing performance than the blank sample and the nano-SiO2 composite sample

under 140 °C for the core with 2 mm of fracture width. Additionally, the favorable degradability of the PINNG system demonstrated that PINNG exhibited great potential in the application of lost circulation control as a temporary plugging agent. © 2022 Elsevier B.V.

Number of references: 36
Main heading: Nanocomposites
Controlled terms: Crosslinking - Fourier transform infrared spectroscopy - Fracture - Hydrogels - Scanning electron microscopy - Silica - Silicon - Thermogravimetric analysis
Uncontrolled terms: Cellulose nanofibrils - Fractured reservoir - High temperatures and high pressures - Lost circulation control - Nano-SiO 2 - Nanocomposite hydrogels - Network nanocomposites - Plugging agent - Strengthening mechanisms - Temporary plugging
Classification code: 549.3 Nonferrous Metals and Alloys excluding Alkali and Alkaline Earth Metals - 761 Nanotechnology - 801 Chemistry - 801.3 Colloid Chemistry - 802.2 Chemical Reactions - 804 Chemical Products Generally - 933 Solid State Physics - 951 Materials Science
Numerical data indexing: Percentage 1.232E+03%, Size 2.00E-03m, Temperature 4.13E+02K
DOI: 10.1016/j.colsurfa.2022.130369

Compendex references: YES
Database: Compendex
Data Provider: Engineering Village

158. Calculation method and geological significance of dissolved and exsolved helium in pore water

Accession number: 20231113711963
Title of translation:

Authors: Zhao, Dong (1, 2); Wang, Xiaofeng (1); Liu, Wenhui (1, 3); Zhang, Dongdong (1); Li, Xiaofu (1); Zhang, Jiayu (1)
Author affiliation: (1) State Key Laboratory of Continental Dynamics, Northwest University, Shaanxi, Xi'an; 710069, China; (2) Laboratory Management Office-Experimental Center, Xi'an Shiyou University, Shaanxi, Xi'an; 710069, China; (3) Sinopec Exploration & Production Research Institute, Beijing; 100083, China
Corresponding author: Wang, Xiaofeng(wangxf@nwu.edu.cn)

Source title: Natural Gas Industry
Abbreviated source title: Natur. Gas Ind.
Volume: 43
Issue: 2
Issue date: 2023
Publication year: 2023
Pages: 155-164
Language: Chinese
ISSN: 10000976
CODEN: TIGOE3
Document type: Journal article (JA)
Publisher: Natural Gas Industry Journal Agency

Abstract: The classical helium accumulation theory emphasizes the "extraction" and "carrying" of dissolved helium in the rock pore water by external fluids (such as CH4 and N2), without giving full consideration how the change of the occurrence environment of in-situ dissolved helium (especially the formation temperature and pressure changes caused by tectonic uplift) influences Helium migration and accumulation, so this theory has a certain limitation in helium resource evaluation and development. In this paper, Bunsen coefficient is used to calculate helium solubility under formation conditions. Based on this, a model for calculating the amount of dissolved and exsolved helium in rock pore water is established by taking the unit volume (1 km3) of granite as an example. Then, the correlation between the changes of formation temperature and pressure and the helium migration and accumulation is researched qualitatively and quantitatively. And the following research results are obtained. First, the helium solubility in the formation condition

is extremely small and varies in a wide range, and its change is mainly under the joint influence of reservoir depth and helium molar partial pressure, which usually increases with the increase of burial depth and partial pressure. Second, the decrease of formation temperature and pressure caused by large tectonic uplift can lead to the large-scale continuous exsolution of in-situ dissolved helium, thus providing sufficient free helium source for the formation of helium-rich gas reservoirs. Third, the 4He generated and accumulated in massive granites for a long time can be exsolved and released from the pore water under proper conditions. In conclusion, the accumulation models of crust-sourced helium-rich natural gas reservoirs are summarized as "uplift-exsolution type" and "replacement-exsolution type" by taking the occurrence of large-scale tectonic uplift in the exsolution and enrichment process of pore dissolved helium as the basis. © 2023 Natural Gas Industry Journal Agency. All rights reserved.

Number of references: 42
Main heading: Solubility
Controlled terms: Dissolution - Granite - Helium - Natural gas - Petroleum reservoir engineering - Tectonics - Water
Uncontrolled terms: Accumulation model - Amount of dissolved helium - Amount of exsolved helium - Bunsen coefficient - Exsolution - Formation pressure - Formation temperature - Pore waters - Tectonic uplift - Temperature and pressures
Classification code: 481.1 Geology - 512.1.2 Petroleum Deposits : Development Operations - 522 Gas Fuels - 801.4 Physical Chemistry - 802.3 Chemical Operations - 804 Chemical Products Generally
Numerical data indexing: Size 1.00E+03m
DOI: 10.3787/j.issn.1000-0976.2023.02.016
Compendex references: YES
Database: Compendex
Data Provider: Engineering Village
Compilation and indexing terms, Copyright 2023 Elsevier Inc.

159. On profiniteness and Hausdorffness of topological residuated lattices

Accession number: 20230066760
Authors: Yang, Jiang (1); He, Pengfei (2); Wang, Juntao (3)
Author affiliation: (1) School of Mathematics, Northwest University, Xi'an; 710127, China; (2) School of Mathematics and Information Science, Shaanxi Normal University, Xi'an; 710119, China; (3) School of Science, Xi'an Shiyou University, Xi'an; 710065, China
Corresponding author: He, Pengfei(hepengf1986@126.com)
Source title: arXiv
Abbreviated source title: arXiv
Issue date: February 22, 2023
Publication year: 2023
Language: English
E-ISSN: 23318422
Document type: Preprint (PP)
Publisher: arXiv
Abstract: The aim of this paper is to study the profiniteness of compact topological residuated lattices and the existence of Hausdorff topological residuated lattices. Firstly, we study profinite residuated lattices and obtain sufficient and necessary conditions for profiniteness in compact topological residuated lattices. These conditions include topological and algebraic characterizations. Moreover, it order to study the existence of Hausdorf topological residuated lattices, we investigate finiteness conditions in residuated lattices. Finally, we investigate linear topological residuated lattices and give the class of residuated lattices that can be endowed with a non-trivial Hausdorff topology. © 2023, CC BY.

Number of references: 41
Main heading: Algebra
Controlled terms: Topology
Uncontrolled terms: Condition - Finiteness condition - Hausdorff - Hausdorff topologies - Hausdorffness - Non-trivial - Profiniteness - Residuated lattices - Sufficient and necessary condition - Topological algebra
Classification code: 921.1 Algebra - 921.4 Combinatorial Mathematics, Includes Graph Theory, Set Theory
DOI: 10.48550/arXiv.2302.11333
Compendex references: YES
Preprint ID: 2302.11333v1
Preprint source website: https://arxiv.org
Preprint ID type: ARXIV
Database: Compendex
Data Provider: Engineering Village

160. Study on spontaneous imbibition and displacement characteristics of mixed-wet tight sandstone reservoir based on high-precision balance and NMR method

Accession number: 20231413834232

Authors: Jiang, Zhihao (1, 2); Li, Gaoren (3, 4); Zhao, Peiqiang (5); Zhou, You (3, 4); Mao, Zhiqiang (5); Liu, Zhidi (1, 2)

Author affiliation: (1) School of Earth Sciences and Engineering, Xi'an Shiyou University, Xi'an; 710065, China; (2) Shaanxi Key Laboratory of Petroleum Accumulation Geology, Xi'an Shiyou University, Xi'an; 710065, China; (3) Exploration and Development Research Institute, PetroChina Changqing Oilfield Company, Xi'an; 710021, China; (4) National Engineering Laboratory for Exploration and Development of Low-Permeability Oil & Gas Fields, Xi'an; 710018, China; (5) State Key Laboratory of Petroleum Resources and Prospecting, China University of Petroleum, Beijing; 102249, China

Corresponding author: Jiang, Zhihao(zhihaoj2021@xsyu.edu.cn)

Abstract: Wettability is the key to understanding the complex seepage characteristics of tight sandstone reservoirs, which will affect the distribution of the residual hydrocarbon resources during the reservoir exploitation process. Complex wettability, strong heterogeneity and tiny pore space make it more challenging to study the imbibition characteristics of mixed-wet tight sandstone reservoirs. In this study, the spontaneous imbibition (SI) and displacement characteristics of mixed-wet tight sandstone reservoirs are studied by high precision balance and nuclear magnetic resonance (NMR) T2 experiment. 3 rock plungers (A1, B1, C1) were put into the $CaCl_2$ solution for SI, while their parallel samples (A2, B2, C2) were carried out SI experiments in the experimental oil. Then all the plungers are respectively displaced by the imbibition liquid after SI experiments. The weight and NMR T2 spectra of the plungers in the above different conditions were measured. According to the experiment results, the pores of tight sandstone can be divided into 3 types with different wettability. The adsorption pores with T2 distribution of 0.01–2.5 ms are water-wet, the capillary bound fluid pores with T2 between 2.5 and 50 ms and the movable fluid pore with T2 greater than 50 ms are mainly oil-wet. The SI and displacement behaviors of different pores were studied, the results show the oil absorbed per cc rock is more than 4 times that of brine. The weight gain after SI in the first 24 h can indicate the total SI result. The study results can accurately characterize the wettability of different pores and contribute to a novel wettability evaluation method in mixed wettable tight sandstone. © 2023 Elsevier Ltd

Number of references: 49

Main heading: Nuclear magnetic resonance

Controlled terms: Chlorine compounds - Nuclear magnetic resonance spectroscopy - Pore fluids - Sandstone - Silicon - Wetting

Uncontrolled terms: Displacement - Displacement characteristic - High-precision - Mix-wettability - Residual hydrocarbons - Resonance methods - Seepage characteristics - Spontaneous imbibition - Tight sandstone reservoirs - Tight sandstones
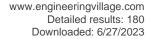
Classification code: 482.2 Minerals - 549.3 Nonferrous Metals and Alloys excluding Alkali and Alkaline Earth Metals - 631.3 Flow of Fluid-Like Materials

Numerical data indexing: Time 1.00E-05s to 2.50E-03s, Time 2.50E-03s to 5.00E-02s, Time 5.00E-02s, Time 8.64E+04s

DOI: 10.1016/j.fuel.2023.128247

161. First-principles study of the behaviors of He atoms at TiC(110)/V(110) interface

Authors: Wang, Yuan (1); Zhang, Jiteng (1); Wang, Chen (2); Jin, Na (1)
Author affiliation: (1) Center for Rare Earth & Vanadium & Titanium Materials, School of Materials Science & Engineering, Sichuan University, Chengdu; 610065, China; (2) School of Materials Science and Engineering, Xi'an Shiyou University, Xi'an; 710000, China
Corresponding author: Jin, Na(jinna319@163.com)

Abstract: The behaviors of He atoms at TiC(110)/V(110) interface with center-site stacking, which has the most covalent-ionic bond, using first-principles calculations are studied to clarify the effect of TiC-precipitate on the He bubble formation in the vanadium alloys. The results show that He atom prefers to dissolve at TiC/V interface compared with bulk vanadium, and the dissolved He atom would cause the interface to swell, but has little influence on the electronic properties of the interface. It can be explained by He atom with a typical closed shell structure, which is hardly chemically reactive with other elements. The TiC-precipitate promotes the vacancies formation at the interface. He atoms are easier to dissolve at the interface where exists vacancies. The maximum number of He atoms that can be trapped by the interface with V monovacancy is thirteen, moreover the interface can trap more He atoms with the increasing of vacancies. In addition, the smallest energy barrier of He atom from the interface to the interior bulk vanadium is 0.67 eV, which is almost six times higher than that in bulk vanadium (0.11 eV), suggesting that the He atom dissolved at the interface is difficult to escape to bulk vanadium. In conclusion, TiC/V interface is a possible nucleation position of He bubbles. The findings can provide the theoretical strategy for further designing, fabricating and processing of vanadium alloys used in nuclear structure materials. © 2022 Elsevier Ltd

162. Effects of detonation initial conditions on performance of pulse detonation chamber-axial turbine combined system

Authors: Liu, Junyu (1); Wang, Zhiwu (1, 2); Qin, Weifeng (1); Li, Junlin (1); Zhang, Zixu (1); Huang, Jingjing (3)

Author affiliation: (1) School of Power and Energy, Northwestern Polytechnical University, Xi'an; 710072, China; (2) Shenzhen Research Institute of Northwestern Polytechnical University, Shenzhen; 518057, China; (3) Mechanical Engineering College, Xi'an Shiyou University, Xi'an; 710065, China
Corresponding authors: Wang, Zhiwu(malsoo@mail.nwpu.edu.cn); Huang, Jingjing(huangjingjing@xsyu.edu.cn)

Abstract: The pulse detonation turbine engine (PDTE) has a potential performance advantage over conventional gas turbine engines due to the self-pressurization feature of detonation. However, pulse detonation exhibits strong unsteadiness, and large flow losses can be generated when the detonation wave interacts with the turbine blades, which severely limits engine performance. Therefore, how to maximize this potential performance advantage is crucial to the application of the PDTE. If the detonation initial conditions could be adjusted to modify the characteristics of detonation so that the pulse detonation chamber (PDC) and turbine are well matched, the performance of the PDTE could be greatly improved. Taking this into account, this paper numerically investigated the performance of the PDC-turbine combined system with different hydrogen-air mixture equivalence ratios and initial temperatures. The turbine efficiency and PDC combustion efficiency were analyzed first, which provided guidance for the thermal efficiency analysis. The results indicated that the combined system was more suitable for operation under lean fuel conditions due to the high thermal efficiency and obvious performance advantage over isobaric combustion. In addition, increasing the initial temperature could improve thermal efficiency under lean fuel conditions, but some of the performance advantage would be sacrificed. © 2023 Elsevier Ltd

Number of references: 38
Main heading: Hydrogen
Controlled terms: Combustion - Combustion knock - Detonation - Gas turbines - Pulse detonation engines - Thermal efficiency - Turbine components - Turbomachine blades
Uncontrolled terms: Combined system - Combustion efficiencies - Detonation chambers - Hydrogen detonation - Performance - Performance advantage - Pulse detonation - Pulse detonation turbine engine - Thermal-efficiency - Turbine efficiency
Classification code: 521.1 Fuel Combustion - 612.1 Internal Combustion Engines, General - 612.3 Gas Turbines and Engines - 617 Turbines and Steam Turbines - 641.1 Thermodynamics - 641.2 Heat Transfer - 654.2 Rocket Engines - 804 Chemical Products Generally
DOI: 10.1016/j.energy.2023.127765

Compendex references: YES
Database: Compendex
Data Provider: Engineering Village

163. Effect of N-doping on Structure and Properties of 3R-CuInO2Oxide by First-principles Study (*Open Access*)

Accession number: 20232114118149
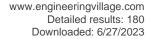**Authors:** Zhang, Xiaojian (1); Liu, Wenting (1); Li, Yangping (2)
Author affiliation: (1) School of Materials Science and Engineering, Xi'An Shiyou University, Xi'an; 710065, China; (2) State Key Lab of Solidification Processing, School of Materials Science and Engineering, Northwestern Polytechnical University, Xi'an; 710072, China
Source title: Journal of Physics: Conference Series

Abbreviated source title: J. Phys. Conf. Ser.
Volume: 2468
Part number: 1 of 1
Issue: 1
Issue date: 2023
Publication year: 2023
Article number: 012042
Language: English
ISSN: 17426588
E-ISSN: 17426596
Document type: Conference article (CA)
Conference name: 10th Annual International Conference on Material Science and Environmental Engineering, MSEE 2022
Conference date: November 25, 2022 - November 27, 2022
Conference location: Virtual, Online
Conference code: 188302
Publisher: Institute of Physics

Abstract: The structural, electronic and mechanical properties of N-doped 3R-CuInO2 were investigated by using the first-principles theory. The lattice constants and internal parameter of 3R-CuInO2 were calculated and the effects of N-doping on the structural parameters were also studied. And the electronic properties of pure and doped 3R-CuInO2 were studied throughout the calculation of band structure and density of states. Moreover, the elastic coefficients, bulk modulus, shear modulus, Young's modulus and Poisson's ratio of pure and doped 3R-CuInO2 with different concentration of N atoms were also investigated. © Published under licence by IOP Publishing Ltd.

Number of references: 30
Main heading: Electronic properties
Controlled terms: Copper compounds - Doping (additives) - Elastic moduli - Lattice constants - Structural properties
Uncontrolled terms: Constant parameters - Densities of state - Elastic coefficient - First-principle study - First-principle theory - Internal parameters - N-doped - N-Doping - Structural parameter - Structures and properties
Classification code: 408 Structural Design - 933.1.1 Crystal Lattice - 951 Materials Science
DOI: 10.1088/1742-6596/2468/1/012042
Funding Details: Number: No.YCS22112062, Acronym: -, Sponsor: -; Number: 51902252, Acronym: NSFC, Sponsor: National Natural Science Foundation of China;
Funding text: This work was supported by National Natural Science Foundation of China (Grant No. 51902252) and Innovation and Practice Ability Training Project for Postgraduates of Xi'an Shiyou University (Grant No.YCS22112062).
Compendex references: YES
Open Access type(s): All Open Access, Gold
Database: Compendex
Data Provider: Engineering Village

164. Small-sized temperature and pressure sensors based on fiber bragg grating for oil and gas wells

Accession number: 20231914073635
Authors: Xu, Dongpo (1); Feng, Dequan (1); Chen, Qiang (2); Liu, Guoquan (2); Qiao, Xueguang (3)
Author affiliation: (1) The Photoelectric Oil and Gas Logging and Detection Laboratory, Xi'an Shiyou University, China; (2) The Logging Technology Research Institute, China Petroleum Logging Company Ltd, China; (3) The Department of Physics, Northwest University, Xi'an, China
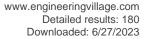**Corresponding author:** Qiao, Xueguang(xgqiao@nwu.edu.cn)
Source title: Sensors and Actuators A: Physical
Abbreviated source title: Sens Actuators A Phys
Volume: 357
Issue date: August 1, 2023
Publication year: 2023
Article number: 114397
Language: English
ISSN: 09244247
CODEN: SAAPEB
Document type: Journal article (JA)

Publisher: Elsevier B.V.

Abstract: This paper presents a novel temperature and pressure sensor with a small volume and large range, which can measure the temperature and pressure accurately in oil and gas wells. The feasibility of the sensor is verified by theoretical calculation and simulation, and the relationship between the sensor structure and the wavelength of fiber Bragg grating is established. The structure of the sensor is optimized by simulation, so that the sensor has good performance. The performance of the sensor is verified by experiments, which can measure temperature and pressure independently, the pressure range of the sensor is 0–40 MPa, the sensitivity is 24.05 pm/MPa, the linearity is 0.9997, and the repeatability is 0.0038. The temperature measurement range is 25–200 and the sensitivity is 31.16 pm/. The sensor is packaged with solid glass particles and it can operate for long periods in high temperature environments. © 2023 Elsevier B.V.

Number of references: 26

Main heading: Pressure sensors

Controlled terms: Fiber Bragg gratings - Temperature measurement - Temperature sensors

Uncontrolled terms: Glass particles - Measurement range - Oil and gas well - Performance - Pressure ranges - Sensor structures - Small-sized sensor - Temperature and pressures - Theoretical calculations - Theoretical simulation

Classification code: 944.3 Pressure Measuring Instruments - 944.5 Temperature Measuring Instruments - 944.6 Temperature Measurements

Numerical data indexing: Pressure 0.00E00Pa to 4.00E+07Pa, Size 2.405E-11m, Size 3.116E-11m

DOI: 10.1016/j.sna.2023.114397

Compendex references: YES

Database: Compendex

Data Provider: Engineering Village

165. Miniaturized High-Sensitivity Temperature Sensor Based on Cascaded Fiber-Optic FPI

Accession number: 20231113736819

Authors: Liu, Yinggang (1); Wen, Junliang (1); Feng, Yanpei (1); Huang, Liang (1); Dong, Jingfei (1)

Author affiliation: (1) Xi'an Shiyou University, Shaanxi Engineering Research Center of Oil and Gas Resource Optical Fiber Detection, Shaanxi Key Laboratory of Measurement and Control Technology for Oil and Gas Wells, Xi'an; 710065, China

Corresponding author: Liu, Yinggang(ygliu@xsyu.edu.cn)

Source title: IEEE Photonics Technology Letters

Abbreviated source title: IEEE Photonics Technol Lett

Volume: 35

Issue: 8

Issue date: April 15, 2023

Publication year: 2023

Pages: 430-433

Language: English

ISSN: 10411135

E-ISSN: 19410174

CODEN: IPTLEL

Document type: Journal article (JA)

Publisher: Institute of Electrical and Electronics Engineers Inc.

Abstract: In letter, a cascaded fiber-optic Fabry-Perot interferometers temperature sensor with high-sensitivity and small-dimension is proposed and demonstrated. The sensor is fabricated by filling the polydimethylsiloxane (PDMS) and air between two single-mode fiber end-faces located in a section of silica capillary, thus a PDMS-based glue cavity, an air cavity and combined PDMS-air cavity are constructed. Due to the similar optical length between PDMS glue cavity and PDMS-air cavity, the conditions for Vernier effect can be easily satisfied in the sensor fabrication. The temperature sensitivity of proposed sensor is effectively improved in experiment. The research results show that the sensitivity of sensor is enhanced from 2.62 nm/°C to 23.22 nm/°C, which is about 8.86 times than that of the single PDMS-based glue cavity, and the linearity of temperature-dependent wavelength shifts is superior to 0.99 in

temperature range of 3250 °C. The sensor has advantages of high sensitivity, simplicity and easy to fabrication, and the small-dimension merit make it more suitable for point-temperature measurement. © 1989-2012 IEEE.

Number of references: 22
Main heading: Temperature measurement
Controlled terms: Fabry-Perot interferometers - Fiber optic sensors - Fiber optics - Glues - Gluing - Microchannels - Optical fiber fabrication - Polydimethylsiloxane - Silica - Silicones - Single mode fibers - Temperature sensors
Uncontrolled terms: Air cavity - End faces - Fabry-perot interferometer - Fiber-optics - High sensitivity - Optical fiber sensing - Sensitivity - Silica capillary - Single-mode fibers - Vernier effect
Classification code: 741.1.2 Fiber Optics - 815.1.1 Organic Polymers - 941.3 Optical Instruments - 944.5 Temperature Measuring Instruments - 944.6 Temperature Measurements
Numerical data indexing: Size 2.322E-08m, Size 2.5146E-02m, Size 2.62E-09m
DOI: 10.1109/LPT.2023.3251412
Compendex references: YES
Database: Compendex
Data Provider: Engineering Village
Compilation and indexing terms, Copyright 2023 Elsevier Inc.

166. Effect of molybdenum content on corrosion resistance and corrosion behavior of Ti-Mo titanium alloy in hydrochloric acid

Accession number: 20224913207539
Authors: Zhao, Heng (1, 2); Xie, Longfei (1); Xin, Chao (1); Li, Ning (2); Zhao, Bin (3); Li, Lanyun (2)
Author affiliation: (1) Xi'an Rare Metal Materials Institute Co., Ltd., Xi'an; 710016, China; (2) School of Materials Science and Engineering Xi'an Shiyou University, Xi'an; 710065, China; (3) Xi'an Surface Material Protection Co., Ltd, Xi'an; 710200, China
Corresponding author: Xie, Longfei(lfeixie@163.com)
Source title: Materials Today Communications
Abbreviated source title: Mater. Today Commun.
Volume: 34
Issue date: March 2023
Publication year: 2023
Article number: 105032
Language: English
E-ISSN: 23524928
Document type: Journal article (JA)
Publisher: Elsevier Ltd
Abstract: In this work, the corrosion resistance and corrosion behavior of Ti-xMo (x = 0, 1, 3, 5 wt%) titanium alloys in 10 wt% HCl solution are systematically studied by microstructural characterization, electrochemical and corrosion weight loss measurements. The results show that with the increase of Mo content, the quantity of β-phase on Ti-xMo alloys surface increases, and the corrosion resistance is enhanced. The electrochemical property showed that corrosion current density decreased, and polarization resistance increased with the increase of Mo content. Moreover, the corrosion weight loss revealed that corrosion rates of Ti-xMo alloys after 10 d of immersion were 0.19, 0.001 and 0.0007 mm/a, respectively. It is found that the corrosion type of Ti-xMo alloys changes from uniform corrosion to pitting corrosion when the Mo addition reaches 3 wt%, and the widths of pitting corrosions for Ti-5Mo are smaller than those for Ti-3Mo. The increase of Mo content and β-phase can significantly improve the corrosion resistance of Ti-xMo alloys. This work will provide referenceable data for designing high corrosion-resistant materials for oil well pipelines through composition optimization. © 2022 Elsevier Ltd

Number of references: 53
Main heading: Corrosion resistance
Controlled terms: Binary alloys - Chlorine compounds - Corrosion rate - Corrosion resistant alloys - Corrosive effects - Electrochemical corrosion - Hydrochloric acid - Molybdenum alloys - Pipeline corrosion - Pitting - Titanium alloys
Uncontrolled terms: Acid corrosion - Corrosion behaviour - Corrosion weight loss - Electrochemical technology - HCl solution - Microstructural characterizations - Mo content - Molybdenum content - Resistance behaviors - Titanium (alloys)
Classification code: 531 Metallurgy and Metallography - 539.1 Metals Corrosion - 542.3 Titanium and Alloys - 543.3 Molybdenum and Alloys - 801.4.1 Electrochemistry - 802.2 Chemical Reactions - 804.2 Inorganic Compounds
Numerical data indexing: Size 1.00E-06m, Size 7.00E-07m
DOI: 10.1016/j.mtcomm.2022.105032

Compendex references: YES
Database: Compendex
Data Provider: Engineering Village

167. Design and analysis of UWB antenna with quintuple band-notched and wide-band rejection characteristics

Accession number: 20221011754409
Authors: Yang, Hailong (1, 2); Zhang, Jinsheng (2); Li, Xuping (1); Li, Yapeng (1); Yang, Junhua (1); Shi, Xiaomin (3)
Author affiliation: (1) Xi'an University of Posts & Telecommunications, Xi'an; 710121, China; (2) Control Science and Engineering from the Xi'an Research Institute of High-Tech, Xi'an; 10024, China; (3) Communication Engineering Department, Xi'an Shiyou University, Xi'an, China
Corresponding author: Yang, Hailong(yanghl68@163.com)
Abstract: In this study, a compact ultra-wideband (UWB) antenna with quintuple band-notched and wide-band rejection characteristics is studied. The proposed antenna mainly consists of a rectangular radiating patch, a microstrip feeding line, and a modified rectangular ground plane. The quintuple band-notched functions with narrow stop bands are achieved at WiMAX (3.3-3.7 GHz), WLAN (5.15-5.35 GHz and 5.725-5.825 GHz), C-band IEEE INSAT/super-extended (6.7-7.1 GHz) by using three modified inverted U-shaped slots and two symmetrical rectangular slots on the radiating path. Each stop band formed in the UWB antenna can be adjusted independently, and deep reflection zeros are formed between the adjacent stop bands. The formation of reflection zeros improves the band-edge selectivity of the stop band, and the notch characteristics are more prominent. To further study the wide stop band (C-band and X-band) with good selectivity characteristics, a pair of L-shaped open slot is added to the edges of two rectangular slots. Additionally, a pair of modified Rho-shaped resonators is located near the feeding line to realize band-notched characteristic at ITU service bands (8.025-8.4 GHz), thus a quintuple band-notched UWB antenna is achieved. The shape factor (ratio of the -3 dB bandwidth to the -10 dB bandwidth) of the wide stop band is 0.56, which indicates that the antenna has excellent band-edge selectivity. To verify the performance of the proposed design, both the time-domain and the frequency-domain characteristics of the antenna have been studied and analyzed. The simulated and measured results verify the design as a good candidate for various portable UWB applications. © 2022 The Author(s). Published by Cambridge University Press in association with the European Microwave Association.
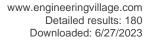**Number of references:** 38
Main heading: Resonators
Controlled terms: Antenna feeders - Antenna grounds - Bandwidth - Frequency domain analysis - Microstrip antennas - Microwave antennas - Mobile antennas - Slot antennas - Time domain analysis - Ultra-wideband (UWB)
Uncontrolled terms: Band notched antenna - Band-notched - Band-rejection characteristics - Notched band - Rho-shaped resonator - Stopband - Ultra-wideband antenna - Ultrawide band - Wide-band - Wideband antenna
Classification code: 716.1 Information Theory and Signal Processing - 716.3 Radio Systems and Equipment - 921 Mathematics - 921.3 Mathematical Transformations
Numerical data indexing: Decibel -1.00E+01dB, Decibel -3.00E+00dB, Frequency 3.30E+09Hz to 3.70E+09Hz, Frequency 5.15E+09Hz to 5.35E+09Hz, Frequency 5.725E+09Hz to 5.825E+09Hz, Frequency 6.70E+09Hz to 7.10E+09Hz, Frequency 8.025E+09Hz to 8.40E+09Hz
DOI: 10.1017/S1759078722000186

Compendex references: YES
Database: Compendex
Data Provider: Engineering Village

168. Integrated fiber-optic sensor based on inscription of FBG in seven-core fiber for curvature and temperature measurements

Accession number: 20225113262749
Authors: Liu, Yinggang (1); Feng, Yanpei (1); Wen, Junliang (1); Huang, Liang (1); Dong, Jingfei (1)
Author affiliation: (1) Shaanxi Engineering Research Center of Oil and Gas Resource Optical Fiber Detection & Shaanxi Key Laboratory of Measurement and Control Technology for Oil and Gas Wells, Xi'an Shiyou University, Xi'an; 710065, China
Corresponding author: Liu, Yinggang(ygliu@xsyu.edu.cn)
Source title: Optical Fiber Technology
Abbreviated source title: Opt. Fiber Technol.
Volume: 75
Issue date: January 2023
Publication year: 2023
Article number: 103197
Language: English
ISSN: 10685200
CODEN: OFTEFV
Document type: Journal article (JA)
Publisher: Academic Press Inc.
Abstract: An integrated fiber-optic sensor with cross-sensitivity elimination effect is proposed and experimented for simultaneous measurements of curvature and temperature. The sensor structure mainly consists of a section of seven-core fiber (SCF) that fiber Bragg gratings (FBGs) were inscribed in each fiber core by phase-mask technique. Since the FBG in the central-core of SCF is only sensitive to temperature, and others in six outer-cores have same temperature responses and different sensitivity for curvature, the sensor can simultaneously measure temperature and curvature through analyzing the wavelength shifts of central-core FBG and every-two cores of FBG. The experiment results show that the maximum curvature sensitivity reaches 0.39 nm/m-1 in the curvature range of 2.53 m-1–8.62 m-1, and temperature response sensitivity is 9.97 pm/°C, which is consistent with ordinary single-mode FBG in temperature range of 30 °C–70 °C. Furthermore, the verified experiment for simultaneous measurement are performed, the central-core FBG can be used as a temperature calibration during the curvature measurement. The relative errors of curvature and temperature are 2.22 % and 2.58 %, respectively. The SCF-based FBG sensor has the advantages of small dimension, easy fabrication, better repeatability, and potential application values in many fields such as machine structure motion monitoring. © 2022 Elsevier Inc.
Number of references: 26
Main heading: Fiber Bragg gratings
Controlled terms: Fiber optic sensors - Fiber optics - Temperature measurement
Uncontrolled terms: Central core - Core fibre - Cross sensitivity - Curvature - Fiber bragg grating - Fibre-optic sensor - Measurements of - Seven-core fiber - Simultaneous measurement - Temperature response
Classification code: 741.1.2 Fiber Optics - 944.6 Temperature Measurements
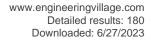**Numerical data indexing:** Percentage 2.22E+00%, Percentage 2.58E+00%, Size 1.00E00m to 8.62E+00m, Size 2.53E+00m, Size 2.54E-02m, Size 3.90E-10m, Size 9.97E-12m, Temperature 3.03E+02K to 3.43E+02K
DOI: 10.1016/j.yofte.2022.103197

169. Investigation of corrosion inhibitor used in cement   (*Open Access*)

Accession number: 20231413833211
Authors: Yan, Wei (1); Hao, Wang (1); Xu, Zhongying (2)

Author affiliation: (1) Drilling and Production Engineering Technology Institute, CNPC Chuanqing Drilling Engineering Company Ltd., Xi'an; 710018, China; (2) Shaanxi University Engineering Research Center of Oil and Gas Field Chemistry, Xi'An Shiyou University, Xi'an; 710065, China
Corresponding author: Xu, Zhongying(zjwyan@cnpc.com.cn)

Source title: Journal of Physics: Conference Series
Abbreviated source title: J. Phys. Conf. Ser.
Volume: 2454
Part number: 1 of 1
Issue: 1
Issue date: 2023
Publication year: 2023
Article number: 012017
Language: English
ISSN: 17426588
E-ISSN: 17426596
Document type: Conference article (CA)
Conference name: 5th International Symposium on Hydrogen Energy and Energy Technologies, HEET 2022
Conference date: November 18, 2022 - November 19, 2022
Conference location: Osaka, Virtual, Japan
Conference code: 187331
Publisher: Institute of Physics

Abstract: Steel bar corrosion inhibitor can be incorporated into concrete (or mortar) with a small amount, or coated on the cement surface to protect the steel materials. It can prevent or delay the corrosion of metal bars by directly acting on the steel bars in concrete (or mortar), but it does not affect the structure and properties of concrete. In this paper, the single component corrosion inhibitor was screened and evaluated at room temperature by salt water immersion test and static coupon weight loss method. The results show that hydrazine hydrate and KNO_3 can effectively prevent the corrosion of reinforcement after being placed in simulated corrosion solution for 7 days. When the concentration of hydrazine hydrate and KNO_3 is greater than 0.5%, the corrosion inhibition rate of KNO_3 is 95.44% (100mg·L-1). © Published under licence by IOP Publishing Ltd.

Number of references: 15
Main heading: Corrosion inhibitors
Controlled terms: Bars (metal) - Cements - Concretes - Corrosion prevention - Corrosion protection - Corrosion rate - Hydrates - Hydration - Hydrazine - Mortar - Potash - Potassium Nitrate - Steel corrosion
Uncontrolled terms: Cement surface - Hydrazine hydrate - Metal bar - Properties of concretes - Single components - Steel bars - Steel materials - Structures and properties - Water immersion tests - Weight loss method
Classification code: 412 Concrete - 412.1 Cement - 414.3 Mortar (Before 1993, use code 412) - 535.1.2 Rolling Mill Practice - 539.1 Metals Corrosion - 539.2 Corrosion Protection - 539.2.1 Protection Methods - 545.3 Steel - 803 Chemical Agents and Basic Industrial Chemicals - 804.2 Inorganic Compounds
Numerical data indexing: Age 1.918E-02yr, Mass density 1.00E-01kg/m3, Percentage 5.00E-01%, Percentage 9.544E+01%
DOI: 10.1088/1742-6596/2454/1/012017
Compendex references: YES
Open Access type(s): All Open Access, Gold
Database: Compendex
Data Provider: Engineering Village

170. The configuring pathways of green technology advance, organizational strategy and policy environment for realizing low-carbon manufacturing from the perspective of simmelian tie: A qualitative comparative analysis of listed companies in China

Accession number: 20224813185778
Authors: Li, Xinhao (1); Ruan, Tianshun (1, 2); Hou, Ke (1); Qu, Rong (3)
Author affiliation: (1) School of Economics and Management, Xi'an Shiyou University, Xi'an; 710065, China; (2) School of Economics and Management, Northwest University, Xi'an; 710127, China; (3) School of Economics and Management, Weinan Normal University, Weinan; 714000, China
Corresponding author: Ruan, Tianshun(180706@xsyu.edu.cn)
Source title: Journal of Cleaner Production
Abbreviated source title: J. Clean. Prod.
Volume: 382
Issue date: January 1, 2023
Publication year: 2023
Article number: 135149
Language: English
ISSN: 09596526
CODEN: JCROE8
Document type: Journal article (JA)
Publisher: Elsevier Ltd

Abstract: Low-carbon manufacturing is an emerging industrial trend and an important way to achieve sustainable development. As the country with the largest manufacturing scale and carbon dioxide emissions, it is of great practical and theoretical significance to study China's low-carbon manufacturing issues. Based on the ternary analysis perspective of simmelian tie, this paper chooses to identify the influencing factors through the technology-organization-environment research framework, and derives the pathways of low-carbon manufacturing through the fuzzy-set qualitative comparative analysis method. The research results show that: (1) Under the low-carbon manufacturing goal, stable industrial chain structure and policy-sensitive are the formation reasons for the simmelian tie. (2) From the perspective of simmelian tie, low-carbon manufacturing will be influenced by the driving role of green technological advances, the supporting role of organizational strategies, and the regulatory role of the policy environment. (3) Manufacturing enterprises' low-carbon pathways are directly related to their industrial chain position. Compared with upstream enterprises, downstream enterprises have more diverse low-carbon manufacturing pathways. (4) Active governmental support can more effectively promote the realization of low-carbon manufacturing than environmental pressure. © 2022

Number of references: 85
Main heading: Sustainable development
Controlled terms: Carbon dioxide - Global warming - Industrial research - Manufacture - Planning
Uncontrolled terms: Carbon dioxide emissions - Green technology - Industrial chain - Low-carbon manufacturing - Manufacturing IS - Manufacturing issue - Organizational policies - Organizational strategy - Qualitative comparative analysis - Technology advances
Classification code: 443.1 Atmospheric Properties - 537.1 Heat Treatment Processes - 804.2 Inorganic Compounds - 901.3 Engineering Research - 912.1 Industrial Engineering - 912.2 Management - 913.4 Manufacturing
DOI: 10.1016/j.jclepro.2022.135149
Compendex references: YES
Database: Compendex
Data Provider: Engineering Village

171. Adsorption of NO gas molecule on the vacancy defected and transition metal doped antimonene: A first-principles study

Accession number: 20224713140481
Authors: Chen, Guo-Xiang (1); Du, Rui-Yun (1); Wang, Dou-Dou (2); Chen, Zhe (1); Liu, Shuai (1); Zhang, Jian-Min (3)
Author affiliation: (1) College of Sciences, Xi'an Shiyou University, Xi'an; 710065, China; (2) College of Science, Xi'an University of Science and Technology, Xi'an; 710054, China; (3) College of Physics and Information Technology, Shaanxi Normal University, Xi'an; 710062, China
Corresponding author: Chen, Guo-Xiang(guoxchen@xsyu.edu.cn)
Source title: Vacuum
Abbreviated source title: Vacuum
Volume: 207
Issue date: January 2023
Publication year: 2023
Article number: 111654

Abstract: The adsorption behaviors of single vacancy defected and transition metal (TM) atoms (Sc, Ti) doped antimonene for NO molecule have been systematically investigated using the first-principles calculations based on the density functional theory (DFT-D2 method). The results show that the NO molecule is physisorbed on pure antimonene with the low adsorption energy. While the NO molecule is chemisorption on single vacancy defected antimonene (SV-antimonene), TM doped antimonene (Sc-antimonene, Ti-antimonene) and TM doped single vacancy defected antimonene (Sc-SV-antimonene, Ti-SV-antimonene). The introduction of vacancy defects and TM atoms can effectively enhance the interaction between the NO molecule and the antimonene by analyzing the density of states (DOS), charge density difference (CDD) and the electron localization function (ELF). In addition, the significant changes in work function (WF) after NO adsorption indicate that defected and doped antimonene are sensitive to NO molecule. The optical properties suggest that the increase in absorption coefficients of all adsorption systems can be observed in the visible region. Therefore, these results provide theoretical guidance for the design of high-sensitive gas sensors based on antimonene. © 2022 Elsevier Ltd

Number of references: 58
Main heading: Molecules
Controlled terms: Adsorption - Calculations - Defects - Density functional theory - Design for testability - Optical properties - Titanium compounds - Transition metals
Uncontrolled terms: Adsorption properties - Antimonene - DFT-d2 - Gas molecules - Metal-doped - NO molecule - Single vacancies - Transition metal atoms - Transition metal doping - Vacancy Defects
Classification code: 531 Metallurgy and Metallography - 741.1 Light/Optics - 802.3 Chemical Operations - 921 Mathematics - 922.1 Probability Theory - 931.3 Atomic and Molecular Physics - 931.4 Quantum Theory; Quantum Mechanics - 951 Materials Science
DOI: 10.1016/j.vacuum.2022.111654

Compendex references: YES
Database: Compendex
Data Provider: Engineering Village

172. Determination of Stabilization Time During Stress-Sensitivity Tests

Accession number: 20230066095

Authors: Yu, Miao (1); Huang, Hai (2); Li, Huazhou (1)
Author affiliation: (1) School of Mining and Petroleum Engineering, Faculty of Engineering, University of Alberta, Edmonton; T6G 1H9, Canada; (2) Shaanxi Key Laboratory of Advanced Stimulation Technology for Oil & Gas Reservoirs, Xi'an Shiyou University, Xian; 710065, China
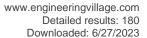**Corresponding authors:** Huang, Hai; Li, Huazhou

Abstract: The stress sensitivity of tight sandstone formations is significantly larger than that of high-permeability sandstone formations. It takes a longer time for the permeability of a tight sandstone to get stabilized when subjected to a change in the confining stress. Such phenomenon is referred as the delayed stress sensitivity phenomenon. To quantify the delayed stress sensitivity phenomenon, a term called stabilization time can be used. It characterizes how much time is required for a given core to reach an unchanging permeability level when the confining pressure is changed from a lower pressure to a higher pressure. In this study, we make a hypothesis that the delayed stress sensitivity can be correlated with one or more pore-structure properties of the reservoir rocks. Stress-sensitivity tests on twelve tight cores are studied to testify the hypothesis that the stabilization time of tight sandstone cores under tri-axial stress test conditions can be related to the pore-structure properties of the reservoir rocks. Twelve cores with

different permeability levels are retrieved from two field (i.e., a gas field and an oil field). Mercury intrusion porosimetry (MIP) tests and tri-axial stress-sensitivity tests have been conducted on these cores. The purpose of the MIP tests is to measure pore structure parameters such as the pore size distribution. Using a trial-and-error approach, we develop an empirical method to split the pores in a given core sample into large pores and small pores based on the pore size distribution charts. Once the pores are split into large pore and small pores, we can further calculate the area ratio of the large pores to the small pores. When conducting the tri-axial stress-sensitivity tests, we apply a constant axial stress of 10 MPa, but change the confining pressure from 5 to 30 MPa. During each tri-axial stress-sensitivity test, we monitor the variation of permeability versus time. By analyzing the permeability variation data, we can determine the stabilization time, i.e., the time required for the permeability to reach a constant value when confining pressure changes to a higher level. We also record the cumulative stabilization time as a function of the confining pressure. The cumulative stabilization time (T) is found to linearly correlate with the logarithm function of the confining pressure (lnP). We discover that the slope of the linear relationship between T and lnP shows a strong correlation with the area ratio of large pores to small pores. Regression using an inverse exponential function results in a regression coefficient of $R^2=0.86$. This indicates that a core sample with a larger area ratio of large pores to small pores has a shorter stabilization time, while a core sample with a smaller area ratio of large pores to small pores has a longer stabilization time. Such finding is in line with the physical understanding that the core sample with a smaller area ratio of large pores to smaller pores tends to have a steadier structure and deform more slowly than the one with a larger area ratio of large pores to smaller pores. © 2023, The Authors. All rights reserved.

Number of references: 23
Main heading: Rock mechanics
Controlled terms: Gas industry - Petroleum reservoir engineering - Pore size - Pore structure - Rock pressure - Sandstone - Sensitivity analysis - Size distribution - Stabilization - Stresses
Uncontrolled terms: Area ratios - Confining pressures - Large pores - Permeability change - Pore-size distribution - Sensitivity tests - Stabilization time - Stress sensitivity - Tight sandstones - Tri-axial stress
Classification code: 482.2 Minerals - 483.1 Soils and Soil Mechanics - 502.1 Mine and Quarry Operations - 512.1.2 Petroleum Deposits : Development Operations - 522 Gas Fuels - 921 Mathematics - 922.2 Mathematical Statistics - 931.2 Physical Properties of Gases, Liquids and Solids - 951 Materials Science
Numerical data indexing: Pressure 1.00E+07Pa, Pressure 5.00E+06Pa to 3.00E+07Pa
DOI: 10.2139/ssrn.4370497
Compendex references: YES
Preprint ID: 4370497
Preprint source website: https://papers.ssrn.com/sol3/papers.cfm
Preprint ID type: SSRN
Database: Compendex
Data Provider: Engineering Village
Compilation and indexing terms, Copyright 2023 Elsevier Inc.

173. Variant selection of massive γ subgrains and corresponding mechanical properties in Ta containing $\gamma-$TiAl-based alloys

Accession number: 20225213292008
Authors: Pan, Hengpei (1); Zhang, Keren (2); Chen, Jieming (1); Zhang, Xinyao (1); Zhao, Hui (2); Hu, Rui (3)
Author affiliation: (1) Luoyang Ship Material Research Institute, Luoyang; 471023, China; (2) School of Materials Science and Engineering, Xi'an Shiyou University, Xi'an; 710065, China; (3) State Key Laboratory of Solidification Processing, Northwestern Polytechnical University, Xi'an; 710072, China
Corresponding author: Zhang, Keren
Abstract: The variant selection of subgrains in massive γ (#m) is systematically studied by 0–2 at.% Ta-containing $\gamma-$TiAl-based alloy. Results show that the precipitation of #m phase increases first, and then decreases with the rising of

Ta. The critical content of Ta, which massive transformation is promoted or inhibited, is identified. EBSD and HRTEM results reveal variant selection process during nucleation and growth inner α matrix along all possible $\{1\ 1\ 1\}\gamma$, in terms of minimization of energy of highly defected α grain caused by Ta, thereafter, the subgrains of #m are refined. These fine subgrains and highly defected α_2 grain can enhance the mechanical properties of TiAl-xTa alloy. © 2022 Elsevier B.V.

Number of references: 15
Main heading: Titanium alloys
Controlled terms: Aluminum alloys - Defects - Intermetallics - Tantalum alloys - Ternary alloys
Uncontrolled terms: Intermetallic alloys and compounds - Massive transformations - Nucleation and growth - Subgrains - Ta - Ta-containing - Variant selection - α matrix - γ_TiAl based alloy - #m phase
Classification code: 531.1 Metallurgy - 541.2 Aluminum Alloys - 542.3 Titanium and Alloys - 543.4 Tantalum and Alloys - 951 Materials Science
DOI: 10.1016/j.matlet.2022.133689
Funding Details: Number: 21JC027, Acronym: -, Sponsor: Education Department of Shaanxi Province; Number: 2021JM-403,2022JQ-359, Acronym: -, Sponsor: Natural Science Basic Research Program of Shaanxi Province;
Funding text: This work was supported by Natural Science Basic Research Program of Shaanxi (Program No. 2022JQ-359 and No. 2021JM-403) and Scientific Research Program Funded by Shaanxi Provincial Education Department (Program No. 21JC027)
Compendex references: YES
Database: Compendex
Data Provider: Engineering Village
Compilation and indexing terms, Copyright 2023 Elsevier Inc.

174. Distributed variational Bayesian adaptive filtering for randomly delayed measurements and unknown noise statistics in multi-sensor networked systems

Accession number: 20232114136196
Authors: Li, Guo (1); Gao, Shesheng (1); Xia, Juan (2); Yang, Jiahui (1); Gao, Zhaohui (3)
Author affiliation: (1) School of Automation, Northwestern Polytechnical University, Xi'an; 710072, China; (2) College of Information Science and Engineering, Henan University of Technology, Zhengzhou; 450001, China; (3) School of Electronic Engineering, Xi'an Shiyou University, Xi'an; 710065, China
Corresponding author: Xia, Juan(xiajuan_dr@163.com)
Source title: Digital Signal Processing: A Review Journal
Abbreviated source title: Digital Signal Process Rev J
Volume: 139
Issue date: July 2023
Publication year: 2023
Article number: 104077
Language: English
ISSN: 10512004
CODEN: DSPREJ
Document type: Journal article (JA)
Publisher: Elsevier Inc.
Abstract: To deal with randomly delayed measurements and unknown noise statistics in multi-sensor networked systems, a distributed variational Bayesian adaptive cubature Kalman filtering algorithm (DVB_ACKF) is presented in this paper. To compensate for the effects induced by randomly delayed measurements, a refined measurement reorganization method is designed via a two-stage estimation strategy. Specifically, we first estimate the time delay step. The measurements are then rearranged based on the estimated results from the first stage. Then, a novel noise estimator with the sliding-window and variational Bayesian method is developed to estimate the mean and covariance of the unknown noise. The network topology attribute and measurement accuracy have been combined to eliminate the distributed fusion error. The tuning parameter and forgetting factor as well as their bounds are analyzed. Furthermore, numerical simulations are carried out to verify the superior performance of the developed algorithm. © 2023 Elsevier Inc.

Number of references: 37
Main heading: Adaptive filtering
Controlled terms: Adaptive filters - Bayesian networks - Kalman filters - Network topology - Sensor networks
Uncontrolled terms: Delayed measurements - Distributed filtering - Distributed filtering algorithm - Filtering algorithm - Measurement Noise - Multi sensor - Noise statistics - Unknown noise - Unknown noise statistic - Variational bayesian
Classification code: 703.1 Electric Networks - 921.4 Combinatorial Mathematics, Includes Graph Theory, Set Theory

175. Hydrophobically modified low molecular weight polymers as high temperature resistant shale inhibitor

Accession number: 20231914066334

Authors: Wang, Zonglun (1); Liu, Jingping (1); Lv, Kaihe (1); Shao, Zihua (1); Zhang, Xianfa (1); Xu, Zhe (1); Zhang, Fan (3); Dong, Xiaodong (1); Sun, Jinsheng (1, 2)
Author affiliation: (1) School of Petroleum Engineering, China University of Petroleum (East China), Shandong, Qingdao, China; (2) CNPC Engineering Technology R & D Company Limited, Beijing, China; (3) School of Petroleum Engineering, Xi'an Shiyou University, Shanxi, Xi'an, China
Corresponding author: Liu, Jingping(liujingping20@126.com)

Abstract: With the exploration and development of deep oil and gas, an efficient shale inhibitor resistant to high temperatures is critical for wellbore stability during drilling. In this paper, a hydrophobically modified low molecular weight polymer (SDY) is studied to maintain wellbore stability at high temperatures during drilling. The inhibition performance of SDY was investigated using linear swelling experiments and rolling recovery experiments at different temperatures. The experimental results showed that SDY had good inhibition performance. At 150 °C, the expansion rate was 61.69 % for 1 % SDY and 175.51 % in water. And the rolling recovery of shale rock chips was 87.53 % for 1 % SDY and 18.92 % in water. Compared with water, it can reduce the hydration swelling rate of bentonite rock mold by 57 % and improve the recovery rate of shale rock chips by 3.37 times at 150 °C. The inhibition mechanism of SDY was analyzed by zeta potential, particle size distribution, contact angle, self-absorbing water, X-ray diffraction and scanning electron microscopy experiments. The good inhibition performance of SDY at high temperatures may be attributed to three aspects. First of all, SDY molecules can neutralize the negative charge on the shale surface by electrostatic effect, and reduce the repulsive force between shales to inhibit the hydration dispersion of shales. Second, SDY can still adsorb on the shale surface at high temperatures to form a hydrophobic film and change the wettability of the shale surface. This increases the adsorption resistance of water molecules on the shale surface thereby inhibiting shale surface hydration. Third, SDY molecules can insert between the layers of bentonite sheets to bind the adjacent clay layers together, effectively inhibiting the permeable hydration of shale. This study provides an approach for addressing wellbore stability in deep wells with higher temperature. © 2023 Elsevier B.V.

Number of references: 52
Main heading: Molecules
Controlled terms: Boreholes - Contact angle - Drilling fluids - Hydration - Hydrophobicity - Infill drilling - Molecular weight - Oil field equipment - Oil wells - Particle size - Particle size analysis - Recovery - Scanning electron microscopy - Wetting
Uncontrolled terms: 150 ° C - Highest temperature - Hydrophobic modification - Inhibition performance - Low-molecular-weight polymers - Rock chips - Shale inhibitors - Shale rocks - Wellbore stability - Wetting reversal
Classification code: 511.1 Oil Field Production Operations - 511.2 Oil Field Equipment - 512.1.1 Oil Fields - 931.2 Physical Properties of Gases, Liquids and Solids - 931.3 Atomic and Molecular Physics - 951 Materials Science
Numerical data indexing: Percentage 1.00E00%, Percentage 1.7551E+02%, Percentage 1.892E+01%, Percentage 5.70E+01%, Percentage 6.169E+01%, Percentage 8.753E+01%, Temperature 4.23E+02K
DOI: 10.1016/j.molliq.2023.121856

Authors: Jiang, Haiyan (1); Liu, Shuai (1); Wang, Jiao (2); You, Yuan (3); Yuan, Shibao (1)
Author affiliation: (1) Xi'an Shiyou University, Shaanxi, Xi'an; 710065, China; (2) The Fourth Oil Production Plant of Dagang Oilfield Branch, Tianjin; 300450, China; (3) Exploration and Development Research Institute of Changqing Oilfield Branch, CNPC, Shaanxi, Xi'an; 710018, China
Corresponding author: Yuan, Shibao(upcysb@126.com)
Abstract: In-situ pyrolysis of oil shale is a sophisticated process that converts solid to gas and liquid. There is currently minimal research on the chemical mechanism of the production process. Using the Chang 7 oil shale in the Ordos basin in China as an example, thermogravimetry, scanning electron microscopy, and oil shale pyrolysis are used to examine the pyrolysis process, mineral composition, and pore structure characteristics of oil shale. The results indicate that organic matter is entirely pyrolyzed as temperature rises. The organic matter is first pyrolyzed into asphaltene at low temperatures (320–450 °C), and the C–H bond of hydrocarbon molecules break and recombine to generate lipid compounds. In the medium temperature pyrolysis (450–600 °C), a substantial amount of organic matter is pyrolyzed, ester compounds undergo pyrolysis reaction, and macromolecular alkanes undergo dehydrogenation and chain breaking reaction to form small molecule hydrocarbons and hydrogen. In the high temperature pyrolysis (600–700 °C), secondary cracking of organic matter pyrolysis products, dehydrogenation of naphthenic hydrocarbons, polymerization of some polycyclic aromatic hydrocarbons to generate colloidal, asphaltene and oil shale semi-coke. As temperature rises, clay minerals are completely pyrolyzed, and the number of micropores and microcracks in oil shale increases as well. © 2023
Number of references: 29
Main heading: Scanning electron microscopy
Controlled terms: Dehydrogenation - Microcracks - Mineral oils - Molecules - Oil shale - Polycyclic aromatic hydrocarbons - Pore structure - Pyrolysis - Thermogravimetric analysis
Uncontrolled terms: Chemical mechanism - Evolution mechanism - Experimental study - In-situ pyrolyse - Ordos Basin - Product analysis - Pyrolyse product analyse - Pyrolyse stage - Pyrolysis products - Temperature rise
Classification code: 512.1 Petroleum Deposits - 513.3 Petroleum Products - 801 Chemistry - 802.2 Chemical Reactions - 804.1 Organic Compounds - 931.2 Physical Properties of Gases, Liquids and Solids - 931.3 Atomic and Molecular Physics
Numerical data indexing: Temperature 5.93E+02K to 7.23E+02K, Temperature 7.23E+02K to 8.73E+02K, Temperature 8.73E+02K to 9.73E+02K
DOI: 10.1016/j.energy.2023.127097
Compendex references: YES
Database: Compendex
Data Provider: Engineering Village

178. First-principles calculations to investigate electronic structures and magnetic regulation of non-metallic elements doped BP with point defects

Accession number: 20224513093795
Authors: Wen, Junqing (1); Li, Ning (1); Shi, Qiulong (2); Wu, Hua (1); Feng, Xia (1); Wang, Chun (1); Zhang, Jianmin (3)

Author affiliation: (1) School of Science, Xi'an Shiyou University, Xi'an; 710065, China; (2) School of Mechanical Engineering, Inner Mongolia University of Technology, Hohhot; 010051, China; (3) School of Physics and Information Technology, Shaanxi Normal University, Xi'an; 710062, China
Corresponding author: Wen, Junqing(wenjq2013@163.com)

Abstract: In order to control the magnetic properties and electronic structures of black phosphorene (BP) monolayer, the structures, electronic and magnetic properties of non-metallic elements doped BP monolayer without or with defects including P vacancy (VP) have been studied by density functional theory (DFT). Defective BP appears ferromagnetic metallicity, and the magnetic moment is 0.086 µB. The magnetism mainly comes from the spin polarization of P atoms near the defect point. For non-metallic elements doped intrinsic BP, system doped with B and N shows P-type semiconductor. C doped shows non-magnetic metal properties. Odoped exhibits magnetic P-type semiconductor. Si and S doped shows ferromagnetic metal properties. The magnetism mainly comes from the spin polarization of P atoms near the defect point, and a small part comes from doped atoms. In the case of non-metallic elements doped defective BP, the results show that flaw-b-C and flaw-s-Si exhibit non-magnetic metallic properties. The flaw-b-S shows P-type semiconductor with indirect band gap of 0.712 eV. Other systems exhibit ferromagnetic metallicity, and the magnetism mainly comes from the spin polarization of P atoms near defect point. Non-metallic elements doped BP monolayer without or with point defects can effectively adjust magnetic properties and electronic structures. © 2022 Elsevier Inc.

Number of references: 39
Main heading: Density functional theory
Controlled terms: Astrophysics - Atoms - Calculations - Electronic structure - Energy gap - Ferromagnetic materials - Ferromagnetism - Magnetic moments - Magnetic properties - Metals - Monolayers - Point defects - Silicon - Spin polarization - Structural properties
Uncontrolled terms: Defective black phosphorene - Density-functional-theory - Electronic.structure - Ferromagnetics - Metal properties - Metallicities - Non-metallic elements - Nonmagnetics - P type semiconductor - Spin-polarization
Classification code: 408 Structural Design - 549.3 Nonferrous Metals and Alloys excluding Alkali and Alkaline Earth Metals - 657.2 Extraterrestrial Physics and Stellar Phenomena - 701.2 Magnetism: Basic Concepts and Phenomena - 708.4 Magnetic Materials - 921 Mathematics - 922.1 Probability Theory - 931.3 Atomic and Molecular Physics - 931.4 Quantum Theory; Quantum Mechanics - 932.1 High Energy Physics - 933.1.1 Crystal Lattice - 951 Materials Science
Numerical data indexing: Electron volt 7.12E-01eV
DOI: 10.1016/j.jmgm.2022.108370

Compendex references: YES
Database: Compendex
Data Provider: Engineering Village

179. Electronic, magnetic and optical properties of zigzag ZnO nanoribbons under the coupling action of electric field and strains

Accession number: 20230613541182
Authors: Wen, Junqing (1); Cui, Weilin (1); Shi, Qiusheng (2); Yu, Fan (1); Lin, Pei (1); Li, Ning (1); Zhang, Jianmin (3)

Author affiliation: (1) School of Science, Xi'an Shiyou University, Xi'an; 710065, China; (2) School of Mechanical Engineering, Inner Mongolia University of Technology, Hohhot; 010051, China; (3) School of Physics and Information Technology, Shaanxi Normal University, Xi'an; 710062, China
Corresponding author: Wen, Junqing(wenjq2013@163.com)
Abstract: The electronic, magnetic and optical properties of zigzag ZnO nanoribbons under electric field and strains are calculated using density functional theory. The results show that Z8-ZnONRs have ferromagnetism, which is mainly caused by the spin polarization of O atoms of O-terminated edge. Under the action of Y-axial electric field, the system has ferromagnetism, which is mainly contributed by O-2p and Zn-3d orbital electrons. Z8-ZnONRs have the characteristics of high-energy storage and low loss. The application of Y-axial electric field can enhance the absorption of visible light. The application of strains can adjust the electronic structures of Z8-ZnONRs and the system remains magnetic. Which mainly comes from the contribution of O atoms of O-terminated edge. The results show that the coupling of electric field and strains makes the system change from ferromagnetic metal to magnetic semiconductor. © 2023

Number of references: 42
Main heading: Density functional theory
Controlled terms: Electric fields - Electronic properties - Electronic structure - Ferromagnetism - II-VI semiconductors - Magnetic semiconductors - Nanoribbons - Optical properties - Spin polarization - Wide band gap semiconductors - Zinc oxide
Uncontrolled terms: Coupling actions - Density-functional-theory - Electronic.structure - Low-loss - Magnetic and optical properties - Orbital electrons - Spin-polarization - Storage loss - Visible light - Zigzag nanoribbon
Classification code: 701.1 Electricity: Basic Concepts and Phenomena - 701.2 Magnetism: Basic Concepts and Phenomena - 708.4 Magnetic Materials - 712.1 Semiconducting Materials - 741.1 Light/Optics - 761 Nanotechnology - 804.2 Inorganic Compounds - 922.1 Probability Theory - 931.3 Atomic and Molecular Physics - 931.4 Quantum Theory; Quantum Mechanics - 932.1 High Energy Physics
DOI: 10.1016/j.tsf.2023.139698
Compendex references: YES
Database: Compendex
Data Provider: Engineering Village

180. Main controlling factors and oil-bearing potential characteristics of a tight sandstone reservoir: A case study of southwest Ordos Basin   (*Open Access*)

Accession number: 20231814026704
Authors: Guo, Feng (1); Peng, Xiaoxia (2); Ma, Xuqing (3); Wang, Haonan (1)
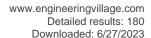**Author affiliation:** (1) School of Earth Sciences and Engineering, Shaanxi Key Lab of Petroleum Accumulation Geology, Xi'an Shiyou University, Xi'an, China; (2) Department of Geology, Northwest University, Xi'an, China; (3) PetroChina Changqing Oilfield Company, No.3 Gas Production Plant, Wushenqi, China
Corresponding authors: Guo, Feng(448073900@qq.com); Peng, Xiaoxia(pengxx2002@sina.com)

Abstract: Clarifying the main controlling factors of reservoirs and their oil-bearing potential is vital for predicting tight sandstone reservoirs. The Chang 8 reservoir in the southwest of Ordos Basin is a typical tight sandstone reservoir and is widely distributed. Observation description and sampling analysis of cores, the grain size analysis, casting thin section, scanning electron microscope, mercury pressure, nuclear magnetic resonance, and conventional physical analysis are used to clarify the main controlling factors and oil-bearing potential characteristics of the Chang 8 reservoir in southwest Ordos Basin. The results show that delta front subfacies are mainly developed in Chang 8 member, including distributary channel, natural dike, estuary bar and distributary bay. The main rock type of reservoir is lithic feldspathic sandstone, followed by feldspathic lithic sandstone. The types of reservoir space are mainly intergranular pores and intragranular dissolved pores, with a small amount of clay-related pores and micro-fractures. The average porosity and permeability of the reservoir are 11.67% and $0.52 \times 10^{-3} \mu m^2$, respectively. The reservoirs with high oil saturation are mainly distributary channels and thicker mouth bar sand bodies. Compaction is the main factor of reservoir compaction (porosity loss rate is 55.73%), followed by cementation (porosity loss rate is 29.23%). The favorable diagenesis is the dissolution of feldspar grains and some cement. The Chang 8 tight reservoir contains various nano-scale pore-throat. For tight reservoirs with similar physical properties, the pore-throat structure controls the oil saturation of the tight reservoir. Favorable conditions for tight sandstone reservoirs oil saturation include favorable sedimentary environment (distributary channel or thick mouth bar) and suitable microscopic pore characteristics. © The Author(s) 2023.